UNIVERSITY OF SOUTHAMPTON

Improvement of Conducting Polymer Gas Sensors

By Isabelle Besnard

A thesis submitted for the Degree of

DOCTOR OF PHILOSOPHY

January 2001

Department of chemistry
University of Southampton
Highfield
Southampton

UNIVERSITY OF SOUTHAMPTON

ABSTRACT

FACULTY OF SCIENCE

CHEMISTRY

Doctor of Philosophy

IMPROVEMENT OF CONDUCTING POLYMER GAS SENSORS

By Isabelle Besnard

The use of gas sensors is rapidly increasing, along with the number of candidate materials for gas sensing applications. In order to improve their competitivity, conducting polymer gas sensors have to be constantly improved. This work on conducting polymer chemoresistive gas sensors consists in improving their quality regarding three aspects: the substrates, the sensitive layer itself and the sensing mechanism of these devices.

A new array of micromachined devices was developed, comprising a new design (array of 4 discrete devices) and a new electrode material (platinum). This array was found to be more suitable for the requirements of our electronic nose applications. The electrochemistry of the electrode material was also employed to check the quality and to condition the substrates prior to every single electropolymerisation, which was reflected by an increase in quality.

Poly(pyrrole) and poly(aniline) doped with alkyl sulfonate were investigated as well as new coatings doped with aromatic sulfonate or metal phthalocyanine sulfonate. Their sensitivity towards CO and NO_2 was evaluated for possible applications in the automotive industry. The reproducibility from sensor to sensor was also addressed. Monitoring *in-situ* the resistance of the film during the electrodeposition, employing a technique specially designed for this purpose led to significant improvement in the reproducibility but also in the response time and in the stability over time.

The conducting polymers gas sensors were also tested towards ethanol and water, both as coatings for chemoresistive devices and QCM sensors. The aim was to get a deeper insight into the sensing mechanism of these gas sensitive materials in order to be able to engineer a coating for a given vapour. Following conductivity, viscoelasticity and mass upon exposure demonstrated that a Langmuir adsorption isotherm model was not suitable. A new model was defined, a double-diffusion model, where the vapour diffuses rapidly in the pores of the polymer before penetrating in the material itself, explaining the large response time of the conducting polymer gas sensors.

Table of contents

Chapter 1 - Introduction

Chapter 2 - Experimental

Chapter 3 - The chemoresistor substrate Description and improvement

Chapter 4 - Improvement of the sensing material

Chapter 5 - Production of conducting polymer gas sensors description, results and discussion

Chapter 6 - Introduction to the QCM experiments

Chapter 7 - Response of the conducting polymer gas sensors to ethanol

List of abbreviations

BVD	Butterworth van-Dyke
QCM	Quartz Crystal Microbalance
EQCM	Electrochemical Quartz Crystal Microbalance
SCE	Saturated Calomel Electrode
THF	Tetrahydrofuran
SEM	Scanning Electron Microscopy
VOC	Volatile Organic Compound
ppm	Part per million
PANPentSA	Poly(aniline) pentane sulfonate
PANDecaSA	Poly(aniline) decane sulfonate
PANptolSA	Poly(aniline) *p*-toluene sulfonate
PANNiPcTs	Poly(aniline) nickel phthalocyanine tetrasulfonate
PANCuPcTs	Poly(aniline) copper phthalocyanine tetrasulfonate
PPyPentSA	Poly(pyrrole) pentane sulfonate
PPyDecaSA	Poly(pyrrole) decane sulfonate
PPyptolSA	Poly(pyrrole) *p*-toluene sulfonate
PPyNiPcTs	Poly(pyrrole) nickel phthalocyanine tetrasulfonate
PPyCuPcTs	Poly(pyrrole) copper phthalocyanine tetrasulfonate

Acknowledgements

There are several scientists I wish to thank, without who this work would not have been so interesting, successful and enjoyable- all three being closely interlinked.
First I would like to thank Prof. P.N. Bartlett, for his supervision, his interest in my subject and for all the discussions during this work. He also introduced me to the field of gas sensors and electronic noses, a subject that highly interests me due to the high technology level employed and the continuous development of the science behind it.

I am grateful to the European Community (Brite-EuRam III BRPR-CT96-0194) as well as to the industrial partners (Centro Ricerche Fiat and Mannesman VDO AG) for funding this research programme, and to all members of the CIA project for the interest they showed in the conducting polymer gas sensors and the knowledge they brought me during this cooperation.

I wish then to thank the Sensor Research Laboratory (Engineering Department- Warwick University) for providing me with the gas test chamber, with the sensor substrates and with the electronics. I especially wish to thank Prof. J.W. Gardner for all his help on various subjects but also R. Tamadoni and Dr P. Ingelby. To finish I wish to thank all the members for their friendship.

I thank Dr G. Attard for lending the Impedance Analyser employed to perform the QCM experiments.

To finish a special thanks to the members of the electrochemistry group, especially Dr J. Elliott for her supervision and Dr P.R. Birkin for his technical and theoretical help. To Karen, Kermit and Lianne for their company, to Sam for his entertainment, to all my friends especially Eric and Juliet, I say thank you. Oh, I was about to forget Stefan for being patient.

To my parents

for their love and education

Chapter 1 - Introduction

1.1 - Electronic Nose technology

Olfaction is one of the five senses of the human being. Already in the infant the sense of smell is highly developed and allows it, for example, to recognise its parents, whereas the visual recognition is only developed later. During its childhood, the child goes through an intensive phase of training where it is exposed to a wide range of smells and is trained to identify them. Progressively it then uses the sense of smell on an everyday basis to appreciate foodstuff, fragrances or to unwillingly detect malodorous smells. A description of biological olfaction and its processing mechanism, which is far beyond the scope of this thesis, can be found elsewhere [1-3].

Olfaction is largely used on an industrial level. **Human panels**, people trained for their sense of smell, are employed in the food industry, the fragrance industry and in many other applications. However there are some limitations to these human "sniffers". As illustrated in Figure 1. 1, such activity can be unpleasant but also hazardous, for example in the case of detection of toxic gases or vapours. Additionally, even if the human panels are highly trained (representing high costs), they are subject to some subjectivity and are physically limited by the saturation of the sensitive cells, making continuous monitoring impossible.

With increasing concern with human's health and the need for industries to have a tool to intensively monitor odours and gases, scientists have developed an analytical tool which reproduces the human olfactory system and aims in going beyond the limits of a human nose: an electronic nose.

Figure 1. 1: efficiency test of deodorant at Rexona (picture originally from a Scientific American article).

1.1.1 - The Olfactory system and the Electronic Nose

A definition of an electronic nose was given in 1996 by Gardner and Bartlett [4]: "an **Electronic Nose** is an instrument which comprises an array of electronic chemical sensors with partial specificity and an appropriate pattern recognition system, capable of recognising simple or complex odours".

The introduction to electronic noses given here is mainly based on the complete and up-to-date review on electronic noses edited by these scientists [1]. The purpose here is to give an overview on the subject, but the reader is advised to refer to this reference for more concise information.

In the mammalian nose, volatiles interact with olfactory receptor cells which then transmit the information to the olfactory bulb where it is pre-processed. Pre-processed data are then transmitted to the brain where they are analysed and recognition can occur [1-3]. In a similar manner to human olfaction, artificial olfaction comprises an array of chemical sensors which interact with the vapour and the chemical information is then transduced into an electrical signal. The information is then pre-processed to take into account various parameters, for example the temperature and the humidity, before being transferred to the artificial intelligence. The data will be analysed by a neural network or any other pattern

recognition technique within the computer to enable identification of the odour or the chemicals mixture. Figure 1. 2 shows this parallel between the mammallian and artificial olfaction.

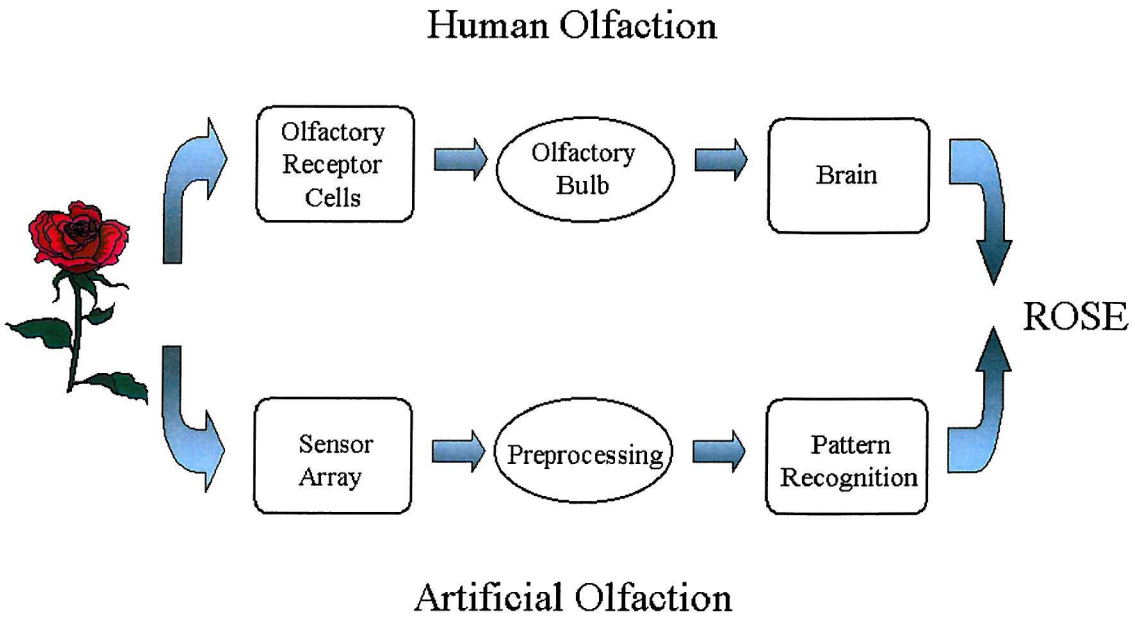

Figure 1. 2: diagram drawing the parallel between mammallian olfaction and artificial olfaction.

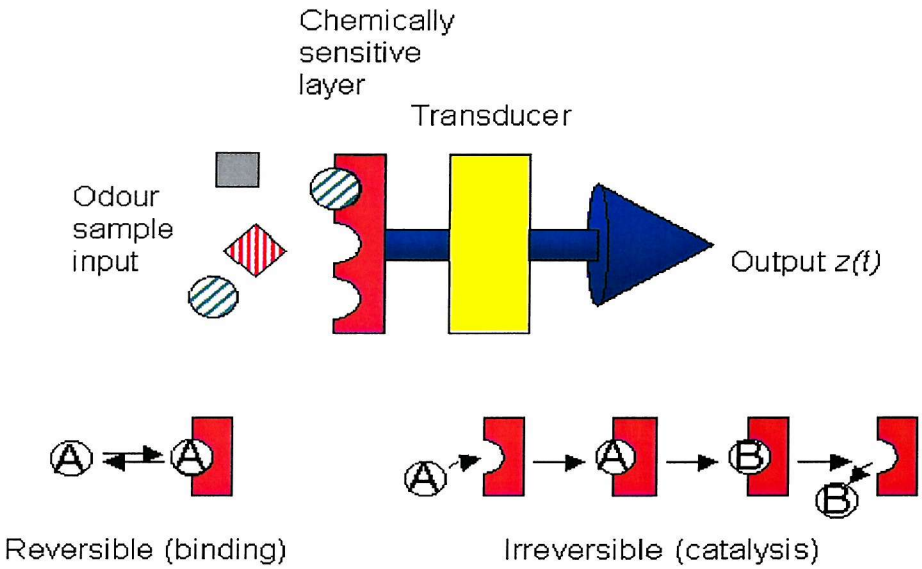

Figure 1. 3 : diagram showing the overall principle of the sensing mechanism as well as the two possible interactions between the vapour and the sensor coating: reversible and irreversible.

There are two ways for the vapour to interact with a sensor: the reversible response and the irreversible one, as shown in Figure 1. 3. In the **reversible response**, the vapour interacts with the coating and is released without any transformation once the vapour is removed. In the **irreversible** case, the vapour undergoes a chemical reaction at the coating and the products of the reaction are released.

Wünsche *et al.* [5] performed the comparison between a human panel composed of 30 persons and an electronic nose (comprising 8 piezoelectric quartz crystal sensors) to detect odours from foodstuff. Table 1. 1 gives some differences between the mammalian nose and the electronic nose observed during this study, as well as general characteristics.

Human Nose	**Electronic nose**
100 millions of olfactory cells	Array of sensors (usually between 6 and 40)
Response time in the second range	Response time in the minute range (varies widely with the type of sensor)
Irreversible response	Reversible (QCM, CP) or irreversible (MO) response
Low detection threshold (below ppm)	Higher detection threshold than human nose
Logarithm sensitivity to concentration	Linear sensitivity to concentration (in major cases at low concentrations)
In-built "sensors" sensitive to a wide range of chemicals	Choice of right coating and pattern recognition software required

Table 1. 1: typical characteristics of human and artificial noses, mainly extracted from a comparison between a human panel and an electronic nose based on 8 QCM sensors [5]. QCM (Quartz Crystal Microbalance), CP (Conducting Polymers) and MO (Metal Oxide) sensors will be detailed in the following section.

The field of electronic nose research is inherently interdisciplinary. A simple view of this analytical tool would be an equipment comprising a batch of sensors and recognition software. There are some components which are also significant in the performance of an electronic nose like the electronics employed, the signal pre-processing technique or the vapour pre-concentration, but which will not be discussed here.

1.1.2 - Gas sensors in the electronic noses

Individual gas sensors have been in use for decades, the most commonly employed are metal oxide sensors (Taguchi). Their general requirements are a high sensitivity to the target vapour and no interference from other vapours, a fast response time, a low sensitivity to external parameters (temperature, humidity), reversibility and reproducibility. For the sensors of an array of an electronic nose the requirements are similar. A major difference is that the sensors should not respond specifically to a given vapour but rather have a broad sensitivity. Indeed, an array should be able to give a pattern of responses to a complex odour which can be composed of hundreds of chemicals like coffee aroma for example [6]. The sensors of the array should also have a low cross-sensitivity to give significantly different patterns for different smells. In addition, for mass utilisation, the production should be cost efficient; and portable applications also require a low power consumption. All these aspects have to be addressed when developing an array of sensors.

The candidate materials for chemically sensitive interfaces include polymers, organic monolayers, metals, semiconductors, biomolecules and any combination of these [7,8]. This field is always expending and is going towards new materials, more sensitive on the nanoscale like the use of a single carbon nanotube as a sensor [9]. Transducing approaches can include mechanical, electrochemical, optical and of electronic types [7,8,10].

The sensing technology employed in electronic nose is at the moment mainly selected from three categories of sensors: metal oxide, quartz resonator and conducting polymer gas sensors. Less common sensor types, like electrochemical sensors, pellistors, optical fibres or devices based on a mass spectrometer, are not going to be described here.

CONDUCTING POLYMERS

Conducting polymers are organic materials containing a dopant, which resistance varies upon exposure to a vapour. This is one example where the response is reversible in the sense defined in Figure 1. 3 as only weak interactions of the Van der Waals type are expected to take place between the film and the vapour. They respond to a wide variety of vapours like NH_3, alcohols, ketones, without interference from common gases such as CO_2, CO, CH_4 and N_2. A whole section (section 1.2) will be dedicated to discussing their nature, properties and applications, as well as their sensing properties.

METAL OXIDE

In contrast to the weak interactions in conducting polymers, the response of a metal oxide sensor operates by a reaction type mechanism. The vapour is burnt at the metal oxide layer which is operated at elevated temperature (typically between 350 and 550°C). By consuming oxygen during the combustion, the conductivity of the coating varies with the amount and nature of the vapour. The sensing material generally employed is tin dioxide containing catalyst particles, platinum or palladium. More recently, ZnO, TiO_2 or WO_3 have also been employed as sensor materials. A complete description of the sensing mechanism can be found elsewhere [7].

This sensing technology has been in use for decades to detect toxic gases and the devices are known as Taguchi sensors. They are now widely employed in electronic nose technology. Following recent advances in heater technology for these devices, the power consumption can be significantly decreased from 800 mW to 75 mW, no longer preventing their use in portable instruments. The advantage of metal oxide sensors is their high sensitivity (down to 50 ppm for alcohols or down to 0.1 ppm for sulfur compounds originating from odours) but the counter-part is the poor selectivity of these materials.

PIEZOELECTRIC SENSORS

Many electronic noses, like products from Alpha MOS, Neotronics and MoTech, employ piezoelectric sensors. These sensors are based on the propagation of acoustic waves in a piezoelectric material, waves which will be modulated by the adsorption of the vapour in a coating. These sensors are composed of two categories, Surface Acoustic Wave sensors (SAW) and Bulk Acoustic Wave sensors (BAW), where the wave propagates at the surface and in the bulk of the crystal respectively. The coatings employed can be polymers (poly(siloxane) and its derivatives are widely employed) [11,12], Langmuir-Blodgett films [13] or Self Assembled Monolayers. Detection can be performed with a monolayer thick coating and sensitivy level of these sensors can be very low (0.5 ppm NO_2 for example for phthalocyanine), but the counter-part can be the high sensitivity to humidity. Quartz Crystal Microbalance sensors (BAW devices) were employed during this work so that a more detailed description of the principle of these sensors will be given in Chapter 5.

MOSFET

MOSFET (Metal Oxide Semiconductor Field Effect Transistor) sensors are less widely employed, mainly only being used in the Nordic Sensor Technology electronic nose. They are based on the classical field effect transistor design: an insulator layer is sandwiched between a metal layer (the gate) and a semiconductor. The conduction between the source and the drain in the semiconductor layer is dependent on the charges at the metal/insulator interface and thus allows detection of vapours.

The metal layer employed is either platinum particles or a palladium layer. In both cases they enable molecular hydrogen, originating from vapour decomposition at the catalyst surface, to reach the metal/insulator interface. Their main disadvantages are a low selectivity and a relatively high operating temperature (100°-150°C).

1.1.3 - Data processing

The strength of an electronic nose is to combine an array of sensors with partial specificity and a recognition software capable of extracting the relevant, but often hidden, information from the response.

In the same way that there is no such thing as a sensor type suitable for all applications, there is no universally suitable pattern recognition software. It depends on the sensors employed, the experimental conditions (humidity, temperature fluctuations, etc.) and on the output of the electronic nose required. There are three main outputs from an electronic nose:

- the vapour is composed of a single gas or a simple gas mixture and the nose is required to determine nature and concentrations.
- the vapour is a complex mixture of gases (for example coffee aroma). In this case, the nature of each chemical and their concentration can not be determined but rather a binary response of whether or not the sample is of suitable quality.
- Still in the case of a complex mixture, the electronic nose can be required to form clusters of similar odour samples and to classify a new vapour in one of these clusters.

A major characteristic in pattern recognition software is whether it is supervised or not. There are **supervised techniques** which require training using a known data set as input, followed by cross-evaluation of the calibration using a second known data set. The parameters set during the training will then be employed to recognise the odour.

Unsupervised techniques discriminate between unknown odours by enhancing the differences between their associated input vectors.

Pattern recognition can be performed by a statistical method or using a neural network. A detailed classification of the different software types employed in electronic noses was written by Gardner and Bartlett [1]. Among the most often encountered are Principal Component Analysis (PCA), Cluster Analysis (CA) and Back-propagation neural networks.

The evaluation of pattern recognition algorithms is done by comparison of qualitative criteria (like speed and ease of training, memory requirements, etc) and the classification accuracy [14]. In the literature, several comparative studies of artificial intelligences have been reported. Shaffer [14] compared seven types of software in detecting warfare agents. In the food area, Gardner treated the response of twelve SnO_2 sensors to some alcohols and beverages with PCA, CA and a neural network [15,16]. As a general conclusion the back-propagation artificial neural network was found to be suitable in most cases, with the limitation that the technique is complex to implement. PCA and CA are also very often employed in electronic nose technology as these methods are simple. The best algorithm remains application specific, defined by trial and error. More information on neural networks can be found elsewhere [17].

1.1.4 - Applications of Electronic Noses

Everywhere where the health or the sense of smell of the customer is involved there is potential use of an electronic nose. Table 1. 2 gives a good overview of the applications, but is not exhaustive. Numerous studies and applications related to the food domain can be found in reference [6].

The numbered electronic noses commercially available is constantly increasing. There are differences in the sampling systems, the pattern recognition and in the sensor array. On the world wide web (www.nose.uia.ac.be) and in references [1,19], a list of the commercial equipment available can be found. Well known in this field are Alpha MOS (France), known for one of the first electronic nose produced, nowadays employing metal oxide, conducting polymer or QCM sensors, MoTech (Germany) employing QCM and metal oxide sensing technology, Nordic Sensor Technologie (Sweden), working with MOSFET

and metal oxide sensors or companies like Neotronics (UK), Cyrano Sciences (USA) or Bloodhound Sensors (UK).

Field of application	Example
Automotive	Engine control, air quality in cabin
Aerospace	Air quality control [18]
Agriculture	Fertiliser and pesticide control, pollutants emissions
Chemical Analysis	Laboratory testing of materials
Safety	Fire warning in mines, buildings
Process Control	Production of foodstuff
Environmental Monitoring	Detection of pollutants in air, water and soil
Medicine	Diagnostic
Military / Customs	Illegal and dangerous substances [14]
Quality Control	Smell and flavour of foodstuff

Table 1. 2: examples of the various fields of application of an electronic nose.

Because a single array and a single pattern recognition software are not available for all applications, the trend at the present is to have available for the customer a wide variety of sensors (strategy of Alpha MOS) and/or artificial intelligences (Cyrano) among which will be selected the most appropriate according to the needs of the user.

A new subject of research is the equivalent of the electronic nose in liquid media: **the electronic tongue**. A review on taste sensors and electronic tongues can be found in reference [20]. Based on the same principle, it can be used as a complement to an electronic nose, when the sample presents a low headspace concentration.

1.1.5 - The "Chemical Imaging for Automotive" project

The work presented in this thesis was part of the multidisciplinary project "Electronic Chemical Imaging for Automotives" (CIA), supported by two car manufactures related companies, Centro Ricerche Fiat (Italy) and Mannesman VDO AG (Germany). With increasing concern with health and environment, they aimed at developing an electronic nose for automotive applications. The first application was to protect the passengers of the

vehicle from outside pollution by closing the vents in case of high toxicity. The second application was to modify this electronic nose to measure pollutants directly at the exhaust.

The CIA project consists in the development of an application specific electronic nose designed to ensure maximum efficiency in the detection of the target gases (CO, NO_2, hydrocarbons, etc.) and fulfil the requirements of a miniature device (the size of a cigarette package). A fairly novel approach was here to combine different sensing technologies in one array to minimise cross-sensitivity of the sensors. So in addition to electronic engineers and artificial intelligence specialists, the project gathered together the leading gas sensing technologies: metal oxide, conducting polymer, MOSFET and QCM sensors. The multidisciplinary aspect of this project will not be investigated here. This thesis rather focuses on the production and the improvement of conducting polymer gas sensors, which were provided to the partners for laboratory and road tests.

1.2 - Conducting Polymers

1.2.1 - Introduction to conducting polymers

Conducting polymers are organic, polymeric forms of acetylene, aromatic compounds (pyrrole, thiophene, aniline) etc. These materials have been known for decades under the name of „polymer black", due to their dark colour. It is only since 1970 that they have been known to be conducting materials, when poly(acetylene) was produced in a conducting form by "mistake" [21]. First produced chemically, it was reported in 1973 by Diaz that conducting polymers could also be produced by electropolymerisation and could thus be obtained directly in the doped conductive state. Several popular articles are related to conducting polymers [21,22] and more information on the historic aspects of these materials can be found in the introduction of the majority of papers related to this subject.

A wide range of **conductivities** has been reported for these materials. For poly(acetylene) alone, the conductivity can vary from 10^{-8} S Ω^{-1} (insulating) to a conductivity of 10^{5} S Ω^{-1} [21,23], close to the conductivity of copper. According to Bidan [23], the conductivity of poly(aniline) can vary between 10^{-13} to 1 S Ω^{-1} and for poly(pyrrole) from 10^{-10} to 10^{2}

S Ω^{-1}. This reference also gathers together, for comparison, the conductivity of a wide range of materials from polystyrene to copper.

Conduction in conducting polymers is believed to occur via the delocalisation of π electrons on the polymer backbone. For this, the polymer should present a conjugated system as well as some charges to enable the charge movement itself. As a general rule, a polymer in a conductive state will have a charge which will be compensated by incorporation of ions (also called dopants) in the coating. With increasing charge density on the polymer backbone, the holes (also called polarons) have the tendency to associate to form bipolarons (two holes) to increase their stability [24].

This can be considered as a brief description of the conduction along the polymer chain. The inter-chain conduction is known to occur via electron hopping [25,26]. The conduction of conducting polymers has been discussed in more detail elsewhere [24].

The wide range of achievable conductivities is easily explained by the tuneable doping level, the tuneable charge mobility (temperature, nature of dopant, etc.) or physical treatment like stretching the material to enhance the 1D conductivity of the polymer [21].

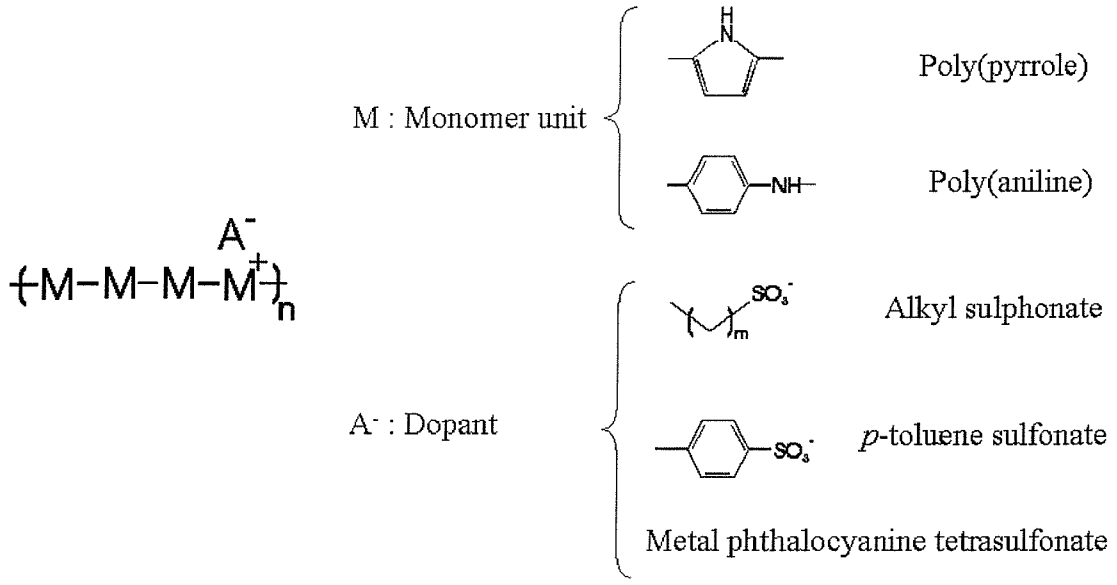

Figure 1. 4: chemical nature of a conducting polymer, as well as the monomers and anions employed in the work presented here.

The **dopant** in conducting polymers can be inorganic (halides and ClO_4^- are often encountered), organic (like *p*-toluene sulfonate or metal phthalocyanines) or even polymeric materials [25]. Figure 1. 4 shows the monomers (aniline and pyrrole) and the

anions (alkyl sulfonate, *p*-toluene sulfonate and metal phthalocyanine tetrasulfonate) used during this study with a simplified formula for a conducting polymer.

Due to their polymeric forms, conducting polymers are insoluble in most of the solvents, so that during the oxidation of the monomer at an electrode (electropolymerisation) the polymer is deposited as a film. Under appropriate conditions they can strongly adhere onto the electrode giving a modified electrode. The full electrodeposition mechanism is not going to be detailed here as it has been described largely in the literature and was found to vary largely with the polymerisation conditions (monomer, electrode material, pH or anion) [6,27]. A simplified view is the production of the radical cations by oxidation of the monomer, which go into solution and react with monomers or oxidised species to form dimers, and then oligomers which themselves undergo further oxidation [28]. After a certain length, the oligomers become insoluble and precipitate at the electrode forming a film.

The electrochemistry of these materials is also well documented in the literature [29,30]. The electrochemical phenomena have been investigated using a wide range of techniques, from the QCM [31-34] to follow ion and solvent molecules in and out of the film to STM [35] to follow the swelling of the film during the redox switching.

The **morphologies** encountered for conducting polymers are broad, depending on the polymer and on the polymerisation. Poly(pyrrole) films are known to have a "cauliflower" structure whereas poly(aniline) can be found as fibrous or homogenous material [36,37]. A general trend is a high porosity, enabling tuneable transport properties and permeability [38].

1.2.2 - Properties and applications

Due to their chemical and physical complexity, conducting polymers are hard to characterise. Their **properties can vary largely with the polymerisation conditions** (chemically or electrochemically, the solvent, the concentrations, the anion [37,39,40], the electrode material [41], the doping level [40], the thickness [38] or any particular treatment [42]). The diversity of materials available make it an advantage for applications, giving the possibility to tune the polymer for a given purpose. Since their discovery, they have been employed for a wide range of applications [23,36,43-45]. In most of the applications, the reversible switching of conducting polymers between their different

oxidation states is exploited. Indeed, these states correspond to different conductivities, colours, densities, chemical nature, etc. making them suitable for all kinds of devices.

Due to the important electron delocalisation, along the polymer backbone, conducting polymers can be obtained with different colours. For example, poly(aniline) is found with three colours. Figure 1. 5 shows the chemical formula of this material, as well as the corresponding cyclic voltammogram. On the plot, two peaks can be seen, corresponding to the two transitions between the three states: from left to right the fully reduced, the semi-oxidised (the only conducting state) and the fully-oxidised states. The corresponding colours of the polymer are also indicated on the diagram. These **electrochromism** properties (a change of colour with the oxidation state) make conducting polymers candidates to electrochromic windows and displays [45].

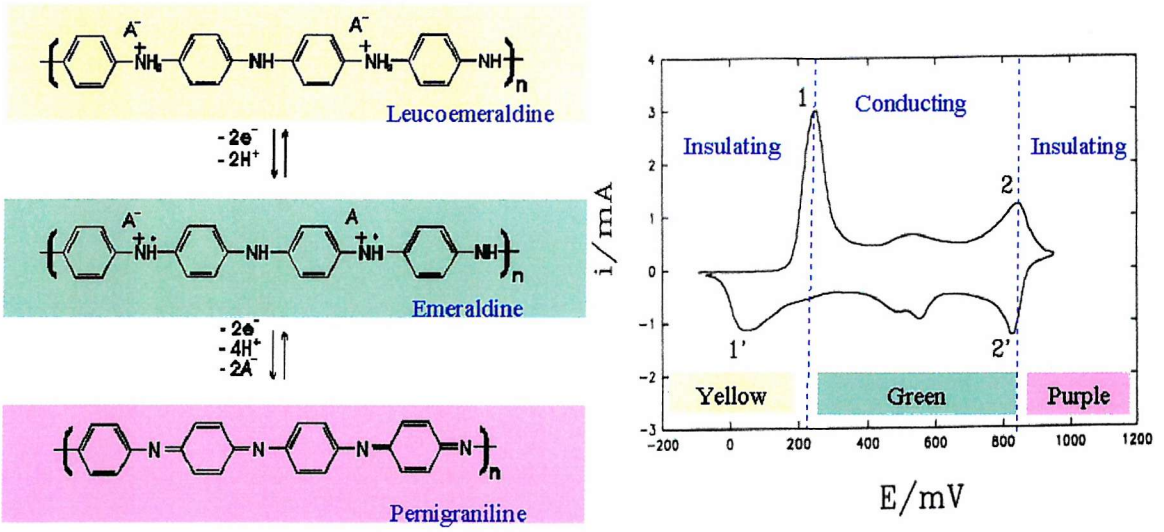

Figure 1. 5 : chemical structure of poly(aniline) as a function of the oxidation state and the cyclic voltammogram showing the two transitions between the three different degrees of oxidation and the corresponding colours.

From the chemical structure of poly(aniline) given in Figure 1. 5, it can be seen that in certain forms only, anions are present in the polymer. This implies that the film is capable of storing and releasing anions according to changes in the potential, which makes it attractive for charge storage, in batteries for example [45].

Upon switching to a form containing a dopant, some structural changes (expansion) are required to accommodate the additional component. In other words, the switching between oxidised and reduced states is accompanied by changes in volume and density which can

be exploited in **actuators**. Thus a conducting polymer membrane can behave like an artificial muscle, whether contracted or relaxed depending on the voltage [46,47].

Conducting polymer are also widely used as a **matrix for immobilisation** of molecules or particles. Moieties can be introduced into the film during electropolymerisation as an anion, as a substituent of the monomer unit, from the solution [48] or after polymerisation by a specific treatment [49].
For example, during electropolymerisation bio-molecules as large as enzymes can be incorporated in a polymer [48] and can lead to biosensors. Metal particles can also be immobilised to create a polymer layer protective against corrosion or for catalytic purposes [49]. Anionic dyes incorporated in a film will complex certain ions like copper ions and will form ionic sensors with optical detection [50]. A review of the applications of conducting polymers as sensors can be found in reference [23].
The use of conducting polymer materials as gas sensors will now be discussed. Due to their high and controllable porosity utilised in gas sensing, conducting polymers are also employed as separation membranes in gaseous [42] and liquid phases [51,52].

1.2.3 - Conducting polymers as gas sensors

As underlined previously, these materials present a wide range of interesting properties, some of which can be modified upon exposure to a vapour, enabling different transducing techniques. They have been employed as **coatings for sensors** with optical (U.V.) detection [53], for QCM [54], as a sensitive layer in Field Effect Transistors [53], Kelvin probe [53] and as chemoresistors [55-57].

The most commonly used technique to detect vapours, mainly due to its ease in setting up, is to monitor the resistance of a conducting polymer film upon exposure to vapours. The vapour acts on the charge delocalisation within the polymer and/or swells the polymer and thus affects the inter-molecular conductivity.

Many studies on the possible detection of a single gas or vapour have already been performed. Conducting polymers, mainly poly(pyrrole), have been reported to respond to a wide range of organic vapours: alcohols [57-59], toluene [54,60] and others [57,58]. Nagase [56] reported the detection of down to 10 ppm methanol with poly(pyrrole) doped with various inorganic anions. Conducting polymers were also found to respond to NO_2,

SO_2, H_2S, ammonia and water [61-63]. On the other hand, they show no response to H_2, CH_4, N_2 or CO [62,63].

The response of conducting polymers to beverages like beer, whisky or coffee has also been investigated for potential application in electronic nose technology [59,64]. The tests were successful as the vapours to sense are composed of a range organic vapours that conducting polymers can detect.

Whereas the results of complex mixtures are limited to applications, many authors exploited the response to individual vapours to investigate the sensing mechanism of conducting polymers [53,54,59,61,65].

In most cases the response to the vapour is reversible. Poor reversibility was however observed for highly electrophilic vapours like NO_2. The sensing mechanism of conducting polymers will be discussed in detail in Chapter 7.

The **advantages of conducting polymer gas sensors**, in addition to vapour detection and their simple design are:

- operated at room temperature, they require a low power consumption which is compulsory for portable equipment and miniaturisation of the electronic nose.
- their broad sensitivity. As an array, coupled with a pattern recognition system, they are suitable for discriminating between complex odours like coffees, beers, perfumes, etc.
- a wide range of materials are available. The main modulations in the sensing properties are introduced by the monomer, substituted or not, and from the anions incorporated in the film. The polymerisation method employed was also found to influence the response to vapour.
- they can be electrodeposited directly onto the sensor substrate by a single step experiment.

In addition, the deposition area is well defined as seen in the photograph in Figure 1. 6 and the amount of polymer deposited is controlled. By controlling the final potential of the polymer it is possible to tune the sensing properties. Sensors can also be produced in a chemical manner by spray, spin coating or patterning by oxidant. The last method has qualities similar to the electrodeposition, but the chemical reaction time required for the production of the sensors remains long (at least 2 hours) [60].

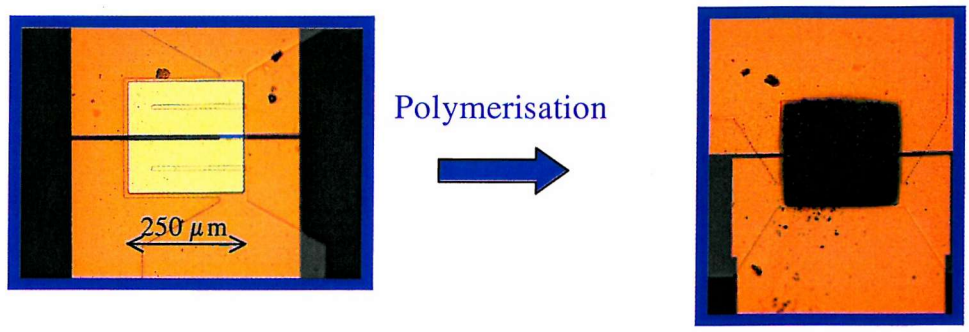

Figure 1. 6 : photograph of a device of 250 µm by 250 µm showing the good definition in the polymer deposition using the electrochemical method.

Conducting polymer gas sensors have been studied for a decade and are largely employed in electronic nose technology. Independent of their success, they still require further investigation imposed by competitive technologies and the non-stop miniaturisation of such devices.

Regarding the coating, several points should be addressed: the reproducibility, the response time, the long time stability and the further diversification of the materials. Regarding industrial applications, it is required to further reduce costs and size. Some of these points were addressed in this work and will be presented in this thesis.

(1) Gardner, J. W.; Bartlett, P. N. *Electronic noses- principles and applications*; Oxford Science Publications: New York, 1999.

(2) Pearce, T. C., *Biosystems*, 1997, **41**, 43-67.

(3) Pearce, T. C., *Biosystems*, 1997, **41**, 69-90.

(4) Craven, M. A.; Gardner, J. W.; Bartlett, P. N., *Trends in analytical chemistry*, 1996, **15**, 486-493.

(5) Wünsche, L. F.; Vuilleumier, C.; Keller, U.; Byfield, M. P.; May, I. P.; Kearney, M. J., *Flavours, Fragrances and Essentials Oils*, 1995, **3**, 295-313.

(6) Elliott, J. M., Conducting Polymer Odour Sensors, PhD thesis, SOUTHAMPTON, 1997.

(7) Moseley, P. T., *Meas. Sci. Technol.*, 1997, **8**, 223-237.

(8) Janata, J.; Josowicz, M.; Vanysek, P.; DeVaney, D. M., *Anal. Chem.*, 1998, **70**, 179R-208R.

(9) Collins, P. G.; Bradley, K.; Ishigami, M.; Zettl, A., *Science*, 2000, **287**, 1801-1804.

(10) Ricco, A. J.; Crooks, R. M.; Janata, J., *Interface*, 1998, **7**, 18-24.

(11) Gopel, W., *Sensors and Actuators*, 1995, **B 24-25**, 17-32.

(12) Schierbaum, K. D.; Hierlemann, A.; Gopel, W., *Sensors and Actuactors B*, 1994, **18-19**, 448-452.

(13) Barker, P. S.; Chen, J. R.; Agbor, N. E.; Monkman, A. P.; Mars, P.; Petty, M. C., *Sensors and Actuators*, 1994, **B 17**, 143-147.

(14) Shaffer, R. E.; Rose-Pehrsson, S. L.; McGill, R. A., *Analytica Chimica Acta*, 1999, **384**, 305-317.

(15) Gardner, J. W.; Hines, E. L.; Tang, H. C., *Sensors and Actuators*, 1992, **B 9**, 9-15.

(16) Gardner, J. W., *Sensors and Actuators*, 1991, **B 4**, 109-115.

(17) Bos, M.; Bos, A.; Linden, W. E. v. d., *Analyst*, 1993, **118**, 323-328.

(18) Persaud, K. C.; Pisanelli, A. M.; Szyszko, S.; Reichl, M.; Horner, G.; Rakow, W.; Keding, H. J.; Wessels, H., *Sensors and Actuators*, 1999, **B 55**, 118-126.

(19) Talou, T.; Dubreuil, B. ISOEN, Tübingen Germany, 1999; p 38-41.

(20) Toko, K., *Meas. Sci. Technol.*, 1998, **9**, 1919-1936.

(21) Kaner, R. B.; MacDiarmid, A. G., *Scientific American*, 1988, **258**, 60-65.

(22) Alper, J., *Science*, 1989, **246**, 208-210.

(23) Bidan, G., *Sensors and Actuators*, 1992, **B 6**, 45-56.

(24) Conwell, E. M.; Mizes, H. A. *Basic properties of semi-conductors*; North-Holland, 1992.

(25) Wegner, G.; Ruhe, J., *Faraday Discuss. Chem. Soc.*, 1989, **88**, 333-349.

(26) Montemajyor, M. C.; Jimenez, R.; Fatas, E., *J. Electroanal. Chem.*, 1993, **361**, 115-119.

(27) Genies, E. M.; Lapkowski, M.; Tsintavis, C., *New J, Chem.*, 1988, **12**, 181-196.

(28) Audebert, P.; Catel, J. M.; Coutumer, G. L.; Duchenet, V.; Hapiot, P., *J. Phys. Chem.*, 1995, **99**, 11923-11929.

(29) Heinze, J., *Synthetic Metals*, 1991, **41-43**, 2805-2823.

(30) MacDiarmid, A. G.; Zheng, W., *MRS Bulletin*, 1997, **22/6**, 24-30.

(31) Bruckenstein, S.; Hillman, A. R., *J. Phys.Chem.*, 1991, **95**, 10748-10752.

(32) Miras, M. C.; Barbero, C.; Kotz, R.; Haas, O., *J. Electroanal. Chem.*, 1994, **369**, 193-197.

(33) Tjarnhage, T.; Sharp, M., *Electrochim. Acta*, 1994, **39**, 623-628.

(34) Xie, Q.; Kuwabata, S.; Yoneyama, H., *J. Electroanal. Chem.*, 1997, **420**, 219-225.

(35) Nyffenegger, R.; Ammann, E.; Siegenthaler, H.; Kötz, R.; Haas, O., *Electrochim. Acta*, 1995, **40**, 1411-1415.

(36) Gardner, J. W.; Bartlett, P. N., *Sensors and Actuators*, 1995, **A 51**, 57-66.

(37) Desilvestro, J.; Scheifele, W., *J. Mater. Chem.*, 1993, **3**, 263-272.

(38) Wang, J.; Chen, S.; Lin, M. S., *J. Electroanal. Chem.*, 1989, **273**, 231-242.

(39) Warren, L. F.; Walker, J. A.; Anderson, D. P.; Rhodes, C. G.; Buckley, L. J., *J. electrochem. Soc.*, 1989, **136**, 2286-2295.

(40) Volfkovich, Y. M.; Bagotzky, V. S.; Zolotova, T. K.; Pisarevskaya, E. Y., *Electrochim. Acta*, 1996, **41**, 1905-1912.

(41) Bade, K.; Tsakova, V.; Schultze, J. W., *Electrochim. Acta*, 1992, **37**, 2255-2261.

(42) Anderson, M. R.; Mattes, B. R.; Reiss, H.; Kaner, R. B., *Science*, 1991, **252**, 1412-1415.

(43) Teasdale, P. R.; Wallace, G. G., *Analyst*, 1993, **118**, 329-334.

(44) Imisides, M. D.; John, R.; Riley, P. J.; Wallace, G. G., *Electroanalysis*, 1991, **3**, 879-889.

(45) Baughman, R. H., *Makromol. Chem., Macromol. Symp.*, 1991, **51**, 193-215.

(46) Baughman, R. H., *Synthetic metals*, 1996, **78**, 339-353.

(47) Otero, T. F.; Sansinane, J. M., *Bioelectrochem. Bioenerg.*, 1995, **38**, 411-414.

(48) Bartlett, P. N.; Cooper, J. M., *J. Electroanal. Chem.*, 1993, **362**, 1-12.

(49) Malik, M. A.; Galkowski, M. T.; Bala, H.; Grzybowska, B.; Kulesza, P. J., *Electrochim. Acta*, 1999, **44**, 2157-2163.

(50) Barisci, J. N.; Conn, C.; Wallace, G. G., *Trends in Polymer Science*, 1996, **4**, 307-311.

(51) Cosnier, S.; Deronzier, A.; Roland, J. F., *J. Electroanal. Chem.*, 1991, **310**, 71-87.

(52) Gros, P.; Gibson, T.; Bergel, A.; Comtat, M., *J. Electroanal. Chem.*, 1997, **437**, 125-134.

(53) Topart, P.; Josowicz, M., *J. Phys. Chem.*, 1992, **96**, 7824-7830.

(54) Vigmond, S. J.; Kallury, K. M. R.; Ghaemmaghami, V.; Thompson, M., *Talanta*, 1992, **39**, 449-456.

(55) Slater, J. M.; Watt, E. J.; Freeman, N. J.; May, I. P.; Weir, D. J., *Analyst*, 1992, **117**, 1265-1270.

(56) Nagase, H.; Wakabayashi, K.; Imanaka, T., *Sensors and Actuators*, 1993, **B 13/14**, 596-597.

(57) Charlesworth, J. M.; Partridge, A. C.; Garrard, N., *J. Chem. Phys.*, 1993, **97**, 5418-5423.

(58) Bartlett, P. N.; Ling-Chung, S. K., *Sensors and Actuators*, 1989, **20**, 287-292.

(59) Slater, J. M.; Paynter, J.; Watt, E. J., *Analyst*, 1993, **118**, 379-384.

(60) Stussi, E.; Stella, R.; Rossi, D. D., *Sensors and Actuators B*, 1997, **43**, 180-185.

(61) Ingleby, P.; Gardner, J. W., *Sensors and Actuators*, 1999, **B 57**, 17-27.

(62) Agbor, N. E.; Petty, M. C.; Monkman, A. P., *Sensors and Actuators*, 1995, **B 28**, 173-179.

(63) Miasik, J. J.; Hooper, A.; Tofield, B. C., *J. Chem. Soc., Faraday Trans. I*, 1986, **82**, 1117-1126.

(64) Pearce, T. C.; Gardner, J. W.; Friel, S.; Bartlett, P. N.; Blair, N., *Analyst*, 1993, **118**, 371-377.

(65) Topart, P.; Josowicz, M., *J. Phys. Chem.*, 1992, **96**, 8662-8666.

Chapter 2 - Experimental

This experimental chapter deals with the description of the equipment used during this work: the chemicals, electrochemical cells and electrodes, quartz crystal microbalance equipment. Additionally this chapter presents special equipment adapted for the production of arrays of conducting polymer sensors. It describes the micro-deposition apparatus, equipment designed to perform electrochemistry onto array devices (devices of small size). It also describes two major pieces of equipment constructed in the course of this work: a bipotentiostat designed to monitor *in-situ* the resistance of the polymer film during its deposition and a mass flow system designed to test the gas sensors produced.

2.1 - General

2.1.1 - Chemicals

All solutions used for electropolymerisation were prepared from de-ionised water from a Whatman RO50 purification system. The aniline was purchased from Aldrich (99,5%) and the pyrrole from Fluka (97%). They were purified by filtering through an alumina (BDH) column packed in a pasteur pipette in order to remove oligomers.

The alkyl sulfonic acid sodium salts were purchased from BDH 98% and were used as received. The copper and nickel phthalocyanine tetrasulfonic acid tetrasodium salts and the *p*-toluene sulfonic acid sodium salt were obtained from Aldrich and used without any further purification.

For the gas test experiments, the carrier gas was zero grade air (BOC, UK). The vapour was generated from ethanol (99,86%- Southampton University) and the water vapour from de-ionised water (Whatman RO50 purification system).

2.1.2 - Electrochemical cell

A standard three-electrode system was used to perform electrochemistry. As reference electrode, a home-made Saturated Calomel Electrode (SCE) was used. All the potentials quoted in this work are quoted against the SCE. The potential of the reference was regularly checked against a commercial SCE (Cole-Parmer, U.S.) and was found to be stable over months. The counter electrode was a platinum gauze, cleaned by heating to red heat in a flame before use. For the micro-deposition, the counter electrode was a gold wire (250 μm diameter), cleaned by cycling in sulfuric acid prior to use. The electrochemical cleaning procedure is detailed in Chapter 3.

Various designs of working electrodes were used. In all cases the electrode material was either gold or platinum. **Disc electrodes** were used to check the purity of solutions, to check the electropolymerisation rate and to investigate new polymers. They were either 1 mm diameter gold (1 mm diameter gold rod 99.9%- Aldrich) sealed in epoxy (Struers Ltd) or 0.5 mm diameter platinum obtained by sealing a platinum rod into glass. Prior to use these electrodes were polished using 1 μm alumina powder (Buehler, U.K.) on a polishing cloth (microcloth, Buehler, U.K.). Another design of working electrode was used to produce chemoresistor gas sensors referred to as **dual micro-gap electrodes**. They are described in detail in Chapter 3. They were square gold or platinum devices with an insulating gap (10 μm wide) and were produced using photolithography (IMT, Neuchatel, Switzerland). In contrast to the disc electrodes, these devices were not reusable.

Three types of cells were used during this work. Most of the experiments were performed in a two-compartment cell fitted with a luggin capillary and thermostated- see Figure 2. 1. For electrodeposition onto gold coated quartz crystals, an Electrochemical Quartz Microbalance cell was used and is described elsewhere [1]. In the case of electrochemistry onto array devices, the cell was limited to a drop of solution (see below).

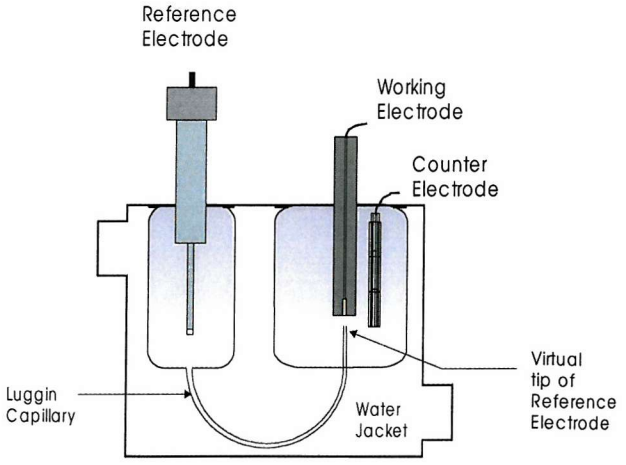

Figure 2. 1: diagram of the electrochemical cell used (except for electrochemistry performed onto quartz crystals and array devices). It comprises two compartments and a luggin capillary. This geometry allows the virtual tip of the reference to be positioned close to the working electrode. The cell is fitted with a water jacket for thermostated experiments.

2.1.3 - Other equipment

Scanning Electron Microscopy was performed on a Jeol 2010 scanning electron microscope.

Resistance of polymers was measured using a battery powered multimeter (Fluke, model 83, U.K.).

2.2 - Quartz crystal microbalance equipment

A quartz crystal microbalance (QCM) was used to investigate the sensing properties of the conducting polymers in parallel with the chemoresistors. AT-cut 10 MHz crystals were employed (International Crystal Manufacturing Company Inc., USA) with the following properties:

Active area (gold disc of 5 mm diameter) = 0.196 cm^2

Diameter of the crystal = 1.4 cm

Thickness of the crystal = 0.0168 cm

Density of the crystal = 2.648 g cm^3

Shear modulus = $2.957.10^8$ N cm^{-2}

Surface finish: un-polished

Electropolymerisation onto the crystals was performed using a cell designed for EQCM

experiments [1]. In this design, only one face of the crystal was exposed to the electrochemical solution and an O-ring was used to seal the crystal in the electrochemical cell. The change in resonant frequency of the crystal was not monitored during the electropolymerisation. More details on the production of the polymer coated quartz crystals will be given in Chapter 5.

During gas test experiments, the response of one quartz crystal microbalance could be interrogated in addition to nine chemoresistors. A HP 4192A Impedance Analyser was used to monitor the real and imaginary parts of the admittance of the crystal. Data acquisition software was written using Quick BASIC 4.5. Data were fitted to the BVD (Butterworth-van Dyke) equivalent circuit using software written in Mathematica 2.2.

2.3 - The micro-deposition apparatus

For the purpose of application of conducting polymer gas sensors in electronic nose technology, array devices of small size were produced. Up to six different polymers could be produced on an array of overall size of about 1 cm by 2 cm. The electrodes in this design were only 2 mm apart from each other.

This design does not allow the substrate to be dipped into the growth solution, and contamination of the neighbouring polymers by the growth solution had to be minimised. Precision equipment was used to perform electrochemistry onto these array devices. A **micro-deposition technique** [2] was employed where the electrochemical cell was reduced to a single drop of solution. Figure 2. 2 shows a diagram of the experimental arrangement. This technique was used with the SRL131 and PtCIA substrates (refer to Chapter 3 for a description of these array devices).

The array (working electrode) was held in a horizontal position with a glass tube, ending with a frit, containing an aqueous solution of electrolyte and the reference electrode (SCE) held perpendicular to the array. This salt bridge prevented chloride ions from the SCE from diffusing into the droplet of the electrochemical cell. Around the tube was a gold wire counter electrode (250 μm diameter) which ended in a spiral at the bottom.

The whole system was set up so that a drop of the growth solution (30 to 50 μl- the electrochemical cell) could be positioned between the desired working electrode and the end of the glass tube. The adjustment was performed using a micro-controller x,y,z stage (Micro-controlle, France). To minimise movement of the apparatus, a Newport anti-

vibration bread board was used as an assembly platform. Prior to electrochemical experiments, the tip of the reference electrode was washed with the electrolyte solution to avoid dilution of the drop by rinsing water. The positioning of the electrodes and the electropolymerisation were followed by optical observation (microscope Meji Techno).
This arrangement allowed four or six different polymers to be deposited onto arrays of small size. Such precision apparatus was required by the small size of the substrates.

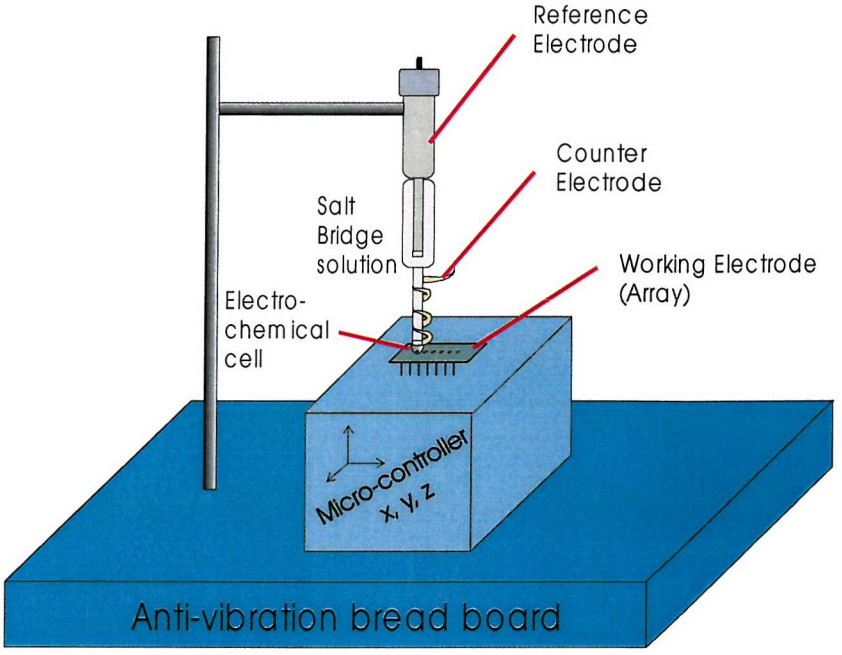

Figure 2. 2: diagram of the micro-deposition apparatus used to perform electrochemistry onto array devices, showing a three-electrode electrochemical cell limited to one drop of solution. The microscope used to position the electrodes and to follow the electropolymerisation is not shown.

2.4 - Potentiostat for electrochemistry

At the beginning of this work, a home-made potentiostat was used to perform electrochemistry and data were recorded using a chart recorder (Bryans Instruments, UK). For the electrodeposition onto chemoresistors, both electrodes of the dual microband were considered as identical and were connected together. Polymerisation was performed by potential step until a sufficient amount of polymer had been deposited. This technique is referred to as "classical", to distinguish it from the following technique used for ***in-situ* resistance measurement**.

A problem occurring during the electrodeposition of conducting polymers, and often ignored, is the lack of reproducibility of the polymerisation due to intrinsic properties of the polymerisation process. As reported in Chapter 4, this problem became significant during this work on small size electrodes, leading to sensors of irreproducible resistance. To overcome this lack of reproducibility, a bipotentiostat was set-up to monitor the resistance of the polymer film during polymerisation.

A bipotentiostat was designed for the *in-situ* measurement of the resistance. Using this bipotentiostat, both electrodes of the dual micro-gap device were controlled independently. The apparatus had the capability:

- to perform electropolymerisation, with both electrodes at the same potential
- to measure the resistance of the film over the insulating gap while no polymerisation was taking place. To do this a small potential difference was applied between the two electrodes of the device and the current flowing between them was measured.

The electropolymerisation conditions as well as the results of this technique will be described in Chapter 4.

A typical polymerisation time used in this work is two minutes. For a maximum efficiency the resistance measurement system was automated. The bipotentiostat was interfaced with a computer. A data acquisition card (CIO-DAS6402/12, Computer Boards, USA) was purchased with a Universal Library Labview extension, so that the programming could be done using Labview (National Instruments Inc., USA) with an interface card of reduced cost. The Labview program controlled the potentiostat: potential step, *in-situ* resistance measurement and the setting of the current gains. It also enabled the measurement and recording of the exact voltages applied and the various currents flowing. The software was used to plot the transients for electropolymerisation for the two channels as well as the device resistance. Finally the software calculated the charge passed during the electropolymerisation for each channel.

2.5 - The mass flow system

No mass flow system was available to test, on a day to day basis, the response to vapours of the polymer sensors produced. Therefore a major task was to design and build a mass flow system. This dynamic sampling system was designed to test vapours generated from solutions. The aim was to be able to test one vapour at different concentrations and at various humidities, under temperature control.

For applications of the chemoresistor sensors in air quality monitoring (CIA project), some tests of response to CO and NO_2 were performed. These tests took place at the University of Warwick, where a test rig for these gases was available. The mass flow system used is not detailed here but was of similar design. The gas was, in this case, generated directly from a gas cylinder.

2.5.1 - The gas delivery system

The **mass flow system** was composed of three lines:

- one line to control the humidity, where the carrier gas was bubbled through de-ionised water
- one line where the vapour was generated by bubbling the carrier gas through the appropriate solvent
- one line of dry carrier gas which allowed a total constant flow rate to be maintained.

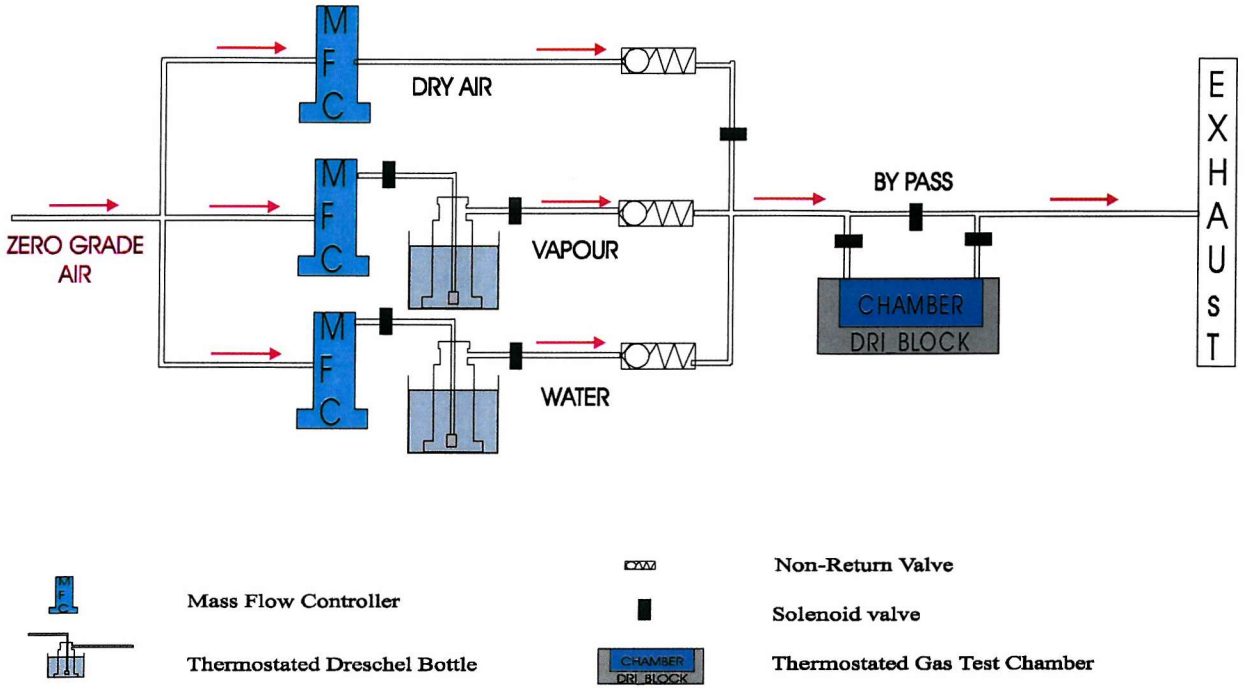

Figure 2. 3: diagram of the mass flow system designed to test one vapour for a range of concentrations and humidities, at a controlled temperature.

Both the Dreschel bottles (containing the solvent and the water) and the sensor chamber were thermostated at 26 ± 0.3 °C, using respectively a water bath (Grant) and a dri-block heater (Techne). During the design, care was taken to avoid leaks, avoid contamination,

minimise dead volumes and to obtain reproducible vapour generation. Figure 2. 3 shows a diagram of the dynamic sampling system.

Three mass flow controllers were purchased from Unit Instruments Ltd (UFC-1100), calibrated with air at a maximum flow rate of 200 cm^3 min^{-1} with a precision of ±1% full scale. They were controlled manually by a read-out box (URS-100 from Unit Instruments Ltd). The URS-100 can control up to five mass flow controllers, either manually or by computer control. A switch (automatic shutdown) was added for each controller to be able to turn off (and on) the flow for each line, without setting the flow rate to zero.

The path of the gas was controlled by solenoid valves (open or closed) (Radio Spares, UK), shown as a solid block in Figure 2. 3. Each vapour generation zone was isolated at both ends to avoid any contamination to the other lines. A by-pass was designed to enable the system to be purged without exposing the sensors to the flow. These valves were controlled manually by home-made electronics. The tubing was ¼'' nylon (Phase Separation Ltd, UK).

It was assumed that the gases were properly mixed, without requiring mixing valves. A later improvement was to add, for each line, a non-return valve (Radio Spare, UK)- symbolised as a ball at the end of a spring in Figure 2. 3.

The **sensor chamber** was designed and provided by the Engineering Department of the University of Warwick. It was carefully designed to minimise dead volumes and contamination. A heat-exchanger was incorporated in the gas inlet to control the temperature of the gas, so that the temperature of the gas equilibrated with the temperature of the chamber before reaching the sensors. The sensor chamber could contain 12 discrete devices and an array of four or six sensors. For the QCM experiments, the quartz crystal replaced one of the discrete devices. Figure 2. 4 shows a diagram of the chamber.

The chamber was composed of three main parts

- the bottom part, with the track of the heat exchanging system
- the middle part, where the dead space for the sensor exposure has been machined out
- the top part with the sensor mounting head

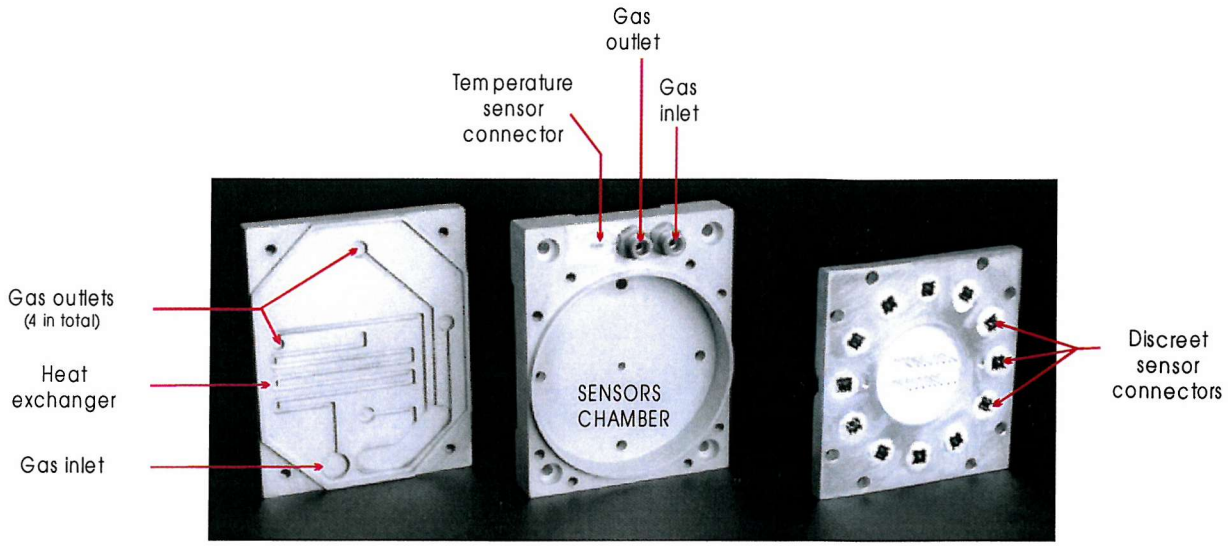

Figure 2. 4: photo of the chamber showing from left to right the heat exchanger block, the sensor chamber (dead space) and the block containing the sensor mounting head for up to 12 discrete devices.

The chamber was made of aluminium coated with a layer of PTFE to minimise contamination. The dead volume of the chamber was less than 38 cm^3. The heat exchange channel was design so that the temperature of gas, flowing at rate up to 500 cm^3 min^{-1}, could equilibrate before reaching the sensors. In the experiments presented here the flow rate was well below this value: 200 cm^3 min^{-1} (identical for all experiments). The heat exchanger had a length of 264 mm and a cross-section of 4 mm^2. The gas inlet was located in the middle of the chamber and the outlet was composed of four holes located in the outside of the chamber to produce a reliable flow across the sensors.

2.5.2 - Vapour generation

Vapour and humidity were generated by bubbling the carrier gas through thermostated Dreschel bottles containing respectively the appropriate solvent and de-ionised water. The inlet of the gas was dipped into the solution and ended with a glass frit, producing a stream of fine bubbles. It was assumed that the bubbles produced were small enough and the flow rate low enough to ensure that the gas was saturated in vapour.

In this work, the concentrations were first expressed in % of the total flow rate. This represents the percentage of the flow rate of one line to the total (200 cm^3 min^{-1}). Then the concentration was expressed in ppm, calculated from the percentage of the flow rate and the vapour concentration at saturation. The vapour concentration at saturation was determined using the **Antoine equation** (1) [3], giving the vapour pressure of a solvent in

equilibrium with its vapour. This assumed that there was constant equilibrium solvent/ vapour and that the gas behaved like an ideal gas.

$$\log V_p = A - \frac{B}{C+T} \qquad (1)$$

where V_p is the vapour pressure in mm Hg, A, B and C are Antoine's coefficients and T is the temperature in °C.

Vapour	A	B / °C	C / °C	Vp / atm at 26 °C	[Vapour] / ppm at saturation at 26 °C
H_2O	8	1686	229.7	0.0335	33536
EtOH	8.16	1624	229	0.0823	82344

Table 2. 1: Antoine's coefficients, vapour pressure and concentration of the saturated vapour in ppm at 26 °C for water and ethanol.

Table 2. 1 gives Antoine's coefficient for water and ethanol, as well as the vapour pressure and the vapour concentration (corresponding to the saturated vapour) at 26 °C. The coefficient for water were determined by fitting the vapour pressure data, obtained from thermodynamic tables [3] for temperatures ranging from –10 °C to 100 °C. The values for ethanol were found in the data handbook [4].

2.5.3 - The sensor output

The response of the polymer chemoresistor (variation of resistance) when exposed to the vapour was converted into a voltage. The electronics, a purpose built linear ohmmeter, was provided by the University of Warwick and can measure the response of up to twelve chemoresistors. It drives a **constant current through the polymer film** and produces an output voltage that is directly proportional to the resistance. The current applied depends on the setting of the range of the resistance of the sensor (see Table 2. 2 for numerical values), and is set manually. In any case, a maximum voltage of 100 mV is applied. A low voltage across the polymer avoids polarisation of the polymer by movement of ions in the electrical field. Using calibration, the resistance of the conducting polymer with time could be determined from the output voltage. For each range, the electronics allows adjustment of the sensor baseline (offset) as well as the response amplitude (larger sensitivity for

expected smaller response) prior to experiments. In an ideal situation, the response of the sensor would cover the full 10 V range of the ADC.

Measurement of the output voltage was performed using a data acquisition card (LPM16, National Instruments Inc., USA), and software written in Labview. The program allows the user to plot and store the voltage across the polymer chemoresistor upon exposure to vapour, as well as the time.

Resistance Range	Current across polymer*/ mA	Colour code
0 Ω - 100 Ω	1	Red
100 Ω - 1 kΩ	0.1	Orange
1 kΩ - 10 kΩ	0.01	Yellow
10 kΩ - 100 kΩ	0.001	Brown

*corresponding to a maximum of 100 mV

Table 2. 2: Current flowing through the polymer chemoresistor as a function of the resistance range setting (with 0.1% accuracy in the current applied) and the colour code for the switches for each setting.

2.5.4 - The gas testing protocol

The procedure to evaluate the response to a vapour (or a change in humidity) at a certain humidity was to let the system equilibrate at the initial humidity. Air of the initial humidity was passed through the bypass for 10 minutes to purge the gas lines, followed by 20 minutes over the sensors to let them equilibrate. The baseline resistance of the sensors was then recorded for 20 minutes before changing the gas composition.

After each experiment, air of relative humidity between 20% and 50%, free of vapour, was passed over the sensors to ensure that the sensors were conditioned in a non aggressive atmosphere.

2.5.5 - Conclusions and further improvements

A mass flow system was designed and build-up in order to test a vapour generated from a solution, for a range of concentrations and humidities, with temperature control. Throughout the design, care was taken to obtain optimum control and efficiency. The dynamic sampling system produced fulfilled the requirements and was largely used to test

chemoresistors and quartz crystals coated with conducting polymers. The mass flow system could be further improved.

One first improvement would be to automate the gas delivery. Up to now, each vapour concentration / humidity combination required intervention of the operator. The mass flow system was designed to be operated manually, but can be easily be upgraded to be computer controlled. The read-out box (URS-100) controlling the mass flow controllers and the electronics controlling the solenoid valves, though operated manually here, were designed to be computer interfaced.
Automation of the mass flow system is of interest in the case of acquisition of a large number of data. The main purpose of this work was to investigate "new" polymers, or to compare the behaviour of chemoresistors with the corresponding polymer coated quartz crystal microbalance. In this situation, the behaviour of the sensors is unknown and the experimenter should have the possibility to modify the settings according to the response of the sensors upon exposure (saturation of the response not reached, off scale electronics, recovery not reached, etc). For this work, an automated mass flow system would have been less flexible.

A second improvement would be to further reduce the length of the tubing used in order to minimise any eventual chemical adsorption and to decrease the delay between the generation of the vapour and the time it reaches the sensors.

(1) Gollas, B.; Bartlett, P. N.; Denuault, G., *Anal. Chem.*, 2000, **72**, 349-356.

(2) Bartlett, P. N.; Gardner, J. W.; Elliott, J. M.; Duke, A.; Beriet, C. ; Patent 9514754.2: Great Britain.

(3) James, A. M.; Lord, M. P. *MacMillan's chemical and physical data*; The MacMillan Press Ltd: London, 1992.

(4) Boublik, T.; Fried, V.; Hala, E. *The vapour pressures of pure substances*; Elsevier Scientific: Amsterdam, 1973.

Chapter 3 – The chemoresistor substrate
Description and improvement

Conducting polymers have largely been studied in the last decades for their wide range of properties and potential applications. One domain of application is their use as gas sensors. Upon exposure to vapours, their properties are modified, including the conductivity, optical properties and density of the coating. Among all these possible transduction methods, the simplest method was selected for this work: to monitor the resistance of the film. The substrate of such chemoresistor consists in two electrodes separated by a thin insulating gap,

the whole being coated by the polymer. The various chemoresistor substrates used, whether discrete or array devices, will be described in the first part of this chapter.

Designed for our specific application, the chemoresistor substrates were fairly complex and not commercially available. Therefore it was necessary to perform a quality check before electropolymerisation in order to detect any defects in the fabrication process. Therefore in a second section, we will show how electrochemistry of the electrode material can be use as a non-destructive screen for the quality of the device.

Electrochemistry can also be employed to follow the multiple steps of the development of a new device. Indeed the application of conducting polymers as gas sensors remains fairly recent and of limited use, so that the substrates are not widely available and research is focussing on improving them. Here the development of a new array of platinum devices will be discussed.

3.1 - Description of the devices

Conducting polymers are used as the vapour sensitive layer for chemoresistors [1-4], Quartz Crystal Microbalances [5], spectroscopic devices [6], Kelvin probe [6,7] or in Suspended Gate Field Effect Transistor structures [8]. Driven by the needs of the industry for sensors capable of monitoring gases and vapours, one first aim of this work was to produce gas sensors for application in electronic noses. This implies a transducer that is simple to produce and use. For this reason a chemoresistor structure was selected, as it requires a simple substrate structure (two electrodes separated by a thin insulating gap) and simple measurement electronics (monitoring a resistance).

Figure 3. 1 a shows the typical cross section of a device used to construct the chemoresistors. They are produced by photolithography, usually with a five-mask process on silicon [9]. A device is composed of a platinum heater[1] embedded in an insulating layer of silicon nitride.

[1] Conducting polymer gas sensors are operated at room temperature, requiring no heater. The existence of the heater is justified by the use of the same substrates for resistive metal oxide sensors which are operated at elevated temperature. The heater can also be used to control the temperature of the polymer film around room temperature or measure it.

Above are the gold (or platinum) electrodes onto which the vapour sensitive layer is electrodeposited. The tracks are insulated from the electrochemical solution by a photoresist. Quick set araldite (Radio Spares, UK) is used to isolate the wires used for bonding the photolithographically produced device onto the support (PCB or metal header).

a -

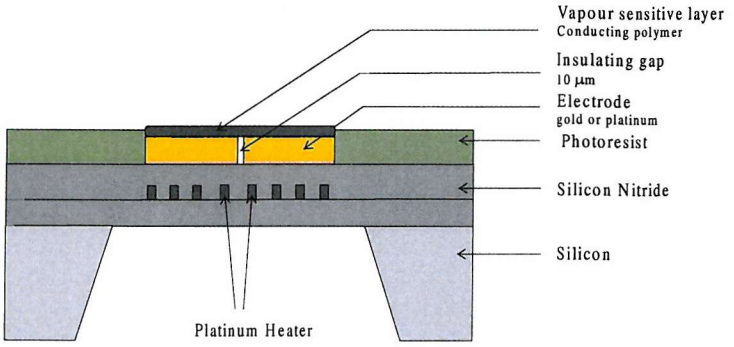

b -

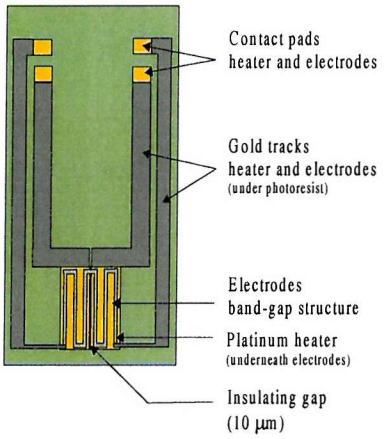

Figure 3. 1: a – Typical cross-section of a device used as substrate for chemoresistor conducting polymer gas sensor.
b - Top-view of the dual micro-gap electrode (discrete device).
These diagrams are not to scale.

The overall electrode is square, as seen in Figure 3. 1 b. The substrate is composed of two half electrodes separated by an insulating gap of 10 µm width. This design is later refereed to as **dual micro-gap** device. The polymer, when electrodeposited, first grows onto the two half-electrodes and ultimately covers the insulating gap. The resistance of the film over the insulating gap, varying upon exposure to vapours, will be monitored during gas test experiments.

Other authors have used more complex chemoresistor structures than the one presented here. Partridge [2] used an array composed of four bands instead of two. Using the technique of the four-probe conductivity measurement, he was able to eliminate the contact resistance between the electrodes and the polymer, increasing the sensitivity of the sensors to vapour. Slater [3] used a device composed of eight bands all coated with the same polymer layer. By monitoring the resistance of the film between electrodes separated by various distances, he was able to discriminate between phenomena taking place at the surface of the polymer to the ones taking place in the bulk. For the purpose of electronic nose applications, this allows discrimination between vapours using a single sensor instead of an array. These designs may consist in an improvement of the final sensors, but in our case would require redesigning the masks for the lithography process and the electronics for the signal monitoring. Thus in this work, switching to a more complex chemoresistor structure was not foreseen.

The substrates used throughout this study were not commercially available. They were designed for this application according to our requirements in collaboration with other partners of the CIA project. They were produced by photolithography at the University of Neuchatel (Switzerland) and were wire-bonded at the University of Warwick (UK).

Reference	Electrode size	Electrode material	Number of devices	Main application	Photoresist
SRL123	1 mm * 1 mm	gold	1	gas sensors for laboratory test	1813 resist
SRL127	500 μm * 500 μm	gold	1	- *in-situ* resistance measurements (Chapter 4) - gas sensors for laboratory test	1813 resist or poly(imide)
SRL131	250 μm * 250 μm	gold	6	gas sensor production for electronic nose	1813 resist
PtCIA	700 μm * 700 μm	platinum	4	gas sensor production for electronic nose	poly(imide)

Table 3. 1: characteristics of the discrete and array devices used in this work. All devices have an insulating gap of 10 μm.
1813 resist = Shipley 1813 photoresist, a copolymer of cresol and formaldehyde.

Table 3. 1 gathers together the description of the four designs used; figures 3. 2 to 3. 5 show photographs of these devices. They can be divided into two categories: discrete devices and array devices.

The SRL123 and SRL127 were discrete devices used to produce gas sensors for laboratory tests. They both consist in gold electrodes, but of different sizes (1 mm^2 and 0.25 mm^2). The SRL123 devices were used as produced and the SRL127 discrete devices were mounted onto a PCB support. The overall size of the discrete devices was about 1 cm by 5 mm.

The SRL131 and PtCIA devices were arrays of respectively six and four micro-gap electrodes and were provided after deposition of suitable polymer films to the CIA partners for tests in electronic noses. The design of these substrates was specific for electronic nose applications as it gathers several sensors on one substrate of small size (the overall size of the array was of about 1 cm by 2 cm). These arrays required the use of the micro-deposition technique (described in Chapter 2) to perform the electropolymerisation. This method consists in a high precision equipment where the electrochemical cell is reduced to one drop of solution. The arrays were mounted onto 14-pin PCB or stainless steel supports.

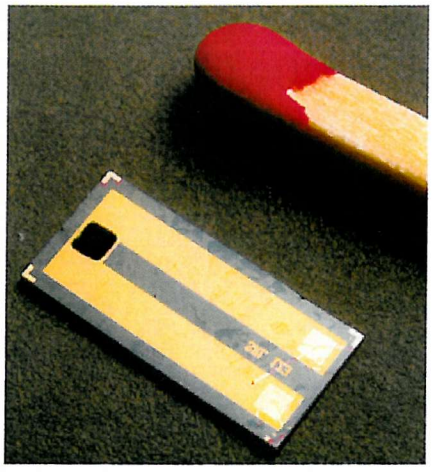

Figure 3. 2: photograph of a SRL123 discrete device here coated with a conducting polymer film. The electrode material is gold and the electrode size is 1000 μm * 1000 μm with a 10 μm insulating gap.

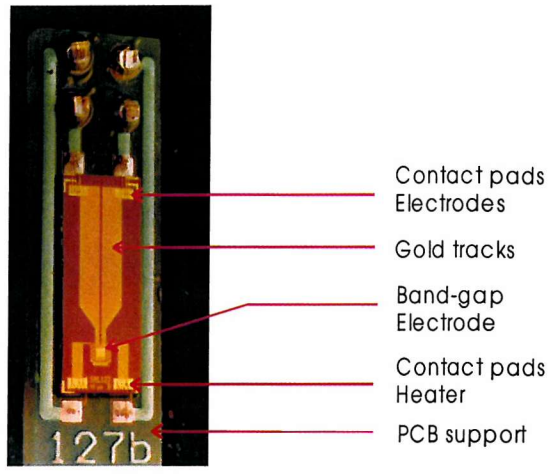

Figure 3. 3: photograph of a SRL127 discrete device. The electrode material is gold and the electrode size is 500 μm * 500 μm with a 10 μm insulating gap.

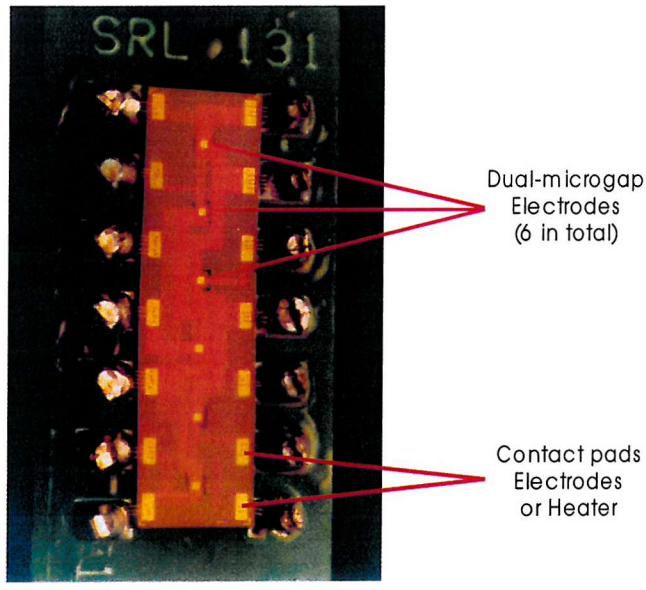

Figure 3. 4: photograph of a SRL131 array, composed of six gold dual micro-gap electrodes of 250 μm * 250 μm with a 10 μm insulating gap (PCB support).

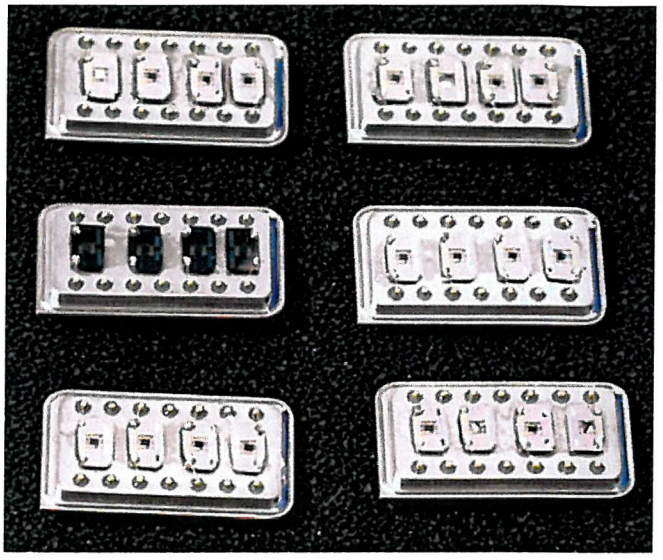

Figure 3. 5: photograph of six PtCIA arrays, each composed of four platinum dual micro-gap electrodes of 700 μm * 700 μm with a 10 μm insulating gap (stainless steel support).

The discrete and array devices just presented are the state-of-the-art. To underline the rapid evolution of the technology used for the substrate production, a photograph of an array device from a previous development stage is included- Figure 3. 6. In 1994, Blair [10], working in the same research group, reported the final design reached at the end of his work. It consisted of an array of three gold devices, 12 mm by 12 mm with a 15 μm gap, deposited onto an alumina tile. The devices produced were of poor quality, leading to poor reproducibility of the polymerisation visible by major polymer deposition outside the electrodes [10,11] [2]. The comparison of this array with the ones used during this work underlines the importance of the substrates in the quality of the sensor, and the importance of their continuous improvement.

[2] The electrodeposition of conducting polymer outside the electrodes of the chemoresistor substrate (onto defects of the photoresist or wire used for wire-bonding) is referred to as **extra-polymerisation**. It is indicative of the quality of the substrate.

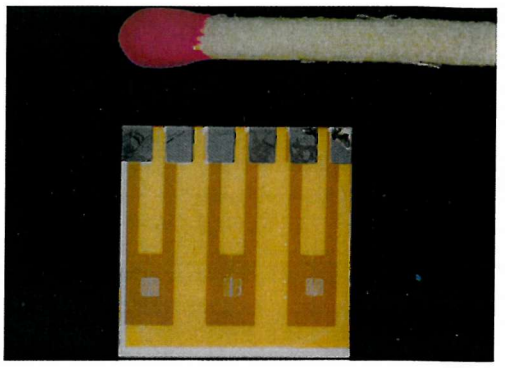

Figure 3. 6: photograph of an array of three gold devices (12 mm *12 mm- 15 μm gap) on an alumina tile, reported to be the state-of-the-art in 1994 [10].

3.2 - Cyclic voltammetry of the electrode material

Electrochemistry was used both to electropolymerise onto the chemoresistor substrates as well as to assess the quality of the devices prior to polymerisation. Electrochemistry of the electrode material, whether of gold or platinum, is a very powerful non-destructive method to "screen" the devices. It is capable of revealing defects in the purity of the metal and in the area of the electrodes.

3.2.1 - Theory

Both gold and platinum have similar behaviours when their potential is cycled in sulfuric acid. They, however, have characteristic differences, which require a separate study.

3.2.1.1 - Cyclic voltammetry of gold

The gold substrates were cycled in 2 M H_2SO_4 at 100 mV s^{-1} (unless otherwise stated) between -0.2 V and +1.8 V vs. SCE (the limits, respectively, for hydrogen and oxygen evolution). Figure 3. 7 shows a typical voltammogram of a polycrystalline gold substrate.

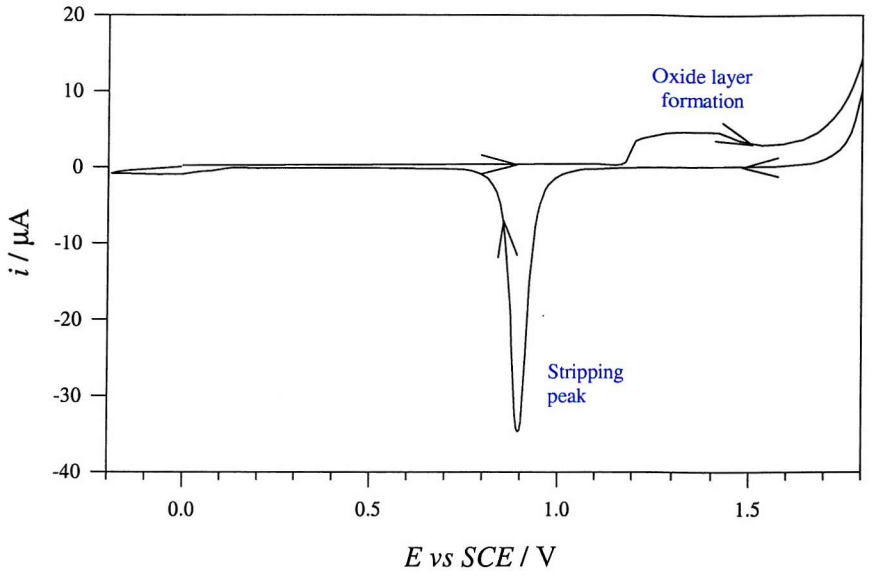

Figure 3. 7: cyclic voltammogram of a 1 mm diameter polycrystalline gold disc electrode in 2 M H_2SO_4 at 100 mV s^{-1}.

When the potential is cycled from 0 V in the oxidative scan, no peak is observed until a potential of *ca* +1.2 V is reached. At this potential there is oxidation of the gold and formation of an oxide layer at the electrode surface. Details of the process involved in the electrochemical oxidation of gold are given by Conway [12]. The oxide layer is reduced-stripped off- when the sweep is reversed at *ca.* +0.9 V. The stripping peak is sharp and its area is directly related to the surface area of the exposed gold. Under the conditions used here, a charge of 200 μC cm^{-2} is required to reduce the oxide layer [12]. Any additional peak on the cyclic voltammogram reveals the existence of electroactive impurities on the gold, or originating from the surroundings.

3.2.1.2 - Cyclic voltammetry of platinum

The cyclic voltammetry of platinum substrates was performed in 1 M H_2SO_4 at 200 mV s^{-1} (unless stated), between -0.2 V and +1.5 V vs. SCE. Figure 3. 8 shows a typical voltammogram of a polycrystalline platinum electrode.

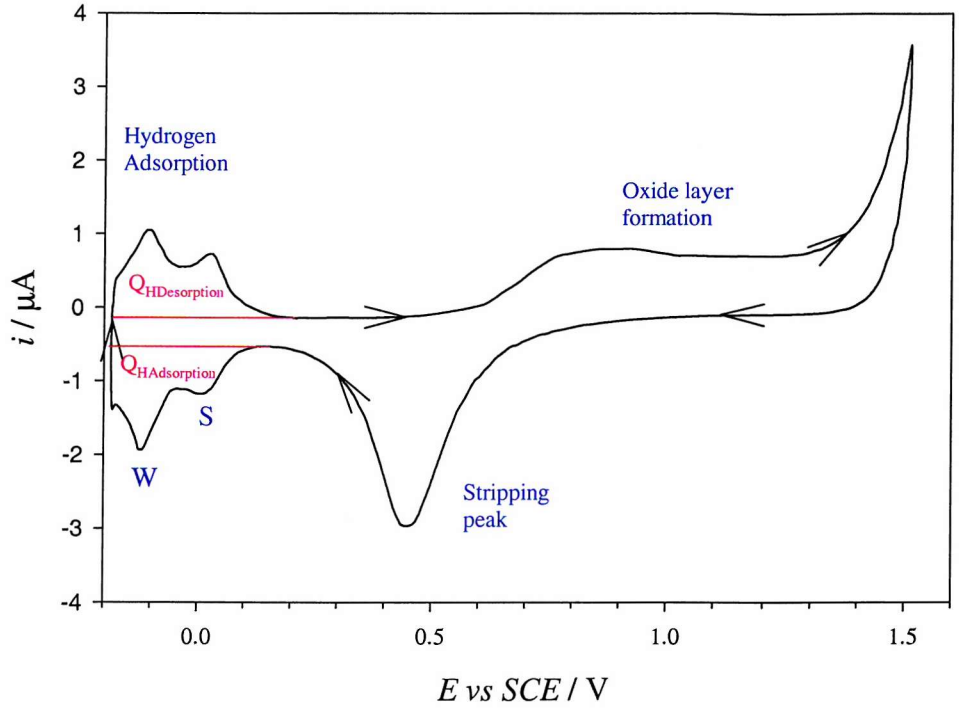

Figure 3. 8: cyclic voltammogram of a 0.5 mm diameter polycrystalline platinum disc electrode in 1 M H_2SO_4 at 200 mV s^{-1}.

As with gold, there is formation of an oxide layer (around + 0.9 V) which is stripped off when the scan is reversed (about +0.45 V). In the region 0 V to -0.2 V (reduction), there is formation and removal of adsorbed hydrogen atoms on the platinum surface following the equation:

$$H^+_{(aq)} + e^- \rightleftharpoons H_{(ads)}$$

where $H^+_{(aq)}$ are protons from the electrolyte and $H_{(ads)}$ are chemisorbed hydrogen atoms [13,14]. For polycrystalline platinum, there are two major peaks and a hint of a third (not visible here, located between the two major peaks). The major peaks are often referred to as the strongly and weakly adsorbed hydrogen peaks [15], labelled S and W respectively on Figure 3. 8. It has been suggested that these three peaks correspond to hydrogen adsorption onto three different crystal faces, the (111) plane for the peak labelled W, the (110) plane for the hidden peak, and the (100) plane for the peak corresponding to the strongly adsorbed hydrogen [15].

If impurities are present on the platinum surface, in addition to a decrease of the stripping peak, the hydrogen adsorption peaks will be largely modified. In other words, the definition and the area of the hydrogen adsorption peaks are closely related to the purity of the metal.

The surface area can be deduced from the hydrogen adsorption region. A charge of 210 μC cm^{-2} is passed in the proton reduction region for adsorption of a monolayer of hydrogen onto platinum (or for its desorption) [15]. The charge is determined by integrating the current from 0 to –0.2 V vs. SCE, after subtracting the current due to the double layer capacitance. The corresponding areas are indicated on the cyclic voltammogram in Figure 3. 8. The roughness (true metal surface/geometrical area) of a pure crystalline platinum surface can be deduced from such calculations.

The electrochemistry of the electrode material, whether gold or platinum, behaves like a fingerprint of the quality of the electrode. Surface area and purity can be evaluated from the cyclic voltammogram in acid. Additionally, forming and removing successively the oxide layer on the metal provides a means of cleaning the surface. The major advantage of this cleaning and quality checking method is that it is non-destructive for the devices, which implies that all substrates can be tested prior to polymer deposition. As a standard experimental procedure, the chemoresistor devices were cycled in acid a minimum of three times before electrodeposition.

3.2.2 - Examples of use of electrochemistry to assess the quality of the devices

Two main applications of the cyclic voltammetry of the electrode material are illustrated here. First, it was used to check the device quality (metal purity and surface area) as well as its reproducibility from device to device. Second, impurities originating from the surroundings of the electrode (substrate or solution) could be detected.

3.2.2.1 - Checking the device quality

As explained above, the electrochemistry of the electrode material allows its quality (both metal purity and electrode area) to be checked as well as the reproducibility from device to device.

Figure 3. 9 shows the cyclic voltammogram of a particular SRL131 device (plain line). The gold substrate does not present any impurity and the charge under the stripping peak is as expected. Thus this device is suitable for electropolymerisation. Figure 3. 9 also shows the cyclic voltammogram of a second device (dashed line). The metal purity is comparable to the first one, but the exposed gold in the electrochemical cell is about 50% of the expected value. At this point it was suspected that this was due to one electrode (electrode b) of the two electrodes (electrodes a and b) of the micro-gap device not being connected properly. This was confirmed both by visual inspection under the microscope and by electrochemistry. By performing the cyclic voltammogram of electrode a alone, the same voltammogram was obtained as when a and b are connected. No current flowed in the circuit if only electrode b was connected.

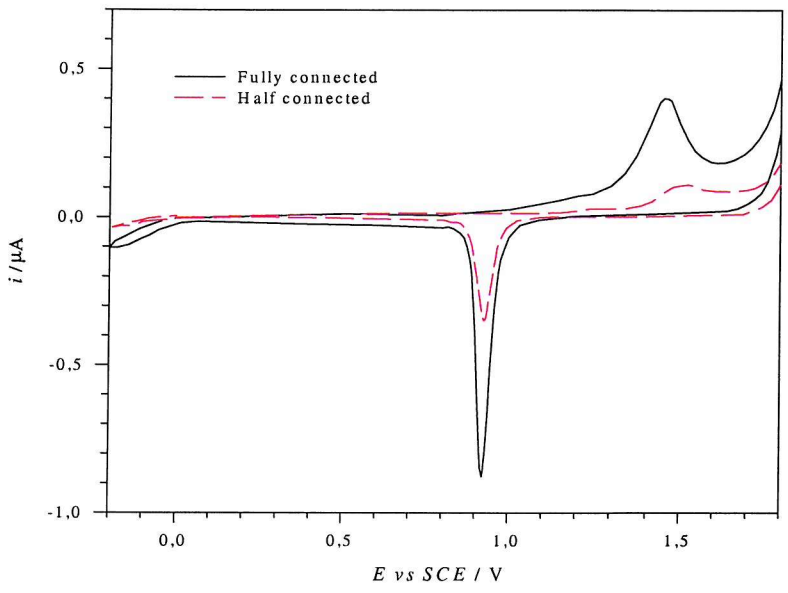

Figure 3. 9: cyclic voltammogram of two SRL131 devices (array of six devices) in 2 M H_2SO_4 at 100 mV s^{-1}. The "reference" device, labelled as fully connected, represents the expected cyclic voltammogram. The second voltammogram, about 50% of the reference and labelled half connected, was one particular device with one out of two electrodes of the micro-gap device not wire-bonded.

This experiment revealed that one electrode of the dual micro-gap device had not been wire-bonded. At this point it was predicted that if polymerisation was performed on this device, it would lead to an unsymmetrical coating unsuitable for use as gas sensor. This implied that it was not worth using this device for polymerisation. More significantly, it implied that the whole array would be unsuitable for application in an electronic nose, as it comprised only five sensors out of six. A strategy to avoid wasting arrays was to have discrete devices composing the array (see design of the PtCIA), instead of a single chip with the six sensors (SRL131), which then could be more easily replaced.

3.2.2.2 - Detection of impurity

Figure 3. 10 shows a typical voltammogram of a gold substrate in a solution of sulfuric acid contaminated with chloride ions. The presence of the impurities is revealed by the extra peaks, at +1.1 V in positive scan, and +0.7 V in negative scan. In addition the stripping peak of the gold was largely reduced due to the formation of a gold-chloride complex which hinders the formation of the gold oxide layer.

Similar voltammograms were frequently encountered after extended use of the sulfuric acid solution. Chloride ions from the reference electrode ($Hg,Hg_2Cl_2/Cl^-$) diffused into the solution introducing contamination. It was found that once rinsed with water, the gold substrates which had been cycled in a contaminated solution did not present this defect anymore when cycled in a fresh acid solution. In other words, devices cycled in a sulfuric acid solution containing a little chloride ion could be used for electropolymerisation after rinsing with de-ionised water, without having to reclean them in pure sulfuric acid.

In Chapter 2, the micro-deposition technique used to perform electrochemistry onto array devices has been described. In the design, the reference electrode is separated from the electrochemical cell (which is reduced to one drop of solution) by an electrolyte bridge. The purpose of this bridge is to avoid contamination of the drop by chloride ions from the reference electrode. This contamination was revealed by the cyclic voltammetry of gold array devices, in absence of the salt bridge, presenting similar additional voltammetric peaks as shown in Figure 3. 10.

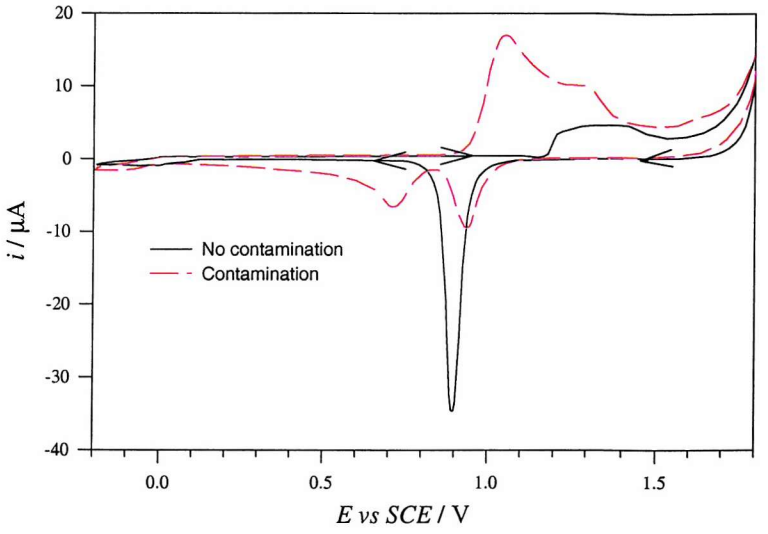

Figure 3. 10: cyclic voltammogram of a 1 mm diameter gold disc electrode in 2 M H_2SO_4 at 100 mV s^{-1} with Cl^- contamination. For comparison the cyclic voltammogram of the same electrode in a pure 2 M H_2SO_4 solution is given.

3.2.3 - Overview of the possible defects and their origins

Throughout this work, electrochemistry of the electrode material (platinum or gold) was used to assess the quality of chemoresistor substrates prior to electropolymerisation or during development of new substrates (details in the following section). Table 3. 2 summarises the possible irregularities presented in the cyclic voltammetry of the devices, both for gold and for platinum devices, and their possible origin.

A general procedure to assess the quality of substrates prior to polymerisation comprises:

- a microscopic inspection to detect any defect, for example the photoresist not fully removed from the electrodes, bad wire-bonding connections, mis-alignment of the masks during the photolithography process, etc.
- the measurement of the resistance of the "insulating" gap, which should be greater than 1 MΩ
- the cyclic voltammogram of the electrode material

Defect in Cyclic Voltammogram	Possible origin of the defect
Smaller Metal Area (stripping peak)	- Defect in photolithography process - Bad connection - Non-electroactive species adsorbed onto the electrode
Larger Metal Area (stripping peak)	- Defect in photolithography process - Dissolution of photoresist - Gold wires for wire bond not insulated- *gold devices only*
Impurity (additional peaks)	Electroactive species originating from: - photolithography process - decomposition of components of device (photoresist, glue, ...) in the solution - impure electrolyte
Hydrogen adsorption peaks ill-defined *- platinum only-*	- non-electroactive species adsorbed onto the metal - platinum of poor crystallinity

Table 3. 2: List (non-exhaustive) of the possible explanations for the defects encountered in the cyclic voltammogram of gold and platinum devices.

3.3 - Development of an array of platinum devices

Cyclic voltammetry of the electrode material, as just illustrated, is an easy-to-perform and non-destructive method to assess the quality of the sensor substrates. During this work a new array of platinum devices was produced and each step of the development was followed using electrochemistry. The aim was to produce an array of conducting polymer sensors for electronic nose applications, which implied an array of small size, of low cost, reliable (quality and reproducibility) and easy to replace. The final array developed was described in the first part of this chapter under the reference "PtCIA".

The new array was composed of both a new photoresist and a new electrode material (platinum) on which the behaviour of electropolymerisation had not been investigated. Therefore it was important to develop it step by step, to evaluate each component of the devices separately in order to be able to trace any source of defects. For this purpose, several batches were produced . By producing several batches of devices it was also possible to investigate the reproducibility of the devices, mainly regarding the quality of the platinum and the electropolymerisation from batch to batch.

3.3.1 - Test of a new photoresist

Electropolymerisation up to now has been limited to aqueous solutions due to the high solubility of the photoresist (1813 Shipley photoresist) in organic solvents. In other words, the photoresist limits the range of polymer that can be investigated as gas sensor materials (poly(thiophene) for example could not be used because it is polymerised from non-aqueous solvents).
The final goal of this experiment was to develop a platinum device with a photoresist resistive to organic solutions. The first step was to test a new photoresist (a poly(imide) photoresist) on gold devices (readily available), in a second step, testing platinum as the electrode material with the old photoresist (1813 Shipley photoresist). Both new materials, the photoresist and the electrode material, would be combined in a later stage of the development.

Two batches of SRL127 gold electrodes were provided, one with poly(imide) photoresist and one with 1813 resist (20 devices in total). In addition to visual examination of the devices, cyclic voltammetry of the gold electrode in sulfuric acid (2 M sulfuric acid at 200 mV s^{-1}, between -0.2 V and +1.8 V vs. SCE) was performed to follow contamination from, or degradation of, the photoresist upon exposure to solvent. The solvents/solutions investigated were 2 M sulfuric acid, acetonitrile, water, propylene carbonate, acetone, tetrahydrofuran, N-Methyl-2-pyrrolidinone, dichloromethane, methanol and iso-propanol. A typical electropolymerisation experiment lasts ten minutes, so times of one hour and one week were chosen as extreme conditions for exposure to organic solvents and aqueous solutions. When defining these conditions the use of the new photoresist for applications other than conducting polymers, which may require longer exposure time was also considered. Indeed the results from this study were shared with Neuchatel which had the possibility to exploit them.

The voltammograms were reproducible and showed good purity of the gold before exposure. One device of each type was dipped in each solution/solvent and left without further handling for one hour. Cyclic voltammetry of the gold and visual examination were performed, and compared to that before exposure. If the device had passed the first stage of the experiment, it was exposed for one week and examined once again.

The **1813 resist** showed poor stability when exposed to organic solvents even after one hour. For all organic solvents tested (except for dichloromethane), the photoresist was dissolved. This was shown by a large increase of the stripping peak on the cyclic voltammogram. By dissolving away the photoresist, the solvent was exposing the gold tracks to the electrochemical solution. For dichloromethane, major impurities were introduced in the cyclic voltammogram masking the signal from the gold. Exposing the 1813 resist to water and sulfuric acid had no effect on the gold device, as expected, even after one week exposure.

For all solutions tested, the electrodes coated with the new **poly(imide)** photoresist showed no degradation upon exposure after one hour. The conclusions were the same after one week, exposure except for dichloromethane. For the device exposed to dichloromethane, the electrode material had to be cycled in acid before recovering the signal of the gold. Even then, the cyclic voltammetry still showed the presence of some impurities, with a slight decrease in stripping peak area (*ca.* 10%).

Table 3. 3 summarises the results of this experiment. The first conclusion is that devices coated with the new poly(imide) photoresist can be used to grow polymers from aqueous solutions, similarly to devices coated with 1813 resist. The second conclusion is clear from Table 3. 3: the poly(imide) photoresist constitutes a major improvement over the 1813 resist. Unlike the 1813 resist, it is resistive to a wide range of organic solvents. It can be exposed for one week to at least seven organic solvents without introducing any contamination to the electrode material or being dissolved.

	1813 Resist		Poly(imide)	
Solvent	**One hour**	**One week**	**One hour**	**One week**
2 M H_2SO_4	FINE	FINE	FINE	FINE
Acetonitrile	Photoresist dissolved	-	FINE	FINE
Water	FINE	FINE	FINE	FINE
Propylene Carbonate	Photoresist dissolved	-	FINE	FINE
Acetone	Photoresist dissolved	-	FINE	FINE
Tetrahydrofuran	Photoresist dissolved	-	FINE	FINE
N-Methyl-2-pyrrolidinone	Photoresist dissolved	-	FINE	FINE
Dichloromethane	Impurities	-	FINE	Some impurities Gold partially recovered
Methanol	Photoresist dissolved	-	FINE	FINE
Iso-propanol	Photoresist dissolved	-	FINE	FINE

Table 3. 3: summary of the chemical resistivity of the 1813 Shipley photoresist and the new poly(imide) photoresist to various solutions/solvents, assessed by cyclic voltammetry of the electrode material and optical observations.
FINE : no impurity was introduced onto the gold and the photoresist was not dissolved.

3.3.2 - Test of the platinum produced by photolithography

Up to now, only gold devices had been used as substrates for conducting polymer gas sensors. Platinum devices were of interest as the processing costs were lower than for gold ones. A device of simple geometry was produced with no gap or platinum heater (1 mm by 1 mm). With this first prototype, four important points were investigated:

- the adhesion of the platinum onto the silicon substrate when its potential is cycled in sulfuric acid
- the purity of the platinum

- the electrodeposition which should be similar to the deposition onto gold devices and reproducible from device to device
- the adhesion of the polymer film onto the device

3.3.2.1 - Behaviour of the electrode material

Five platinum electrodes were provided and cycled in sulfuric acid at 100 mV s^{-1}. During the voltammetry, the platinum did not peel off, showing that the adhesion layer used (titanium, 15 nm thick) was appropriate.

Figure 3. 11 shows a typical cyclic voltammogram obtained. The voltammograms were reproducible for the five electrodes. The voltammetry showed that there was no additional electroactive species on the platinum and the voltammetry was characteristic for polycrystalline platinum. For comparison the cyclic voltammogram of a polycrystalline platinum disc electrode recorded under the same conditions is shown. Close inspection of the voltammograms of the gas sensor substrates showed that the charge density of the stripping peak was lower than expected and that the hydrogen adsorption peaks in the region 0 to -0.2 V vs. SCE were poorly resolved. This was indicative of adsorption of organic species at the platinum surface. High purity platinum (99.99%) was used to produce the device, but some contamination occurred during the photolithographic process as revealed in the cyclic voltammogram[3]. As no major contaminant was present, the purity of the platinum device was estimated to be suitable for application as a substrate for the conducting polymer chemoresistor.

[3] The first contamination source could be the underlying titanium seeding layer. The second source would be the insertion in the metal matrix of some impurities, or impurities could also be adsorbed onto the metal surface.

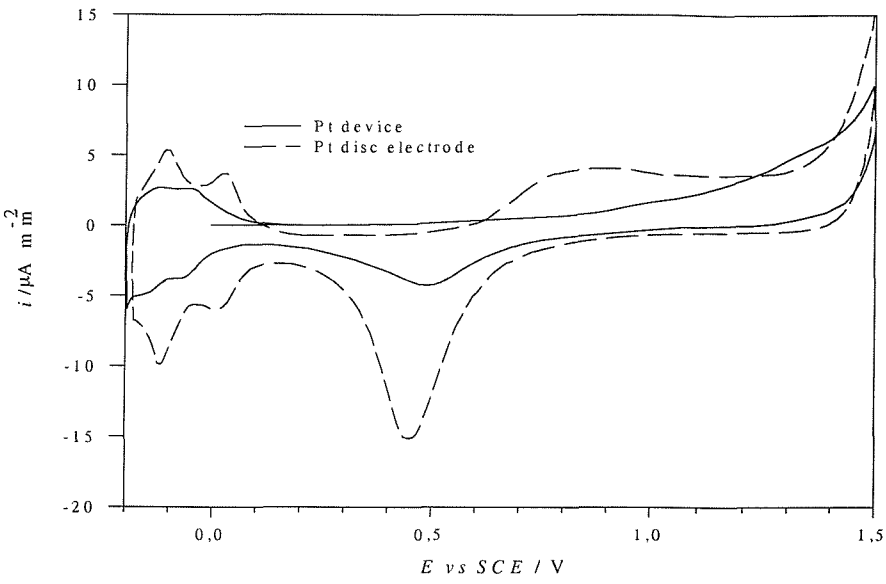

Figure 3. 11: typical cyclic voltammogram of a discrete platinum device produced by photolithography (1 mm by 1 mm, without any gap) in 2 M H_2SO_4 at 100 mV s^{-1}. For comparison, the cyclic voltammogram of a 0.5 mm diameter platinum disc electrode in the same conditions is given. The large difference in current density can partially be explained by a larger roughness of the disc electrode.

3.3.2.2 - Behaviour towards electropolymerisation

Poly(pyrrole) pentane sulfonate, a well characterised system, was electrodeposited onto four of the discrete devices. The growth was reproducible from sensor to sensor and the polymerisation transient was also similar to that obtained on gold substrates, in both shape and current density. Finally, visual examinations did not revealed any defects in the adhesion of the films.

The platinum device quality and the electropolymerisation were satisfactory for this first batch of substrates. A more complex device was then produced to study the behaviour of the polymer deposited over the gap.

3.3.3 - Test of a platinum micro-gap device

A second platinum device (1 mm by 1 mm) was designed, with a 10 µm (5 devices) or a 50 µm (3 devices) insulating gap and a platinum heater. In addition to recheck the platinum

quality and the polymerisation properties on the platinum devices, the behaviour of the polymer over the insulating gap was investigated.

The conclusions drawn on the purity of the electrode material were consistent with the ones for the first batch. Poly(aniline) decane sulfonate was electrodeposited onto three devices and the conclusion on the electrodeposition were found similar to the first batch. Two of the devices, 7 days after the polymerisation, had a resistance in the range 120-130 Ω. The third one had a resistance over 1 MΩ, either due to a poor adhesion or breaking of one contact after deposition.

Globally, the results of the tests performed here were satisfactory in the sense that the films electropolymerised from aqueous solution showed good polymerisation and good conducting characteristics. The next step in the development of the array of platinum devices was to produce a batch of arrays for application in electronic nose technology.

3.3.4 - First batch of arrays for production of chemoresistors

3.3.4.1 - Discussion of the design of the array

The final array of platinum devices, referred to as PtCIA, was composed of four discrete devices, 700 μm by 700 μm each with a 10 μm insulating gap (Figure 3. 5). It was developed in conjunction with the CIA project, to be used in an electronic nose. Therefore several modifications in the design were made from the SRL131 used previously to better fit the requirements of this application. The SRL131 consisted of six gold electrode pairs of smaller size (250 μm by 250 μm with a 10 μm insulating gap), all six electrode pairs being on a single wafer.

The first modification was to decrease the number of polymers on each array from six to four as these chemoresistors were used in conjunction with other types of sensors (metal oxide, QCM and MOSFET sensors). Another major difference from the SRL131 was to have discrete devices (instead of all the devices on a single wafer). This design makes defective devices easier to replace, as underlined in section 3.2.2.1. Finally electrodes of larger size were preferred due to an inherent property of the conducting polymer nucleation. It was found that the electropolymerisation tends to be irreproducible on electrodes of small size as detailed

in the following chapter dealing with the improvement of the deposition by *in-situ* resistance measurement.

In all, seven arrays of four electrode pairs were provided. All electrochemical experiments were performed on the platinum electrode substrates using the micro-deposition technique (see chapter 2 for a description of the set-up).

3.3.4.2 - Characterisation of the platinum

The quality of the platinum array devices was reproducible from the first two batches. However, the ill-definition of the hydrogen adsorption peaks was increased. It was expected that the use of a single drop of electrolyte would more easily bring contamination to the electrode than in the bulk solution, explaining the previous observation.

For the present electrodes the roughness, calculated from the charge passed in the hydrogen adsorption region, was less than 1 (exposed platinum area/geometric area = 0.9- see the theory on the cyclic voltammetry of platinum for more details on the calculations). A roughness close to 1 was expected due to the fabrication process giving smooth metal films. The roughness inferior to 1 is, similarly to the ill-defined hydrogen adsorption peaks, indicative of some organic impurities adsorbed onto the metal. Whether the impurities were originating from the photolithography process or from the micro-deposition was not determined.

3.3.4.3 - Discussion on the electropolymerisation onto the arrays

Four different polymers were grown onto each of the seven arrays of devices, so that each 14 pin structure had an array of four different devices. The four polymers were 1) poly(pyrrole) pentane sulfonate, 2) poly(pyrrole) decane sulfonate, 3) poly(aniline) pentane sulfonate and 4) poly(aniline) octane sulfonate.

The electrodeposition conditions were similar to those used throughout this work. For poly(pyrrole), the growth solution was 0.1 M in pyrrole and 0.1 M in alkyl sulfonate in H_2O. A voltage of 0.85 V was applied for a variable time ranging from 80 to 150 s, at room temperature. Aniline was polymerised from a solution of 0.5 M aniline and 0.5 M alkyl sulfonate salt in 2M H_2SO_4 at room temperature. The voltage was stepped from 0 to 0.9 V for

5 s, followed by a step at 0.78 V until a defined charge was passed: 3.25 mC or 5 mC for poly(aniline) pentane sulfonate, and 7.5 mC for poly(aniline) octane sulfonate.

To investigate the reproducibility of the polymerisation onto the platinum, a large number of devices is required. The substrates were fragile and many were broken during handling. For each polymer type, only four to six sensors (instead of seven) were produced. Additionally, the amount of extra-polymerisation was significant in certain cases and difficult to estimate. Hence the small number of comparable devices available made the analysis problematic. Poly(pyrrole) pentane sulfonate is selected here to illustrate the reproducibility of the deposition and of the final resistance.

As already observed for SRL131 gold arrays (not reported here), the electropolymerisation of both poly(pyrrole) and poly(aniline) films was irreproducible, independent of the dopant. Figure 3. 12 illustrates the irreproducibility of the growth of poly(pyrrole) pentane sulfonate onto PtCIA array devices and Table 3. 4 summarises the results of the polymerisation.

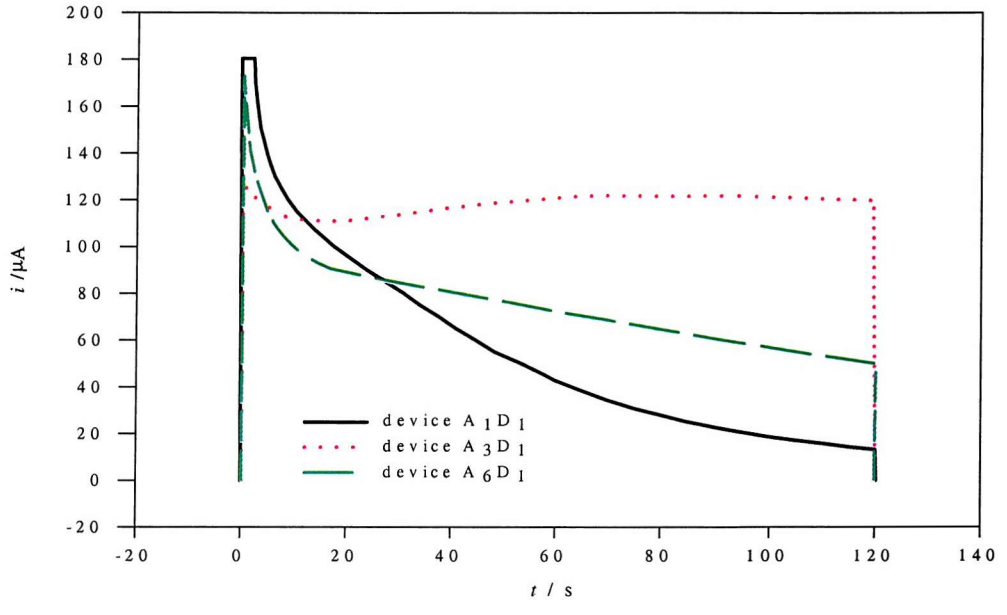

Figure 3. 12: current transients for the growth of poly(pyrrole) pentane sulfonate films onto three array electrodes, showing the irreproducible growth from device to device. The current transient for the device A_3D_1 presents the expected behaviour.

	Array 1	Array 2	Array 3	Array 4	Array 5	Array 6	Array 7
Polymer quality	OK	OK	OK 50% extra polymer	OK	Pt impure array not used	OK	OK
$t_{polymerisation}$ / s	120	120	120	90	_	120	120
Q / mC	6.38	8.13	13.13	6.85	_	8.45	6.0
R / Ω (7 days)	675	1600	210	1100	_	1200	3500

Table 3. 4: results of the electrodeposition of poly(pyrrole) pentane sulfonate onto the first batch of PtCIA arrays.

The current transient of the device A_3D_1 presented the expected shape (roughly constant current during the deposition) and the expected current density (about 0.12 mA mm^{-2}, once 50% of the current has been subtracted, corresponding to the visually estimated amount of extra-polymerisation). The other two devices presented a different behaviour. The current was initially larger than expected, then decreased rapidly below the expected value. Similar irreproducibility was encountered during electropolymerisation onto gold arrays. However, this behaviour was not observed for discrete platinum devices. The conclusion is that the high irreproducibility originates from the micro-deposition technique, and is not a characteristic of the platinum electrodes.

Table 3. 5 compares the reproducibility of the polymerisation charge and the resistance of the devices for gold electrode arrays (SRL131) and platinum electrode arrays (PtCIA). The first observation is that the polymerisation charge density is larger for the gold devices than for the platinum devices. It is therefore expected that the resistance of the polymers on the gold devices would be lower. However the sizes of the electrodes have to be taken into account. The first contribution of the electrode sizes on the resistance is that the conductance of the device increases linearly with the increase of the electrode length. So for films of similar thickness and conductivity the resistance should be reduced by a factor of 2.8 when increasing the electrode length from 250 to 700 μm. The conclusion is that the decrease in the electrode length does not, on its own, account for the large increase in resistance from the platinum to the gold devices (by a factor over 40 here). In the calculation performed earlier it was assumed that the films were grown to comparable thickness. However another implication of the

reduction of the size of the electrodes is that it is expected that the faraday efficiency would decrease when switching from the platinum devices (behaving like macro-electrodes) to the gold devices (going towards a microelectrode behaviour) because the intermediates of the electropolymerisation diffuse more rapidly away from the electrode in the case of the smaller electrodes.

The variation of contact resistance polymer/electrode material is assumed to be of minor contribution in the increase in resistance from the platinum to the gold devices as the resistance of poly(pyrrole) pentane sulfonate was found to be as low as 1 kΩ on larger electrodes.

A second observation from Table 3. 5 is a larger spread in the polymerisation charge onto the gold devices (53%) compared to the platinum devices (27%). Once more, the size of the electrodes has to be taken into account. If the extra-electroactive material area is assumed to be constant for all array devices, the coefficient extra-polymerisation/polymerisation on the electrodes increases with decreasing the electrode area and explains the behaviour observed.

	SRL131 (n=6)	PtCIA (n=4)
Q / mC mm^{-2}	21.9	14.8
error Q / mC mm^{-2}	11.5	4.0
error Q / %	53	27
R / Ω	74 500	1 745
error R / Ω	113 800	1 960
error R / %	153	112

Table 3. 5: results of the electrodeposition of poly(pyrrole) pentane sulfonate onto gold and platinum array devices, showing the poor reproducibility of the deposition, and thus of the final resistance of the chemoresistors. The data of six SRL131 devices and four PtCIA devices (arrays 1, 2, 6 and 7) were used for this table. The errors are given within 95% confidence.

When comparing the reproducibility of the resistance, it appeared to be slightly more reproducible for the platinum devices, 112% spread instead of 153% for the gold arrays. On this aspect the new platinum devices represent an improvement for the array devices. However, the polymerisation charge of poly(pyrrole) pentane sulfonate onto discrete SRL123

devices was found to be much more reproducible (4.1%) as well as the final resistance (36%)- see Chapter 5 for details. The exact origin of the irreproducibility of the growth onto array devices was not determined. As it was not possible to control the irreproducibility in the growth, it was decided to monitor it. As demonstrated in the following chapter, monitoring *in-situ* the resistance of the polymer film during the deposition significantly increases the reproducibility.

3.3.5 - Second batch of arrays for production of chemoresistors

Five arrays were provided with the same design as the first batch. They originated from another photolithographic batch and presented a defect. The resistance over the "insulating" gap was measured prior to polymerisation. Resistances as low as 100 Ω were measured between the two electrodes of the devices, well below the 1 MΩ minimum value expected. Two out of five arrays (array 1 and 2) were not suitable for polymerisation. The low resistance in parallel to the sensitive layer would short-circuit the chemoresistive polymer film.

The resistance between different points on the device (A, B, C and D, located on Figure 3. 13) was measured in an attempt to locate the conduction path. The resistances R_{AB}, R_{CD}, R_{AC} and R_{BD} respectively represents the resistances between the points A and B, between C and D, between A and C and between B and D and are given in Table 3. 6.

A resistance of about 80 Ω was measured for the platinum heater (typical value expected). The lowest resistances were measured between the electrode and the heater, indicating that the defect was not directly in the 10 μm insulating gap but rather due to pinholes in the insulating layer between the electrodes and the heater (much thinner than the gap- 250 nm).

Device	R_{AB} / Ω	R_{CD} / Ω	R_{AC} / Ω	R_{BD} / Ω
Array1 Device 1	125	80	26	139
Array1 Device 3	102	61	70	92
Array2 Device 1	335	83	164	148
Array2 Device 2	158	81	27	86

Table 3. 6: resistance values for four uncoated platinum devices, showing a low resistance over the "insulating" gap. The diagram in Figure 3. 13 locates the various points on the device.

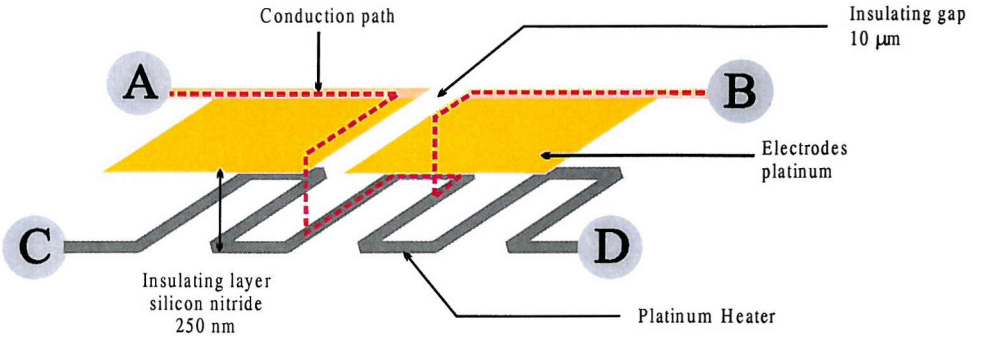

Figure 3. 13: diagram showing a possible conduction path over the "insulating" gap (between points A and B) due to contact between the electrodes and the platinum heater located below. For clarity the diagram was not made to scale and the insulating layer between the electrodes and the heater is not symbolised.

The cyclic voltammetry of the platinum substrates showed that the metal on these electrodes was of better quality than the first batch of arrays. Polymerisation was performed on three arrays presenting a high resistance across the insulating gap. The same polymers as for the first batch were deposited, but unsuccessfully. The growth did not take place uniformly onto the electrode but rather following a pattern similar to the pattern of the platinum heater underneath. Figure 3. 14 shows a typical pattern observed. This was observed for all nine polymer films produced, whether the polymer was poly(pyrrole) or poly(aniline). This behaviour was indicative of a voltage drop across the electrodes during polymerisation. The exact reason was not investigated, but reported to the group in Neuchatel providing us with the devices. The conclusion from this experiment is that, even if extreme precaution is taken during the photolithography, this process is very sensitive to any minor process modification.

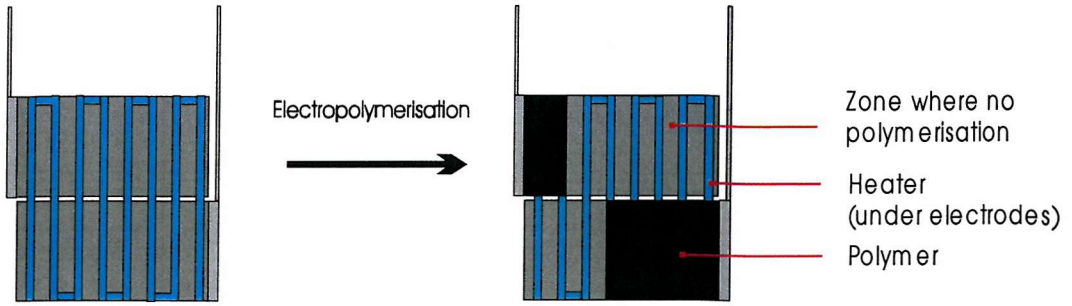

Figure 3. 14: typical polymer pattern resulting from electrodeposition onto the second batch of platinum array devices presenting defect, probably due to contacts between the electrodes and the heater through the 250 nm thick "insulating" layer.

3.3.6 - Third batch of arrays for production of chemoresistors

A third batch of arrays was provided. The design of the array was the same as for the two previous batches, except that the heater had been removed to avoid the problem encountered by the second batch. For the application of these arrays for conducting polymer this was not significant as they are operated at room temperature.

This design was the final design. The array was composed of four discrete platinum devices of 700 μm by 700 μm each with a 10 μm gap. The 130 nm thick platinum electrode was placed onto a 15 nm thick titanium layer (adhesion layer) on silicon nitride.

Eight arrays were provided. During the first use of the array, the platinum electrode was of good purity but decreased with the number of polymers deposited onto the array. The growth solution and the solution used to rinse the polymer previously deposited onto the structure is suspected to have contaminated the platinum left uncoated. The cyclic voltammogram of a device was performed only before polymerisation so this assumption was not proven, but suggests that platinum electrodes are more prone to contamination than gold devices.

Electropolymerisation was performed using the micro-deposition technique to produce arrays of sensors. The results of the polymerisation were similar to those for the first batch: an irreproducible growth leading to an irreproducible resistance from sensor to sensor. These arrays were provided to partners within the CIA project. No conclusion on the sensing properties of the films deposited onto these structures will be discussed here.

3.4 - Conclusions

Electrochemistry of the electrode material, whether gold or platinum, is an efficient non-destructive tool to assess the quality of the devices, prior to electropolymerisation or to follow the development of a new device. Cyclic voltammetry allows the detection of defects in the connection, impurities (electroactive or not) and defaults induced by the photolithography process.

The general conclusion on the gold substrates produced by photolithography employed in this work is that the devices provided were of good quality regarding the reproducibility of the electrode area, good quality of the electrode material and good definition of the growth area.

Electrochemistry was used to develop a new array of platinum devices, comprising a new photoresist and a new electrode material. The design of the array was also modified to fit the requirements of the electronic nose application. The first results from the array of platinum devices were satisfactory, but need further improvement.

The tests performed for the development of these platinum devices were beneficial in various aspects as they consisted in:

- the development of an array for conducting polymer sensors
- the development of a substrate also suitable for metal oxide sensors, sensors used within the CIA project
- the evaluation of new materials (electrode material and photoresist) beneficial for the producer of the devices (University of Neuchatel)

Improvement of the substrates should be accompanied with improvement of the coating itself. Therefore some new materials were investigated as gas sensitive layer along with the evaluation of a new technique consisting in measuring the resistance of the polymer during the deposition in order to increase the reproducibility of the gas sensors. These topics will be discussed in the following chapter.

(1) Bartlett, P. N.; Archer, P. B. M.; Ling-Chung, S. K., *Sensors and Actuactors*, 1989, **19**, 125-140.

(2) Partridge, A. C.; Harris, P.; Andrews, M. K., *Analyst*, 1996, **121**, 1349-1353.

(3) Slater, J. M.; Paynter, J.; Watt, E. J., *Analyst*, 1993, **118**, 379-384.

(4) Hwang, B. J.; Yang, J. Y.; Lin, C. W., *J. Electrochem. Soc.*, 1999, **146**, 1231-1236.

(5) Vigmond, S. J.; Kallury, K. M. R.; Ghaemmaghami, V.; Thompson, M., *Talanta*, 1992, **39**, 449-456.

(6) Topart, P.; Josowicz, M., *J. Phys. Chem.*, 1992, **96**, 7824-7830.

(7) Topart, P.; Josowicz, M., *J. Phys. Chem.*, 1992, **96**, 8662-8666.

(8) Josowicz, M.; Janata, J., *Anal. Chem.*, 1986, **58**, 514-517.

(9) Gardner, J. W.; Pike, A.; Rooij, N. F. d.; Koudelka-Hep, M.; Clerc, P. A.; Hierlemann, A.; Gopel, W., *Sensors and Actuators B*, 1995, **26-27**, 135-139.

(10) Blair, N., The development and characterisation of conducting polymer based sensors for use in an electronic nose, PhD thesis, SOUTHAMPTON, 1994.

(11) Pearce, T. C.; Gardner, J. W.; Friel, S.; Bartlett, P. N.; Blair, N., *Analyst*, 1993, **118**, 371-377.

(12) Angerstein-Kozlowska, H.; Conway, B. E.; Hamelin, A.; Stoicoviciu, L., *Electrochimica Acta*, 1996, **31**, 1051-1061.

(13) Parson, R. In *Electrified interfaces in physics, chemistry and biology*; Guidelli, R., Ed.; NATO ASI Series:; Vol. 355.

(14) Barna, G. G.; Frank, S. N.; Teherani, T. H., *J. Electrochem. Soc*, 1982, **129**, 764-749.

(15) Gilman, S. In *Electroanalytical Chemistry*; Bard, A. J., Ed.; E. Arnold TDL: London, 1967; Vol. 2.

Chapter 4 – Improvement of the sensing material

4.1 - Improvement of the electrodeposition of conducting polymers
by *in-situ* resistance measurement

4.1.1 - Electropolymerisation onto devices- state of the art at the beginning of this work
4.1.1.1 - Electrodeposition conditions and limitations
4.1.1.2 - Investigation of the irreproducibility of deposition
4.1.1.2.1 - Results
4.1.1.2.2 - Discussion
4.1.2 - A new electrodeposition technique: use of *in-situ* resistance measurement
4.1.2.1 - Description of the technique
4.1.2.2 - Discussion of the technique
4.1.2.3 - Evaluation with a dummy cell
4.1.2.4 - Evaluation with conducting polymer
4.1.3 - Results of the *in-situ* resistance monitoring technique
4.1.3.1 - Electropolymerisation and resistance
4.1.3.1.1 - Current transient
4.1.3.1.2 - Film resistance
4.1.3.2 - Optical and Scanning Electron Microscopy
4.1.3.3 - Gas sensing property
4.1.3.3.1 - Sensor production
4.1.3.3.2 - Response to vapour
4.1.3.4 - Conclusions on the *in-situ* resistance monitoring

4.2 - Investigation of new sensing materials
Poly(pyrrole) and poly(aniline) doped with a range of anions

4.2.1 - Discussion of the choice of the vapour sensitive material
4.2.1.1 - Alkyl and aromatic sulfonates as dopant
4.2.1.2 - Metal phthalocyanine tetrasulfonates as dopant
4.2.2 - Gas sensing property of the new polymers
4.2.2.1 - Response to water and ethanol vapours
4.2.2.2 - Response to CO and NO_2
4.2.2.2.1 - Response to CO
4.2.2.2.2 - Response to NO_2

Conducting polymers have been widely studied and are now employed as gas sensors in electronic noses. However, further research in this field remains important. As shown in the previous chapter, this research can be motivated by technological innovations like the miniaturisation of the devices.

A second motivation for research is the requirement of significantly improve the devices. In the domain of gas sensors, a general interest is in increasing the reproducibility from sensor to sensor. This is illustrated here, in the first part of the chapter, for the example of the conducting polymer gas sensors. The approach to the problem was to improve the coating reproducibility by measuring the resistance of the polymer *in-situ* during the electrodeposition in an attempt to improve the reproducibility of the base resistance.

Research can also be driven by the need to perform pure research in order to developp new materials. Conducting polymer materials tested up to now give suitable responses but other materials may be more effective. This reason motivated the work done on designing the sensing material in order to modulate its sensitivity towards target vapours or gases. This will be illustrated in the second part of this chapter, where the influence of the anion on the gas sensitivity will be investigated.

4.1 - Improvement of the electrodeposition of conducting polymers by *in-situ* resistance measurement

The electropolymerisation conditions first used in this work were established in previous studies within the research group. They were the most appropriate for electrodeposition onto the devices used at that time. These polymerisation conditions were found to be no longer optimal, mainly because of the change in the design of the substrates and significant improvement of their quality. The polymerisation conditions had to be modified to better fit the newer technology.

One main interest was to improve the reproducibility of sensor production, an important feature when applications in electronic noses are considered. Irreproducible sensor fabrication implies retraining the neural network of the electronic nose each time one sensor is replaced. For this purpose, a new technique was set-up to measure the resistance of the polymer *in-situ* during electropolymerisation.

4.1.1 - Electropolymerisation onto devices- state of the art at the beginning of this work

4.1.1.1 - Electrodeposition conditions and limitations

Blair [1] reported that the most reproducible method to produce conducting polymers, regarding the quality of the film, was to electropolymerise galvanostatically. However, he also concluded that galvanostatic growth was not suitable for deposition onto the sensor devices available at that time due to the poor quality of the substrates. They presented a large surface of extra-electroactive material (corresponding to pinholes in the photoresist) where polymerisation was also taking place. Because the surface area due to these pinholes was not reproducible and could not be estimated, the amount of material deposited galvanostatically onto the sensing area was largely irreproducible. At this stage, potentiostatic growth for a fixed time was found to be the most suitable method even thought this technique was reported to be less reproducible and produced films of inferior quality to galvanostatic growth. Since then the same method has been employed [2] .

The conditions for the growth of poly(pyrrole) and poly(aniline) defined by Blair and Elliott [1,2] were first employed in this work. In addition to using a potentiostatic method, they also used a combination of high monomer concentration and long polymerisation time to ensure full coverage of the insulating gap. Due to the lack of tool to study the behaviour of the film during its deposition and to detect the moment when the polymer crossed the gap, the choice was to have a thicker film rather than incomplete coverage of the gap. Consequently, the films obtained were rather thick (over 4 μm for poly(pyrrole) and over 10 μm for poly(aniline)). The sensing properties of the resulting films were not optimal, the response time was rather long.

4.1.1.2 - Investigation of the irreproducibility of deposition

4.1.1.2.1 - Results

The irreproducibility of the polymerisation of conducting polymer, whether chemically [3] or electrochemically [4] has already been reported. In addition, the irreproducibility was increased upon electropolymerisation onto array devices (PtCIA and SRL131) as shown in Chapter 3. The origin of the irreproducibility of the growth was not investigated in this case but appeared to be characteristic of the use of the micro-deposition technique.

Irreproducibility in the polymerisation was also observed during polymerisation of aniline onto electrodes of small size (500 μm by 500 μm and below) and it was of interest to locate its origin.

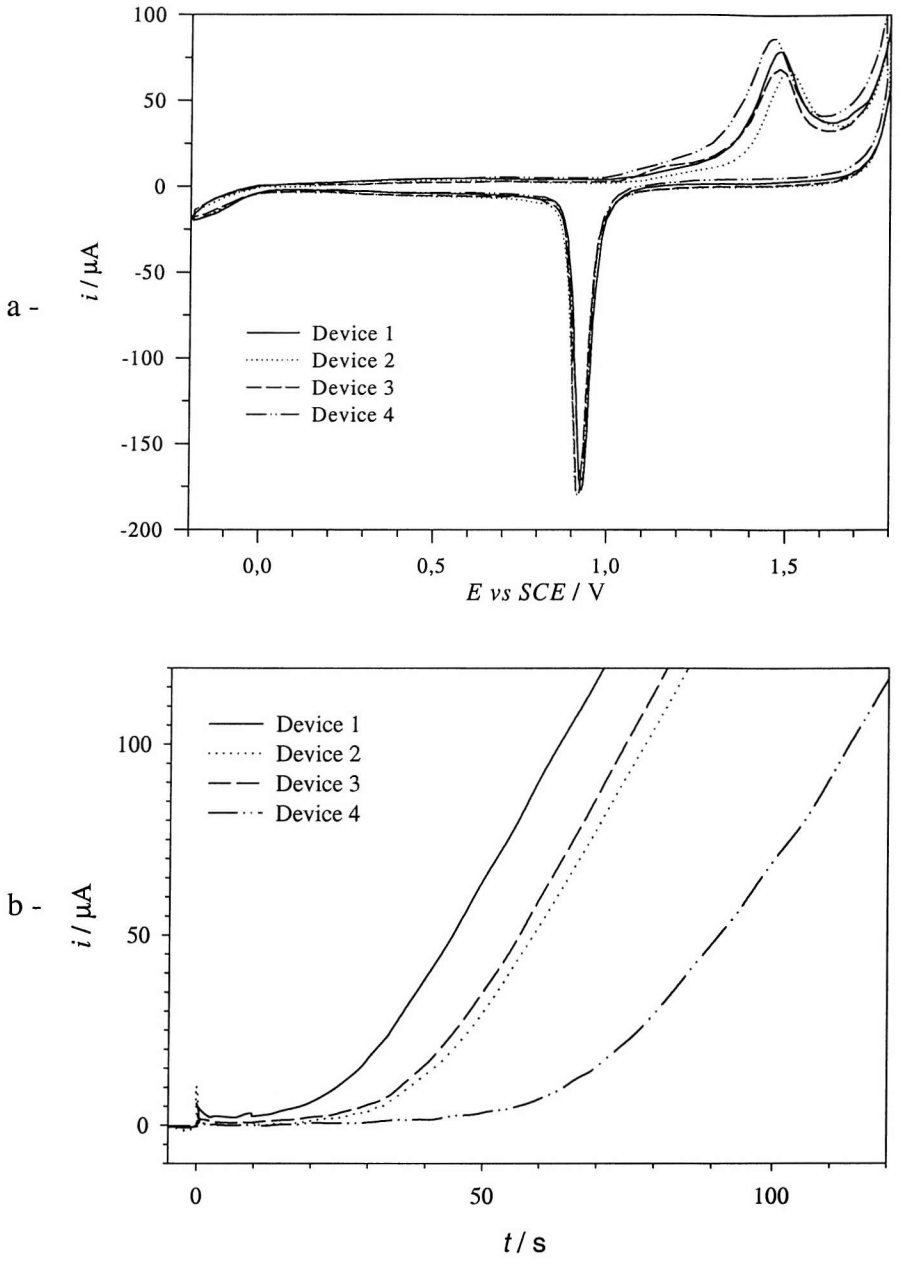

Figure 4. 1: a - Cyclic voltammogram of four SRL127 devices (500 μm by 500 μm) in 2 M H_2SO_4 at 100 mV s^{-1}.
b - Current transients for the growth of poly(aniline) pentane sulfonate onto the same devices showing the variable delay in nucleation.
The electropolymerisation conditions: 0.5 M aniline, 0.5 M pentane sulfonate in 2 M H_2SO_4. +0.9 V for 10 s followed by +0.78 V.

The first step in the investigation of the irreproducibility was to check the reproducibility of the substrates. In Chapter 3, it was reported how electrochemistry of the electrode

material could be used to assess the purity of the metal and the area of the electrode. Figure 4. 1a shows the gold cyclic voltammogram for four SRL127 devices in sulfuric acid. None of the gold electrodes presented impurities as no additional peak was present. The stripping peak, indicative of the amount of exposed gold, was of Q = 112 ± 7 μC, corresponding to a spread of only 6%. It was then concluded that the four substrates were similar.

Even though the substrates were similar the polymerisation current transient for these same electrodes was irreproducible from device to device, as shown in Figure 4. 1b. The pattern followed by the curves is peculiar. It comprises two parts: first a very low current zone, followed by a rapidly increasing current. All four current transients followed this pattern. The irreproducibility originated from the time off-set for the large current to flow. For electrode 1 about 20 s were required to obtain a significant current, much less than for electrode 4 (about 60 s).

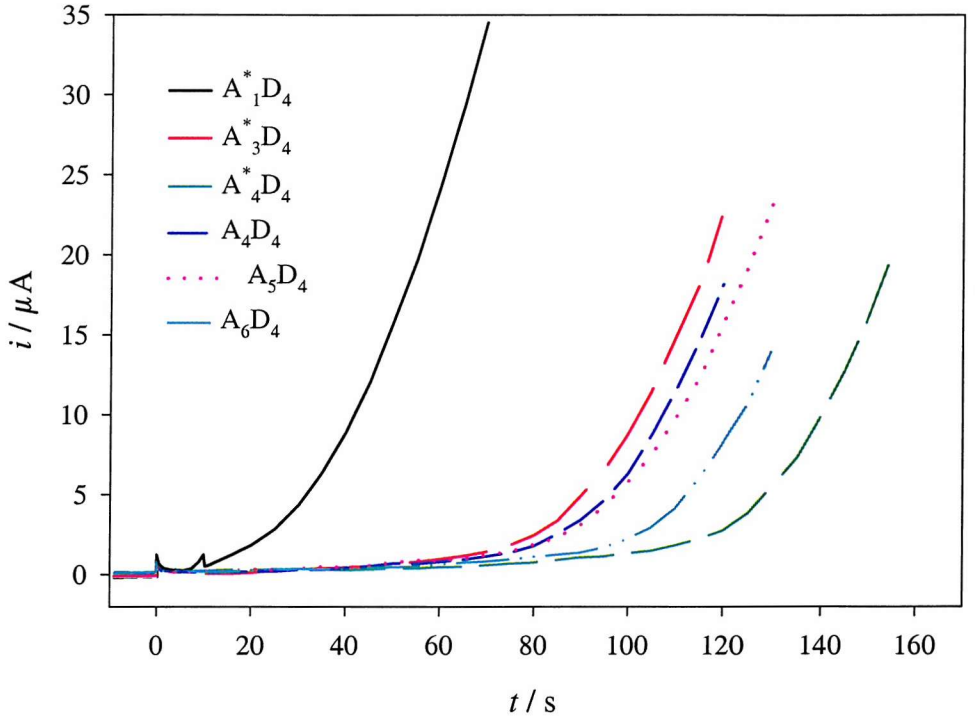

Figure 4. 2: current transients for electropolymerisation of poly(aniline) pentane sulfonate onto six gold array devices SRL131 (250 μm by 250 μm) showing the irreproducibility of the electropolymerisation.
The electropolymerisation conditions are the same as Figure 4. 1.

This behaviour was not characteristic of all polymers. For example it was not observed for poly(pyrrole) films nor for poly(aniline) decane sulfonate. This pattern of

electropolymerisation was also observed for other electrode types, as shown in Figure 4. 2. In general, this behaviour was observed with electrodes of small size (500 μm by 500 μm and below), but not on large ones (eg SRL123).

4.1.1.2.2 - Discussion

Assuming that the difference in electrode area between two substrates is small enough to imply no change in polymerisation mechanism, the current density transients for the polymerisation onto two substrates with a slight difference in surface area are expected to be identical. The pattern observed during the irreproducibility of the deposition behaves differently, which implies that it is not due to a simple variation in electrode area.

It could be argued that the irreproducibility of the growth comes from the presence of by-products from previous polymerisation in solution varying the rate of electropolymerisation. This possibility is ruled out by the fact that this phenomenon was observed on SRL131 devices (Figure 4. 2), array devices using the micro-deposition technique. For these substrates, the electropolymerisation solution was renewed for each deposition, and therefore free of by-products (but still from the same preparation implying no change in composition).

A simple view of the deposition mechanism of conducting polymers is a nucleation mechanism followed by the growth of the nuclei, corresponding to the low current region and the rapidly increasing current respectively in the transient, Figure 4. 1b. The delay in the deposition would then correspond to a change in the nucleation rate, the nucleus growth being itself reproducible. The reason why a nuclei would form at one location on the electrode and not at another one is not yet clear. It can be due to an impurity adsorbed onto the electrode, a defect or a certain crystal plane of the metal. In other words, the nucleation of polymer appears to be a random process, which could explain the irreproducibility of the electrodeposition observed for poly(aniline) pentane sulfonate onto electrodes of small size. Unfortunately, there is at the moment no way of predicting, or controlling, this nucleation.

The irreproducibility of the deposition onto small size electrodes, behaviour not observed for electrodes of larger size, can be explained by the lower probability to have one nucleus on the electrode at a given time with decreasing the size of the electrode. In addition, the

irreproducibility in nucleation may be enhanced by the fastest diffusion of oxidation products away from the electrode in the case of a microelectrode (for example SRL131) than for macroelectrodes (in this case SRL123).

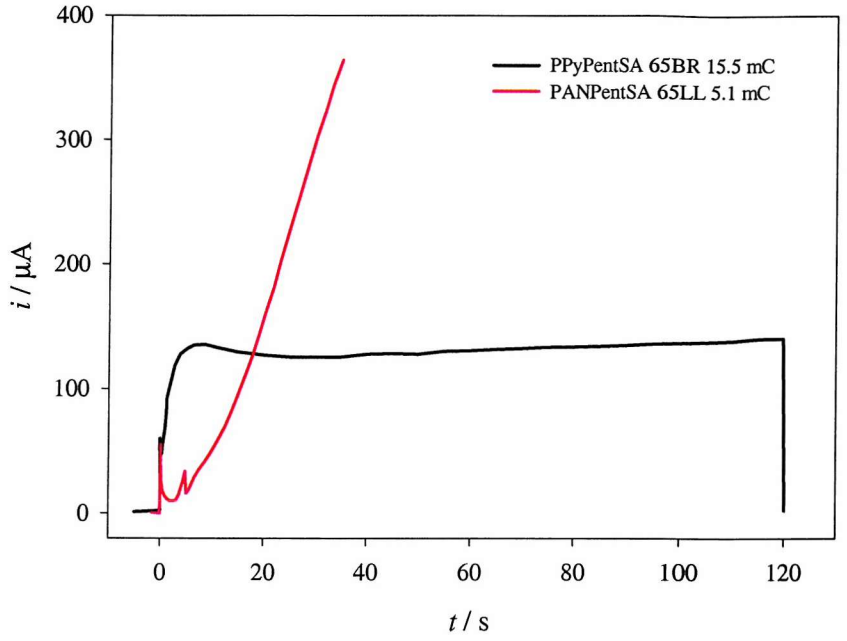

Figure 4. 3: typical current transients for the electropolymerisation of poly(pyrrole) pentane sulfonate and of poly(aniline) pentane sulfonate onto SRL123 devices (1 mm^2) illustrating the different behaviour in electropolymerisation for the two polymers.
a – 0.1 M pyrrole, 0.1 M pentane sulfonate in H_2O; + 0.85 V for 120 s.
b – 0.5 M aniline, 0.5 M pentane sulfonate acid in 2 M H_2SO_4; + 0.9 V for 5 s followed by + 0.78 V for 30 s.

Random nucleation was not observed during the electrodeposition of poly(pyrrole) films, even on devices of small size. Figure 4. 3 compares a typical current transient for the electropolymerisation of poly(aniline) pentane sulfonate and for poly(pyrrole) pentane sulfonate films, illustrating the difference in electropolymerisation mechanism and rate for these two polymers. As already seen for poly(aniline) films, little current flows at first, followed by a sudden and continuous increase. During oxidation and polymerisation of pyrrole, the current rises rapidly and remains relatively constant during the whole potential step. The rapid rise in current seems to indicate a fast nucleation in contrast to poly(aniline). This difference in nucleation could explain the better reproducibility from sensor to sensor in the case of poly(pyrrole) growth.

4.1.2 - A new electrodeposition technique: use of *in-situ* resistance measurement

4.1.2.1 - Description of the technique

Due to the lack of reproducibility of the electrodeposition of conducting polymers, in order to follow the nucleation and polymerisation, a bipotentiostat was set-up to monitor the resistance of the polymer film *in-situ*. The equipment used was described in Chapter 2.

In the previous electropolymerisations onto chemoresistor devices a mono-potentiostat was used. Both halves of the device were connected together and a constant voltage was applied for a fixed time. This procedure led to a thick film with little control over the amount deposited onto the electrode.

In the new set-up, both half-electrodes of the device were connected independently to each channel of a bipotentiostat. Figure 4. 4 represents the logic used in the program controlling the bipotentiostat. Electropolymerisation was still performed by potential step, but the potential step is interrupted at regular interval to measure the resistance of the film in the solution. As a minimum time was required for the polymer to nucleate, grow and start crossing the gap, the potential was applied for a large step duration t_1 (typical value of 30 s). Just before interrupting the polymer growth by turning the cell off, the potential of electrode 2 was decreased to (E_{Elec} – 20 mV) while electrode 1 remained at the potential E_{Elec}. To minimise polarisation of the film only a small potential difference was applied between the two working electrodes (typically 20mV), and that for a duration in the millisecond range, time required to perform the resistance measurement. This short measurement time was also minimising chemical reactions and diffusion process which occurred during the loss in the control of the electrode potential. The current flowing through the polymer film was measured, as well as the exact potential difference between the electrodes. The resistance was calculated using ohm's law[1]. If the polymer film resistance was below the target value the polymerisation was stopped. Otherwise the potential of the working electrode 2 was reset to E_{Elec}, the cell was reconnected and polymerisation resumed. Further resistance measurements were carried out until the control point was reached. A typical value for t_2 (frequency of the resistance

[1] Bartlett *et al.* [5] and also Harris *et al.* [6] reported that conducting polymers show an ohmic behaviour for small applied voltages.

measurement) was one measurement every 2 s as it was found to allow good control of the final resistance.

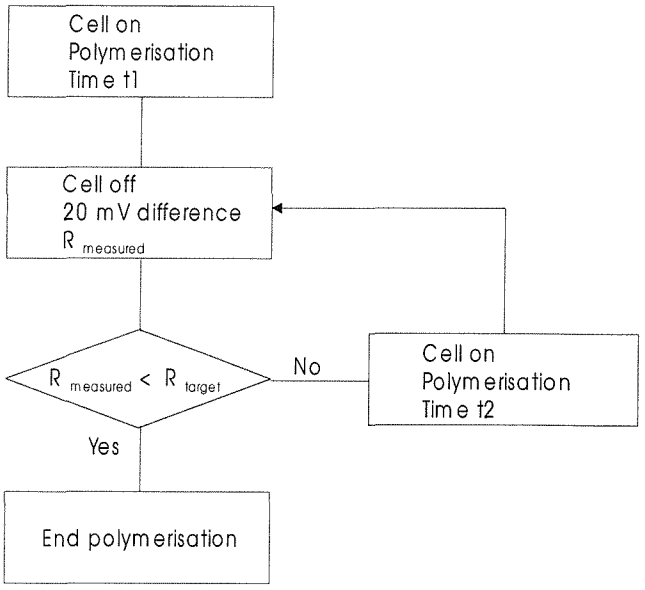

Figure 4. 4: diagram representing the logic used to electrodeposit conducting polymer onto micro-gap devices, measuring the resistance of the film at regular interval until the target resistance is reached.

4.1.2.2 - Discussion of the technique

The principle of the *in-situ* resistance measurement has already been employed by many researchers in more or less complex ways [4,7-9]. In this work, the technique selected to measure the resistance was straightforward, applying a small voltage across the polymer film and measuring the current flowing across the insulating gap of the chemoresistor.

The first one was described by Nishizawa [9]. As just described, the two electrodes are independently connected to a bipotentiostat but the small potential difference is applied during the whole polymerisation process. The advantage of this technique, in addition to employing classical equipment, is that it allows detection of the exact moment where the gap is crossed. It was observed that under these conditions the current behaved similarly for the two electrodes, the amplitude of the current being slightly larger for the electrode at the higher potential (electrode 1) until the polymer crossed the gap. Then the current on electrode 1 increased significantly, whereas on electrode 2 the current decreased significantly. At this point the polymer film made contact between the two electrodes of the micro-gap device which then behaved like a single electrode maintained at a mean potential. This method is an efficient way to estimate the time required for the film to cross the gap since a significant change in behaviour occurs when the gap is crossed.

However it is unsuitable for the production of conducting polymer gas sensors as the resulting film is asymmetrical (more polymer is deposited onto electrode 1 than electrode 2).

The technique used by Partridge [4] is more appropriate to the production of sensors. He used the principle of the four-point measurement to monitor R, applying a voltage between two external electrodes and measuring the current flowing through the polymer using two internal electrodes. With this procedure the contact resistance between the polymer and the electrode was eliminated making the resulting chemoresistor sensors more sensitive to vapours. However, this technique requires a more complex design for the substrate and more complex measurement electronics.

The *in-situ* resistance measurement technique set up in this work remains fairly simple. In order to conclude whether it is beneficial for our application, the technique was evaluated using a dummy cell (network of resistors) and then applied to the deposition of polymers.

4.1.2.3 - Evaluation with a dummy cell

The *in-situ* resistance monitoring program was evaluated using the dummy cell shown in Figure 4. 5, where R represents the solution resistance (typically 100 Ω) and R_1 and R_2 the charge transfer resistances which determine the currents flowing at the electropolymerisation potential for electrodes 1 and 2 respectively (equal in value as both electrodes are equivalent). Typical electrodeposition currents in our experiments are about 10 μA, corresponding to a voltage of about 1 V (typical potential for electropolymerisation) across a resistance of 10^5 Ω (R_1 and R_2). R_p represents the resistance of the polymer film, measured each time the electropolymerisation is interrupted. Maximum values of R_p were about 10 kΩ, and minimum values not less than 100 Ω.

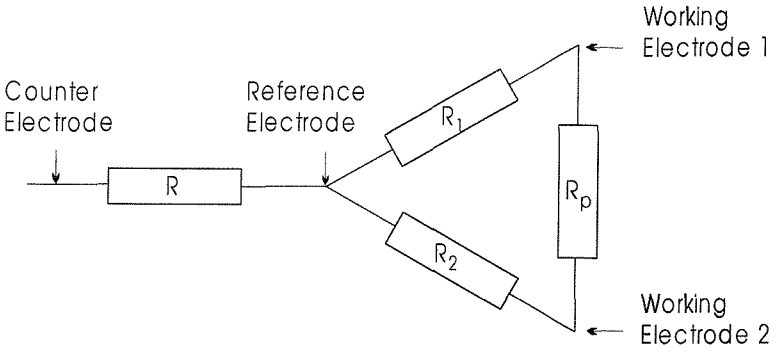

Figure 4. 5: Diagram of the dummy cell used to simulate polymer growth and *in-situ* resistance measurement. R_1 and R_2 are representative of the current flowing during the electropolymerisation at the electrodeposition potential and R_p the resistance of the polymer film. R is the electrolyte resistance.

$R_1 = R_2 = 100\ 000\ \Omega$			$R_1 = R_2 = 10\ 000\ \Omega$		
$R_{p\ expected}/\ \Omega$	$R_{p\ measured}/\ \Omega$	Error/ %	$R_{p\ expected}/\ \Omega$	$R_{p\ measured}/\ \Omega$	Error/ %
99.3	99.6 ± 0.8	0.3	99.2	98.7 ± 5	-0.5
328.7	330 ± 2.5	0.4	329.2	323 ± 2	-1.9
999	983 ± 7	-1.6	1004	998 ± 9	-0.6
4677	4520 ± 57	-3.4	4676	4512 ± 57	-3.5

Table 4. 1: Values of the resistances of the "polymer" in the dummy cell. $R_{p\ expected}$ is the expected value (measured with a multimeter), $R_{p\ measured}$ the resistance measured using the bipotentiostat expressed within 95% confidence. The error in the measurement is the error between the measured value and the expected value. The results are given for two values of $R_1 = R_2$, simulating the current flowing during polymerisation (different polymerisation currents are obtained for different polymers or electrode sizes).

The program written to perform polymerisation was tested with the dummy cell. For each configuration (R_1=R_2 and R_p couples) the resistance of R_p was measured 11 times and determined within 95% confidence. The results are shown in Table 4. 1.

Table 4. 1 shows that the technique is able to measure the resistance of R_p with good precision as the error is inferior to 5% in all cases. At relatively high R_p values, the error on the measurement increases. The systematic error is due to a zero offset error in the ADC measurement channels for the small currents measured. These experiments were performed in absence of a Faraday cage. Preliminary results show that the spread in the measured resistance (95% interval) could be significantly reduced using a Faraday cage.

4.1.2.4 - Evaluation with conducting polymer

The results obtained by the *in-situ* resistance monitoring method were satisfactory on a dummy cell. The next step was to investigate the behaviour on a real electrochemical system. The *in-situ* resistometry technique was tested by electrodepositing poly(aniline) pentane sulfonate onto SRL123 or SRL127 substrates. The experiments to evaluate the technique had to be performed onto dual micro-gap devices and it was therefore necessary to strike a compromise between using a large number of devices to obtain a complete statistical study and keep a number of devices to a minimum due to their limited availability. This explains why this study may not be as complete as necessary in some cases.

Originally, the poly(aniline) films were deposited from a 0.5 M aniline solution. In these conditions, to reach a target resistance of 100 Ω, less than 30 s were required. In order to gain a better control on the electrodeposition, the rate of polymerisation was decreased by reducing the concentration of aniline to 0.2 M. The electrolyte and electropolymerisation potentials were kept the same.
Electropolymerisation was undertaken from a 0.2 M aniline, 0.5 M pentane sulfonate solution in 2 M H_2SO_4 for all experiments reported in the following sections. The potential was first stepped to + 0.9 V for 5 or 10 s, followed by a step to + 0.78 V. The target polymer resistance was determined by trial and error. A range of films with a target resistance between 50 and 200 Ω were grown and inspected under the microscope. The correct target resistance should produce a thin film with full coverage of the gap.

Figure 4. 6 shows a typical curve obtained during electropolymerisation using the *in-situ* resistance measurement. The middle plot shows the current transients for the electropolymerisation onto the working electrodes (both halves of the dual micro-gap device). Both electrodes were exposed to the same potential sequence, giving similar currents. The slight difference in current may be due to a slight difference in the size of the two electrodes or in the zero current offset of the two channels of the bipotentiostat. In the bottom part is plotted the transient for the resistance of the polymer, measured across the gap every two seconds. For the first thirty seconds, the resistance was not monitored as the polymer film resistance was far from the target value.

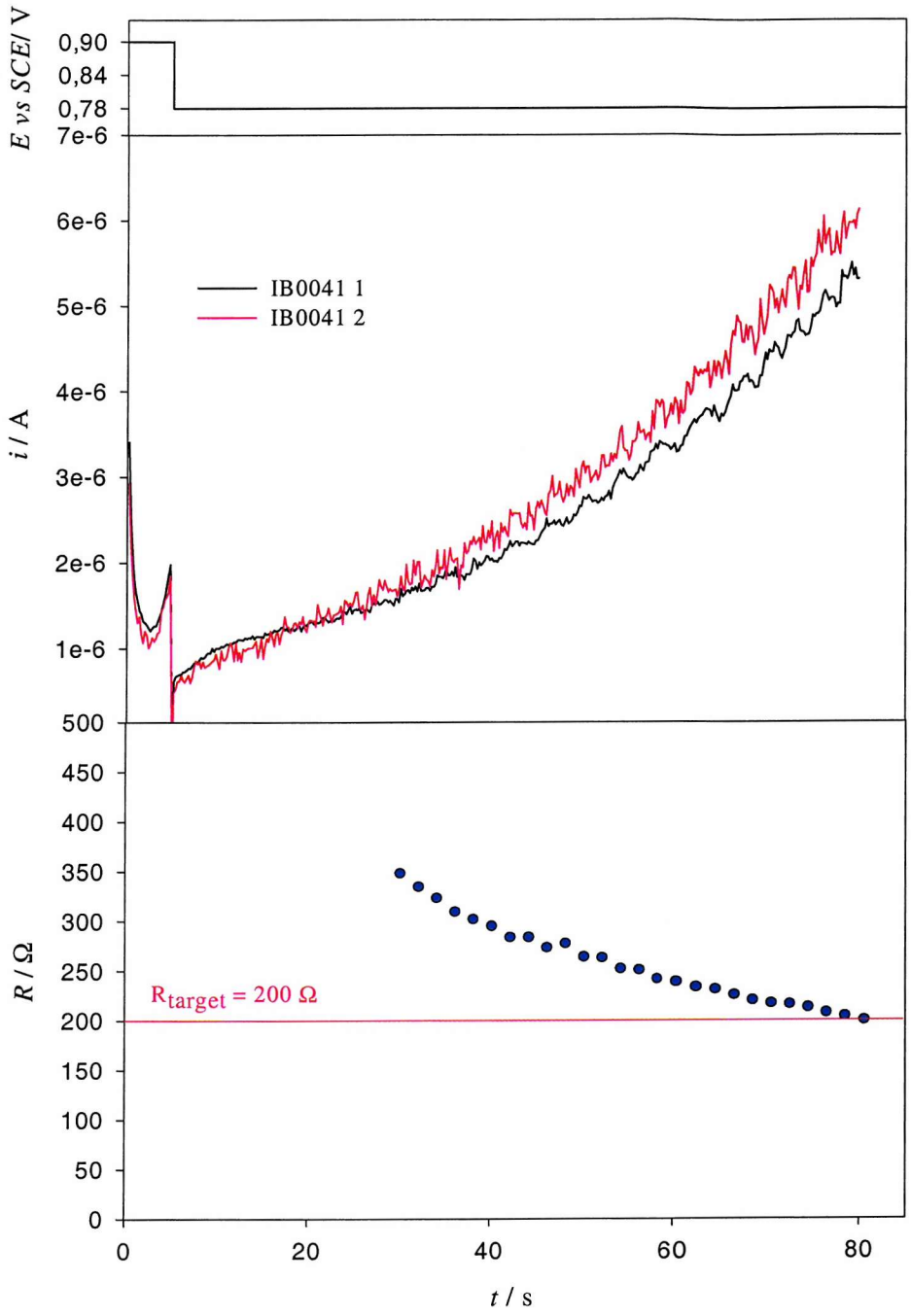

Figure 4. 6: typical current transients (both working electrodes are shown in the middle graph) for the electrodeposition of poly(aniline) pentane sulfonate onto SRL127 together with the potential applied (top graph) and the resistance of the resulting film (device IB0041) (bottom). The solution was 0.2 M aniline, 0.5 M pentane sulfonate in 2 M H_2SO_4, + 0.9 V for 5 s followed by + 0.78 V for 25 s with one resistance measurement every 2 s (here 26 resistance measurements) until the target resistance (200 Ω) was reached.

4.1.3 - Results of the *in-situ* resistance monitoring technique

The equipment has been shown to be able to monitor *in-situ* the resistance of polymer films during the electrodeposition. Before employing this method to produce gas sensors a

study was carried out to see if the interruption of the polymerisation significantly modified the properties of the film, which would then influence its sensing properties. To what extend this method produces in an improvement in the reproducibility of the dry polymer film was also evaluated.

4.1.3.1 - Electropolymerisation and resistance

4.1.3.1.1 - Current transient

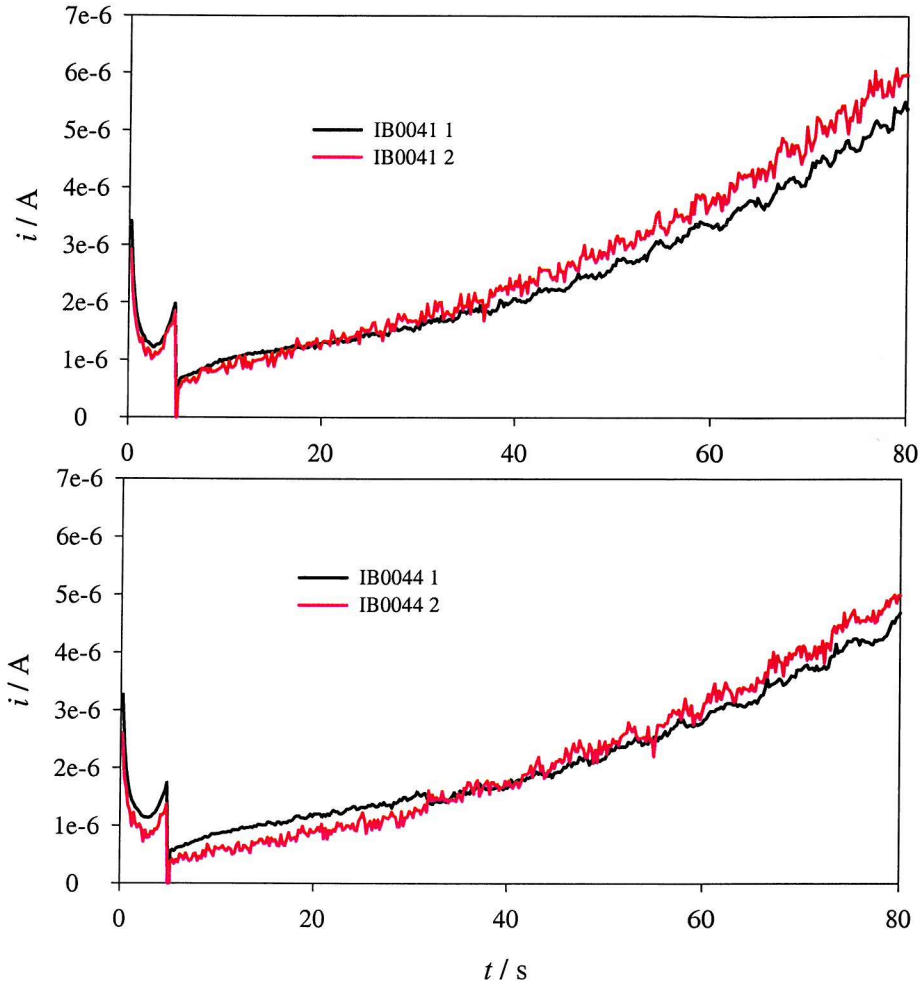

Figure 4. 7: current transients for the electropolymerisation of poly(aniline) pentane sulfonate onto SRL127 devices with the *in-situ* resistance measurement (top-device IB0041) and without (bottom- device IB0044) using in both cases a bipotentiostat.

In order to compare films grown with and without the *in-situ* resistance measurement the following experiment was performed: a first batch of films were grown using the *in-situ* resistance measurement. The electropolymerisation time for these devices was averaged and a second batch of polymers was grown using a "classical" method for a fixed time (the average polymerisation time for the first batch) under the same experimental conditions.

Figure 4. 7 compares typical current transients obtained in the two cases. Within the random nucleation no major difference was observed between the films grown using the new set-up and the films deposited in a classical manner.

4.1.3.1.2 - Film resistance

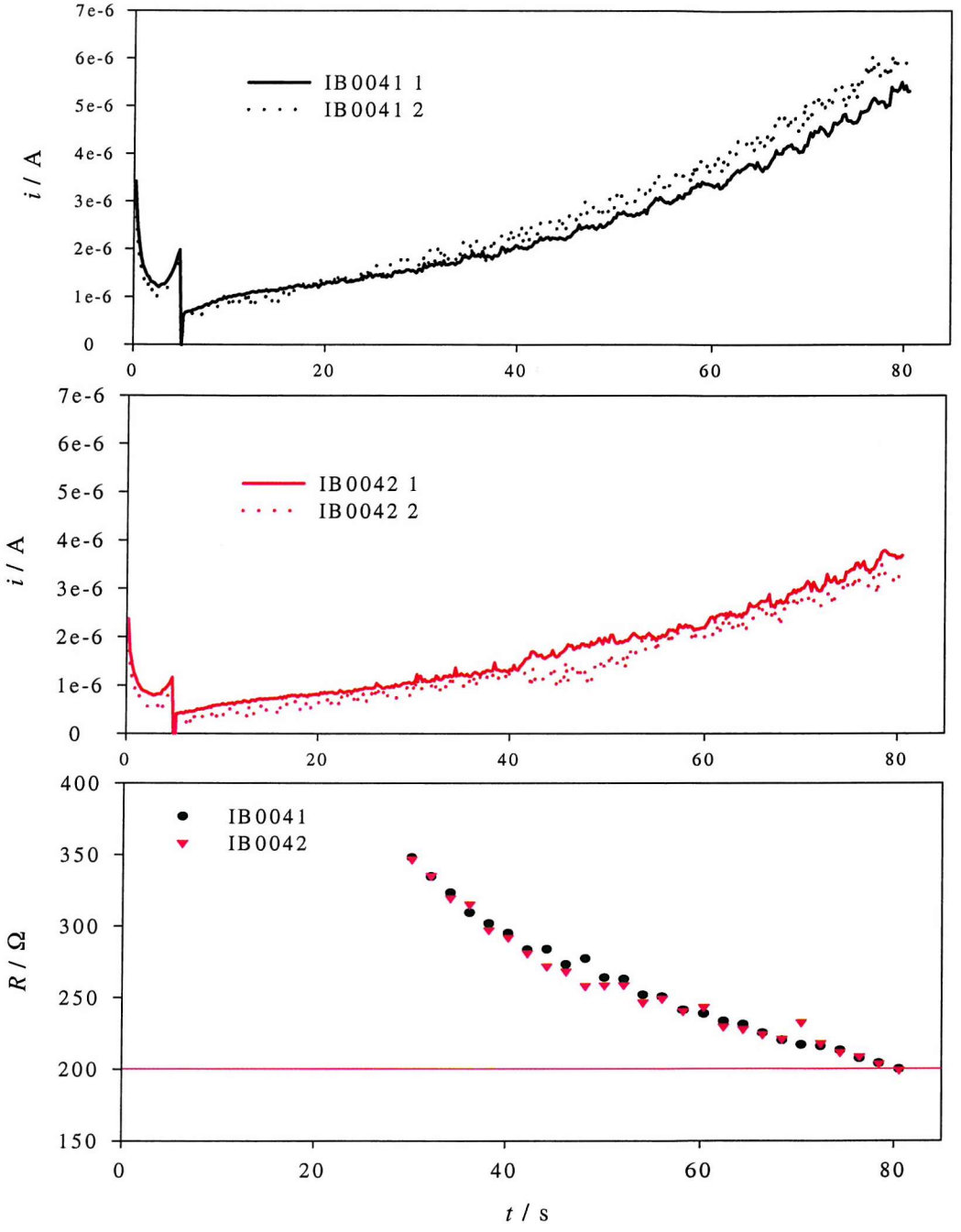

Figure 4. 8: current transients for the electrodeposition of poly(aniline) pentane sulfonate onto two SRL127 devices used in the same conditions (top, device IB0041, bottom, device IB0042) and the resistance of the resulting films. These plots show the irreproducibility of the electropolymerisation but the reproducibility of the resistance (199.9 and 199.5 Ω for IB0041 and IB0042 respectively).

Due to the inherent properties of poly(aniline), the current transients for the electropolymerisation were not reproducible from device to device, even used in the same conditions, as illustrated in Figure 4. 8. This figure also illustrates that the resistance of the wet film could be reproduced with a precision higher than one ohm, which consists in a major improvement. However this same conclusion can not be drawn for the dry coatings as the resistance will vary upon disconnection of the electrochemical cell and upon drying.

Before investigating in detail the resistance measurement, it is interesting to comment on the shape of the resistance transient during polymerisation. Typical current and resistance transients are shown in Figure 4. 9. These two graphs can be converted into one, where the conductance of the film is given as a function of the polymerisation charge (Figure 4. 10). Assuming that the density of the polymer is constant, the charge is linearly related to the thickness of the film[2].

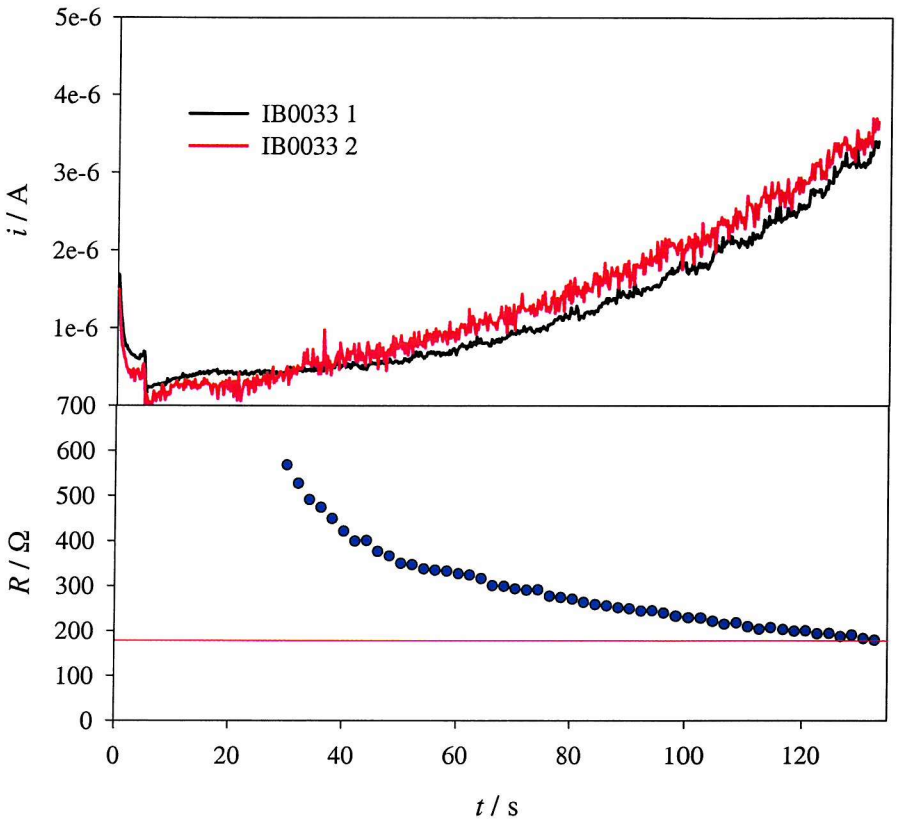

Figure 4. 9: current and resistance transients for a poly(aniline) pentane sulfonate film onto a SRL127 substrate (R_{target} = 180 Ω) showing the behaviour of the resistance over a long time. Device IB0033.

[2] Desilvestro [10] has reported that the morphology of poly(aniline) varies with the film thickness, the film being less dense for films thicker than 150 nm, so that this assumption may not be fully correct.

From Figure 4. 10, three distinct regions can be defined during the polymerisation. By extrapolating the curve to the X axis, a first section can be observed, where polymerisation takes place but the conductance of the film remains zero. This corresponds to charges from 0 to about 15 μC (or 60 μC mm^{-2}) and corresponds to the minimum amount of polymer required to first cross the insulating gap. In a second section, the conductance of the film across the gap increases rapidly for small increases in polymerisation charge. This corresponds to the growth of the film across and covering the gap. Finally, in the third region, the conductance increases less rapidly as a large amount of polymer is deposited. This corresponds to the thickening of the film. The contribution of additional polymer on the resistance is then less significant.

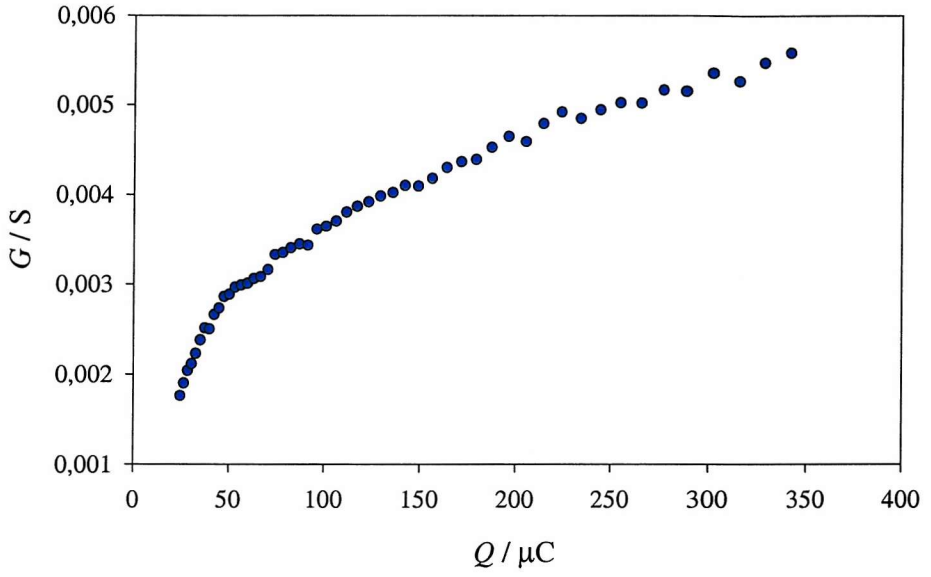

Figure 4. 10: conductance of a poly(aniline) pentane sulfonate film as a function of the polymerisation charge measured in the growth solution close to the electrodeposition potential- data from Figure 4. 9.

Another interesting point is to investigate the variation of resistance from the value measured during the deposition (close to + 0.78 V) and the value at equilibrium in the electrolyte. Once at open circuit, the potential of the polymer relaxes to reach an equilibrium value around + 0.5 V, corresponding to a decrease in resistance by a factor of 3. Figure 4. 11 shows how the resistance of a poly(aniline) film varies with the potential, similar results having already been reported for poly(aniline) [11] and for poly(pyrrole) [7]. This plot is also useful for interpretation of the gas test results, when the interactions between a strongly oxidising (or reducing) vapour and such a polymer are considered. By changing the polymer oxidation state, the vapour can significantly vary the resistance of the coating leading to a large response of the polymer gas sensor. This will be discussed further when the response to NO_2 will be analysed in the second part of this chapter.

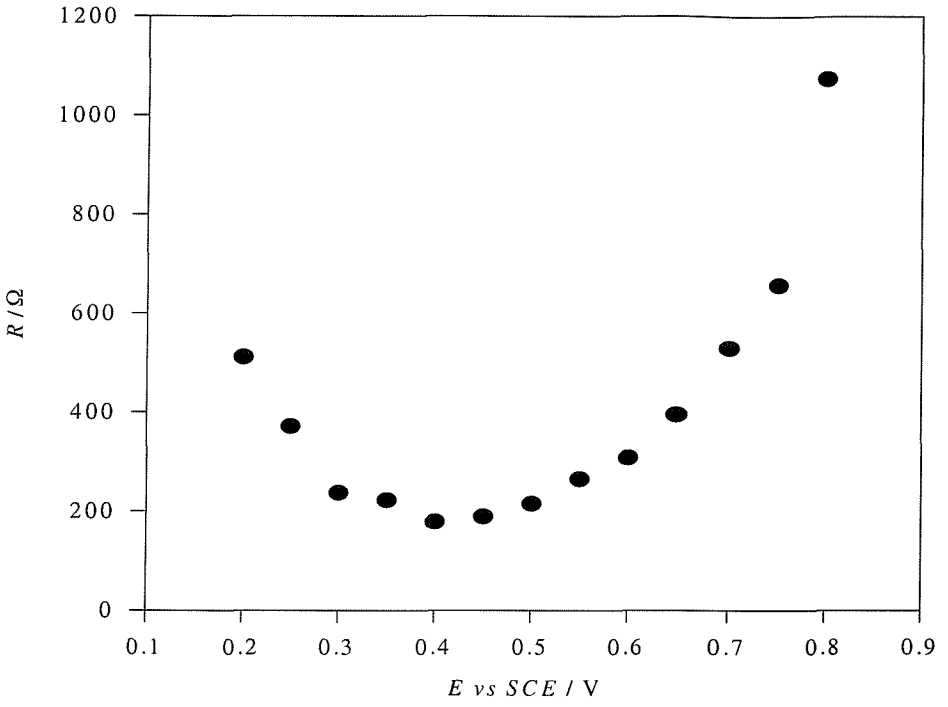

Figure 4. 11: resistance of a poly(aniline) pentane sulfonate film (SRL123 substrate) as a function of the electrode potential in 0.5 M pentane sulphonate in 2 M H_2SO_4. The polymer was obtained under similar conditions to the film shown in Figure 4. 6. The potential was controlled by the bipotentiostat, which also measured the resistance.

In the previous section, it was shown that the interruption of the electropolymerisation to perform the resistance measurement had little effect on the current transient. The second stage of the evaluation of the technique is to see if the reproducibility in the final resistance of the sensors is increased. For this purpose the experiment already described in the previous section was performed. Six sensors were produced with the resistance measurement technique and four sensors in the classical manner. Table 4. 2 gathers the values of the resistances of the resulting films measured in the electropolymerisation solution and in air, and their values within 95% confidence. The difference for the wet films, whether grown with resistance monitoring or in the classical manner, was not significant. The resistances were spread by 20% and 22% respectively for these two methods. However the results from the dry films were conclusive. Whereas the resistance of the films deposited using the *in-situ* resistance measurement technique was spread of 50%, the resistance of the films deposited by classical potential step varied by a factor of two.

	R_t = 200 Ω						Fixed time			
Device	1	2	3	4	5	6	7	8	9	10
Ref.	CR0040	CR0041	CR0042	CR0043	CR0045	CR0046	CR0047	CR0048	CR0049	CR0050
R_{wet}/Ω	37	44	31	52	44	34	33.7	35.3	26.7	27.6
R_{wet}/Ω 95%	40.3 ± 8.1						30.8 ± 6.8			
R_{air}/Ω	214	137	96	105	94	-	545	1355	382	210
R_{air}/Ω 95%	129 ± 63						623 ± 806			

Table 4. 2: resistance of poly(aniline) pentane sulfonate films (SRL123 substrates) measured in the growth solution at open circuit after polymerisation (R_{wet}) and in air 3 days after polymerisation (R_{air}). Devices 1 to 6 were produced using the *in-situ* resistance measurement technique, whereas devices 7 to 10 were produced using a classical potential step (total polymerisation time of 102 s, average of the polymerisation time for the devices 1 to 6).

In addition to the spread of the resistance, another interesting feature is the variation of the resistance upon drying. The resistance of the wet films is higher for the films deposited using the resistance monitoring technique compared to the classical method yet lower for the dry film. This implies that the resistance of the polymer deposited using the *in-situ* resistance measurement technique is more stable upon drying than the resistance of the film deposited in a classical manner. The average resistance increased from 40 to 129 Ω using the new technique, against a change from 30,8 to 623 Ω for the classical method. The same conclusion was reached for another batch of sensors produced onto SRL127 substrates.

A similar behaviour was observed during gas test experiments as shown by Table 4. 3. Over five days of experiments, the drift in the base resistance of sensors produced using the *in-situ* resistance measurement (method a) was less than 2%, whereas it was between 8 and 24% for the sensors produced in a classical manner (method b). For films produced using the original condition (classical potential step with a high monomer concentration, method c), the resistance drift was even more important.

No explanation is available for this increase in stability of the poly(aniline) films induced by interruption of the polymerisation, as revealed by a higher stability of the base resistance. Sabatini [12] reported an increase in long-range order, in stability and in electronic conductivity of poly(aniline) when a cathodic bias was applied during polymerisation. The experimental technique employed in Sabatini's work is similar to cyclic voltammetry in the sense that the polymer is switched between its oxidised and

reduced forms during polymerisation. During the redox process, the movement of ions and solvent molecules in and out of the film induces a rearrangement of the polymer. However this can not account for the increase in stability of the poly(aniline) in this work since the potential was maintained throughout the experiment close to the deposition potential so that the film remains in its oxidised state.

Reference	IB0042	IB0043	IB0044	IB0045	IB0046	IB0047	IB0048
$\Delta R/R_{ini}$ / %	0	- 1.5	- 9.0	+ 8.6	+24.0	+34.0	+22.8
Polymerisation conditions	a	a	b	b	b	c	c

Table 4. 3: relative change in the base resistance of poly(aniline) pentane sulfonate films during five days of gas tests. The sensors were exposed simultaneously to the vapours. Electrodeposition conditions:
a - 0.2 M aniline, 0.5 M pentane sulphonate in 2 M H_2SO_4. + 0.9 V for 5 s followed by + 0.78 V for 25 s and then one resistance measurement every 2 s until the target resistance of 200 Ω was reached. This corresponds to the *in-situ* resistance measurement technique.
b - 0.2 M aniline, 0.5 M pentane sulphonate in 2 M H_2SO_4. + 0.9 V for 5 s followed by + 0.78 V for 100 s, method "intermediate" between methods a and c[3].
c - 0.5 M aniline, 0.5 M pentane sulphonate in 2 M H_2SO_4. + 0.9 V for 10 s followed by + 0.78 V for 60 s. This corresponds to the original conditions.

The final optimised conditions for the deposition of poly(aniline) pentane sulfonate onto SRL127, regarding adhesion and film thickness, was, from 0.2 M aniline, 0.5 M pentane sulfonate solution in 2 M H_2SO_4, first step to + 0.9 V for 5 s followed by + 0.78 V for 25 s and then one resistance measurement every 2 s until the target resistance (200 Ω) was reached (typically 25 measurements). These experimental conditions give a slow polymerisation rate and a film with good mechanical properties. They produce sensors with fairly reproducible resistances which are also stable with time.

4.1.3.2 - Optical and Scanning Electron Microscopy

The influence of the *in-situ* resistance measurement on the morphology was investigated by optical observations and SEM (Scanning Electron Microscopy). The *in-situ* resistance measurement did not have any major effect on the visual appearance of the films when

[3] The polymerisation time should have been of 80 s for the sensors produced using the conditions b to be fully comparable with method a. However, due to an experimental error, the polymerisation time was increased to 105 s. The consequence was to have thicker films, but the results were still believed to be comparable.

observed under the optical microscope. Some samples on SRL127 substrates were characterised by Scanning Electron Microscopy (SEM). Figure 4. 12 a shows a poly(aniline) pentane sulfonate film of target resistance 200 Ω over the gold electrode, and Figure 4. 12 b over the 10 μm wide insulating gap (black band). The film appears to form a network of fibres. It is extremely thin and highly porous. Indeed the gold substrate can easily be seen through the polymer film. It is important to notice that the film uniformly covers the electrodes as well as the gap.

Two films of each type of polymers were observed by SEM- two films grown using the *in-situ* resistance measurement sequence and two films using the classical potential step method. The micrographs obtained were similar for each given type of polymer, as well as for both samples of poly(aniline). Therefore the *in-situ* resistance measurement has not influenced the polymerisation in a way which is evident in the morphology on the SEM scale.

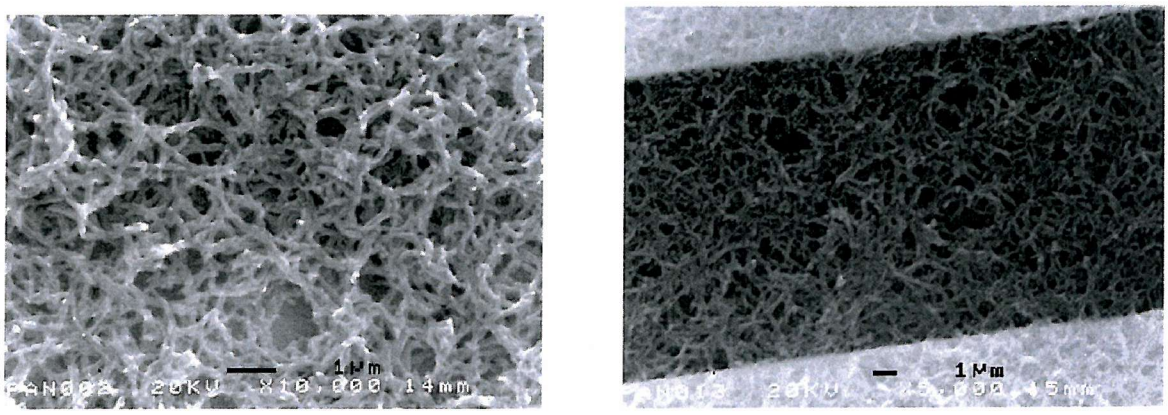

a b

Figure 4. 12: SEM micrographs of a poly(aniline) pentane sulfonate film (R_{target} = 200 Ω) grown onto SRL127

a) over the gold electrode

b) across the insulating gap (10 μm wide)

4.1.3.3 - Gas sensing property

4.1.3.3.1 - Sensor production

The aim of the *in-situ* resistance measurement technique was to improve the reproducibility of the response of the gas sensors. So after showing that the characteristics of the film were rather improved during the production using the in-situ resistance measurement, any eventual improvement in the gas response should be evaluated.

Eight sensors were placed in the gas test chamber and exposed to the same vapours under the same conditions. Table 4. 4 gathers together the polymerisation details for these sensors. Three sensors (devices 1 to 3) were produced using the *in-situ* resistance measurement (method a). Three other sensors (4-6) were electropolymerised from the same solution by the classical potential step method in order to see if there was any influence of the polymerisation interruption (method b). In order to evaluate any improvement of the resistance measurement, sensors 7 and 8 were produced using the original conditions: a classical potential step and a higher monomer concentration (0.5 M) (method c). All the sensors used the SRL127 device as substrate.

Sensor	Reference	Polymerisation conditions	Q / μC	$t_{polymerisation}$ / s
1	IB0041	a	414	80
2	IB0042	a	255	80
3	IB0043	a	284	82
4	IB0044	b	667	105
5	IB0045	b	700	105
6	IB0046	b	707	105
7	IB0047	c	4625	70
8	IB0048	c	4175	70

Table 4. 4: polymerisation conditions and results for poly(aniline) pentane sulfonate coated sensors used for the gas test experiments. See Table 4. 3 for the electropolymerisation conditions. The sensor number 1 was found to present a defect when used as gas sensor, so no results on the sensing properties will be presented here.

4.1.3.3.2 - Response to vapour

Preliminary gas test results are presented to evaluate any improvement of the *in-situ* resistance measurement technique. The first experiment was to expose the sensors to a change of humidity. Figure 4. 13 shows the response to an increase of 6706 ppm in water vapour for polymers produced using the *in-situ* resistance measurement (sensors 2 and 3) and compares it to the response obtained for sensors produced using the original electropolymerisation conditions (sensors 7 and 8). The transients present the same overall shape and the same response time, independent of the electropolymerisation technique used, both for the on and off responses. The main difference is that the response of the sensors produced by *in-situ* resistance measurement are more reproducible from sensor to

sensor. The amplitude of the response for sensor 8 is of about 50% of the response of sensor 7, whereas for sensors 2 and 3 the amplitudes are similar. The number of sensors tested here (two of each type) was encouraging but not statistically significant.

To see if the interruption of the electropolymerisation had any effect on the response, the response of sensors 2 and 3 (produced by *in-situ* resistance monitoring) were compared to the response of sensors 4 to 6 (also thin films but produced in a classical manner)- see Figure 4. 14. Both types of polymers presented similar amplitudes of response, similar response times and similar reproducibility from sensor to sensor.

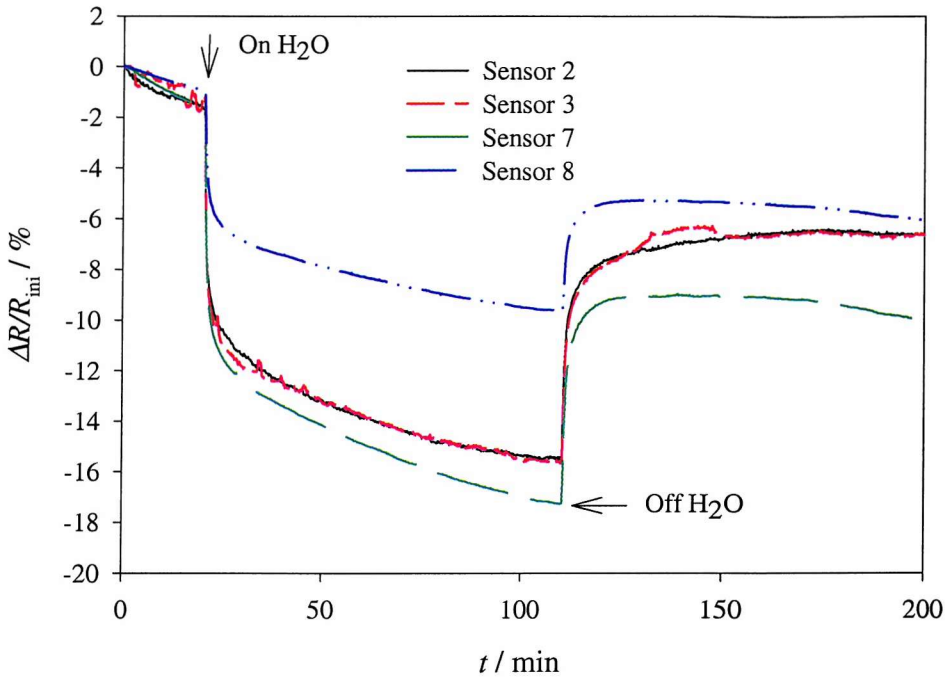

Figure 4. 13: response to a change of 6706 ppm in water vapour (from 6706 to 13412 ppm) for poly(aniline) pentane sulfonate films of target resistance 200 Ω (sensors 2 and 3) and for films deposited using the original electropolymerisation conditions (sensors 7 and 8).

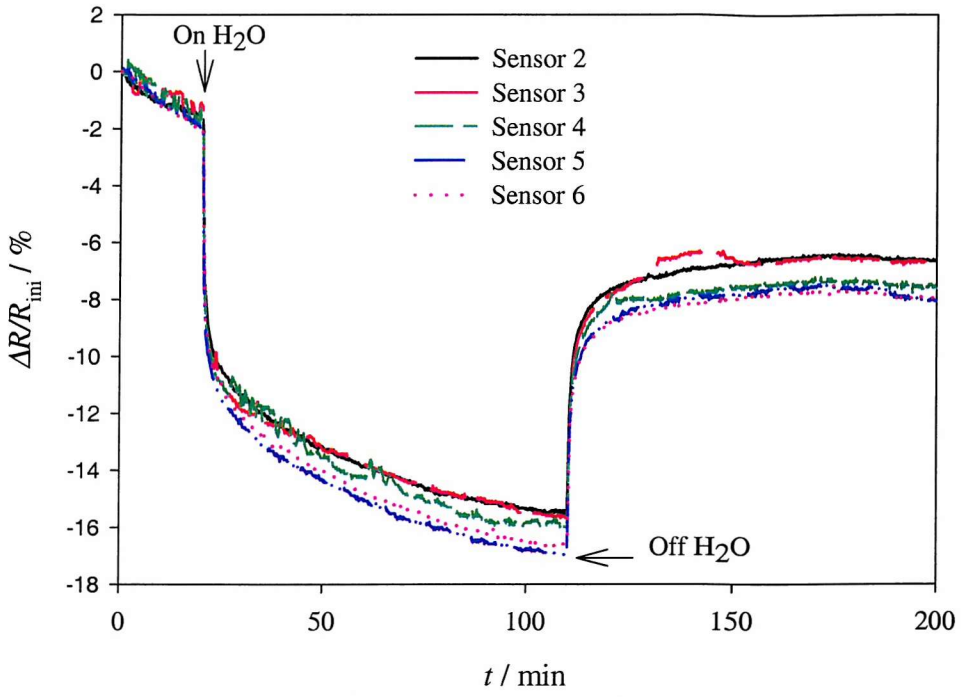

Figure 4. 14: response to a change of 6706 ppm in water vapour (from 6706 to 13412 ppm) for poly(aniline) pentane sulfonate films of target resistance 200 Ω (sensors 2 and 3) and for films deposited using the "intermediate" method (sensors 4, 5 and 6).

The response of the poly(aniline) films to ethanol vapour was also investigated. Figure 4. 15 shows the response to 32937 ppm ethanol for sensors 2, 3, 7 and 8. For water, it was shown that the shape of the transient was independent of the electrodeposition technique employed, which is not the case upon exposure to ethanol. The time required to reach saturation is much larger in the case of the thicker films. After 110 min exposure to vapour, the films produced using the original method reach about 90% of the response at saturation, whereas the other films have a t_{90} of about 50 min. The amplitude at saturation was consistent with the behaviour upon exposure to water: the amplitude was the same for sensors 2, 3 and 7, and the amplitude of the response of sensor 8 was 50% of the response of sensor 7.

Figure 4. 16 shows the response upon exposure to ethanol for thin poly(aniline) films deposited whether by *in-situ* resistance measurement or using the "intermediate" technique. The conclusions are similar to the conclusions drawn from the exposure to water vapour: there is no major difference between the films polymerised with interruption of the growth and those polymerised without interruption.

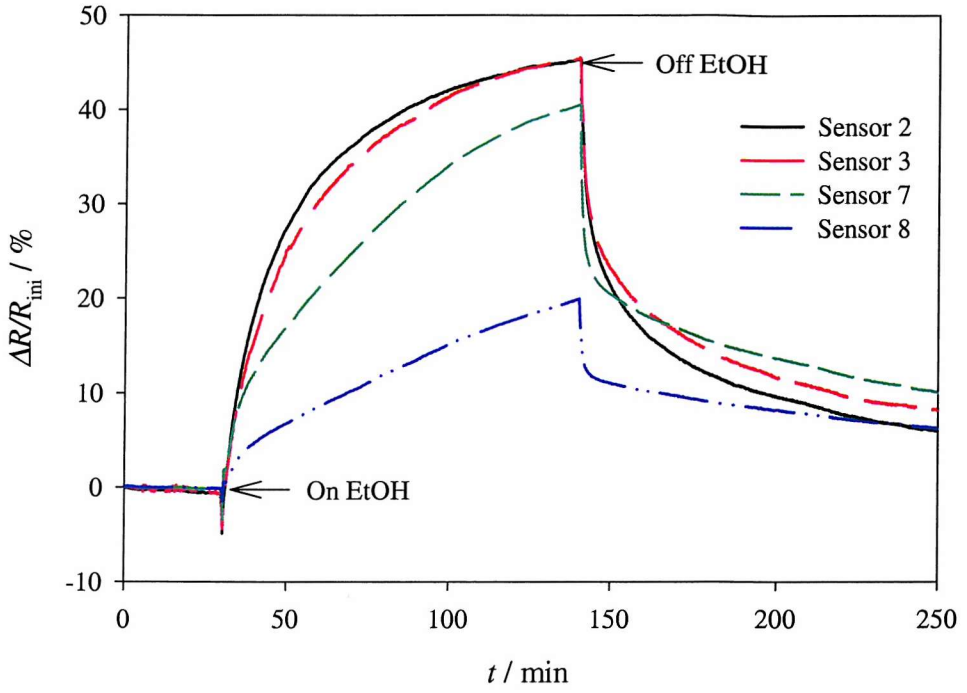

Figure 4. 15: response to exposure to 32937 ppm ethanol vapour for poly(aniline) pentane sulfonate films of target resistance 200 Ω (sensors 2 and 3) and for films deposited in the original conditions (sensors 7 and 8), at 6706 ppm humidity.

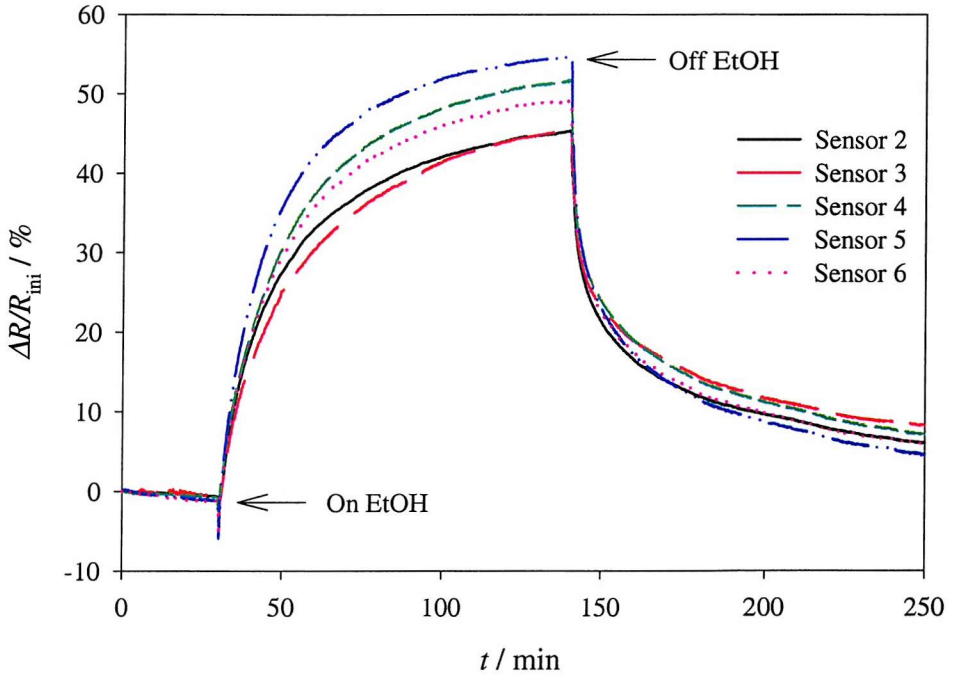

Figure 4. 16: response to exposure to 32937 ppm ethanol vapour for poly(aniline) pentane sulfonate films of target resistance 200 Ω (sensors 2 and 3) and for films deposited using the "intermediate" method (sensors 4, 5 and 6), at 6706 ppm humidity.

An aspect, hidden from the results presented here is that the *in-situ* resistance measurement method consists in a major improvement from the engineering point of view. By growing the polymers thinner, the base resistance has been increased (from about 100 Ω for sensors 7 and 8 to 1kΩ for sensors 1 to 6) and the ratio of signal to noise in the measurement is increased. Indeed, the results just presented show that the response to gas $\Delta R/R_{ini}$ is roughly independent of the deposition technique and of the initial resistance. So if $\Delta R/R_{ini}$ is, for example, of 10%, then by increasing the initial resistance from 100 Ω to 1000 Ω, the measured signal is increased from 10 Ω to 100 Ω. In other words the measured output voltage is multiplied by 10 and the measurement electronics then become less sensitive to noise.

4.1.3.4 - Conclusions on the *in-situ* resistance monitoring

To overcome the lack of reproducibility from sensor to sensor occurring during the electrodeposition of conducting polymers, a new technique was developed and tested. Using a specially designed bipotentiostat, the resistance of the polymer film can be monitored *in-situ* during polymerisation. The technique consists in interrupting the electropolymerisation at regular intervals and measuring the resistance of the film until a target resistance is reached.

A detailed study was performed on poly(aniline) pentane sulfonate. It was shown that the interruption of the electropolymerisation did not have any major influence on the current transient or on the morphology of the film on the SEM scale. The improvements induced by the use of the *in-situ* resistance measurement technique were significant. It was found that the *in-situ* resistance measurement produced a higher stability with time in the base resistance of the chemoresistor. Most important, this technique enables the growth of thinner films in a more reproducible manner, which is reflected by a faster and more reproducible gas response as shown in Figure 4. 15.

However, if compared to the "intermediate" technique, the improvement of the *in-situ* resistance measurement technique in the study performed here appears less significant. Indeed, whether the resistance was monitored during deposition or not, the sensing properties are similar. This would imply that the *in-situ* resistance measurement is not required because, as long as a low monomer concentration is employed, the control on the

electropolymerisation is high and the results are comparable. Assuming that the electrodeposition is reproducible from sensor to sensor, the technique employed by Nishizawa [9] would be sufficient to determine the optimal electrodeposition conditions. By the sacrifice of some devices, the time required for the polymer to cross and cover the gap can be determined and applied for the production of gas sensors.

In chapter 3 it was shown that the deposition onto array devices using the micro-deposition technique was highly irreproducible, more irreproducible than the poly(aniline) pentane sulfonate illustration given here. So, whereas the improvement brought by the *in-situ* resistance measurement is not significant here, it is expected that it will be more beneficial when polymerising onto array devices. Therefore the next step would be to extend the *in-situ* resistance measurement to the electropolymerisation onto array devices, as well as to apply the technique to other conducting polymers.

4.2 - Investigation of new sensing materials

Poly(pyrrole) and poly(aniline) doped with a range of anions

In the previous chapter and in the previous section of this chapter it has been shown that the substrate and the electropolymerisation technique could be improved to give sensors of better quality. A third goal was to improve the gas sensitive material. By investigating new sensing materials, one or more aspects like the amplitude of the response, the response time, the specificity to certain vapours, the recovery time and the stability of the sensor baseline may be improved[4].

4.2.1 - Discussion of the choice of the vapour sensitive material

All the polymer coatings investigated here were limited to poly(aniline) and poly(pyrrole) films. These polymers were selected as they have shown suitable sensing properties and they can be deposited from aqueous solutions[5]. Limiting oneself to two polymers does not imply being limited to two coatings. Indeed it is well known that the properties of a conducting polymer film depend on the monomer, on the electrode material [13], on the electrochemical method employed (potential step, cyclic voltammetry or galvanostatic method) [10] but also on the electrolyte used for the electrodeposition [14]. During the electropolymerisation, anions are incorporated in the polymer film to compensate the positive charge on the polymer backbone. The anion is integrated within the polymer taking into account both its size and its chemical nature, and thus can influence the crystallinity of the polymer, its porosity, its electrical conductivity and its mechanical properties. In this work, the strategy was to investigate different coatings varying "only" in the anion incorporated, which has been already proven to be a successful approach to modulate the response to gases [15,16].

[4] The term "new materials" is here employed for materials which have not previously been investigated as vapour sensitive layer within the research group.

[5] The electrodeposition is limited to aqueous solutions due to a limiting factor of the substrates used at this time, as discussed in Chapter 3.

A significant remark has to be made at this point: even if "only" the anion is modified from one coating to another, as already indicated the whole morphology of the polymer is influenced during the deposition. This anion enhances the differences between coatings made from the same monomer, which is of interest regarding the production of an array of sensors. But this also makes it harder to the interpret the interactions between gases and conducting polymer, as the pure influence of the chemical nature of the dopant can not be isolated in the response from the contribution induced by morphological changes.

4.2.1.1 – Alkyl and aromatic sulfonates as dopant

Sodium salts of alkyl sulphonates have been largely used in the research group as dopants for electrodeposited poly(pyrrole) and poly(aniline) films [2,5,17,18]. They were found to give films with good mechanical and sensing properties. The length of the alkyl chain can be varied from butane (C_4) to dodecane (C_{12}). In the present work the alkyl sulfonates were limited to the pentane and the decane salts to simulate short and long chain length respectively.

It was of particular interest to compare the alkyl sulfonates with **aromatic sulfonates**, both in sensing aliphatic and aromatic vapours. Poly(pyrrole) and poly(aniline) were deposited from a solution containing *p*-toluene sulphonate sodium salt in a similar manner to films doped with alkyl sulfonate. The literature covers the electropolymerisation [19], the characterisation [20,21], the electrochemistry and the structure of poly(pyrrole) *p*-toluene sulfonate. As a coating, this material has already been found to respond to different vapours [15,22]. Little has however been reported on poly(aniline) *p*-toluene sulfonate.

4.2.1.2 - Metal phthalocyanine tetrasulfonates as dopant

A third type of anion was of interest: **metal phthalocyanines**. Metal phthalocyanines are large molecules composed of a central metal atom surrounded by a large organic ring. The most frequently used metals are iron, cobalt, nickel and copper. Figure 4. 17 shows the structure of the metal phthalocyanines used in this work. Phthalocyanines with two different metals were here investigated because the metal of the phthalocyanine, similarly to the anion incorporated in the polymer, has been found to influence the film properties [23] and the sensing properties of the chemoresistors [24].

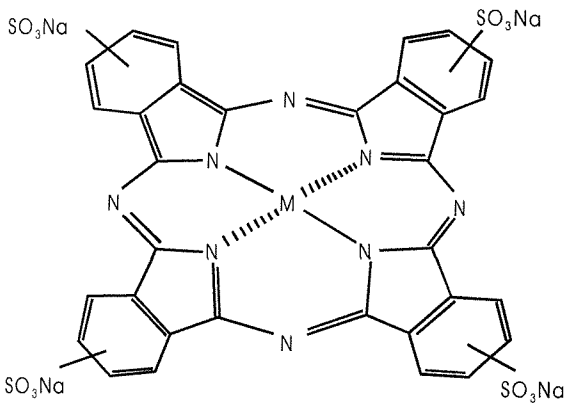

Figure 4. 17: structure of the metal phthalocyanine tetrasulfonate tetrasodium salt. M = Ni or Cu. The sulfonate groups on the ring enhance the solubility in aqueous media.

Metal phthalocyanines used have many interesting properties. The first application is their use as dye stuffs due to their strong optical absorption. Their pigment properties originate from the highly delocalised electrons on the organic ring. They are also widely used as catalyst [25,26], for their electrochromic properties [27] or as gas sensors. As gas sensors, phthalocyanines were found to respond to NO_2 in the range 2.8 ppb to 200 ppm, but also to halogens or ammonia [28]. As a general rule, phthalocyanines respond specifically to strong electron acceptor gases and show no interference from many gases like N_2, CO, CO_2, H_2S or benzene. More information on phthalocyanines can be found in reference [28].

As part of the CIA project, it was required to monitor levels of CO and NO_2. On one hand metal phthalocyanines are known for their gas sensing properties, especially for detection of NO_2 [28]. On the other hand conducting polymers are also known for their gas sensing properties and their capability to immobilise large molecules [29]. The two sensing technologies of the conducting polymers and of the metal phthalocyanine were combined by immobilising the later in the polymer matrix. Such a combination of poly(pyrrole) and various phthalocyanines has already been reported successful for sensing applications by Cabala [24].

The electrochemical properties of the metal phthalocyanines, whether in solution or immobilised in the polymer film, were not investigated in detail in the work presented here. Many articles report on these subjects: electrochemistry in solution [30-33], electrochemistry immobilised in a conducting polymer [27,31,34], conductivity [23] or spectroscopy [23,27,30,33]. Prior to electropolymerisation, cyclic voltammetry of the

metal phthalocyanine tetrasulfonate tetrasodium salt was performed in sulfuric acid to ensure that no decomposition of the anion took place at the polymerisation potential. Oxidation of the metal phthalocyanines used along this work was found to take place at potentials greater than + 0.9 V vs. SCE and therefore larger than the deposition potentials for poly(pyrrole) or poly(aniline).

4.2.2 - Gas sensing property of the new polymers

Conducting polymer chemoresistors were produced on SRL123 substrates by coating poly(pyrrole) and poly(aniline) films doped with pentane sulfonate, decane sulfonate, *p*-toluene sulfonate, copper phthalocyanine tetrasulfonate and nickel phthalocyanine tetrasulfonate. The production of the chemoresistors will be described and discussed in the following chapter.

4.2.2.1 - Response to water and ethanol vapours

Figure 4. 18 shows the response of three poly(pyrrole) films to ethanol and water. Each transient is representative of each polymer type. The dopants were either pentane sulfonate, *p*-toluene sulfonate or decane sulfonate.

The example given here illustrates the fact that a same polymer backbone can have different sensing properties depending on the anion incorporated within the film, all other parameters being equals (solvent, electrodeposition technique, etc.). Indeed, this figure shows major differences in the response between the three poly(pyrrole) films:

- ✓ in the amplitude of the response
- ✓ in the relative amplitude of the response to ethanol compared to the response to water
- ✓ in the shape of the transient
- ✓ in the stability of the base resistance
- ✓ in the recovery

Such modulation of the response is a way of generating a batch of sensors with different sensitivities, required for electronic nose applications. How the polymer senses the vapour appears to be complex and the observed differences cannot be explained at the light of this single experiment. Chapter 7 will be dedicated to the elucidation of the sensing mechanism.

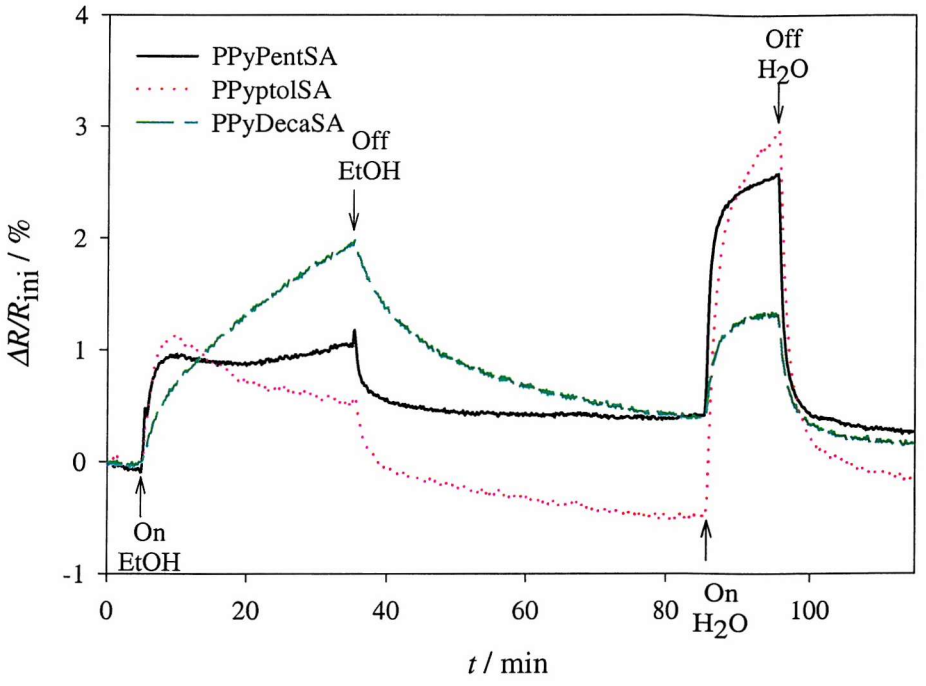

Figure 4. 18: relative change in resistance upon exposure to 32937 ppm ethanol vapour and 16768 ppm water vapour at a base humidity of 6707 ppm for three poly(pyrrole) films. The dopants are pentane sulfonate, *p*-toluene sulfonate and decane sulfonate. The figure illustrates the differences in response to vapours introduce by the anion immobilised in the polymer film.

4.2.2.2 - Response to CO and NO_2

As part of the study of the application of conducting polymer gas sensors in automotive applications, the responses to CO and NO_2 were investigated. The aim of this experiment was to find out if poly(pyrrole) and poly(aniline) films respond to CO and NO_2. If this is the case, the sensitivity should be estimated. The reversibility of the response is also an issue. If they do not respond, they can still be used within the CIA project to detect other vapours in combination with CO and NO_2 sensors. From an academic point of view, the effectiveness of the engineering of the coating towards an increased sensitivity towards NO_2 by coupling metal phthalocyanine and conducting polymers should be evaluated.

According to the literature, poly(aniline) films [35] and more generally conducting polymers [36] were reported not to respond to CO. Additionally, phthalocyanines do not show any sensitivity to CO as already indicated. Therefore it is expected that none of the poly(pyrrole) and poly(aniline) films will respond to CO. This is mainly due to the lack of reactivity of the gas towards electron transfer.

However metal phthalocyanines are known to respond to NO_2 [28,36], which is consistent with the fact that they are sensitive to strongly electrophilic vapours. Agbor [35] tested poly(aniline) films produced according to three different procedures, leading to films of different oxidation states and thicknesses. He reported that poly(aniline) responds to NO_2, but in different ways depending on the preparation mode. Blanc [37] and Miasik [36] reported that p-doped poly(pyrrole) responds to NO_2, whereas Hanawa reported the opposite [38]. He showed that poly(pyrrole) films only responded if they were reduced (insulating state) prior to exposure to NO_2. The different behaviours observed by these authors will be discussed while interpreting the response to NO_2 obtained here.

Sensors coated with poly(pyrrole) and poly(aniline) doped with metal phthalocyanine were tested. In order to estimate the eventual contribution of the phthalocyanine in the response poly(pyrrole) and poly(aniline), films doped with alkyl sulfonate and aromatic sulfonate were also employed. The concentrations of CO tested ranged from 20 to 50 ppm and the concentration of NO_2 from 1 to 40 ppm. The literature reports on the irreversible increase of resistance for poly(pyrrole) films exposed to NO_2 for concentrations varying from 40 to 2100 ppm [38]. Care was taken to limit the number of sensors for the first exposure, and low concentrations of gases were first applied. The temperature of the sensor chamber and the carrier gas was 33°C.

Once exposed to the gas stream in the test chamber, the poly(pyrrole) films doped with metal phthalocyanine lifted off the electrode so that no data is available on the sensing properties of poly(pyrrole) nickel phthalocyanine or poly(pyrrole) copper phthalocyanine. The incorporation of the large metal phthalocyanine apparently induces stress in the polymer film leading to poor mechanical properties. Saunders has also reported poor adhesion of poly(pyrrole) metal phthalocyanine tetrasulfonate films grown from propylene carbonate [23]. This highlights the need for good mechanical properties as a prerequisite for a sensor application, one of the main reason for using alkane sulfonate dopants.

4.2.2.2.1 - Response to CO

As expected, neither poly(aniline) nor poly(pyrrole) films respond to CO, even at concentrations as high as 50 ppm. As an indication, a detection level of 30 ppm is generally required for safety purposes. Figure 4. 19 shows the typical behaviour observed for poly(pyrrole); similar results were obtained for poly(aniline) films. The sensors show

no response to CO as the resistance remained constant upon exposure to the gas. Before and after exposure to CO, the humidity was increased (corresponding to the large peaks around 30 and 140 mn) to evaluate any inhibition of the sensing properties of the polymers towards other vapours. The signals were similar before and after exposure to CO, implying that no contamination had occurred upon exposure to carbon monoxide and showing that the sensors were responding during the experiment.

Even though the conducting polymers tested here do not respond to CO, they are still suitable for use in automotive applications to sense other vapours, as no contamination effect by CO was observed, even at high concentration.

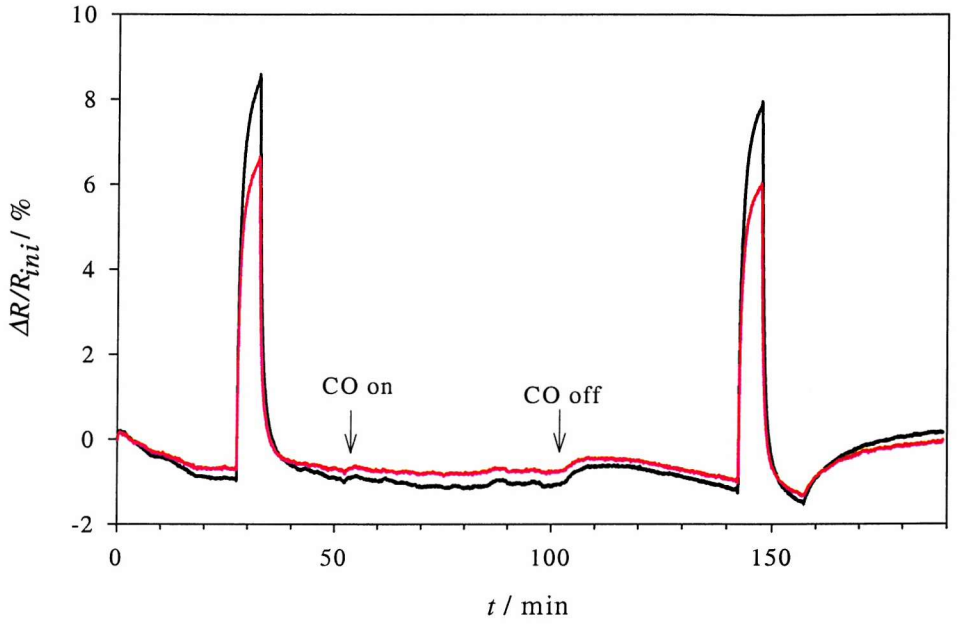

Figure 4. 19: relative change in resistance for two poly(pyrrole) pentane sulfonate films upon exposure to 50 ppm CO at 6707 ppm of water vapour. A pulse at 16768 ppm humidity was used as reference before and after exposure to CO to detect eventual inhibition of the sensing properties towards other vapours.

4.2.2.2.2 - Response to NO_2

None of the poly(pyrrole) films responded to NO_2, even at concentrations as high as 40 ppm. Responses similar to those shown in Figure 4. 19 were obtained when NO_2 was applied in-between two water pulses, showing that the sensors were gas sensitive but not to NO_2.

The first case where poly(pyrrole) films have been reported to respond to NO_2 in the literature quoted earlier was for sensors operated at high temperature (100°C or higher) [36,37]. In this case, the high temperature is suggested to enhance the partition coefficient

of the gas in the film, thus enhancing the response compared to a sensor operated at room temperature.

A second author reported the detection of NO_2 for poly(pyrrole) films in a reduced state [38]. Hanawa went further demonstrating that the same polymer in an oxidised state did not respond, showing the importance of the oxidation state to detect NO_2. Several authors [35-37] agree that the sensing mechanism of conducting polymers towards NO_2 is as following. As strong oxidising agent, the gas withdraws electrons from the polymer, acting like a p-doping reagent and modulating the electron density and conductivity of the polymer. Hanawa showed that the species resulting from the charge transfer was NO_2^-, confirming this model. If the conducting polymer is already in an oxidised state, electron transfer does not occur and no response is observed. This explains the lack of response observed here for the as-synthesised poly(pyrrole) film (in an oxidised state).

Five types of poly(aniline) films were tested, using two sensors of each type. No data were available for poly(aniline) decane sulfonate due to a significant noise level in the signal. Figure 4.21 shows typical responses to a 15 minute exposure to 3 ppm NO_2 for poly(aniline) films doped with pentane sulfonate, *p*-toluene sulfonate, copper and nickel phthalocyanine tetrasulfonates. They all respond in a similar manner to the gas: an increase in resistance upon exposure to NO_2, followed by a further increase once the gas has been removed, corresponding to about 20% of the response. No recovery was observed on the time scale investigated (at least 30 minutes).

The sensing mechanism of NO_2 by poly(aniline) is as described for the poly(pyrrole) films. The gas, a strong oxidising agent, removes electrons from the polymer backbone. Upon exposure to NO_2, the as-synthesised poly(aniline) is switched from a semi-oxidised conducting state (emeraldine) to a fully oxidised insulating state (pernigraniline), and thus the resistance is found to increase upon exposure to NO_2. The fully-oxidised state of poly(aniline) is known to be rather unstable, as shown, for example, in the cyclic voltammetry. This could account for the lack of reversibility observed in the response, also reported by Agbor [35].

The amplitude in the response increases with the dopant in the order copper phthalocyanine, *p*-toluene, pentane and nickel phthalocyanine sulfonate. From the nickel phthalocyanine sulfonate response, the principle of being able to engineer a coating for a

defined target vapour has been proven successful. The amplitude of the response if about double than for the largest response observed for the poly(aniline) films free of metal phthalocyanine. The effect on the film doped with the copper phthalocyanine is however minor. As shown later in Chapter 5, there was significant differences in the electrodeposition of the two poly(aniline) films doped with metal phthalocyanine, introducing different film properties and thus may account for the large difference in sensitivity of the two sensors. Similarly Cabala [24] reported the opposite sensitivity trend for the nickel and the copper doped films upon investigation of the work function.

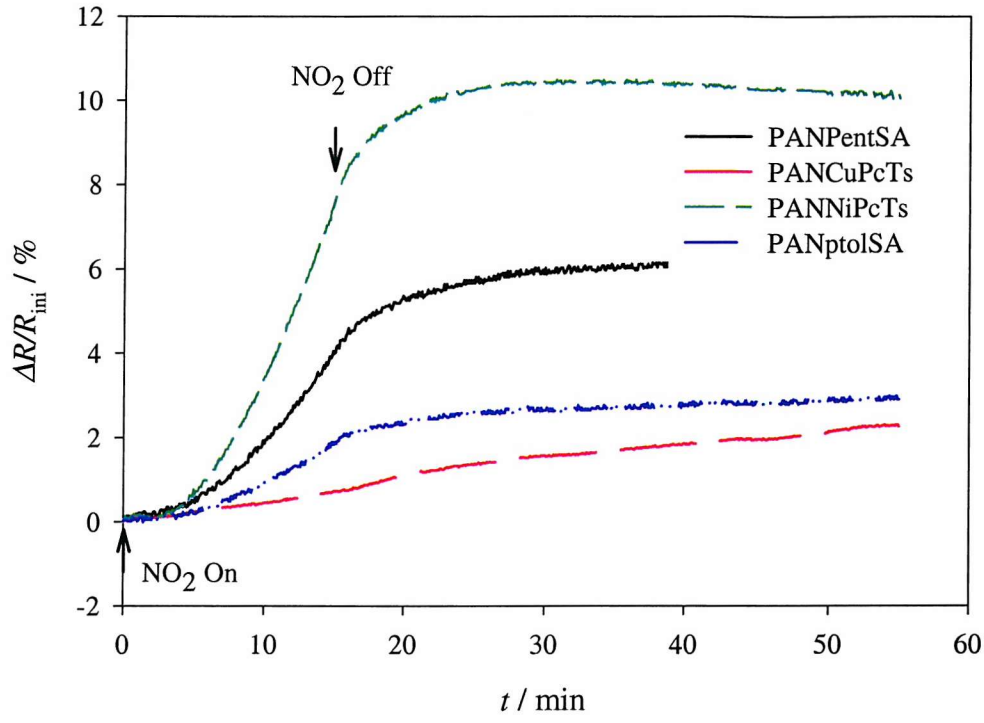

Figure 4. 20: exposure to 3 ppm NO_2 for 15 min for four poly(aniline) films, illustrating the dependence of the sensitivity on the anion and the irreversible response upon exposure to NO_2. It also shows the enhanced sensitivity for the nickel phthalocyanine doped film.

Insufficient data were available to conclude whether or not the exposure of the poly(aniline) films to NO_2 reduces the response to other vapours. Further tests would be required to conclude whether or not poly(aniline) films can be used in automotive applications.

On the improvement of the gas sensitive layer, no clear conclusion can be drawn yet. Poly(aniline) doped with nickel phthalocyanine showed a much larger sensitivity to NO_2 than the other poly(aniline) films tested, however it is not clear if it is due to the additional sensitivity introduced by the metal phthalocyanine.

To conclude if the incorporation of a range of anions in the poly(pyrrole) and the poly(aniline) films improves the sensors towards other vapours, more gas tests are required. The response towards water and ethanol of the films employed here will be detailed later.

(1) Blair, N., The development and characterisation of conducting polymer based sensors for use in an electronic nose, PhD thesis, SOUTHAMPTON, 1994.

(2) Elliott, J. M., Conducting Polymer Odour Sensors, PhD thesis, SOUTHAMPTON, 1997.

(3) Hailin, G.; Yucheng, L., *Sensors and Actuators*, 1994, **B 21**, 57-63.

(4) Partridge, A. C.; Harris, P.; Andrews, M. K., *Analyst*, 1996, **121**, 1349-1353.

(5) Bartlett, P. N.; Archer, P. B. M.; Ling-Chung, S. K., *Sensors and Actuactors*, 1989, **19**, 125-140.

(6) Harris, P. D.; Arnold, W. M.; Andrews, M. K.; Partridge, A. C., *Sensors and Actuators*, 1997, **B 42**, 177-184.

(7) Kankare, J.; Kupila, E. L., *J. Electroanal. Chem.*, 1992, **322**, 167-181.

(8) Talaie, A.; Wallace, G. G., *Solid State Ionics*, 1994, **70/71**, 692-696.

(9) Nishizawa, M.; Miwa, Y.; Matsue, T.; Uchida, I., *J. Electrochem. Soc.*, 1993, **140**, 1650-1655.

(10) Desilvestro, J.; Scheifele, W., *J. Mater. Chem.*, 1993, **3**, 263-272.

(11) Paul, E. W.; Ricco, A. J.; Wrighton, M. S., *J. Phys. Chem.*, 1985, **89**, 1441-1447.

(12) Sabatani, E.; Redondo, A.; Rishpon, J.; Rudge, A.; Rubinstein, I.; Gottesfeld, S., *J. Chem. Soc. Faraday Trans.*, 1993, **89**, 287-294.

(13) Bade, K.; Tsakova, V.; Schultze, J. W., *Electrochim. Acta*, 1992, **37**, 2255-2261.

(14) Tang, H.; Kitani, A.; Shiotani, M., *Electrochim. Acta*, 1996, **41**, 1561-1567.

(15) Topart, P.; Josowicz, M., *J. Phys. Chem.*, 1992, **96**, 8662-8666.

(16) Nagase, H.; Wakabayashi, K.; Imanaka, T., *Sensors and Actuators*, 1993, **B 13/14**, 596-597.

(17) Bartlett, P. N.; Ling-Chung, S. K., *Sensors and Actuators*, 1989, **20**, 287-292.

(18) Bartlett, P. N.; Ling-Chung, S. K., *Sensors and Actuators*, 1989, **19**, 141-150.

(19) Lin, Y.; Wallace, G. G., *Electrochimica Acta*, 1994, **39**, 1409-1413.

(20) Kuwabata, S.; Okamoto, K.; Yoneyama, H., *J. Chem. Soc., Faraday Trans. 1*, 1988, **84**, 2317-2326.

(21) Warren, L. F.; Walker, J. A.; Anderson, D. P.; Rhodes, C. G.; Buckley, L. J., *J. Electrochem. Soc.*, 1989, **136**, 2286-2295.

(22) Charlesworth, J. M.; Partridge, A. C.; Garrard, N., *J. Chem. Phys.*, 1993, **97**, 5418-5423.

(23) Saunders, B. R.; Murray, K. S.; Fleming, R. J.; Korbatieh, Y., *Chem. Mat.*, 1993, **5**, 809-819.

(24) Cabala, R.; Meister, V.; Potje-Kamloth, K., *J. Chem. Soc., Faraday Trans.*, 1997, **93**, 131-137.

(25) Coutanceau, C.; Hourch, A. E.; Crouigneau, P.; Leger, J. M.; Lamy, C., *Electrochim. Acta*, 1995, **40**, 2739-2748.

(26) Perez, E. F.; Kubota, L. T.; Tanaka, A. A.; Neto, G. D. O., *Electrochimica Acta*, 1998, **43**, 1665-1673.

(27) Toshima, N.; Tominaga, T.; Kawamura, S., *Bull. Chem. Soc. Jpn*, 1996, **69**, 245-253.

(28) Lezwoff, C. C.; Lever, A. B. P. *Phthalocyanines- Porperties and applications*; VCH Publishers Inc., 1989.

(29) Bartlett, P. N.; Cooper, J. M., *J. Electroanal. Chem.*, 1993, **362**, 1-12.

(30) Choi, C. S.; Tachikawa, H., *J. Am. Chem. Soc.*, 1990, **112**, 1757-1768.

(31) Reynolds, J. R.; Pyo, M.; Qiu, Y. J., *J. Electrochem. Soc.*, 1994, **141**, 35-40.

(32) Sasaki, H.; Iwabuchi, Y.; Toshima, S., *J. Electroanal. Chem.*, 1982, **131**, 243-255.

(33) Rollmann, L. D.; Iwamoto, R. T., *J. AM. Chem. Soc.*, 1968, **90**, 1455-1463.

(34) Coutanceau, C.; Rakotondrainibe, A.; Crouigneau, P.; Leger, J. M.; Lamy, C., *J. Electroanal. Chem.*, 1995, **386**, 173-182.

(35) Agbor, N. E.; Petty, M. C.; Monkman, A. P., *Sensors and Actuators*, 1995, **B 28**, 173-179.

(36) Miasik, J. J.; Hooper, A.; Tofield, B. C., *J. Chem. Soc., Faraday Trans. I*, 1986, **82**, 1117-1126.

(37) Blanc, J. P.; Derouiche, N.; Hadri, A. E.; Germain, J. P.; Maleysson, C.; Robert, H., *Sensors and Actuators*, 1990, **B1**, 130-133.

(38) Hanawa, T.; Kuwabata, S.; Yoneyama, H., *J. Chem. Soc., Faraday Trans. I*, 1988, **84**, 1587-1592.

Chapter 5 - Production of conducting polymer gas sensors description, results and discussion

Much effort has already been put into understanding the sensing mechanism of conducting polymers, but till now no universally agreed model has been proposed. As for many researchers working on polymer coatings [1,2] and on conducting polymers [3-9], one topic of interest here was to elucidate the interactions between polymer and vapour. By identifying the nature of these interactions, it may be possible to increase the sensor specificity and decrease cross-sensitivity of the sensors in an array and therefore further improve the sensors. The strategy employed here will be to couple the chemoresistor generally employed with a QCM coated with identical polymers to monitor the mass of vapour adsorbed by the coating.

The production of both chemoresistor and QCM sensors employed for this purpose will be described and discussed in this chapter, mainly to throw light on possible relations between the polymerisation characteristics and the response to vapours. The reproducibility of the sensors, both in terms of deposition and of final resistance, will be discussed and further compared with the polymer coated quartz microbalances.

5.1 - Introduction to sensor production

5.1.1 - Comments on the electropolymerisation

The choice of polymers and the experimental conditions have already been discussed in detail in Chapter 4. The polymers used were poly(pyrrole) and poly(aniline) films, as they are known to give suitable response to the vapours of interest and have already been investigated by others in the research group [11,12]. The poly(pyrrole) and poly(aniline) films were doped with five different anions: pentane sulfonate, decane sulfonate, *p*-toluene sulfonate, copper phthalocyanine tetrasulfonate and nickel phthalocyanine tetrasulfonate.

The substrates used for the electrodeposition of the conducting polymers were SRL123 devices (1 mm by 1 mm square gold electrode with a 10 μm gap), cleaned prior to the deposition by cyclic voltammetry in 2 M sulfuric acid. The substrates used for the QCM sensors were AT-cut 10 MHz crystals with gold disc electrodes of 5 mm diameter (active area of 0.196 cm^2). A substrate comprising both the chemoresistor and the QCM sensors has been described [7] but in the present work separate structures were employed.

The alkyl sulfonate salts used in this work are surfactants, composed of an anionic hydrophilic head group (SO_3^-) and an hydrophobic tail (alkyl chain). Above the **Critical Micelle Concentration** (CMC), these molecules form aggregates in aqueous solutions in which the hydrophobic tails pack in a sphere with the outer-surface composed of the hydrophilic head groups. Water molecules are then excluded from the hydrophobic core.

The critical micelle concentration for a range of alkyl sulfonates can be found in reference [12]. In this work, pentane sulfonic acid was used at concentrations below the critical micelle concentration (the highest concentration used was 0.5 M and the CMC is 1.23 M).

Both poly(pyrrole) and poly(aniline) films were grown from a solution containing decane sulfonic acid sodium salt above its critical micelle concentration (CMC of 0.04 M).

Polymer films were deposited by potential step. This method is easy to perform and gives sensors with suitable properties. The *in-situ* resistance measurement detailed in Chapter 4 was shown to be successful in improving the sensors (both in terms of reproducibility from sensor to sensor and response time). This technique was, however, developed in parallel with the production of the sensors employed for the gas test experiments and therefore was not used for the production of the films described here.

5.1.2 - Introduction to the discussion

Previous work has shown that poly(pyrrole) and poly(aniline) films form well behaved sensors once doped with alkyl sulfonate counter ions. These coatings will be used as "reference" materials to evaluate the reproducibility of the deposition, and later the sensing properties of the same polymers doped with *p*-toluene sulfonate and metal phthalocyanine tetrasulfonate not investigated up to now.
During the gas test experiments, only one QCM sensor could be tested at a time. So the number of polymers tested with the quartz crystal microbalance was restricted to the same "reference" coatings: poly(pyrrole) and poly(aniline) films doped with pentane and decane alkyl sulfonate.

For each polymer, the average polymerisation charge and the resistance (measured for the dry film) are given within 95% confidence limits, the raw values being gathered together in Annex A. The error is expressed both as an absolute value and as percentage. The discussion will be mainly based on the reproducibility of the polymerisation charge and the film resistance, within each combination anion/polymer, both for poly(pyrrole) and poly(aniline). The chemoresistors for the gas test experiments were then selected from a batch of 6 to 8 sensors by selecting the most reproducible regarding the polymerisation and the baseline resistance. This method of selection seems to be the most logical but was not demonstrated experimentally.

5.2 - Poly(pyrrole) sensors

5.2.1 - Poly(pyrrole) chemoresistors

5.2.1.1 - Electropolymerisation conditions

The electropolymerisation conditions for the five poly(pyrrole) films grown can be found in Table 5. 1. After deposition, the potential was stepped back to zero to reduce the interfacial charges, but did not correspond to the reduction of the poly(pyrrole) films. At a potential of 0 V, poly(pyrrole) remains in its oxidised (conductive) state. Reduction of poly(pyrrole) only occurs at potential of about –0.3 V.

Anion	[Monomer]	[Anion]	Solvent	E vs SCE / V	t / s
Pentane SA	0.1 M	0.1 M	H_2O	+ 0.85	120
Decane SA	0.1 M	0.1 M	H_2O	+ 0.85	120
p-toluene SA	0.1 M	0.1 M	H_2O	+ 0.85	120
CuPcTs	0.1 M	saturated	0.5 M H_2SO_4	+ 0.85	120
NiPcTs	0.1 M	saturated	0.5 M H_2SO_4	+ 0.85	100 to180

Table 5. 1: electropolymerisation conditions for poly(pyrrole) films doped with five different anions onto SRL123 devices. The polymerisation was performed at room temperature.

5.2.1.2 - Results and discussion for the poly(pyrrole) chemoresistors

Electrodeposition of poly(pyrrole) pentane sulfonate

Eight sensors were coated with poly(pyrrole) pentane sulfonate. Figure 5. 1 shows a typical current transient for the deposition onto SRL123 device (device 65BR). The shape was reproducible for the eight sensors as illustrated in Figure 5. 2. However the current amplitude slightly decreased with the number of sensors produced also shown in Figure 5. 2 and in Annex A. During electrodeposition, by-products are believed to pass into solution and decrease the subsequent rate of polymerisation. Warren [13] found that in an electrolysis mode, a pyrrole solution was stable over only three hours. Even thought the polymerisation rate decreased, the reproducibility of the polymerisation charge was satisfactory, Q = 14.8 mC ± 0.9 mC (corresponding to 4.1%, average over 8 sensors). The resistance of the dry film was 578 ± 331 Ω (36%). At first sight, the error on the resistance appears to be large but will be better commented in light of results obtained for other coatings.

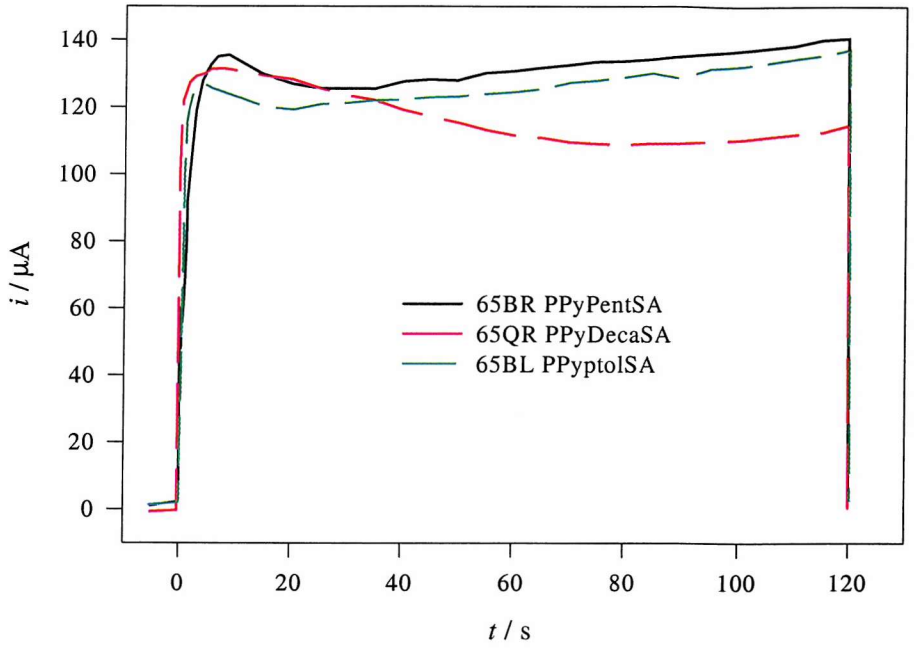

Figure 5. 1: typical current transients for the electropolymerisation of poly(pyrrole) doped with pentane sulfonate, decane sulfonate and *p*-toluene sulfonate onto SRL123 devices. See Table 5. 1 for the polymerisation conditions.

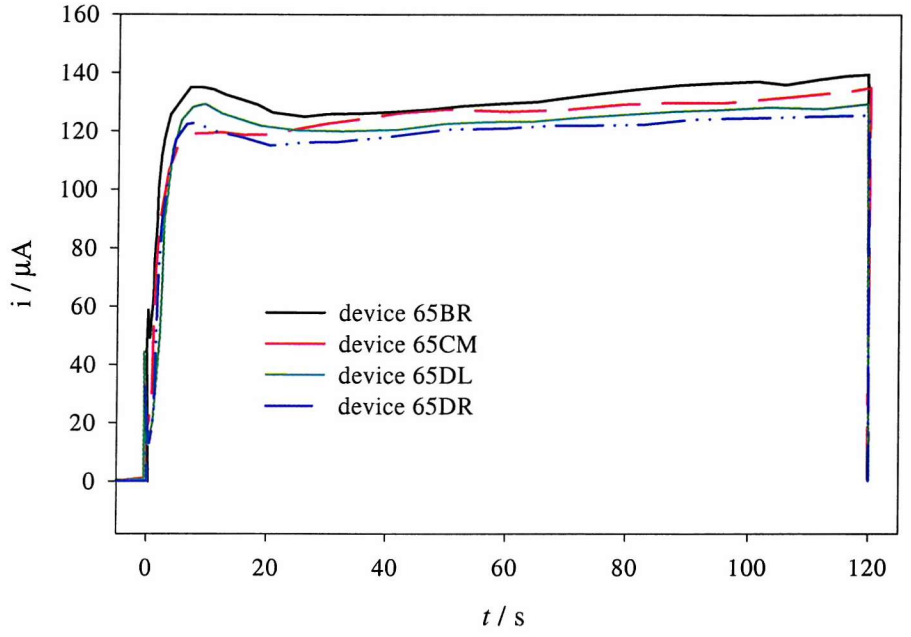

Figure 5. 2: current transients for the electrodeposition of poly(pyrrole) pentane sulfonate films onto four SRL123 devices illustrating the reproducibility of the transients in shape and in current density from sensor to sensor.

It was shown in Chapter 4, by monitoring the resistance during the electropolymerisation, that the resistance of a given chemoresistor decreases with increasing amount of polymer deposited. This is however valid for one device, but within a given polymer type, some deviation are observed from sensor to sensor as illustrated in Figure 5. 3. For two identical

polymers of supposedly identical thicknesses (deduced from the polymerisation charge) the resistance can present some deviations. For example, devices 65CM and 65CR in Figure 5. 3 were both polymerised by passing a charge of 14.75 mC, but the dry resistance varies significantly: 237 Ω for the first film and 760 Ω for the second.

The chemoresistors selected for gas tests were not randomly selected, but rather according to the reproducibility of the polymerisation charge and resistance of the dry film. Graphically, it can be illustrated by Figure 5. 3, where the resistance is plotted versus the polymerisation charge. Seven sensors are found to form a cluster around 14-15 mC and 200-800 Ω for poly(pyrrole) pentane sulfonate. The eighth device from the batch (reference 65CL) appears to be apart with a charge of 17 mC and a resistance around 1500 Ω. Due to this significant difference this chemoresistor will not be selected first for gas experiments.

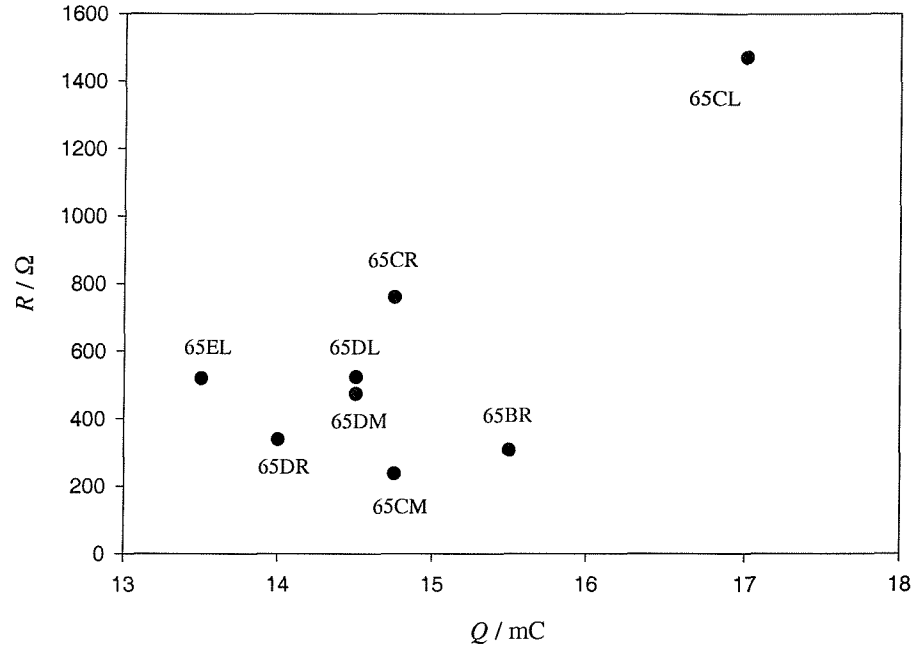

Figure 5. 3: resistance of the dry poly(pyrrole) pentane sulfonate films versus the polymerisation charge, showing some deviation in the sensor production. Such visualisation of the electrodeposition results allows the selection of the "best" sensors (most reproducible in polymerisation charge and in resistance).

Electrodeposition of poly(pyrrole) decane sulfonate and poly(pyrrole) p-toluene sulfonate

The conclusions drawn for poly(pyrrole) pentane sulfonate were also found to be valid for the electrodeposition of poly(pyrrole) decane sulfonate and poly(pyrrole) *p*-toluene sulfonate. The shape of the transients was reproducible from sensor to sensor and a slight but noticeable decrease of the current was observed with increasing number of sensors produced. The current transients were also similar for the three polymers, as shown in

Figure 5. 1. For these polymers, the polymerisation charge was 15.1 ± 1.0 mC and 16.0 ± 1.0 mC, and the resistances 121 ± 108 Ω and 69 ± 28 Ω for the decane doped polymer (averaged over six sensors) and for the *p*-toluene doped polymer (averaged over seven sensors) respectively.

The comparison of the three poly(pyrrole) films just described (PPyPentSA, PPyDecaSA and PPyptolSA) is interesting. First of all, the similarity in the current transients is remarkable (Figure 5. 1). The shape and current amplitude of the transients were not strongly dependent on the anion. Consequent the charges passed during electrodeposition were similar. However the final resistance of the devices can vary with the anion incorporated in the film by a factor of 6 from poly(pyrrole) pentane sulfonate (451 Ω) to the *p*-toluene doped film (69 Ω). Before concluding that the conductivity of the film varies with the anion, the electrodeposition efficiency has to be considered. Indeed the amount of pyrrole which is oxidised at the electrode is not the same as the amount deposited onto the device as polymer. Some of the polymerisation intermediates produced in the reaction escape into solution together, and possibly, with some polymer fragments.
The electrodeposition efficiency was calculated for these three polymers- see Chapter 6 for details of the calculations. The deposition efficiency was 20%, 62% and 22% for the pentane, the decane and the *p*-toluene doped films respectively. This implies that, even if the three films were electropolymerised using the same charge, the amount of material deposited is about three times greater on devices coated with poly(pyrrole) decane sulfonate than on the two others. The high deposition efficiency of the poly(pyrrole) doped with decane sulfonate may be explained by the surfactant properties of the anion, preventing the reaction intermediates from leaving the solution/electrode interface [12].

Table 5. 2 shows for the three polymers the relationship between the estimated amount of polymer and the resistance of the devices. In order to comment this table it has to be remembered that the resistance of the polymer film does not vary linearly with the amount of polymer deposited (or thickness of the film) as seen in Chapter 4 for poly(aniline) pentane sulfonate. Talaie *et al.* [14] reported a similar variation of the resistance of a poly(pyrrole) *p*-toluene sulfonate as a function of the thickness of the film.
From Table 5. 2 it can be concluded that the poly(pyrrole) *p*-toluene sulphonate films have a much higher conductivity than the pentane and decane doped films, because a small amount of polymer ($Q_{deposition}$ = 3.52 mC) corresponds to a low resistance (69 Ω).

However, little can be said on the relative conductivity of the pentane and decane sulfonate films because the amounts of material deposited vary greatly from one to the other.

Anion (number of devices)	$Q_{oxidised}$ / mC	Deposition efficiency / %	$Q_{deposited}$ / mC	R / Ω
Pentane SA (8)	14.8	20	2.96	579
Decane SA (6)	15.1	62	9.36	121
p-toluene SA (7)	16.0	22	3.52	69

Table 5. 2: table showing the relationship between the amount of poly(pyrrole) deposited as a polymer film ($Q_{deposited}$) and the resistance of the final devices for three dopants deduced from the polymerisation charge and deposition efficiency. The data were averaged from three experiments for the deposition efficiency and from six to eight experiments for the other data (number in brackets indicated next to the anion). See Chapter 6 for the deposition efficiency calculations.

In addition to the poly(pyrrole) films doped with the two alkyl sulfonates and with *p*-toluene sulfonate, chemoresistors coated with poly(pyrrole) metal phthalocyanine (M = Cu or Ni) were produced.

The previous films investigated were polymerised from solutions of the anion in water. Polymerisation in water was found to give films with poor mechanical properties. Indeed these films were easily lifted off the electrodes. According to Cabala [15] the competitive doping between a large anion (here MPcTs) and a small one (HSO_4^- for example), even in small quantity, decreases the density of the film and improves the mechanical properties. In addition other authors have also grown poly(pyrrole) films doped with metal phthalocyanine tetrasulfonate from sulfuric acid solution [16,17] . Therefore the metal phthalocyanine doped films were polymerised from a solution of 0.5 M H_2SO_4.

Electrodeposition of poly(pyrrole) copper phthalocyanine tetrasulfonate and poly(pyrrole) nickel phthalocyanine tetrasulfonate

The current transients for the deposition of poly(pyrrole) doped with copper and nickel phthalocyanine were similar to each other as shown in Figure 5. 4. These transients can be compared with the transients for poly(pyrrole) doped with alkyl or aromatic sulfonates shown in Figure 5. 1. Whereas for the first three polymers discussed the current was

constant over the whole deposition (about 120 μA), here the current was initially large (over 500 μA), and then decreased rapidly to reach a final value similar to the electrodeposition current for the first batch of polymers. In addition, as seen in the polymerisation charge (Annex A), the irreproducibility from sensor to sensor was significantly increased, from the first three polymers to the metal phthalocyanine tetrasulfonate doped poly(pyrrole), but also from the copper to the nickel phthalocyanine tetrasulfonate poly(pyrrole). For this reason, the polymerisation time was increased for successive polymerisations of pyrrole with nickel phthalocyanine. The origin of the decrease in the polymerisation rate was not investigated. Even given this increase in polymerisation time, the irreproducibility remains large for the poly(pyrrole) nickel phthalocyanine (16.1 ± 2 mC, averaged over seven sensors), larger than the copper equivalent (12.2 ± 1.6 mC averaged over eight sensors). On one hand the irreproducibility of the deposition is high and on the other hand, the resistance shows a good reproducibility compared to the first series of polymers (1107 ± 239 Ω and 937 ± 340 Ω for the copper and the nickel doped film respectively). If the gas tests of the poly(pyrrole) metal phthalocyanine tetrasulfonates are promising, the sensor production should then be improved as it is expected that the lack of reproducibility in the production will be reflected in the response to gas and vapour.

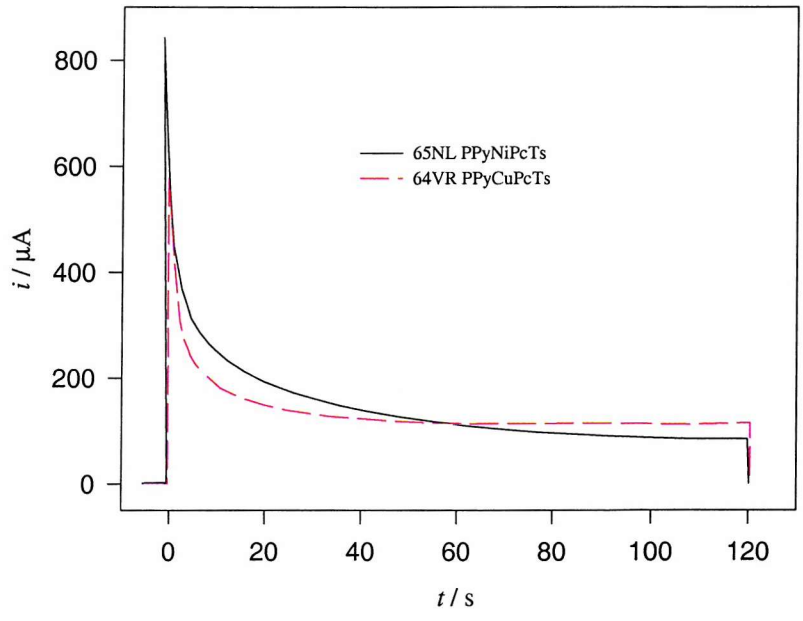

Figure 5. 4: typical current transients for the electropolymerisation of poly(pyrrole) copper phthalocyanine tetrasulfonate and poly(pyrrole) nickel phthalocyanine tetrasulfonate. See Table 5. 1 for the polymerisation conditions.

Anion (number of devices)	Q / mC	Error Q/ mC 95% confidence	Error Q/ % 95% confidence	R / Ω	Error R/ Ω 95% confidence	Error R/ % 95% confidence
Pentane SA(8)	14.5	0.6	4.1	451	163	36
Decane SA (6)	15.1	1.0	6.6	121	108	89
p-toluene SA (7)	16.0	1.0	6.2	69	28	40
CuPcTs (8)	12.2	1.6	13.1	1107	239	21
NiPcTs (7)	16.1	2.0	12.4	937	340	36

Table 5. 3: average polymerisation charge and resistance of the dry poly(pyrrole) films expressed within 95% confidence for a number of sensors varying from 6 to 8 (number in brackets indicated next to the anion).

Table 5. 3 gathers together the average polymerisation charge and average resistance for the five poly(pyrrole) types electrodeposited, as well as the errors in these values expressed within 95% confidence limits. These poly(pyrrole) films can be classified into two groups, from their deposition conditions and from the results of the polymerisation:

- the pentane, the decane and the *p*-toluene doped films, grown from aqueous solution, which have a polymerisation charge reproducible within 7% but with a base resistance which is rather irreproducible (up to 89%). Globally, the results were satisfactory.
- the copper and the nickel phthalocyanine tetrasulfonate doped poly(pyrrole) grown from 0.5 M H_2SO_4 showing a sharp decrease of the polymerisation rate with increasing number of successive polymerisations. This leads to an irreproducible polymerisation charge (higher than 12 %) but the reproducibility of the resistance is surprisingly high (36% or less) when compared to the first group. Globally the polymerisation of this first batch of poly(pyrrole) metal phthalocyanine tetrasulfonate was satisfactory. The lack of reproducibility of the deposition should be further investigated if more sensors are to be produced.

5.2.2 - Poly(pyrrole) coated Quartz Crystal Microbalance

Electrodeposition of poly(pyrrole) pentane sulfonate and poly(pyrrole) decane sulfonate was performed onto the quartz crystal microbalance, a separate structure to chemoresistors. In order to be able to compare the responses of the two sensor types coated with the same polymer, any difference between the two coatings should be minimised. Therefore the same polymerisation conditions as used for the chemoresistors were employed.

5.2.2.1 - Poly(pyrrole) pentane sulfonate coated QCM

Poly(pyrrole) pentane sulfonate was deposited onto two quartz crystal microbalance electrodes, referred to as QCM4 and QCM5 (subscript 4 for the quartz 4 and subscript 5 for the quartz 5) using the conditions from Table 5. 1. The growth was reproducible for the two depositions, both in terms of charge ($Q_{growth4}$ = 41 mC and $Q_{growth5}$ = 42 mC) and in terms of shape of the current transients.

Comparing the deposition onto the chemoresistors and onto the quartz crystal microbalance, the shape of the current transients were similar but the current density was lower by a factor of seven in the case of the QCM electrodes. For the chemoresistors, the charge density was 1408 mC cm^{-2}, but only 202 mC cm^{-2} for the QCM substrates.
The iR drop may be responsible for the decrease in current density observed from the SRL123 to the QCM may be the iR drop. First of all, the surface area of the working electrode was multiplied by 20. In addition, the electrolyte was only composed of the alkyl sulfonate which shows surfactant properties and therefore probably presents poor conductivity (this was not measured). These two factors may imply that the electropolymerisation onto QCM shows iR drop. Even though the reference electrode was placed close to the working electrode (about 1 cm), this was probably insufficient to eliminate all iR drop. In addition to the iR drop, the substrate (nature of the metal, crystallinity, etc.) is known to influence on the polymerisation rate [18] which could also take part in the variation in polymerisation rate.

The consequence from this difference in electropolymerisation rate is that, assuming similar deposition efficiencies and densities, the film onto the chemoresistor is about seven times thicker than on the QCM. For interpretation of the sensing properties of the poly(pyrrole) pentane sulfonate, this difference in thickness may be significant.

The amount of polymer deposited onto the quartz crystal could be estimated more precisely by performing cyclic voltammetry of the film in background electrolyte. The signal would be directly linked with the amount of polymer deposited. However, during the redox switching, there is movement of ions and solvent molecules in and out of the film, and rearrangement of the polymer chains to accommodate these molecules. Such redox process has been found to largely influence the permeability of the film [19], and thus is a destructive method for the sensors. For this reason it was not applied here.

5.2.2.2 - Poly(pyrrole) decane sulfonate coated QCM

Poly(pyrrole) decane sulfonate was deposited onto two QCM electrodes, referred to as QCM8 and QCM9. The solution was the same as the one used for the chemoresistors but the potential step time to + 0.85 V was increased from 120 s for the chemoresistors to 480 s for the QCM electrodes. The growth was fairly reproducible for the two depositions, both in terms of the total charge ($Q_{growth8}$ = 185 mC and $Q_{growth9}$ = 161 mC) and in terms of the shape of the current transients.

The shape of the current transients was similar for the deposition onto the chemoresistors and the quartz crystal microbalance substrates. As observed for the deposition of poly(pyrrole) doped with pentane sulfonate, the current density was smaller than expected for the QCM by a factor of 8. For this reason the potential step was applied for 480 s for the QCM instead of 120 s for the chemoresistors. By increasing the polymerisation time, the differences between the two sensor types were decreased, but the coating on the QCM remains about half as thick as that on the chemoresistor (charge density of 785 mC cm^{-2} for the former and 1440 mC cm^{-2} for the later).

5.3 - Poly(aniline) sensors

5.3.1 - Poly(aniline) chemoresistors

5.3.1.1 - Electropolymerisation conditions

Monomer concentration

Monomer concentrations of 0.4 or 0.5 M were employed. 0.5 M aniline was found to be the optimal concentration from previous studies [11], but to reduce the polymerisation rate, in some cases the concentration was decreased to 0.4 M.

Electrolyte

The poly(aniline) films were grown from a solution containing the sulfonic acid sodium salt (0.5 M unless stated) and sulfuric acid to decrease the pH to a value suitable for the polymerisation of aniline. During polymerisation, anions from the electrolyte are incorporated into the polymer film to compensate for the positive charge on the polymer backbone. In the case of the poly(aniline) films, there is competition between HSO_4^- (from the sulfuric acid) and RSO_3^- (from the sulfonic acid). A higher concentration of RSO_3^- is expected to increase the ratio RSO_3^-/ HSO_4^- in the polymer which is beneficial on two

aspects. First of all, it enhances the differences in response of the various poly(aniline) sensors and secondly large anions are known to produce films of better mechanical properties [13].

Potential

Poly(aniline) was deposited using a bipotential step. An initial step at + 0.9 V, of short duration, was used to produce a thin poly(aniline) layer presenting good adhesion properties. The potential was then decreased to + 0.78 V, as the poly(aniline) formed at + 0.9 V deposits in an over-oxidised state, corresponding to a less conducting form [11,20,21]. A single potential step at + 0.78 V would lead to a film presenting poor adhesion [11]. Unlike poly(pyrrole), the polymer modified electrode was disconnected from the polymerisation cell at the potential of deposition. Stepping the potential to zero would have for implication to reduce the poly(aniline) film into an insulating state.

Potential step duration

The potential step duration was varied as a function of the polymerisation rate of aniline, varying with the anion, in order to have a film of suitable thickness. +0.9 V was applied for 5 s to have a suitable poly(aniline) underlayer. This step was of 10 s duration in the case of poly(aniline) copper phthalocyanine tetrasulfonate as the polymerisation rate was very low for this given polymer. For this same polymer, the second step was also much longer in duration than for the other anions, 230 s compared to 30 s at maximum. The second step for the other polymers varied from 15 to 30 seconds, depending mainly on the aniline concentration and the deposition temperature.

Temperature

Polymerisation was performed at room temperature except for poly(aniline) decane sulfonate and poly(aniline) *p*-toluene sulfonate where polymerisation was performed from a solution thermostated at 40°C to ensure solubility of the anion at a concentration of 0.5 M.

Table 5. 4 gathers the polymerisation conditions for the deposition of the poly(aniline) films for the five anions employed.

Anion	[Monomer]	[Anion]	Solvent	E vs SCE / V step 1 / step 2	t / s step 1 / step 2
Pentane SA	0.5 M	0.5 M	2 M H_2SO_4	+ 0.9 / +0.78	5 / 30
Decane SA	0.4 M	0.5 M	2 M H_2SO_4	+ 0.9 / +0.78	5 / 25
p-toluene SA	0.5 M	0.5 M	2 M H_2SO_4	+ 0.9 / +0.78	5 / 15
CuPcTs	0.4 M	saturation	2 M H_2SO_4	+ 0.9 / +0.78	10 / 230
NiPcTs	0.4 M	saturation	2 M H_2SO_4	+ 0.9 / +0.78	5 / 30

Table 5. 4: electropolymerisation conditions for poly(aniline) films doped with five different anions onto SRL123 devices. The polymerisation was performed at room temperature or at 40 °C for the decane and the *p*-toluene sulfonate doped films.

5.3.1.2 - Results and discussion of the poly(aniline) chemoresistors

Electrodeposition of poly(aniline) pentane sulfonate and poly(aniline) nickel phthalocyanine tetrasulfonate

Figure 5. 5 shows the current transients for the deposition of poly(aniline) films doped with pentane sulfonate and nickel phthalocyanine tetrasulfonate. Both are similar in the shape and in the current density.

For both polymers, the shape of the transients was reproducible from sensor to sensor. As previously observed for the poly(pyrrole) films, the polymerisation charge was however decreasing with the increasing number of polymerisations for poly(aniline) pentane sulfonate. The nickel phthalocyanine tetrasulfonate doped film (see Annex A) behaved rather in the opposite direction with Q_{growth} increasing. The polymerisation charges show a larger scatter than the poly(pyrrole) films: 5.0 ± 0.9 mC for PANPentSA, (corresponding to18%, average over seven sensors) and 6.7 ± 0.7 mC for PANNiPcTs (corresponding to10%, average over six sensors). The reproducibility in the baseline resistance was however higher than for the poly(pyrrole) equivalents: 13.7 ± 2.8 Ω (20% error) and 47 ± 14 Ω (30% error).

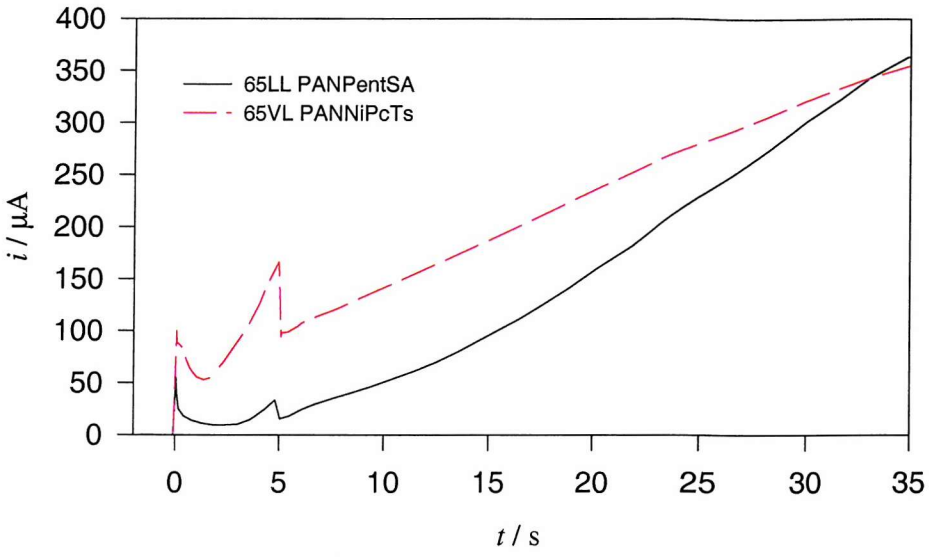

Figure 5. 5: typical current transients for the deposition of poly(aniline) pentane sulfonate and poly(aniline) nickel phthalocyanine tetrasulfonate onto SRL123 devices- see Table 5. 4 for the polymerisation conditions.

Electrodeposition of poly(aniline) copper phthalocyanine tetrasulfonate

Whereas at first sight there is little difference between the copper and the nickel phthalocyanine tetrasulfonate from a structural point of view, the electrodeposition behaves significantly differently for the two poly(aniline) films doped with metal phthalocyanine as shown in Figure 5. 5 and Figure 5. 6 for the nickel and copper phthalocyanine respectively. First of all, the shape is slightly different, but most significantly the current density is decreased by a factor of 50 from the nickel to the copper phthalocyanine.

The origin of this extremely low polymerisation rate was not investigated. Similar current transients were obtained by a previous co-worker [11], which eliminates the possibility of error during the preparation of the solution. The slow rate could come from an impurity originating from the copper phthalocyanine tetrasulfonate tetrasodium salt, or is simply a characteristic of the copper phthalocyanine somehow slowing down the aniline polymerisation rate. Such a decrease in polymerisation rate was not observed for pyrrole.

Seven chemoresistors were produced. The shape for the transient was reproducible from sensor to sensor, but as for the nickel equivalent, the growth charge increased with the number of successive polymerisations performed from the solution. The growth charge

showed poor reproducibility (1.16 ± 0.38 mC, corresponding to 33% error, average over seven sensors) which was reflected in the resistance values: 3187 ± 1633 Ω, 51% error. The resistance of the film was very sensitive to the exact amount of polymer deposited because the film was deposited thinly as seen from the low polymerisation charge.

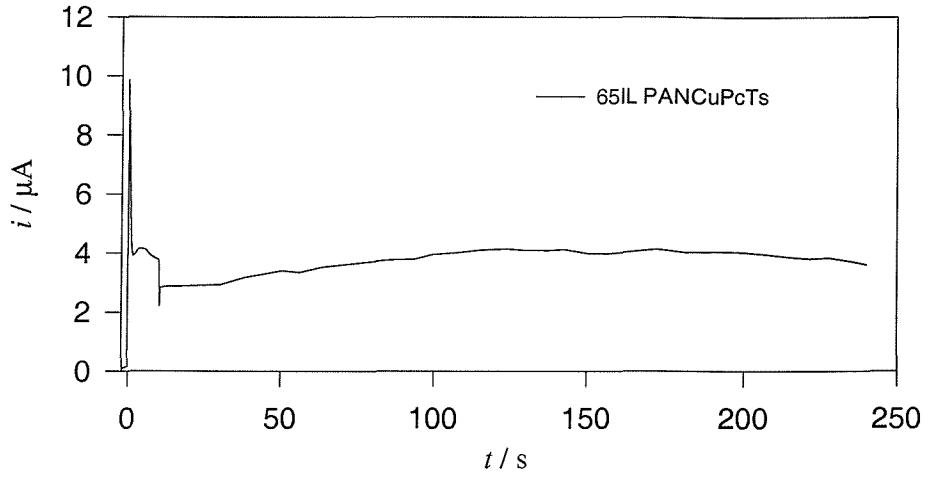

Figure 5. 6: typical current transient for the deposition of poly(aniline) copper phthalocyanine tetrasulfonate onto SRL123 devices- see Table 5. 4 for the polymerisation conditions.

Electrodeposition of poly(aniline) decane sulfonate and poly(aniline) p-toluene sulfonate

The current transient is similar for these two polymers as shown in Figure 5. 7. Compared to, for example, poly(aniline) pentane sulfonate, the current was significantly greater at least partially due to the elevated temperature of polymerisation which significantly increases the polymerisation rate. Elliott [11] reported that the polymerisation charge is doubled on increasing the deposition temperature for poly(aniline) butane sulfonate from 28° to 40°C. This corresponds, roughly, to the magnitude of increase observed on going from the pentane (deposited at room temperature) to the decane (deposited at 40°C) doped poly(aniline). In any case, the polymerisation rate should be decreased for further production of these poly(aniline) in order to enable better control of the coating characteristics (thickness and therefore resistance).

Six chemoresistors were coated with poly(aniline) decane sulfonate and six others with poly(aniline) *p*-toluene sulfonate. Again, the transient shape was reproducible from sensor

to sensor and the electropolymerisation current decreased with the number of successive polymerisations from the solution for the poly(aniline) decane sulfonate.

The polymerisation charge for PANDecaSA was poorly reproducible, 21.8 ± 3.7 mC, corresponding to an error of 17%. The resistance of the dry film was 3.6 ± 0.4 Ω. The variation in the resistance was only 11%, less than the spread in the polymerisation charge. The opposite was observed for all polymers investigated here. From visual observations, the poly(aniline) decane sulfonate films were thick, which was also confirmed by the low resistance of these films. In this case, the polymer is so thick that extra material has little influence on the base resistance, which then becomes highly reproducible. The growth charge for poly(aniline) *p*-toluene sulfonate did not decrease with the increasing number of successive polymerisations from the same solution. There is still however a relatively large spread in the charge (18.9 ± 2.5 mC, corresponding to 13% error). The resistance was 6.8 ± 1.0 Ω, corresponding to 15% error.

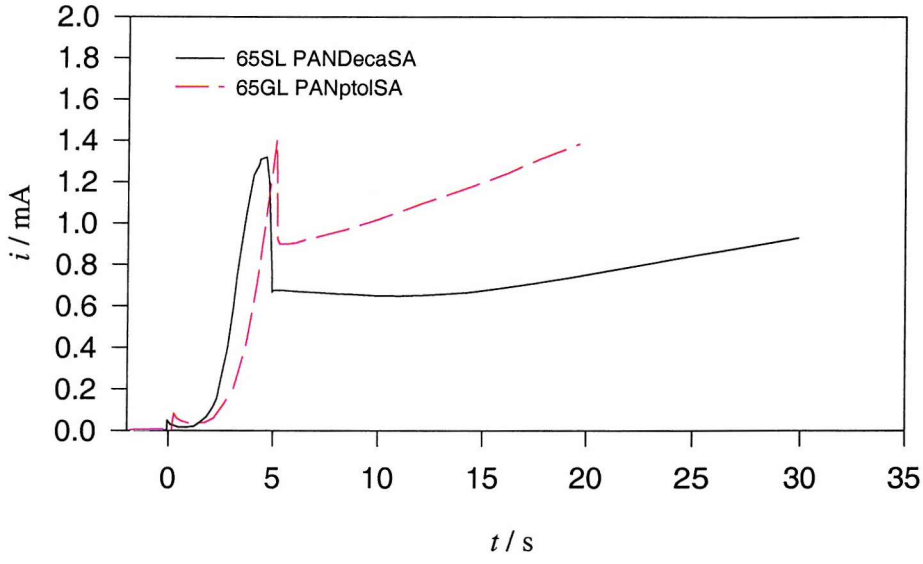

Figure 5. 7: typical current transients for the deposition of poly(aniline) decane sulfonate and poly(aniline) *p*-toluene sulfonate onto SRL123 devices- see Table 5. 4 for the polymerisation conditions.

Conclusions

The five types of poly(aniline) coated chemoresistors can be divided into three groups:

1. Poly(aniline) pentane sulfonate and poly(aniline) nickel phthalocyanine tetrasulfonate

These polymers presented a medium rate of deposition, performed at room temperature. The polymerisation charge was of about 5 mC, within 10-20% and the resistance of 10 to 50 Ω.

2. Poly(aniline) copper phthalocyanine tetrasulfonate

For some unknown reason, the polymerisation rate of aniline was extremely low, about 50 times lower than for poly(aniline) nickel phthalocyanine tetrasulfonate. Even if the polymerisation time was largely increased compare to the other poly(aniline) films, the charge passed remained small- about 1 mC- and the resistance of the polymers high- about 1500 Ω.

3. Poly(aniline) decane sulfonate and poly(aniline) *p*-toluene sulfonate

These polymers presented a high deposition rate, mainly due to elevated electropolymerisation temperature. The polymerisation charge was of about 20 mC within 15% and the resistance of the dry film was inferior to 4 Ω.

Table 5. 5 gathers together the polymerisation charges and the resistances of the dry films, with the associated errors, for the poly(aniline) films. In percentage terms, the error in the resistance of the film over the gap was larger than the error in the polymerisation charge, except for poly(aniline) decane sulfonate. In this case, the film was grown so thickly (as shown by the large polymerisation charge and the small resistance) that even a spread in the polymerisation charge (17%) would not create a large spread in the resistance of the device (11%). It is difficult to define the reproducibility of the polymer resistance for such low resistance as the contribution of the electrode tracks is no longer negligible.

In the case of the poly(aniline) metal phthalocyanine tetrasulfonate film, the variation in the resistance was much larger than the variation in the polymerisation charge, compared to the results obtained for the alkyl and *p*-toluene sulfonate films. A general observation for poly(aniline) is that the higher the resistance, the larger the variation in R, which nearly correspond to the smaller the polymerisation charge. This was not observed for poly(pyrrole) films.

Anion (number of devices)	Q / mC	Error Q/ mC 95% confidence	Error Q/ % 95% confidence	R / Ω	Error R/ Ω 95% confidence	Error R/ % 95% confidence
Pentane SA (7)	5.0	0.9	18	13.7	2.8	20
Decane SA (6)	21.8	3.7	17	3.6	0.4	11
p-toluene SA (6)	18.9	2.5	13	6.8	1.0	15
CuPcTs (7)	1.16	0.38	33	3187	1633	51
NiPcTs (6)	6.7	0.7	10	47	14	30

Table 5. 5: polymerisation charge and resistance of the dry poly(aniline) films expressed within 95% confidence limits for a number of sensors varying from 6 to 8 (number indicated in brackets next to the anion).

5.3.2 - Poly(aniline) coated Quartz Crystal Microbalance

Polymerisation was performed onto quartz crystal microbalance electrodes using the same deposition conditions as for the production of the chemoresistors.

5.3.2.1 - Poly(aniline) pentane sulfonate coated QCM

Poly(aniline) pentane sulfonate was deposited onto three crystals, referred to as QCM1, QCM6 and QCM7. The solution contained 0.2 M aniline, 0.5 M pentane sulfonate in 2M H_2SO_4. A potential of + 0.9 V was applied for 5 s followed by step at 0.78 V for 75 s.
The growth was reproducible for quartz crystals 1 and 6, with a polymerisation charge densities of 587 and 540 mC cm^{-2} respectively. The charge density was significantly smaller for the quartz crystal 7: 396 mC cm^{-2}.

Two batches of chemoresistors coated with poly(aniline) pentane sulfonate were produced. The batch described in the previous section was used first as chemoresistors. The second batch was produced using the *in-situ* resistance measurement technique described in Chapter 4. Gas test experiments showed that the response was significantly improved from the first batch. Consequents, the QCM coatings were produced in a similar manner, mainly with a low aniline concentration to gain control in the electrodeposition. The charge density was on average 501 mC cm^{-2} for the chemoresistors and 508 mC cm^{-2} for the quartz. Thus the quartz crystal microbalances coated with poly(aniline) pentane sulfonate were comparable to the chemoresistors produced using the *in-situ* resistance measurement technique (devices IB0041, IB0042 and IB0043).

The decrease in current observed for the deposition of poly(pyrrole) films onto QCM electrodes was not observed for the poly(aniline) pentane sulfonate films even thought the current was larger (2 mA) than for the poly(pyrrole) deposition (0.35 mA was flowing and 2.8 mA was expected). The absence of iR drop in the case of poly(aniline) can be explained by a smaller solution resistance due to the combination of a higher alkyl sulfonic acid concentration and additional sulfuric acid increasing the conductivity of the solution. The conductivity of the solution was not measured to quantify the resistive loss.

5.3.2.2 - Poly(aniline) decane sulfonate coated QCM

Poly(aniline) decane sulfonate was deposited onto two QCM electrodes, referred to as QCM10 and QCM11. The solution was the same as used for the chemoresistors but the second potential step duration was increased from 25 s for the chemoresistors to 100 s for the QCM. The growth was reproducible for the two depositions, both in terms of the charge ($Q_{growth10}$ = 316 mC and $Q_{growth11}$ = 319 mC) and in terms of the shape of the transients.

In a similar manner to PPyDecaSA, the polymerisation duration was increased from the chemoresistor to the QCM to compensate for the decrease in current density on the QCM electrodes. The final amounts of polymer deposited expressed as charge density were similar: 1835 mC cm^{-2} for the chemoresistors and 1458 mC cm^{-2} for the quartz crystal microbalances. The shape of the current transients compared in the region 0 to 30 s was also reproducible. Assuming that the deposition rate has no influence on the film properties (density, crystallinity, etc), the chemoresistors and the quartz coated with poly(aniline) decane sulfonate are comparable.

A first possible explanation for the difference in polymerisation rate in the case of poly(aniline) decane sulfonate from one substrate to an other is the effect of iR drop and that for two reasons. First, the current expected to flow during the deposition onto the quartz crystal microbalance was large- about 16 mA, eight times the current flowing during the deposition of the pentane sulfonate doped film. In this case the high concentration of decane sulfonate and the presence of sulphuric acid would not be sufficient to increase the solution conductivity. In fact only 3 mA was found to flow. Second, for practical reasons, due to the thermostat of the electrochemical cell, the

reference electrode could not be brought as close to the working electrode as before. By increasing the distance between the two electrodes to about 20 mm, the contribution to the iR drop was increased.

Another possible explanation for the slow rate of polymerisation is an effective temperature of the growth solution below 40°C. The cell employed for the deposition onto chemoresistor electrodes was thermostated with a water jacket surrounding the whole solution, ensuring a good control of the temperature of the solution. The cell used to deposit onto the QCM was thermostated using a spiral glass tube dipped in the solution. It is possible that in this case the temperature control was not as efficient. Elliott showed that, for the deposition of poly(aniline) butane sulfonate, the polymerisation rate decreased by 1/3 on decreasing the temperature from 40 °C to 30 °C, all other deposition conditions being identical [11]. She also reported that for this same polymer, the temperature had little influence on the shape of the current transient. This implies that the decrease in temperature would not have been detected by a change in the shape of the chronoamperogram. The temperature of the growth solution was not measured so that it is not possible to separate the contribution of the iR drop and of the temperature in the decrease in current density.

5.4 - Conclusions

5.4.1 - Chemoresistors

Ten different polymers were electrodeposited onto chemoresistor substrates, five poly(pyrroles) and five poly(anilines). For each polymer different anions were incorporated as dopant: pentane sulfonate, decane sulfonate, *p*-toluene sulfonate, copper phthalocyanine tetrasulfonate and nickel phthalocyanine tetrasulfonate. Comparison between poly(pyrrole) and poly(aniline) films is not straightforward as within each type of polymer the behaviour varies significantly. No simple relationship between the monomer, the anion, the polymerisation conditions, the polymerisation charge and the final resistance was observed.

A general comment on the production of the chemoresistors is that the irreproducibility in the deposition for identical polymerisation conditions, showed up to 18% variation in Q_{growth} for poly(aniline) pentane sulfonate. The irreproducibility in the polymerisation

induces an irreproducibility in the resistance of the devices, up to 89% for poly(pyrrole) decane sulfonate. A general trend is that there is a larger variation in the resistance than in the polymerisation charge (in %). However the largest variation in the polymerisation charge does not correlate with the largest variation in resistance as seen by comparing PPyDecaSA (6.6% error in Q and 89% error in R) with PPyCuPcTs (13.1% error in Q and only 21% error in R).

There are two experimental implications from the production of the chemoresistors detailed in this chapter:

- the range of resistances obtained varies from about 4 Ω to at least 3 kΩ. In order to minimise the noise compared to the signal, the electronics should be able to select various ranges according to the base resistance of the polymer.
- some polymer films were deposited leading to devices with a resistance as low as 4 Ω. The resistance of the various electrical contacts can be estimated as 1 Ω. Let assume that the response to a vapour from the polymer only, $\Delta R/R_{ini}$, is independent of the initial resistance R_{ini}. If the electrical connections have a non-negligible contribution to R_{ini}, (here 1 Ω for a 4 Ω device) then the sensitivity of the sensor decreases significantly- 25% for the values illustrating the case of poly(aniline) decane sulfonate. The implication is that the polymer films should be deposited more thinly in order to increase the base resistance and avoid this decrease in sensitivity.

One purpose for the deposition of poly(pyrrole) and poly(aniline) doped with various anions was to investigate the influence of the anion on the sensing properties. For example it should be possible to study the influence of the length of the carbon chain both in poly(pyrrole) and in poly(aniline) alkyl sulfonate by comparing the pentane and the decane doped films. An other example would be the influence of the nature of the metal in the metal phthalocyanine doped film. However an important point to take into account during this comparison, is that the polymer may have very different properties. For example, is it possible to compare the influence of the anion in poly(aniline) pentane sulfonate and in poly(aniline) decane sulfonate, the first one being deposited at room temperature, the second one at 40°C? Is it possible to compare poly(aniline) copper phthalocyanine tetrasulfonate with the nickel equivalent knowing from the polymerisation charge that the thickness of the former is about 6 times larger than the later? The

conclusion from this comment is that purely the influence of the anion on its own can not be investigated. Some changes in properties (thickness, crystallinity, doping level, etc) induced by different polymerisation conditions are expected to play a part in the difference in gas sensitivity. In the literature some authors have ignored this point and purely report on the influence of the anion [8], whereas others underline the fact that the contribution of the polymer's properties, influenced by the anion, is not negligible [3].

5.4.2 - QCM

Quartz Crystal Microbalance structures were coated with four polymer types: poly(pyrrole) pentane sulfonate, poly(pyrrole) decane sulfonate, poly(aniline) pentane sulfonate and poly(aniline) decane sulfonate. These polymers were selected as they are known to produce well behaved chemoresistors. The purpose was to compare their responses to vapours with the equivalent chemoresistors responses to investigate the interactions taking place between the conducting polymer and the vapour. During the interpretation it should be kept in mind that the poly(pyrrole) pentane sulfonate coating is seven times thinner on the QCM than on the chemoresistors; for the poly(pyrrole) decane sulfonate the difference in thickness is only of a factor 2. For both poly(aniline) coatings, chemoresistors and QCM are assumed comparable.

(1) Grate, J. W.; Abraham, M. H., *Sensors and Actuators B*, 1991, **3**, 85-111.

(2) Zellers, E. T.; Han, M., *Anal. Chem.*, 1996, **68**, 2409-2418.

(3) Topart, P.; Josowicz, M., *J. Phys. Chem.*, 1992, **96**, 8662-8666.

(4) Topart, P.; Josowicz, M., *J. Phys. Chem.*, 1992, **96**, 7824-7830.

(5) Vigmond, S. J.; Kallury, K. M. R.; Ghaemmaghami, V.; Thompson, M., *Talanta*, 1992, **39**, 449-456.

(6) Slater, J. M.; Watt, E. J.; Freeman, N. J.; May, I. P.; Weir, D. J., *Analyst*, 1992, **117**, 1265-1270.

(7) Kunugi, Y.; Nigorikawa, K.; Harima, Y.; Yamashita, K., *J. Chem. Soc., Chem. Commun.*, 1994, 873-874.

(8) Nagase, H.; Wakabayashi, K.; Imanaka, T., *Sensors and Actuators*, 1993, **B 13/14**, 596-597.

(9) Charlesworth, J. M.; Partridge, A. C.; Garrard, N., *J. Chem. Phys.*, 1993, **97**, 5418-5423.

(10) Patrash, S. J.; Zellers, E. T., *Anal. Chem.*, 1993, **65**, 2055-2066.

(11) Elliott, J. M., Conducting Polymer Odour Sensors, PhD thesis, SOUTHAMPTON, 1997.

(12) Blair, N., The development and characterisation of conducting polymer based sensors for use in an electronic nose, PhD thesis, SOUTHAMPTON, 1994.

(13) Warren, L. F.; Anderson, D. P., *J. Electrochem. Soc.*, 1987, **134**, 101-105.

(14) Talaie, A.; Wallace, G. G., *Solid State Ionics*, 1994, **70/71**, 692-696.

(15) Cabala, R.; Meister, V.; Potje-Kamloth, K., *J. Chem. Soc., Faraday Trans.*, 1997, **93**, 131-137.

(16) Hourch, A. E.; Rakotondrainibe, A.; Beden, B.; Crouigneau, P.; Leger, J. M.; Lamy, C.; Tanaka, A. A.; Gonzalez, E. R., *Electrochim. Acta*, 1994, **39**, 889-898.

(17) Coutanceau, C.; Hourch, A. E.; Crouigneau, P.; Leger, J. M.; Lamy, C., *Electrochim. Acta*, 1995, **40**, 2739-2748.

(18) Desilvestro, J.; Scheifele, W., *J. Mater. Chem.*, 1993, **3**, 263-272.

(19) Pellegrino, J.; Radebaugh, R.; Mattes, B. R., *Macromolecules*, 1996, **29**, 4985-4992.

(20) Lacroix, J. C.; Diaz, A. F., *J. Electrochem. Soc.*, 1988, **135**, 1457-1463.

(21) Tang, H.; Kitani, A.; Shiotani, M., *Electrochim. Acta*, 1996, **41**, 1561-1567.

Chapter 6 - Introduction to the QCM experiments

Conducting polymer chemoresistors are suitable as sensors to detect organic vapours. However understanding of the nature of the interactions taking place between the vapour and the polymer is poor. Resistance measurements do not give any information on the amount of vapour adsorbed, the location in the polymer layer, the strength of the forces between the vapour and the polymer or any reconfiguration of the polymer. The Quartz Crystal Microbalance coated with conducting polymer can, on its own, give some information both on the mass adsorbed and on viscoelastic effects occurring in the film. The origins and the limits of these properties will be now discussed to enable appropriate use. In the following chapter, the QCM will be employed to investigate the sensing mechanism.

In the second part of this chapter, some preliminary QCM experiments will be described and discussed, most importantly the calculations of the number of pyrrole or aniline units contained in the coating will be presented.

6.1 - Introduction to the Quartz Crystal Microbalance

6.1.1 - Piezoelectricity

In 1880, the Curie brothers, Pierre and Jacques, discovered surface electric charges on tourmaline crystals due to mechanical stress [1]. This phenomenon was called **piezoelectricity**. It consists of electrical polarisation of the crystal caused by deformation of the crystal in particular directions, causing the separation of the centres of oppositely

charged species. The polarisation is proportional to the applied pressure. One year later they showed experimentally the **converse effect**: mechanical deformation of crystals due to an applied electrical field [2], illustrated in Figure 6. 1. Since then piezoelectricity has been widely used and the QCM is one application.

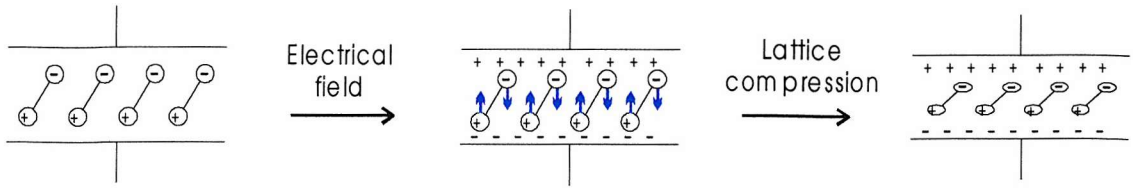

Figure 6. 1: diagram representing the converse effect of piezoelectricity. An electrical field is applied to an acentric material by two electrodes. It provokes a displacement of the oppositely charged species of the crystal creating a lattice deformation.

6.1.2 - The Quartz Crystal Microbalance principle

The principle of the Quartz Crystal Microbalance has been employed for a long time by the crystal manufacturers to adjust the resonant frequency of the crystals: by adding mass to the crystal they were able to decrease the resonant frequency of the oscillator to a desired value. It was only in 1957 that Sauerbrey applied this property to measure mass changes [3]. He demonstrated that the change in resonant frequency of a crystal is directly related to the mass changes on the crystal according to equation (1), known as the **Sauerbrey equation**. The QCM is a very sensitive balance and can easily detect monolayers of substances, with a precision in the range nanograms for a 10 MHz crystal.

$$\Delta m = -\Delta f * \frac{A(\mu_q \rho_q)^{1/2}}{2 f_0^{\,2}} \qquad (1)$$

where Δm : mass change

Δf : shift in resonant frequency due to the variation in mass (Hz)

A : area of the electrodes producing the electrical field (cm^2)

μ_q : shear modulus of the crystal (N cm^{-2})

ρ_q : density of the crystal (g cm^{-3})

f_0 : resonant frequency of the crystal (Hz)

Figure 6. 2 shows a diagram of a Quartz Crystal Microbalance using the converse piezoelectric effect. Both faces of the crystal are coated with an electrode, between which

an electrical field is applied. The active area of the QCM is limited to the cylinder containing the two electrodes which act as energy trapping. Generally, only one face of the crystal is coated or exposed to a solution, and the phenomenon taking place at this electrode can be monitored.

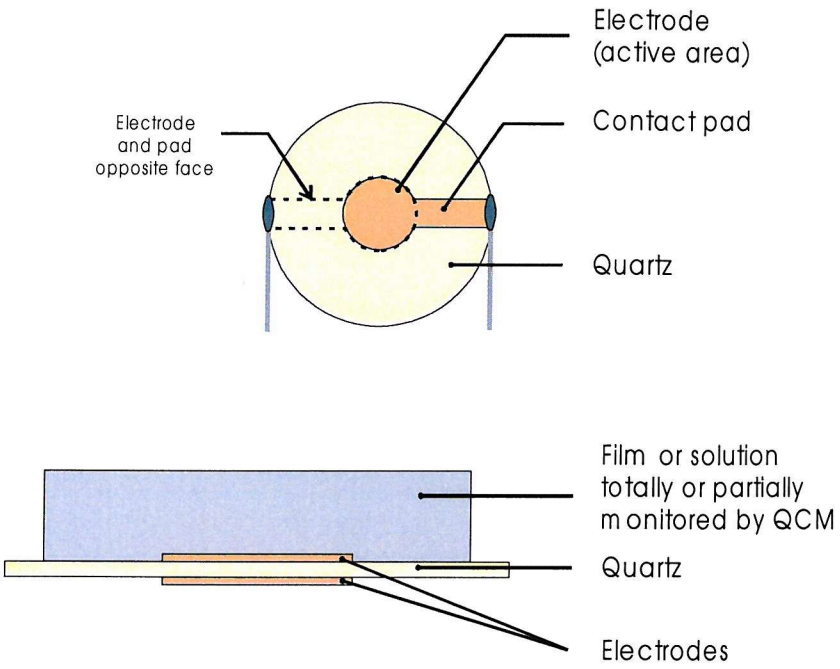

Figure 6. 2: typical quartz crystal microbalance design (top view and cross-section). The quartz is sandwiched between two disc electrodes and an electrical field is applied. The solution or film deposited over the electrodes can be sensed for mass and viscoelastic changes.

For the application of the QCM as a gas sensor, monitoring the resonant frequency of the crystal upon exposure is satisfactory as knowledge of the exact mass of adsorbed vapour is not required. **Impedance analysis** of the crystal is however a more complex but complete method which should be employed for research purposes. It gives information on both mass changes and viscoelastic effects. The QCM electrical equivalent circuit, known as the Butterworth van Dyke (BVD) circuit, is shown in Figure 6. 3. It comprises a resistance, a capacitance and an inductance in series, which are referred to as the **motional branch**. In parallel to the motional branch is another capacitance, C_0.

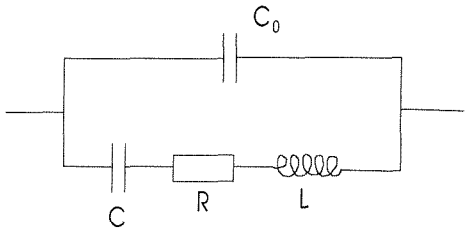

Figure 6. 3: Butterworth van Dyke (BVD) equivalent electrical circuit of a QCM.

The physical interpretation of the different components of the equivalent circuit are:

- R : energy dissipation (internal friction, mechanical and acoustical losses), indicative of the viscoelasticity
- L : inertial component, related to the displaced mass, so directly depending on the loading of the crystal
- C : energy stored during oscillation by the crystal
- C_0 : static capacitance of the quartz resonator with the electrodes

In a QCM experiment, a pure increase in mass will be reflected by an increase in L and a pure change in viscoelasticity by a change in R. C_0, which represents the capacitance of the measurement circuit, is constant during the experiment. C, the capacitance between the two electrodes, is also assumed to be independent of the sensitive layer and therefore constant.

In the work presented here, the output of the impedance analysis of the QCM was the real (Y_{real}) and the imaginary (Y_{ima}) parts of the admittance, which were then fitted to the corresponding equations, (2) and (3) respectively. Taking C and C_0 as constants, the values of R and L could be deduced from the fitting program.

$$Y_{real} = \frac{R}{R^2 + (Lw - \frac{1}{Cw})^2} \qquad (2)$$

$$Y_{ima} = C_0 w - \frac{Lw - \frac{1}{Cw}}{R^2 + (Lw - \frac{1}{Cw})^2} \qquad (3)$$

where w is the angular frequency.

6.1.3 - Discussion of the rigid film approximation

The Sauerbrey equation, relating the shift in resonant frequency to the mass uptake, is limited to the case of a coating behaving as a rigid layer (R constant). The gravimetric mode of the QCM is often limited by viscoelastic effects occurring in the coating. In the literature, there are different approaches to the problem of possible viscoelastic effects taking place in conducting polymer gas sensors. Many authors [4-7] have simply ignored the limitations of the rigid film approximation and used the Sauerbrey equation, probably because of the difficulty in estimating the contribution of the viscoelastic effects to the shift in resonant frequency.

In their review on EQCM, Buttry *et al.* [8] reported that a coating can be approximated to a rigid layer if it corresponds to less than 2% of the mass of the crystal, equivalent to a maximum shift of 200 kHz for a 10 MHz crystal. Slater [9] has employed this same approximation in the case of conducting polymers quoting a study performed on metallic films [10]. However due to the very different viscoelasticity of polymers compared to metals, as well as the larger porosity where solvent can be trapped, the validity of the argument is open to question.

A more complete approach was adopted by Topart [11] who recorded the impedance of the QCM over a range of vapour concentrations and was able to detect a significant change in the viscoelasticity behaviour in a poly(pyrrole) film once exposed to about 12 % methanol vapour.

Contribution of viscoelastic effects to the shift of resonant frequency of a QCM was estimated in this work using the method suggested by Calvo *et al.* [12]. According to this approach, the deposition of a rigid layer leads to a shift in resistance, ΔR, which is negligible compared to ΔX_L. ΔX_L represents the shift in mass expressed in ohm, therefore allowing direct comparison with ΔR, and is calculated according to equation (4),

$$\Delta X_L = 2\pi f_0 \Delta L \qquad (4)$$

where f_0 is the resonant frequency of the crystal.

For a rigid layer it is expected that the contribution to R of any additional mass is zero, or in other words $\Delta X_L >> \Delta R$. In this case, the plot of ΔR versus ΔX_L gives a horizontal line. For a semi-infinite Newtonian liquid, the viscoelasticity is zero and the curve becomes a straight line of slope + 1. If $\Delta R \leq 10^{-2} \Delta X_L$, the viscoelasticity effects are negligible and the coating can be considered as a rigid layer. Unfortunately, to the best of my knowledge,

when ΔR and ΔX_L are of the same order, there is no way with the data available of predicting the effect of the viscoelasticity on the shift in resonant frequency.
Etchenique and Brudny reported in reference [13] the polar plot of a poly(aniline) film upon drying which could be approximated to a spiral centred at the initial wet film coordinates. In other words, upon drying, X_L was both increasing and decreasing, and both for ΔX_L positive and negative R was found to increase and decrease. This implies that calculating the mass using the Sauerbrey equation would lead to mis-interpretation, finding both increase and decrease in the content of water upon drying. The impossibility of predicting the effect of viscoelasticity on the Sauerbrey equation is also illustrated by the contradictory results reported by Luklum *et al.* [14] and Rodahl *et al.* [15]: the first group reported an amplification of the sensitivity of QCM sensors due to viscoelastic effects while the second group reported an under-estimation of the mass due to the decrease in the propagation depth of the acoustic wave.

In the work presented here, QCM sensors are coupled with chemoresistor sensors to investigate the interactions between the polymer and the vapour. In a similar manner, many authors have coupled QCM coated with conducting polymers with chemoresistors [4-6,9], as well as with Kelvin probe measurements [11,16] or used the QCM on its own [7].

The combination of the conducting polymer chemoresistors with the QCM here may enable us:

- to determine the amount of gas absorbed per monomer unit, for water and/or for vapour.
- to study the effect of one vapour molecule on the resistance as a function of the vapour concentration in the polymer.
- to determine the amount of vapour adsorbed as a function of humidity
- to detect physical changes of the polymer from the viscoelasticity contribution of the QCM.
- to have a time resolution between the adsorption of the vapour by the film (QCM) and the change in resistance of the chemoresistor and any reconfiguration of the polymer.

6.2 - Preliminaries to the QCM experiments

6.2.1 - Determination of the amount of monomer units on the QCM sensors

As just described, the combination of the QCM with chemoresistors may bring some information on the molecular scale of the sensing mechanism, for example on the number of vapour molecules adsorbed per monomer unit. To do this, the number of monomer units immobilised onto each quartz crystal microbalance has to be determined prior to the gas test experiments. For this, two approaches are available: electrochemical determination and use of the microbalance property of the quartz crystal. In all methods, limits to the validity have to be made, so that the number of monomer units will be given as a range rather than as an absolute value. The calculations, the approximations required and the results are now described and discussed.

6.2.1.1 - Determination of the number of pyrrole units

Poly(pyrrole) pentane sulfonate

Method 1: electrochemical determination

During electropolymerisation of pyrrole, n electrons are required for the formation of the polymer backbone per monomer unit. In addition, the polymer is produced in its oxidised form, with one positive charge delocalised on the polymer chains, over m monomer units, requiring withdrawing of a further 1/m electron per monomer unit. 1/m is called the **doping level**. The total number of electrons required for the electrodeposition of the material effectively deposited onto the electrode is then n+1/m per pyrrole unit. During electrodeposition, part of the oxidation products pass into solution, themselves contributing to a number of electrons n'+1/m'. The growth charge can therefore be expressed as:

$$Q_{growth} = N_{ox}\left[\left(n+\frac{1}{m}\right)DE+\left(n'+\frac{1}{m'}\right)(1-DE)\right]F \qquad (5)$$

where DE is the deposition efficiency, N_{ox} the number of moles of monomer oxidised and F the Faraday constant.

The deposition efficiency of the electropolymerisation, DE, is defined as:

$$DE = \frac{N_{dep}}{N_{ox}} \qquad (6)$$

where N_{dep} is the number of moles of monomer units deposited onto the electrode.

If the polymer modified electrode is removed from the solution and is transferred to a solution of background electrolyte, free of monomer, the polymer can be switched between its oxidised and reduced states. The charge passed will ideally be proportional to the amount effectively deposited, N_{dep}, according to:

$$Q_{elec} = N_{dep} \frac{1}{m} F \qquad (7)$$

where Q_{elec} is the charge passed to reduce or oxidise the polymer in the electrolyte.

Let assume that the Faradaic efficiency for the growth onto a disc electrode and onto a QCM electrode are the same, that the oxidation state of the material lost in both cases is the same and that the degree of oxidation of the deposited polymer is the same, the deposition efficiency can be determined from the electrodeposition onto a disc electrode further cycled in the background electrolyte.

From equations (5) and (7), the deposition efficiency can be calculated:

$$DE = \frac{N_{depD}}{N_{oxD}} = \frac{Q_{elecD} m}{F} \frac{F[ADE + B(1 - DE)]}{Q_{growth\,D}} \qquad (8)$$

where the index D refers to the disc electrode, A=n+1/m and B=n'+1/m'.

By rearranging equation (8), the deposition efficiency is:

$$DE = \frac{BQ_{elecD} m}{Q_{growthD} - Q_{elecD}(A - B)m} \qquad (9)$$

By combining equations (5), (6) and (9) the number of moles of monomer units deposited onto the QCM can be determined:

$$N_{depQCM} = N_{oxQCM} DE$$

$$= \frac{Q_{growthQCM}}{F\left[A\left(\frac{BQ_{elecD} m}{Q_{growthD} - Q_{elecD}(A - B)m}\right) + B\left(1 - \frac{BQ_{elecD} m}{Q_{growthD} - Q_{elecD}(A - B)m}\right)\right]} \frac{BQ_{elecD} m}{Q_{growthD} - Q_{elecD}(A - B)m} \qquad (10)$$

where the index QCM refers to the QCM electrode.

Rearranging equation (10) leads to:

$$N_{depQCM} = \frac{mQ_{growthQCM}Q_{elecD}}{FQ_{growthD}} \qquad (11)$$

Knowing the doping level, the electropolymerisation charge onto the QCM, the charge for the polymerisation onto the disc electrode and the charge passed in background electrolyte, the number of monomer units effectively deposited onto the QCM can be calculated. Bearing in mind the assumptions made earlier, equation (1) shows that the number of monomer units deposited onto the QCM is independent of the nature of the by-products (length of the polymer chain and degree of oxidation).

It is of interest for the discussion of the results to calculate the deposition efficiency and therefore a number of limitations need to be discussed, here for the coating of the QCM 4. An Excel spreadsheet was created to calculate the different minimum and maximum values originating from the limits of validity (Table 6. 1).

Limit of validity 1

The first approximation was made when a number of 2+1/m electrons per pyrrole unit was assumed. In theory, two electrons are required per monomer unit for the formation of the polymer backbone. This assumes that the polymer chain is long enough to neglect the contribution of the two end units, each contributing only one electron. No experiment has been performed to determine the exact length of the polymer chain for the polymers employed here. It was assumed that the polymer chain contained, at a minimum, 8 repeats, corresponding to 1.75 electrons per monomer. 8 is the value often assumed as the length for the precipitation of the oligomers onto the electrodes [17].

Limit of validity 2

The doping level, 1/m, for poly(pyrrole) pentane sulfonate was determined by elemental analysis for films grown in identical conditions [18]. A value of 0.33 was calculated, corresponding to one positive charge delocalised on three monomer units. For similar materials Wernet [19] and Shimidzu [20] reported lower dopant level, down to 0.254. So the minimum number of electrons required per pyrrole unit for the doping was taken as 0.25, and the maximum as 0.33.

Combining approximations 1 and 2, the total number of electrons required for the formation of poly(pyrrole) pentane sulfonate lies between 2.0 and 2.33 electrons per pyrrole unit.

Number of electrons per monomer unit

	Minimum	Maximum
n backbone	1.75	2
n doping	0.25	0.33
n total	2	2.33

Determination of Deposition Efficiency

Experiment	1	2	3
Q_{growth} / mC	14.2	11.3	12.1
Q_{elec} / mC	0.451	0.236	0.389
Deposition Efficiency Minimum / %	19.2	12.7	19.5
Deposition Efficiency Minimum / %	32.6	21.4	33.0

Quartz Crystal Microbalance – QCM 4 (Q_{growth} = 41 mC)

	Minimum	Maximum
Extra-polymerisation / %	2	10
Q_{growth} active area / %	37.27	40.20
Deposition Efficiency / %	12.7	33.0
Q_{elec} expected / mC	5.04	13.25
Number of units deposited / mol	2.24E-08	6.86E-08

Table 6. 1: spreadsheet used to calculate the number of pyrrole units contained in the poly(pyrrole) pentane sulfonate film deposited onto the QCM 4 using the electrochemical method (referred to as method 1). It gathers together the different approximations as well as the minimum and maximum values at each step of the discussion (see text). The **extra-polymerisation** corresponds to the amount of polymer deposited onto the electrode tracks, not contributing to the mass measurement of the QCM.

The deposition efficiency was calculated from the electrodeposition onto a 1 mm diameter gold disc electrode. Three poly(pyrrole) pentane sulfonate films (referred to as experiment 1 to 3 in Table 6. 1) were deposited in the same conditions as the film deposited onto the quartz crystal. They were then washed with deionised water and transferred into background electrolyte, free of monomer. The films were then cycled three times between their oxidised and reduced states (between + 0.4 and – 0.9 V *vs.* SCE). Then the electrode potential was maintained at +0.4 V for five minutes to ensure full oxidation of the

poly(pyrrole) before stepping to – 0.9V until the current had decayed to zero. The charge passed to reduce the poly(pyrrole) is related to the doping level and the amount of electroactive polymer deposited on the electrode according to equation (7).

For all three experiments, the minimum and maximum deposition efficiencies (DE_{min} and DE_{max} respectively) were calculated from the growth charge, the charge passed in the electrolyte during the redox switching, the minimum and maximum number of electrons for the doping and the total number of electrons (found in Table 6. 1), according to equations (12) and (13),

$$DE_{min} = \frac{Q_{elec}}{Q_{growth}} * \frac{n_{totmin}}{n_{dopmax}} \qquad (12)$$

$$DE_{max} = \frac{Q_{elec}}{Q_{growth}} * \frac{n_{totmax}}{n_{dopmin}} * 1.1 \qquad (13)$$

where n_{totmin} is the minimum of the total number of electrons required (2 electrons), n_{totmax} the corresponding maximum (2.33 electrons), n_{dopmin} the minimum of electrons required for the doping (0.25 electron) and n_{dopmax} the corresponding maximum (0.33 electron).

Limit of validity 3

The coefficient 1.1 in equation (13) is here justified by a percolation argument. As Aoki [21] showed for poly(aniline), during the redox switching, due to the interruption of the conducting path before reduction could occur, some electroactive material remains in its oxidised state. This material does not take part in Q_{elec} but does in the sensor response. Here the amount was roughly estimated at 10%. Aoki only performed percolation studies on poly(aniline) films and further showed that the level of reduction was dependent on the electrochemical conditions employed for the reduction. Therefore no exact value is here given.

The maximum deposition efficiency calculated for poly(pyrrole) pentane sulfonate was 33%, far below the expected value. Indeed, Wainright [22] reported a much larger deposition efficiency for poly(pyrrole), lying between 67 and 97% depending on the anion used and Baker [23], without reporting an exact value, reported a deposition efficiency close to 100%. Even thought a lower pyrrole concentration was used in his work (which could improve the deposition efficiency due to the slower polymerisation rate), it is

unlikely that it accounts for the large difference in deposition efficiency. In addition, for a deposition efficiency of 33%, coloured by-products are expected to be visible in the growth solution, which was not observed. Thus it appears that the deposition efficiency calculated here has been under-estimated. One possible explanation for the low deposition efficiency could be the loss of material during the transfer between the growth and the electrolyte solutions.

Limit of validity 4

The deposition efficiency values were used to calculate the amount of poly(pyrrole) deposited onto the quartz crystal coated with poly(pyrrole) pentane sulfonate- third table in Table 6. 1. In doing this it was assumed that the deposition efficiency was independent of the substrate and of the polymerisation rate. As seen in Chapter 5, the polymerisation rate was lower on the QCM substrates than on the chemoresistor substrates, the later being similar to a 1 mm diameter gold electrode, which then probably also influence the deposition efficiency. Because its contribution could not be quantified, this was not taken into consideration in the calculations.

Method 2: QCM determination

Using the values and approximations discussed above, the interval $2.24.10^{-8}$ to $6.86.10^{-8}$ mol was defined electrochemically (method 1) as comprising the number of pyrrole units deposited onto QCM 4. For comparison, the number of monomer units can be determined from the mass loading of a QCM, calculated from the shift in resonant frequency from the bare crystal to the polymer coated crystal using the Sauerbrey equation (method 2).

In order to employ the Sauerbrey equation, the rigid film approximation was verified according to Calvo's criteria [12] as discussed earlier. The shift in R (ΔR= 8 Ω) was found to be negligible compared to the change in X_L (ΔX_L= 1885 Ω) so that it was concluded that the poly(pyrrole) film deposited onto QCM4 was behaving like a rigid layer in the dry state. Then using the Sauerbrey equation leads to a corresponding mass of 15.5 μg.

To calculate the corresponding number of pyrrole units, the molecular weight has to be determined. From the elemental analysis [18], a molecular weight per pyrrole unit of 115.3 g mol^{-1} was determined, corresponding to C_4H_3N, 1/3 $C_5H_{11}SO_3$. The number of pyrrole units deposited was then $1.35.10^{-7}$ mol, 2.5 to 9 times larger than the number of pyrrole units determined by electrochemistry (method 1).

Limit of validity 1'

The calculations performed above supposed that the polymer film was free of solvent. The shift in resonant frequency was measured by flowing dry air over the QCM, so it is first expected that any contribution of residual solvent in the film to the mass on the microbalance would be eliminated. However, for poly(aniline) some non-negligible amount of residual water, even in the dry state, has already been reported (Matveeva [24] reported 0.3 molecule H_2O per aniline unit). So it seems reasonable to consider a similar phenomena for poly(pyrrole). Assuming that only polymerisation solvent (water) is incorporated, the amount of water deduced from QCM would be at least of 5.7 molecule per pyrrole unit to compensate for the extra weigh, which seems unlikely because it is so large. It is assumed here that any pentane sulfonate trapped in the film as salt, which would account for extra mass is already taken into consideration in the molecular weight deduced from the elemental analysis.

Conclusion on the determination of the number of monomer units- method 3

The number of pyrrole units deposited onto the QCM4 as poly(pyrrole) pentane sulfonate has been determined both by electrochemistry (method 1) and using the microbalance property of the quartz crystal (method 2). The amount determined by the first method ($0.2.10^{-7}$ to $0.7.10^{-7}$ mol of units) is at least 2.5 times smaller than the amount determined by the second ($1.35.10^{-7}$ mol of units). The results of these experiments are represented in Figure 6. 4, showing the disagreement between these two methods. For reasons already detailed, it is suspected that electrochemistry has led to an underestimation, mainly due to a very low calculated deposition efficiency. However some assumptions were also made when employing the QCM, so that the validity of the results is not well defined. Both calculations do not appear to lead to significant results. They failed in determining a reduced interval containing the number of pyrrole units. A more appropriate determination is now proposed.

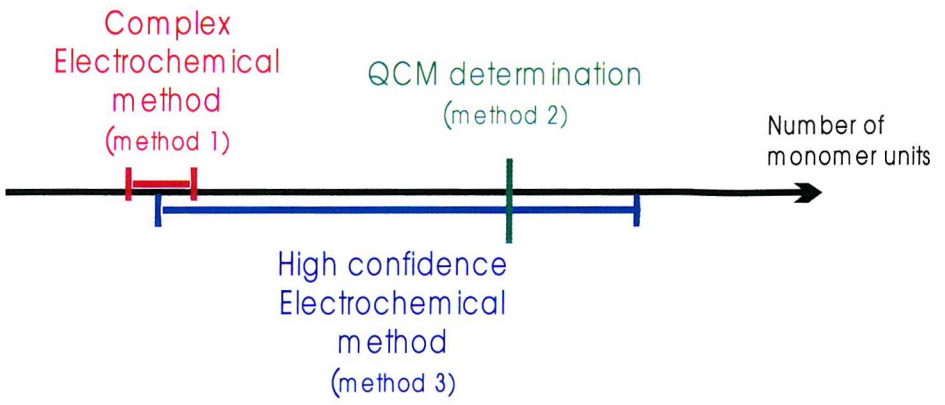

Figure 6. 4: schematic diagram showing the number of monomer units deposited onto QCM determined by three different techniques. The lack of agreement between methods 1 and 2 requires the use of method 3, less precise but of higher confidence. This diagram is typical for the poly(pyrrole) films investigated here.

Regarding the confidence in the validity, a more satisfactory method exists to determine the range of monomer units deposited, but with the counter-part of loss of precision (method 3 in Figure 6. 4). The maximum number of units deposited can be calculated from the polymerisation charge assuming 100% efficiency in the deposition. Using 2.3 electron per monomer unit for the polymerisation, a maximum value of $1.75.10^{-7}$ pyrrole units was determined for the QCM 4 using equation (8). The lower limit of the range, $0.38.10^{-7}$ mol units, is calculated from the polymerisation charge and the deposition efficiency (20%). The later is here a rough estimation calculated without taking into account all the approximations discussed in Table 6. 1 as they are shown to lead to unsatisfactory results.

Poly(pyrrole) decane sulfonate

Blair [18] determined a doping level of 0.33 for poly(pyrrole) decane sulfonate which is in agreement with the reported value by Wernet [19] and Shimidzu [20]. A similar spreadsheet to the one described for poly(pyrrole) pentane sulfonate was developed. Using this value a higher deposition efficiency than for PPyPentSA was calculated (68%). However, the conclusions were similar: a careful determination of the number of monomer units led to contradictory results when comparing electrochemical technique (method 1) and QCM technique (method 2). So the minimum and maximum number of monomer units were determined following method 3, using the polymerisation charge and a deposition efficiency of 68% and 100% for the minimum and the maximum of the range respectively.

Two QCM were coated with poly(pyrrole) pentane sulfonate (QCM 4 and 5), and two others with poly(pyrrole) decane sulfonate (QCM 8 and 9). Table 6. 2 gives the range for the number of pyrrole units for each of them, determined as discussed.

QCM	4	5	8	9
Polymer	PPyPentSA	PPyPentSA	PPyDecaSA	PPyDecaSA
Q_{growth} / mC	41	42	184.4	160.8
Extra-polymerisation / %	5	5	12	12
Max number units / mol **100% DE**	$1.75.10^{-7}$	$1.79.10^{-7}$	$7.30.10^{-7}$	$6.35.10^{-7}$
Min number units / mol **calculated DE**	$0.38.10^{-7}$	$0.39.10^{-7}$	$4.96.10^{-7}$	$4.32.10^{-7}$

Table 6. 2: polymerisation data onto quartz crystals coated with poly(pyrrole), as well as the estimated ranges for the number of pyrrole units deposited determined using method 3. The maximum value was calculated assuming 100% deposition efficiency and the minimum using the calculated deposition efficiency (20% for the pentane sulfonate and 68% for the decane sulfonate doped films).

Other authors have performed similar calculations. A detailed discussion is given by Baker [23] who investigated the electropolymerisation of pyrrole by QCM. The main conclusion, even if some of the approximations detailed here are ignored, is that, unlike here, he found agreement between both electrochemical and QCM methods.

Topart [11], in his analysis of QCM gas sensors, quoted a value for the number of adsorbed vapour molecules per monomer unit. From the slope of the linear variation of the shift in resonant frequency with the electropolymerisation charge, he deduced the number of electrons per monomer unit (2.20 for poly(pyrrole) *p*-toluene sulfonate and 1.70 for poly(pyrrole) tetrafluoroborate). Unfortunately, the calculations of the number of monomer units are not detailed. At the same time, he underlines that there is possibly incorporation of solvent in the film, but no attempt to estimate its contribution is reported. Most of the authors investigating the response of QCM gas sensors simply ignore this point.

6.2.1.2 - Determination of the number of aniline units

The polymerisation of aniline is similar to pyrrole in the sense that it requires 2 electrons per monomer to form the backbone. The electrochemistry of the polymer is different in the sense that poly(aniline) exists in three different oxidation states: the fully reduced, the semi-oxidised and the fully oxidised states [25]. The degree of oxidation of the as electropolymerised poly(aniline) is located between the semi and the fully oxidised states

so, for the electropolymerisation, 2.5 to 3 electrons are required per aniline unit. 0.5 electrons are required to reach the semi-oxidised state, and between 0 to 0.5 further electron are required to reach the as-synthesised oxidation state. In the background electrolyte, the charge passed to switch from reduced to semi-oxidised state corresponds to 0.5 electron per aniline unit and can be used to determine the number of aniline molecules deposited onto the QCM substrates.

The discussion on the determination of the number of monomer units is similar to the discussion for poly(pyrrole). A spreadsheet was developed using the QCM 1 coated with poly(aniline) pentane sulfonate. The number of aniline units deposited, determined by the different techniques described for PPyPentSA, are gathered together in Table 6. 3.

Technique	Number of monomer units / mol
Minimum deduced from method 1	$1.20.10^{-7}$
Maximum deduced from method 1	$2.64.10^{-7}$
Method 2	$8.10.10^{-7}$
Maximum deduced from method 3	$4.75.10^{-7}$

Table 6. 3: number of aniline units deposited onto the QCM1 as poly(aniline) pentane sulfonate, determined by three different methods. The minimum and maximum were determined using a detailed and rigorous method, as in the spreadsheet discussed for PPyPentSA (method 1). For comparison, the value determined by QCM (method 2) is given, as well as the value deduced from the polymerisation charge assuming 100 % deposition efficiency and 2.5 electrons (method 3).

From Table 6. 3 it can be concluded that again there is disagreement between the electrochemical and the QCM techniques.

On one hand, a relatively low deposition efficiency was calculated (44%) and for the same reasons as given for poly(pyrrole), it was suspected that the obtained value was an under-estimate. On the other hand, if the number of monomer units was determined using a deposition efficiency of 100%, which confidently indicates the maximum, the value was still below that determined by mass measurement. This implies that the QCM was unsuitable to define a relevant value for this coating. There are at least two possible sources of error:

- water trapped in the film, expected to be in a larger amount than for poly(pyrrole)

- viscoelastic effects which could account for over-estimation of the mass deposited, even if for the dry film the rigid film approximation applies according to Calvo's criteria.

As for poly(pyrrole), the results of our attempt of estimate a well defined interval were unsatisfactory. To increase confidence, the number of aniline units was calculated from the polymerisation charge using the calculated deposition efficiency (44% for poly(aniline) pentane sulfonate and 47% for poly(aniline) decane sulfonate) and 100%. The results are gathered together in Table 6. 4.

QCM	1	3	6	10	11
Polymer	PANPentSA	PANPentSA	PANPentSA	PANDecaSA	PANDecaSA
Q_{elec} / mC	123.2	119.8	111.2	316	318.6
Extra-polymerisation / %	7	7	5	10	12
Maximum units / mol 100% DE	$4.75.10^{-7}$	$4.62.10^{-7}$	$4.38.10^{-7}$	$11.79.10^{-7}$	$11.62.10^{-7}$
Minimum units / mol calculated DE	$2.09.10^{-7}$	$2.03.10^{-7}$	$1.93.10^{-7}$	$5.54.10^{-7}$	$5.46.10^{-7}$

Table 6. 4: polymerisation data onto quartz crystals coated with poly(aniline), as well as the interval containing the number of aniline units deposited (method 3). The maximum value is calculated assuming 100% deposition efficiency and the minimum value using the calculated deposition efficiency (44% for the pentane sulfonate and 47% for the decane sulfonate doped films).

In the calculations performed to determine the number of monomer units deposited onto the QCM, it was first concluded that detailed calculations were unsuccessful. Indeed, there is disagreement between the electrochemical method and the QCM method. It was concluded that the number of monomer units could, with a higher confidence, be located in an interval determined from the polymerisation charge, employing a deposition efficiency lying between a value estimated experimentally and 100 %. The drawback is the lack of precision which will make the interpretation of the gas sensing results more complex. Before interpreting the response of the QCM gas sensors, further points regarding the microbalance experiments need to be addressed.

6.2.2 - Fitting program

The good fitting of the program of the real and imaginary admittance values to the BVD equivalent circuit (equations (2) and (3)), written using Mathematica, was verified in two ways:

- the values of R, L, C and C_0 obtained from the fitting program were reintroduced into the equations and the curves obtained from these were compared to the experimental curve.
- One set of data was fitted using Sigma Plot in addition to Mathematica, and the fitted parameters were compared.

This procedure showed that the parameters required to interpret the QCM response could be successfully extracted.

6.2.3 - Bare crystal experiment

In order to estimate any contribution of the bare crystal to the response of the gas sensor, an uncoated QCM was placed in the gas test chamber and its response to humidity and vapour concentration changes analysed. The resonant frequency of the crystal decreased by about 14 Hz when switching from dry air to air containing 16768 ppm water, and by a further 10 Hz when adding 41172 ppm ethanol vapour. Comparing these values for the bare crystal with the values for coated QCM (responses detailed in the next chapter), it can be concluded that the intrinsic sensitivity of the gold electrode is low and can be neglected.

6.2.4 - Transfer function

The responses of the QCM to vapours were analysed by following the values of R and L in the BVD equivalent circuit, indicative of the mass and viscoelastic effects. Before going into details in the analysis, the raw data, the admittance curve, gives some preliminary information on the behaviour we can expect from the coated QCM.

The curve of the real part of the admittance as a function of the frequency shows a single peak as shown, for example, in Figure 6. 5. The position of the peak on the frequency axis gives the resonant frequency. On one hand, a pure gravimetric response of the QCM would correspond to a shift in the peak along the x axis without any modification in the shape. On the other hand, purely viscoelastic changes are signalled by a change in peak

shape but not in position. For conducting polymers, both gravimetric and viscoelastic effects are expected to take place simultaneously, leading to a shift in resonant frequency as well as a change in the shape of the admittance curve.

Figure 6. 5 and Figure 6. 6 show the real part of the admittance at 0 ppm and 13414 ppm water for the four QCM coatings tested (poly(pyrrole) pentane sulfonate, poly(pyrrole) decane sulfonate, poly(aniline) pentane sulfonate and poly(aniline) decane sulfonate).
A first comment is required on the behaviour of the poly(aniline) decane sulfonate coated QCM. In contrast to the other polymers, the peak is not well defined (very broad and of low amplitude). From the large polymerisation charge and the shape of the transfer function it is believed that the loading on the crystal and the viscoelastic effects are so important that they prevent any vibration of the crystal and its resonance. This further implies that the QCM coated with PANDecaSA could not be used as gas sensor.

A general behaviour seen on the graphs is the shift to lower frequency of the peak upon exposure from dry air to air containing 13414 ppm due to water adsorption in the coating and therefore mass increase. For the pentane sulfonate doped films, a broadening of the peak is observed, whereas for PPyDecaSA the peak sharpens. This would correspond to two opposite viscoelastic behaviours. The exact reason behind these opposite behaviours is not yet clear.

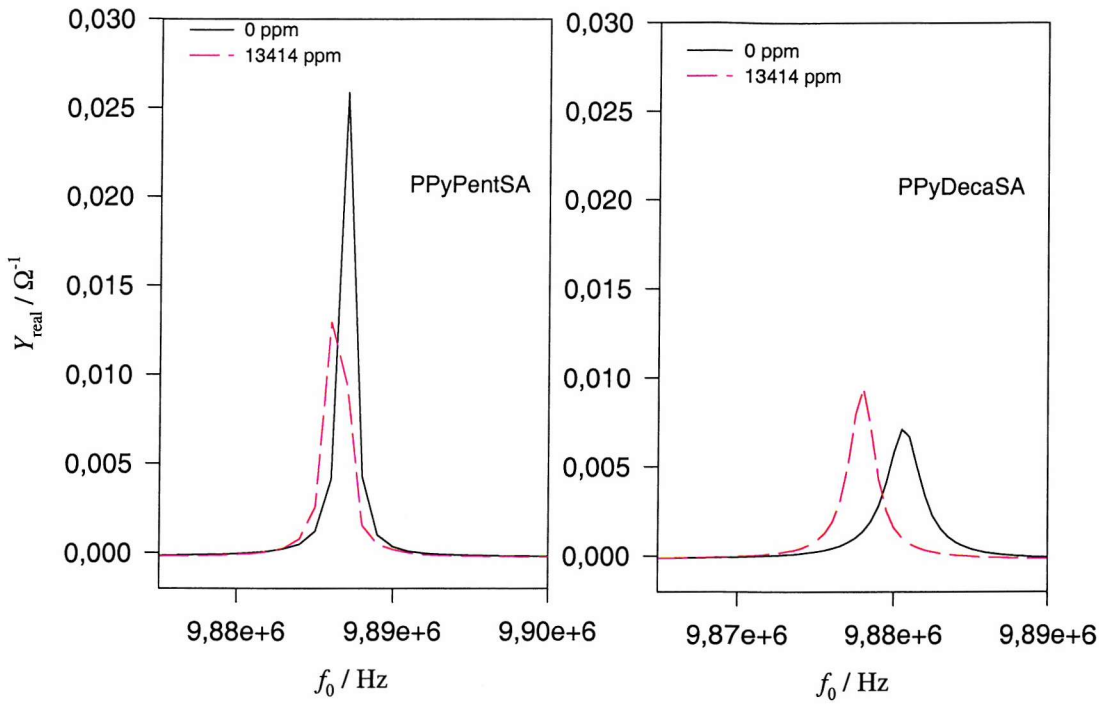

Figure 6. 5: real part of the admittance of a QCM coated with poly(pyrrole) pentane sulfonate and a QCM coated with poly(pyrrole) decane sulfonate at 0 ppm and 13414 ppm water.

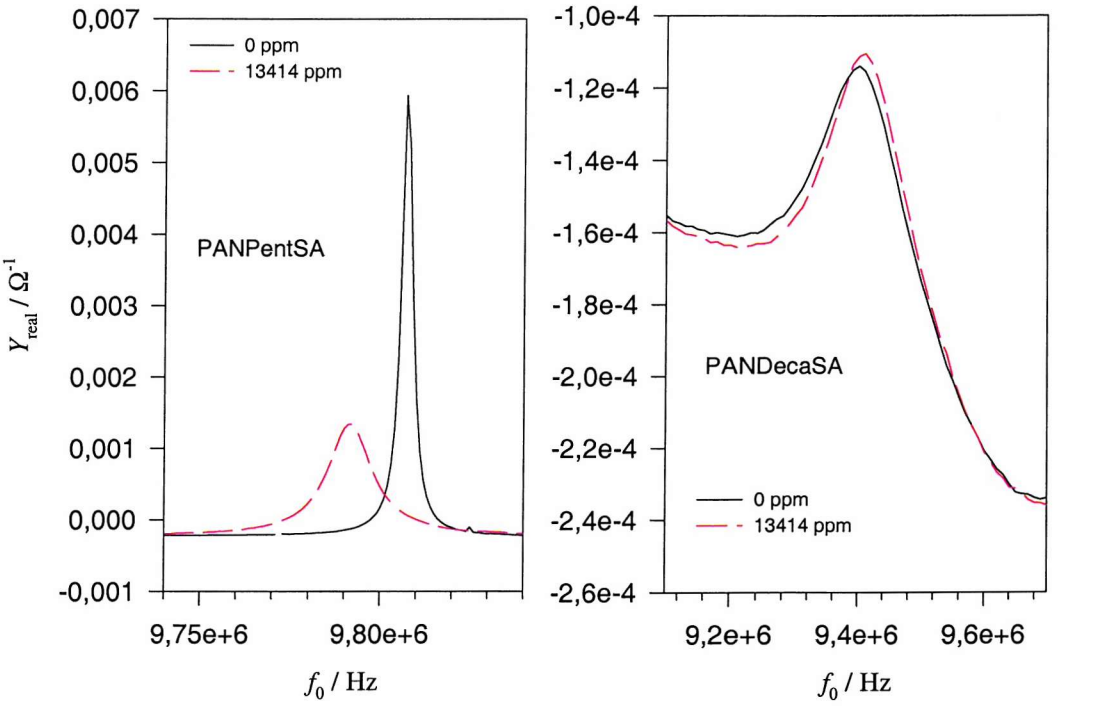

Figure 6. 6: real part of the admittance of a QCM coated with poly(aniline) pentane sulfonate and a QCM coated with poly(aniline) decane sulfonate at 0 ppm and 13414 ppm water.

The QCM is a useful tool as a sensor or as a balance to investigate mechanism. However, it should be used with caution mainly due to the limitations of the Sauerbrey equation to rigid layers. By performing the impedance analysis of the QCM it should be possible to conclude whether any significant viscoelastic effects are observed upon exposure to vapour and therefore if the mass of adsorbed vapour can be determined (see Chapter 7).

For the investigation of the sensing mechanism, the amount of monomer units deposited onto the crystal was determined. Unfortunately, due to the large number of approximations required for these calculations, an interval, rather than an exact value, was obtained. The main problem encountered during the discussion was the disagreement between the electrochemical method and the QCM based mass measurement. To gain in confidence, a broad interval was taken, which implies that drawing conclusions from gas test measurement may be difficult.

(1) Curie, P.; Curie, J., *Bull. Soc. Min. de France*, 1880, **3**, 90.

(2) Curie, P. *Oeuvre de Pierre Curie*; Gauthier- Villars: Paris, 1908.

(3) Sauerbrey, G. Z., *Phys. Verha.*, 1957, **8**, 113.

(4) Kunugi, Y.; Nigorikawa, K.; Harima, Y.; Yamashita, K., *J. Chem. Soc., Chem. Commun.*, 1994, 873-874.

(5) Charlesworth, J. M.; Partridge, A. C.; Garrard, N., *J. Chem. Phys.*, 1993, **97**, 5418-5423.

(6) Nagase, H.; Wakabayashi, K.; Imanaka, T., *Sensors and Actuators*, 1993, **B 13/14**, 596-597.

(7) Vigmond, S. J.; Kallury, K. M. R.; Ghaemmaghami, V.; Thompson, M., *Talanta*, 1992, **39**, 449-456.

(8) Buttry, D. A.; Ward, M. D., *Chem. Rev.*, 1992, **92**, 1355-1379.

(9) Slater, J. M.; Watt, E. J.; Freeman, N. J.; May, I. P.; Weir, D. J., *Analyst*, 1992, **117**, 1265-1270.

(10) Lu, C. S., *J. Appl. Phys.*, 1972, **43**, 43854390.

(11) Topart, P.; Josowicz, M., *J. Phys. Chem.*, 1992, **96**, 7824-7830.

(12) Calvo, E. J.; Etchenique, R.; Bartlett, P. N.; Singhal, K.; Santamaria, C., *Faraday Discuss.*, 1997, **107**, 141-157.

(13) Etchenique, R.; Brudny, V. L., *Langmuir*, 2000, **16**, 5064-5071.

(14) Lucklum, R.; Behling, C.; Hauptmann, P., *Anal. Chem.*, 1999, **71**, 2488-2496.

(15) Rodahl, M.; Kasemo, B., *Sensors and Actuators*, 1996, **A 54**, 448-456.

(16) Topart, P.; Josowicz, M., *J. Phys. Chem.*, 1992, **96**, 8662-8666.

(17) Scharifker, B. R.; Fermin, D. J., *Journal of Electroanalytical Chemistry*, 1994, **365**, 35-39.

(18) Blair, N., The development and characterisation of conducting polymer based sensors for use in an electronic nose, PhD thesis, SOUTHAMPTON, 1994.

(19) Wernet, W.; Monkenbusch, M.; Wegner, G., *Makromol. Chem., Rapid Commun.*, 1984, **5**, 157-164.

(20) Shimidzu, T.; Ohtani, A.; Honda, K., *Bull. Chem. Soc. Jpn.*, 1988, **61**, 2885-2890.

(21) Aoki, K.; Teragishi, Y., *J. Electroanal. Chem.*, 1998, **44**, 25-31.

(22) Wainright, J. S.; Zorman, C. A., *J. Electrochem. Soc.*, 1995, **142**, 379-383.

(23) Baker, C. K.; Reynolds, J. R., *J. Electroanal. Chem.*, 1988, **251**, 307-322.

(24) Matveeva, E. S., *Synthetic Metals*, 1996, **79**, 127-139.

(25) Genies, E. M.; Lapkowski, M.; Tsintavis, C., *New J, Chem.*, 1988, **12**, 181-196.

Chapter 7 - Response of the conducting polymer gas sensors to ethanol

In Chapter 5, the production of chemoresistors coated with poly(aniline) and poly(pyrrole) films doped with various anions was discussed. The first target in generating a batch of coatings was to produce an array of sensors for electronic nose applications. These sensors have already been tested towards some inorganic gases (Chapter 4). Here their responses towards ethanol, employed as a reference VOC, is briefly reported in the first part of this chapter, along with their sensitivity to humidity. The data collected can be used to select the most appropriate sensors for applications in an electronic nose.

The second purpose in investigating different polymers with different dopants was to investigate the contribution of the dopant to the sensing mechanism. To a larger extent, better understanding of the interactions between polymer and vapour should enable one to engineer a coating to detect given vapours. Even thought a lot of research is ongoing in this field, no agreed mechanism yet exists. Here further investigation in this direction was performed. To increase the information acquired during gas test experiments, chemoresistors were coupled with Quartz Crystal Microbalance sensors with the main aim of monitoring the amount of vapour adsorbed in the coating. The models described in the literature, as well as a possible model, will be discussed in the light of the results obtained with the chemoresistors and the QCM sensors in the second part of this chapter.

7.1 - Response of the chemoresistors

A wide variety of conducting polymer materials is available. This work focussed on poly(pyrrole) and poly(aniline) as they demonstrated suitable sensing properties [1-3]. The choice of the anions has already been discussed in Chapter 4. The aim of this section is to give an overview of the characteristics of the various coatings to enable a selection of polymer sensors following the "sss" criteria defined by Göpel [4], "sss" standing for high sensitivity to a vapour (and low to humidity), high selectivity and high stability. In addition to the "sss" criteria, the response time and reproducibility (of the response to a given vapour and from sensor to sensor) should also be taken into account. The results for chemoresistors will also be used later in the discussion of the sensing mechanism.

7.1.1 - Response of poly(pyrrole)

The response of poly(pyrrole) pentane sulfonate, poly(pyrrole) decane sulfonate and poly(pyrrole) *p*-toluene sulfonate chemoresistors towards water and ethanol was investigated.

To evaluate the **sensitivity of a sensor to water**, two points have to be addressed. The first is to investigate the response of a given sensor to a change in the humidity level. The second regards the influence that humidity has on the response to a vapour. Ideally both should be minimised to ensure minimum cross-sensitivity from the water and also that the presence of ambient humidity has little effect on the sensitivity to other vapours.

Regarding the responses to a humidity increase, the conductance of the three poly(pyrrole) materials was found to decrease. Figure 7. 1 shows the conductance plot for three poly(pyrrole) pentane sulfonate films over a range of humidity levels, representative of the three poly(pyrrole) coatings investigated. The sensitivity to water for this film is high as from 0 to 25000 ppm the relative change in resistance is about 10 %.

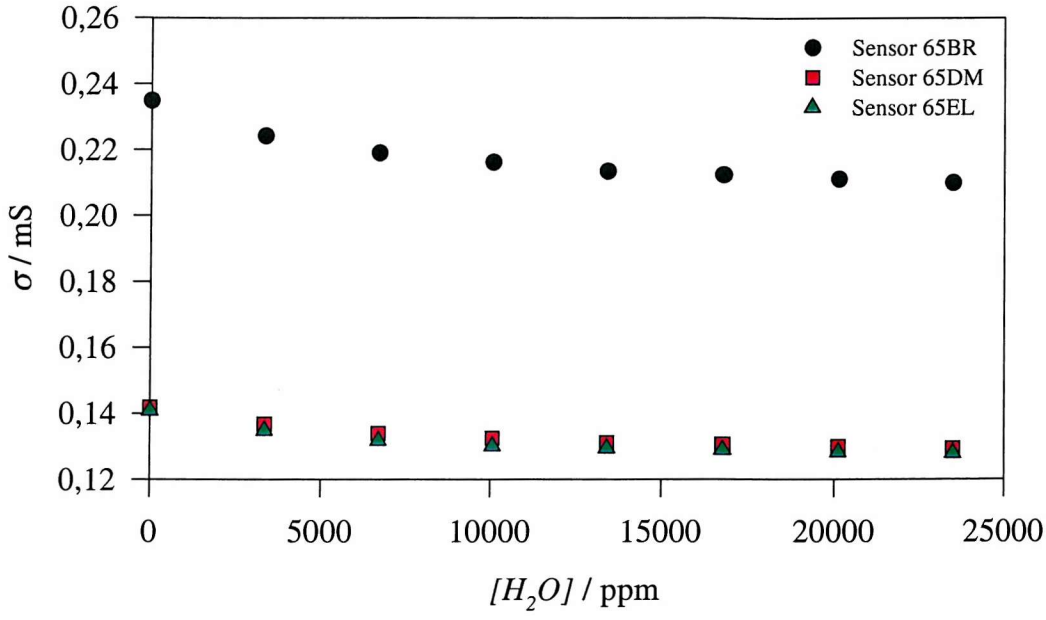

Figure 7. 1: conductance of poly(pyrrole) pentane sulfonate films as a function of the humidity.

For poly(pyrrole), the sensitivity to water was increased with the dopant in the order decane < pentane < *p*-toluene sulfonate. This order in sensitivity corresponds both to the change in conductivity observed upon a change of the humidity level and the decrease in the response to ethanol with increasing water content, the later being illustrated in Figure 7. 2. As shown in Figure 7. 2, for poly(pyrrole) pentane sulfonate, the amplitude of the response to ethanol is decreased by 50 % with increasing humidity from 0 ppm to 1677 ppm, and further decreased to about 30 % of the original response at 6707 ppm. Poly(pyrrole) decane sulfonate showed little sensitivity as from 0 ppm to 1677 ppm the response to ethanol decreased by only 20 % and was little dependent on the humidity at higher water contents.

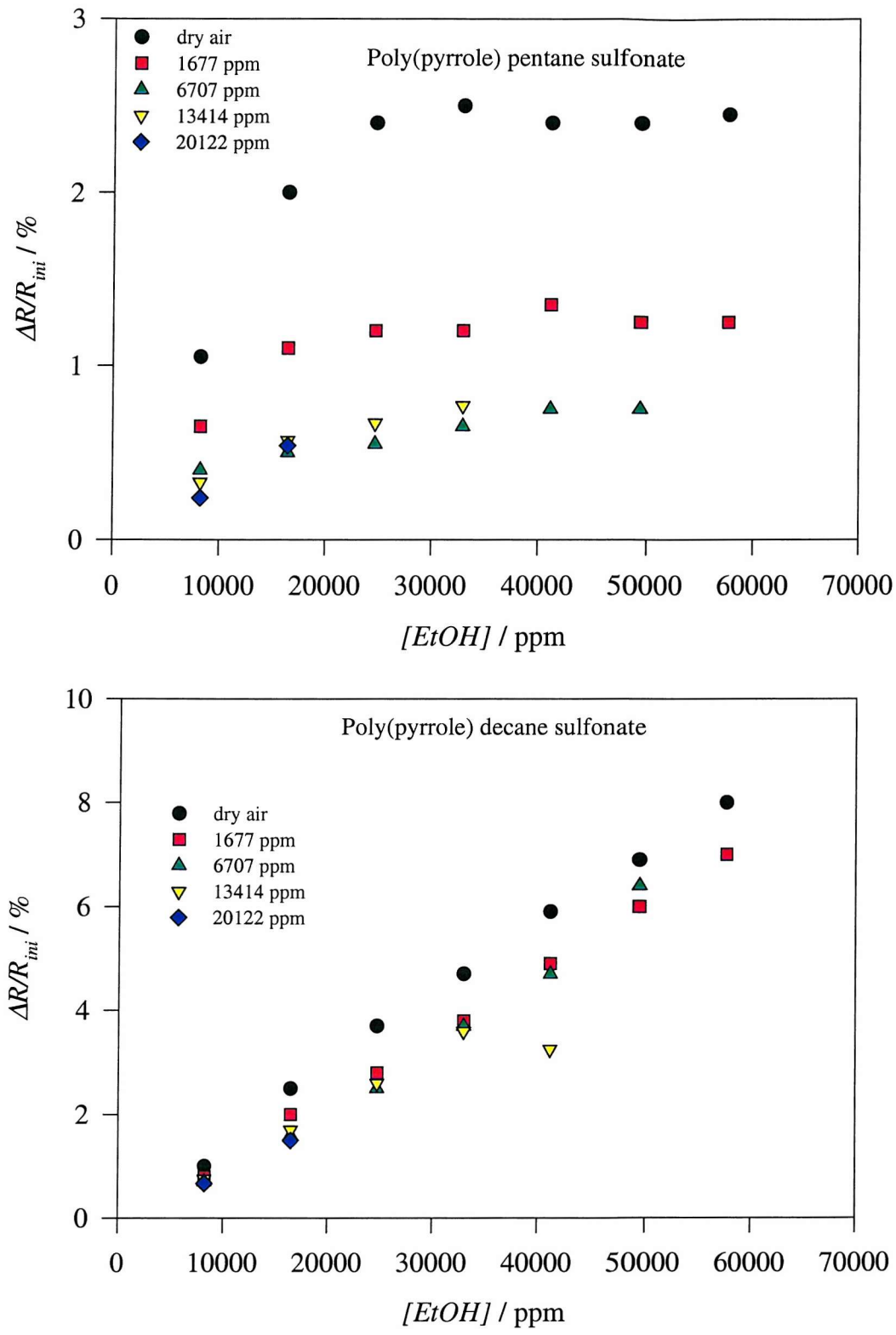

Figure 7. 2: response to ethanol as a function of the concentration for different humidity levels both for poly(pyrrole) doped with pentane sulfonate (sensor 65BR) and decane sulfonate (sensor 65QM). These graphs show the relative sensitivities to water and to ethanol.

As shown in Figure 7. 1 and in Figure 7. 2, both water and ethanol induce an increase in resistance of a poly(pyrrole) coating once exposed separately. With increasing humidity, the amplitude of the response of a poly(pyrrole) film to ethanol decreases, implying that there are apparently some interactions between the vapour and the water in the film and that a competition between the two molecules should be considered when defining a model.

The three types of poly(pyrrole) film investigated showed different behaviours upon exposure to ethanol. Whereas the response of the poly(pyrrole) decane sulfonate increases over the whole range of concentrations investigated, Figure 7. 2 also shows that for poly(pyrrole) pentane sulfonate the response to ethanol at a given humidity saturates from about 25000 ppm ethanol. At this point it is interesting to raise the question of the origin of such behaviour and to determine whether this is due to saturation of the amount of vapour adsorbed by the coating or to the lack of influence of further adsorbed molecules on the resistance of the coating. This question will be addressed later because in order to reach a conclusion, the adsorbed mass must first be determined.

Regarding the sensitivity to ethanol, for the pentane sulfonate and the *p*-toluene sulfonate doped films, the sensitivities were similar (about 2.5 % at maximum), but smaller than the decane sulfonate doped film (a response up to 8 % was obtained for the same concentrations)- see Figure 7. 2. Coupled with the low sensitivity to water, the high sensitivity of the poly(pyrrole) decane sulfonate to ethanol make it attractive for gas sensing applications.

In addition to the "sss" criteria, when considering a coating for sensing applications, the response time, as well as other characteristics, have to be considered.
Regarding the transient for the response to a humidity change, the response was relatively slow to reach saturation (around 20 min), of similar shape for the three poly(pyrrole) types (not shown here).
The response time to ethanol largely varied with the anion, being fast for the poly(pyrrole) films doped with pentane sulfonate and *p*-toluene sulfonate (about 5 min) and slow for poly(pyrrole) decane sulfonate (about 60 min). Figure 7. 3 compares the transients for poly(pyrrole) pentane sulfonate and poly(pyrrole) decane sulfonate to ethanol. Several comments are required on the shape of the transients.

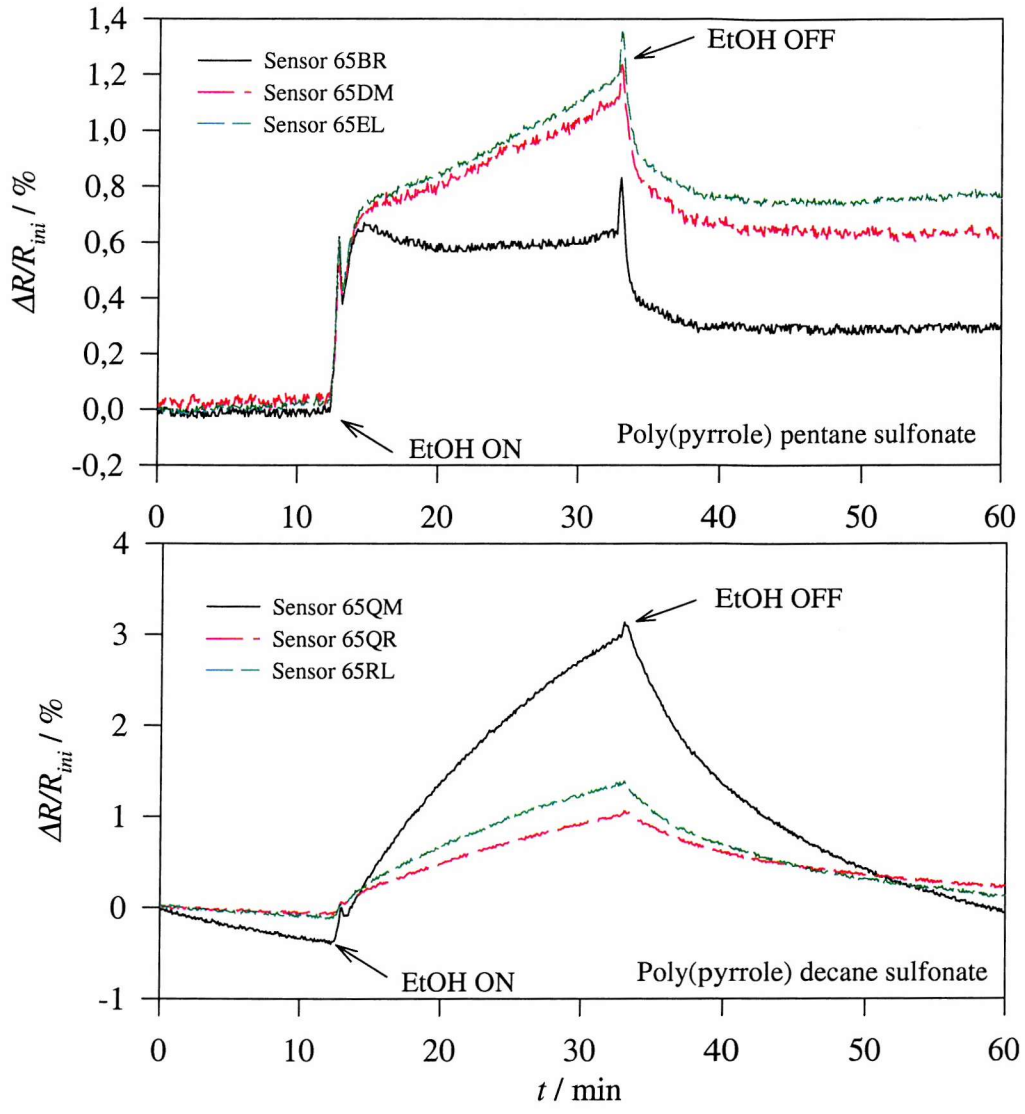

Figure 7. 3: transients for the response to 32938 ppm ethanol at 6707 ppm water for the three poly(pyrrole) pentane sulfonate coated chemoresistors and three poly(pyrrole) decane sulfonate coated chemoresistors.

The response of poly(pyrrole) pentane sulfonate to ethanol is composed of two components: a rapid reversible increase in the resistance followed by a slow increase in resistance which was irreversible, the longer the exposure the larger the irreversibility. The implication of the irreversible component from an experimental point of view is that the exposure time should be limited to 5 min in order to avoid any possible loss of sensitivity of the poly(pyrrole) pentane sulfonate sensor. In other words, this rules out application where continuous monitoring is required, for example for toxic gases for automotive applications (CIA project). This irreversibility in the response was not observed for poly(pyrrole) doped with *p*-toluene sulfonate nor with decane sulfonate and was not explained at this stage.

The response of poly(pyrrole) decane sulfonate was found to be extremely slow, of about one hour, composed of a slightly curved response. From SEM photographs, Blair [1] reported that poly(pyrrole) decane sulfonate was denser than poly(pyrrole) pentane sulfonate, both deposited in conditions similar to those used here. The low porosity may account for the long response time of poly(pyrrole) decane sulfonate, the dense structure slowing down the diffusion of the vapour in the polymer. If further considering that diffusion is rate limiting, the slower response may also be due to the thicker films obtained for poly(pyrrole) decane sulfonate. Indeed it was seen in Chapter 5 that all three poly(pyrrole) films discussed here were electropolymerised with similar growth charge, but that the deposition efficiency was three times larger for the decane sulfonate doped film than for the two others. This implies that the poly(pyrrole) decane sulfonate coating was three times thicker than the poly(pyrrole) doped with pentane and *p*-toluene sulfonate. The sensing mechanism along with the diffusion of the vapour in the film will be discussed in more detail in the second part of this chapter.
Regarding the application of poly(pyrrole) decane sulfonate synthesised here as a gas sensor, the large response time is then a disadvantage which should be compensated by the high sensitivity to the vapour of interest.

The **reproducibility from sensor to sensor** must also be taken into consideration for the use of a coating layer in an electronic nose, where minimum recalibration should be required when exchanging one batch of sensors for another. For the three coatings tested, poly(pyrrole) pentane sulfonate showed the best reproducibility in the polymerisation charge, the base resistance and in the response to vapours. Poly(pyrrole) decane sulfonate did not show any major difference in the polymerisation charge compared to the other poly(pyrrole), but the irreproducibility was large both for the base resistance (89%) and the response to vapour (about 100%) as seen in Figure 7. 3. Indeed, whereas the sensors tested for this polymer (65QM, 65QR and 65RL) showed good reproducibility in Q_{growth} and R (see Annex A), the response for 65QM is about double the response of the two others. Again this is another disadvantage for the use of poly(pyrrole) decane sulfonate as a sensor coating. Another implication is that there is no clear trend between the reproducibility of the polymerisation charge, the resistance and the response to vapours for the poly(pyrrole) investigated, especially because not all sensors produced have been tested to perform proper statistics.

7.1.2 - Response of poly(aniline)

Five poly(aniline) types were tested as chemoresistor coatings: poly(aniline) pentane sulfonate, poly(aniline) decane sulfonate, poly(aniline) *p*-toluene sulfonate, poly(aniline) copper phthalocyanine tetrasulfonate and poly(aniline) nickel phthalocyanine tetrasulfonate.

All poly(aniline) films responded in a similar manner to a change of humidity: the conductance increased with increasing humidity with a relatively fast response time (less than 10 min). The sensitivity to a humidity change increases with the anion in the order CuPcTs~DecaSA<*p*-tolSA<PentSA~NiPcTs. A similar curve to the one for poly(pyrrole) was found for the variation of the conductance as a function of the humidity, as illustrated in Figure 7. 4 for PPyDecaSA.

The sensitivities of poly(pyrrole) and poly(aniline) to water can be compared by comparing the relative change in conductance from dry air to 23475 ppm for the two polymers. The conductance, in this range of water concentration, was about 30-50% for poly(aniline), whereas it was at maximum 20% for the poly(pyrrole) films investigated. It can therefore be concluded that chemoresistors coated with poly(aniline) are more sensitive than the ones coated with poly(pyrrole) to changes in humidity.

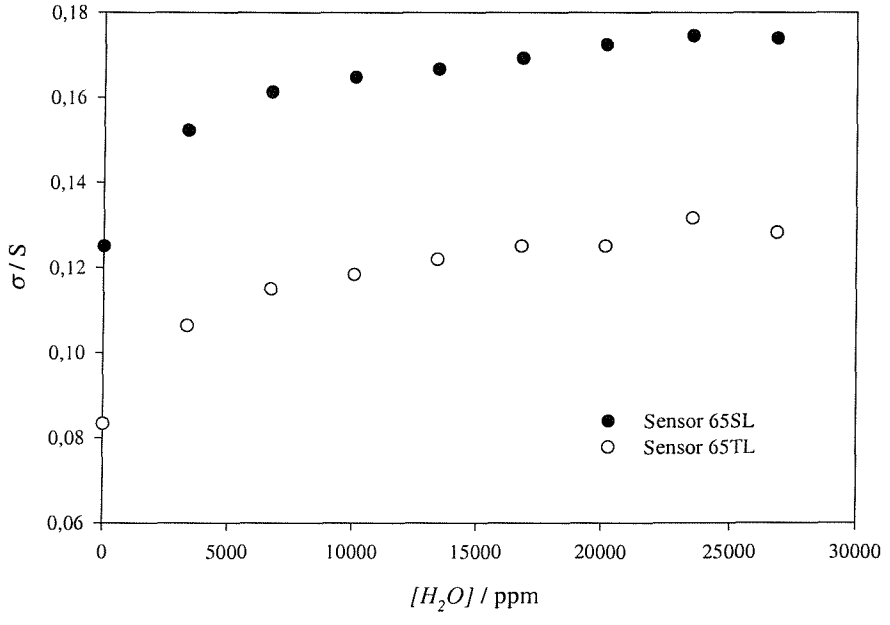

Figure 7. 4: typical conductance variation of poly(aniline) decane sulfonate with humidity.

An interesting feature from the response of poly(aniline) to water is that the conductivity increases with increasing water content, the opposite to the behaviour of poly(pyrrole). One possible explanation is that the water molecules form H-bonds with the protonated aniline which then facilitates charge delocalisation along the polymer backbone.

Insufficient data were gathered to meaningfully compare the sensitivity of the five different poly(aniline) films towards the influence of the humidity on the response to ethanol. Nevertheless, some discrete comparison can be performed.

As for the poly(pyrrole) films, the sensitivity to ethanol decreased with increasing humidity, however the relative sensitivity of poly(pyrrole) and poly(aniline) is largely dependent on the dopant. For poly(aniline) pentane sulfonate, the response to 32938 ppm EtOH is only reduced by a factor of 2 on increasing the humidity from 1677 ppm to 13414 ppm, whereas under the same conditions the amplitude of the response is reduced by a factor of 3 for poly(pyrrole) pentane sulfonate. This implies that, with respect to the influence of water on the response to ethanol for the pentane sulfonate doped polymers, poly(pyrrole) is more sensitive to water than poly(aniline). The inverse conclusion is reached for the decane sulfonate doped polymers. The response to ethanol was weakly dependent of the humidity for poly(pyrrole) decane as shown in Figure 7. 2 but the estimated amplitude of the response to 32938 ppm EtOH is reduced by a factor of 4 when increasing the humidity from 1677 ppm to 13414 ppm for the poly(aniline) film. This also implies that the response to ethanol of the poly(aniline) decane sulfonate is more sensitive to humidity than the poly(aniline) pentane sulfonate. The opposite was however concluded from the investigation of the response to water alone.

The poor sensitivity to a change in humidity is in agreement with the poor water sensitivity found for poly(pyrrole) decane sulfonate. This may be explained by the hydrophobicity of the long alkyl chain, compared to the pentane equivalent. However, no explanation is available for the high sensitivity to humidity of the response of PANDecaSA to ethanol.

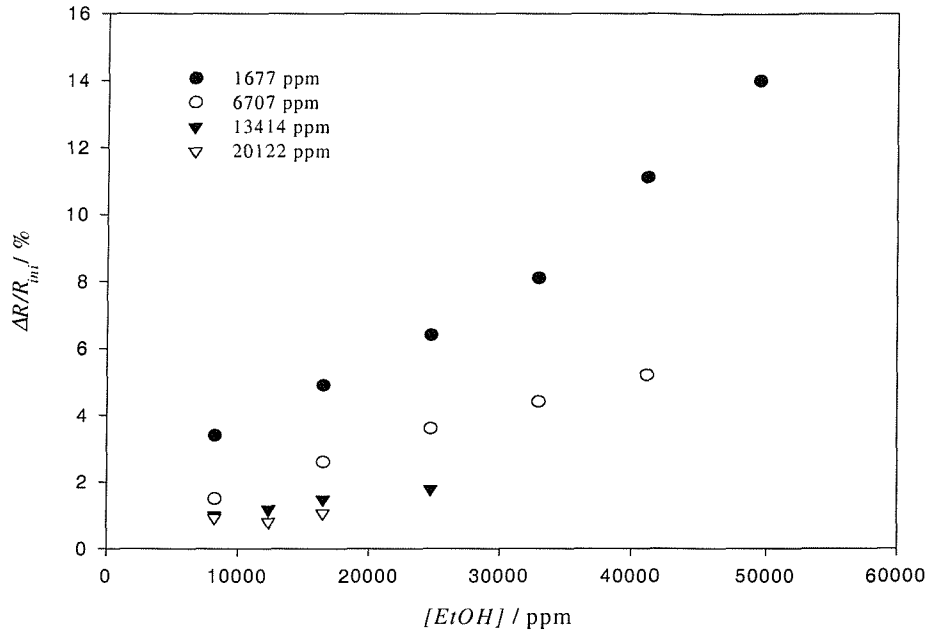

Figure 7. 5: response of poly(aniline) decane sulfonate (sensor 65SL) to ethanol as a function of the humidity showing the high sensitivity to humidity, which is in contradiction with the low sensitivity deduced from the response to a simple change in humidity.

Regarding the influence of the anion on the **response to ethanol**, a significant characteristic of the poly(aniline) films is the change in the sign of the response with the dopant implying a high discrimination power. As illustrated in Figure 7. 6, the resistance of poly(aniline) doped with decane sulfonate and with copper phthalocyanine tetrasulfonate decreases upon exposure to ethanol, whereas the resistance increases for the other three poly(aniline) films. Such behaviour was not observed for the response to water. Figure 7. 6 also shows that in fact, the transient for the response can be divided into two parts: a fast response which gives the final sign of the response, followed by an increase in the resistance for all poly(aniline) films. Regarding the absolute value of the amplitude of the response, the sensitivity to ethanol increases in the order CuPcTs~DecaSA<*p*tolSA<PentSA~NiPcTs, in the same order as the water sensitivity, which makes the selection of the most appropriate gas sensors more complex. At this stage, no explanation of the observed behaviours is available.

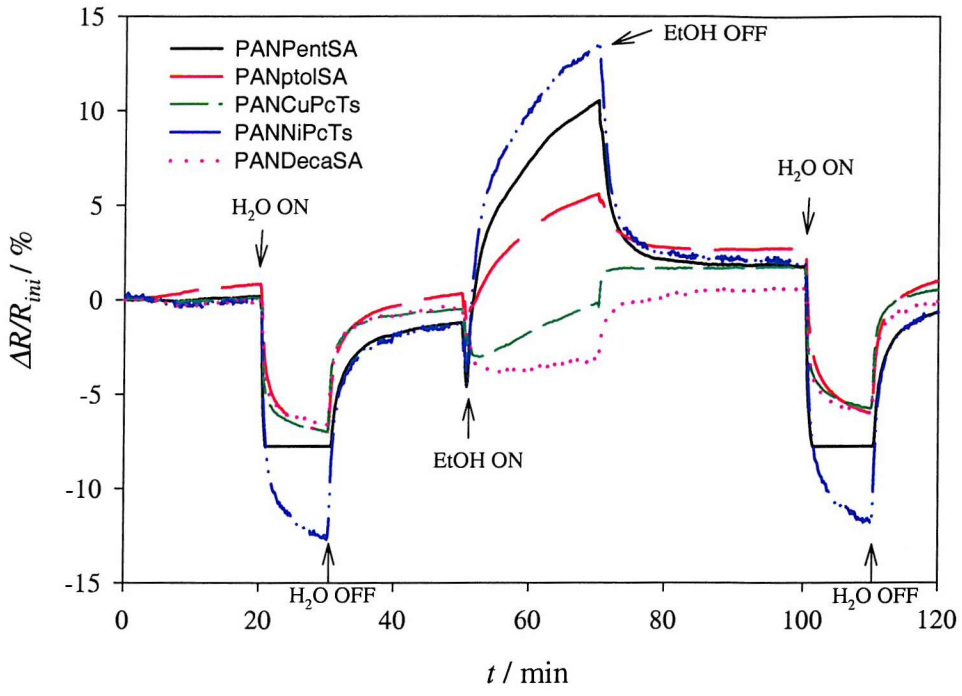

Figure 7. 6: transients to 13414 ppm H_2O, 32938 ppm EtOH and once more 13414 ppm H_2O at 6707 ppm H_2O for poly(aniline) films doped with five different anions. For this experiment, the electronics of the poly(aniline) pentane sulfonate film saturates upon exposure to water.

For each coating, only two sensors were tested, which make impossible the analysis of the reproducibility from sensor to sensor. Still, all poly(aniline) films showed a satisfactory reproducibility, except for the poly(aniline) doped with decane sulfonate where the response amplitude varied from 1 to 4. A similar conclusion was reached for the poly(pyrrole) films.

7.1.3 - Conclusions on the chemoresistor responses

The response of several conducting polymer gas sensors to ethanol was analysed, as well as the influence of humidity. Poly(pyrrole) decane sulfonate presented good sensitivity characteristics (high sensitivity to ethanol and low sensitivity to water). The drawback is the large response time which prevents its use in the CIA project where immediate detection and action are required. Poly(pyrrole) pentane sulfonate responds faster but the irreversibility of the response upon long exposures makes it unsuitable for continuous monitoring. Poly(pyrrole) *p*-toluene sulfonate represents a compromise with medium sensitivity, fast response and good reversibility.

The application of poly(aniline) as a sensor coating in an electronic nose is, for the films investigated here, limited by its high sensitivity to humidity. In addition, the sensitivity to

humidity was found to increase with increasing sensitivity to ethanol, making the selection of one, or several, poly(aniline) coatings difficult. On the one hand, PANDecaSA and PANCuPcTs both give a negative response and were found to respond fast, on the other hand for PANDecaSA the response was irreproducible. The advantage in using PANPentSA, PANptolSA or PANNiPcTs is that anyone of these sensors is capable of differentiating between H_2O and EtOH due to the opposite signs of the responses. Therefore, PANPentSA and/or PANCuPcTs may be an appropriate selection for application in the CIA electronic nose.

Some selection criteria for conducting polymer chemoresistor coatings were briefly discussed. The CIA partners performed further tests "on the road", not detailed here. The results are rather complex as they were taking into account other sensor types as well as the analytical capabilities of the associated artificial intelligence system so that they are not going to be detailed here. On the laboratory side, further tuning the selection could have been performed by testing a wider range of vapours.

The information gained on the chemoresistors revealed that the coatings were not optimised, limiting their use in electronic noses. There are two directions to overcome this problem: either the coating is improved or the whole instrument is adapted to fit the behaviour of the sensors. For example, regarding the high sensitivity to water, incorporating hydrophobic groups, or molecules, in the film, or coating the polymer with a hydrophobic film may lower the humidity sensitivity. In addition it has been demonstrated in Chapter 4 that depositing a thinner film could reduce the response time. A study performed by Vigmond *et al.* [5] on the influence of the degree of oxidation on the response to vapours revealed that when switching between oxidised and reduced states the sign of the response of poly(pyrrole) to water was inverted. Therefore, it seems possible to minimise the response to water by modulating the degree of oxidation of the polymer. In terms of the instrument, a humidity sensor could be added, if of course the sensitivity of this sensor to the vapours of interest is minimised. Pre-saturation with water of the gaseous sample could also be considered. Some software solutions to the problem of high humidity sensitivity are also possible.

7.2 - Response of the chemoresistors coupled with QCM sensors

Investigation of the sensing mechanism

The motivation for part of this work on conducting polymer gas sensors was to compensate for the lack of a universally accepted model for the interactions between a conducting polymer and a vapour. The aim is to gain maximum information on the mechanism in order to foresee the response of a sensor coated with these materials, whatever the transduction mechanism. Simply by investigating the response of chemoresistors coated with different polymers, the information collected on the sensing mechanism is poor. The problem lies in relating the response of the chemoresistors to the amount of adsorbed vapour. This deficit may be compensated by the use of QCM sensors. The use of the Sauerbrey equation is one of the important bases of the discussion as it may enable us to precisely measure the mass of adsorbed vapour from the QCM data. Therefore the applicability of the rigid film approximation, which enables its use, will first be discussed in respect of some of the poly(pyrrole) and the poly(aniline) coatings investigated earlier. A predominant model for polymer vapour sensitivity, the Langmuir isotherm model, will be discussed in the light of the results obtained, before proposing and discussing a more suitable model, a double-diffusion model coupled with a BET adsorption isotherm.

7.2.1 - Viscoelastic effects

By coupling the chemoresistor with the QCM sensors, the first aim was to be able to relate the change in conductivity of the film with the amount of vapour adsorbed. As seen from the theory in the QCM (Chapter 6), to be able to measure a mass using the Sauerbrey equation, the coating on the quartz should behave as a rigid layer. Viscoelastic effects were estimated by monitoring ΔR and ΔX_L as discussed in Chapter 6, both from the bare crystal to the polymer free of vapour and upon exposure to vapour.

7.2.1.1 - Viscoelastic behaviour of the coating free of vapour

Electrodeposition was performed on the QCM substrates without monitoring the impedance of the crystal as our interest was mainly the use of the QCM sensors in the gas phase. However the viscoelastic behaviour of the dry coating prior to applying any vapour was relevant for later comparison of the viscoelastic effects upon exposure to vapours.

Coating	PPyPentSA (QCM4)	PPyDecaSA (QCM8)	PANPentSA (QCM1)
$\Delta R / \Omega$	8	139	96
$\Delta X_L / \Omega$	1885	11310	13825
$\Delta X_L / \Delta R$	235	81	144
Rigid film	Yes	Some viscoelastic effects	Yes

Table 7. 1: changes in R and in X_L from the bare crystal to the crystal coated with the polymer free of vapour, extracted from the impedance analysis of the QCM. The coefficient $\Delta X_L/\Delta R$ gives an indication of viscoelasticity in the coating. If it is superior to 100, the viscoelastic effects are considered negligible.

Table 7. 1 gathers together the changes in R and in X_L from the bare crystal to the conducting polymer free of vapour. Both poly(pyrrole) and poly(aniline) films doped with the pentane sulfonate can be considered as behaving rigidly in the dry state as ΔX_L is at least 100 times larger than ΔR. The poly(pyrrole) decane sulfonate film shows some deviation from the rigid behaviour in the dry state ($\Delta X_L/\Delta R$ of 81).

7.2.1.2 - Viscoelastic behaviour upon exposure to vapours

Once exposed to an analyte, conducting polymers adsorb part of the vapour from the gas phase. By incorporation of this gas/liquid in the coating, the viscoelastic characteristics of the material may be changed significantly. Here, the rigid/non-rigid behaviour of the polymers was investigated both upon a single exposure and over the whole range of concentrations.

7.2.1.2.1 - Poly(pyrrole) pentane sulfonate

Upon exposure to vapours, the resonant frequency (f_0, correlated to X_L) and the equivalent electroacoustic resistance, R, were monitored for two QCM sensors coated with poly(pyrrole) pentane sulfonate films. As shown in Figure 7. 7, the resonant frequency behaviour was reproducible and well defined for the two sensors, in contrast to the electroacoustic resistance changes. The resistance was rather noisy and the trend in the behaviour upon exposure was not clear. Such behaviour was typical both upon exposure to water and to ethanol. The lack of a trend in the behaviour of R for the poly(pyrrole)

pentane sulfonate on the scale of a single exposure prevented us from making any conclusion on any viscoelastic effect.

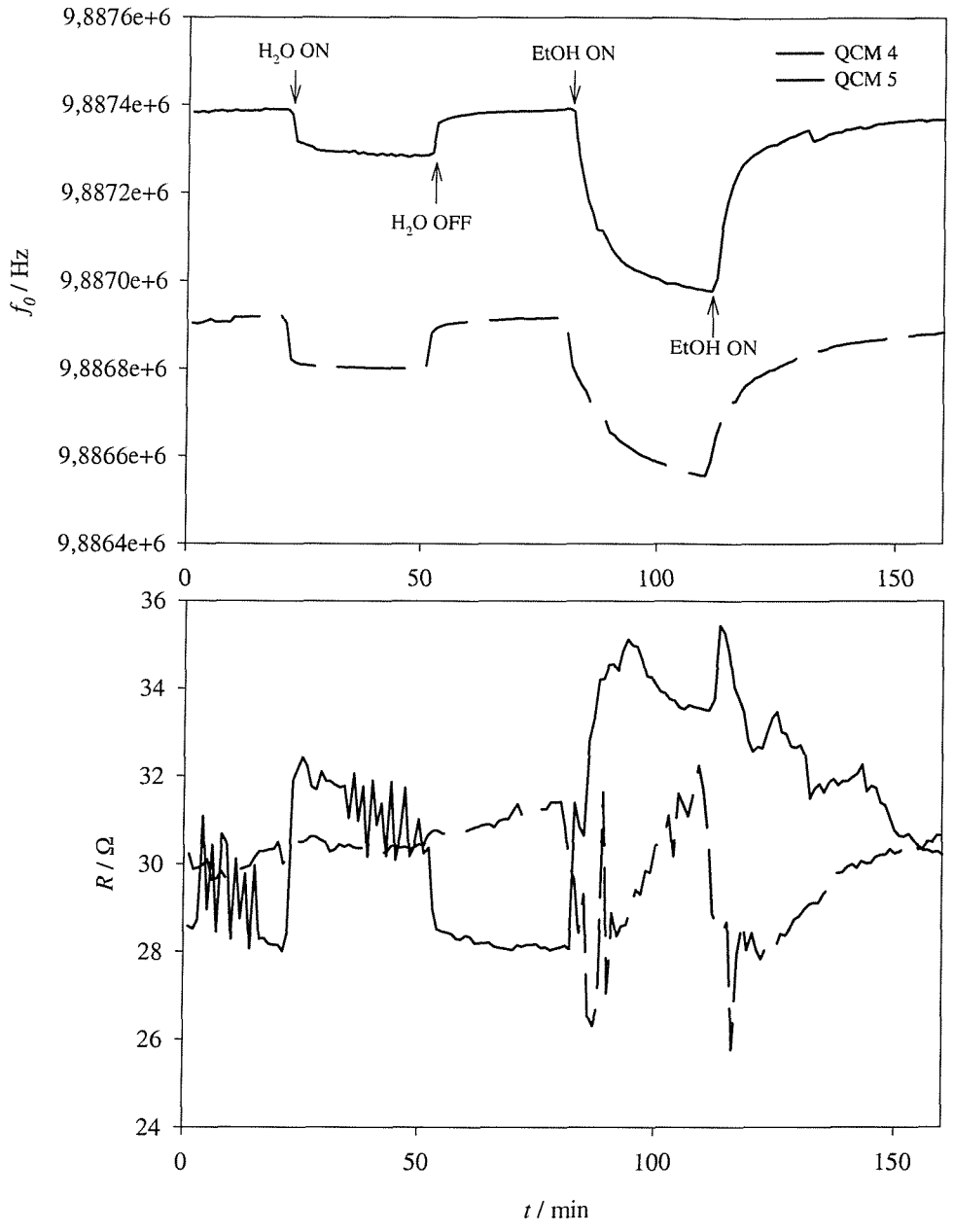

Figure 7. 7: resonant frequency and electroacoustic resistance of QCM4 and QCM5 both coated with poly(pyrrole) pentane sulfonate illustrating on one hand the reproducibility of the shift in resonant frequency from sensor to sensor and on the other hand the lack of definition in the behaviour of R. The sensors were exposed to 13414 ppm water and 32938 ppm ethanol at 6707 ppm water.

In absolute terms, the electroacoustic resistance for PPyPentSA was in the same range as for poly(pyrrole) decane sulfonate. However, as seen later, the change in R observed upon exposure was more important for this later polymer (about -40 Ω). So on the scale of a

single exposure, the change in resistance may be in the noise level, which would account for the poor definition in the signal.

From the coating free of vapour to a water content close to saturation (26829 ppm), $\Delta X_L/\Delta R$ was 10 (ΔR and ΔX_L were 9 and 91 Ω respectively). A similar ratio was obtained upon exposure to ethanol. For example, from 0 to 41172 ppm EtOH at 6707 ppm H_2O the ratio $\Delta X_L/\Delta R$ was 7. From the lack of rigidity over the range of concentration investigated and the lack of definition of R on the scale of a single exposure, whether or not the film behaves rigidly for a given vapour concentration could not be defined. Therefore it was assumed that the poly(pyrrole) pentane sulfonate film did not behave rigidly upon exposure to vapour.

It has been shown that at a high humidity level (26829 ppm), the viscoelastic effects for the poly(pyrrole) pentane sulfonate are not negligible, and that the layer cannot be considered as rigid. The Sauerbrey equation can still be employed to estimate the corresponding increase in mass. 0.61 μg were added by incorporation of the water molecules (3% of the mass of the polymer), the total mass loading being 20.6 μg.
Now recalling the rigid film criteria reported by Buttry *et al.* [6], the layer, according to this reference, can be approximated as rigid if its mass loading is less than 2% of the crystal mass (here a 10 MHz crystal), or 175 μg. Therefore, from the experiments performed here with poly(pyrrole), it can be concluded that the rigid film criteria defined by Buttry is not appropriate for the material considered here. Indeed, viscoelastic effects were observed for mass changes 8 times smaller than the criteria defined by Buttry (or 0.25% mass loading). It is unlikely that the difference by a factor of 8 between Buttry's rigid film criteria and the 0.25% mass loading where viscoelastic effects were observed are simply due to the error in the Sauerbrey equation introduced by non-rigidity of the layer.
Concerning the viscoelasticity changes observed for the poly(pyrrole) film upon exposure to vapour and more generally for conducting polymers, the loss of rigidity is somehow expected. The loss in rigidity introduced by a mass m of vapour is expected to be larger than the loss in rigidity introduced by addition of the same mass m of polymer, which is itself larger than for a mass m of metal.

7.2.1.2.2 - Poly(pyrrole) decane sulfonate

Two types of viscoelastic effects were observed for poly(pyrrole) decane sulfonate as shown in Figure 7. 8. First, on the scale of a single exposure, the equivalent electroacoustic resistance showed clear viscoelastic changes. The viscoelastic effects were significant once the pyrrole film was exposed to water (from the dry film to the film exposed to 1676 ppm, the $\Delta X_L/\Delta R$ ratio was 15.5) and to ethanol ($\Delta X_L/\Delta R$ ratio of 2.2 from 8234 to 16469 ppm EtOH at 1676 ppm H_2O).
On the scale of the whole range of concentrations investigated, a second type of viscoelastic change was revealed by plotting ΔR versus ΔX_L. The polar plot, shown in Figure 7. 8, has a sigmoid shape, showing a inflection around ΔR =-40 Ω. This sharp transition seems to indicate a radical change in the physical properties of the polymer.

Viscoelastic changes shown over the whole vapour concentration range have already been reported by Topart [7] for poly(pyrrole) doped with tetrafluoroborate and *p*-toluene sulfonate exposed to methanol. At about 12% methanol, the equivalent resistance was found to vary significantly whereas the additional mass was not significant. He explained it as due to plasticisation of the polymer.

At this point, some comment on the sign of the variation of electroacoustic resistance is required. The decrease observed for poly(pyrrole) upon exposure to ethanol for QCM8 would imply that the viscoelastic losses decrease and the polymer becomes more rigid. This observation is in contradiction with the results from Topart [7], where the electroacoustic resistance was found to increase upon exposure. This is also in contradiction with the results obtained with the second QCM tested coated with poly(pyrrole) decane sulfonate (QCM9) where the electroacoustic resistance was increasing upon exposure to ethanol. For both QCM, the response was well defined, unlike the QCM coated with poly(pyrrole) pentane sulfonate shown in Figure 7. 7. However, the amplitude of the changes in the electroacoustic resistance were about 10 times smaller for the QCM9 than for the QCM8 at comparable concentrations. The initial value was also lower. No explanation for this behaviour is available here.

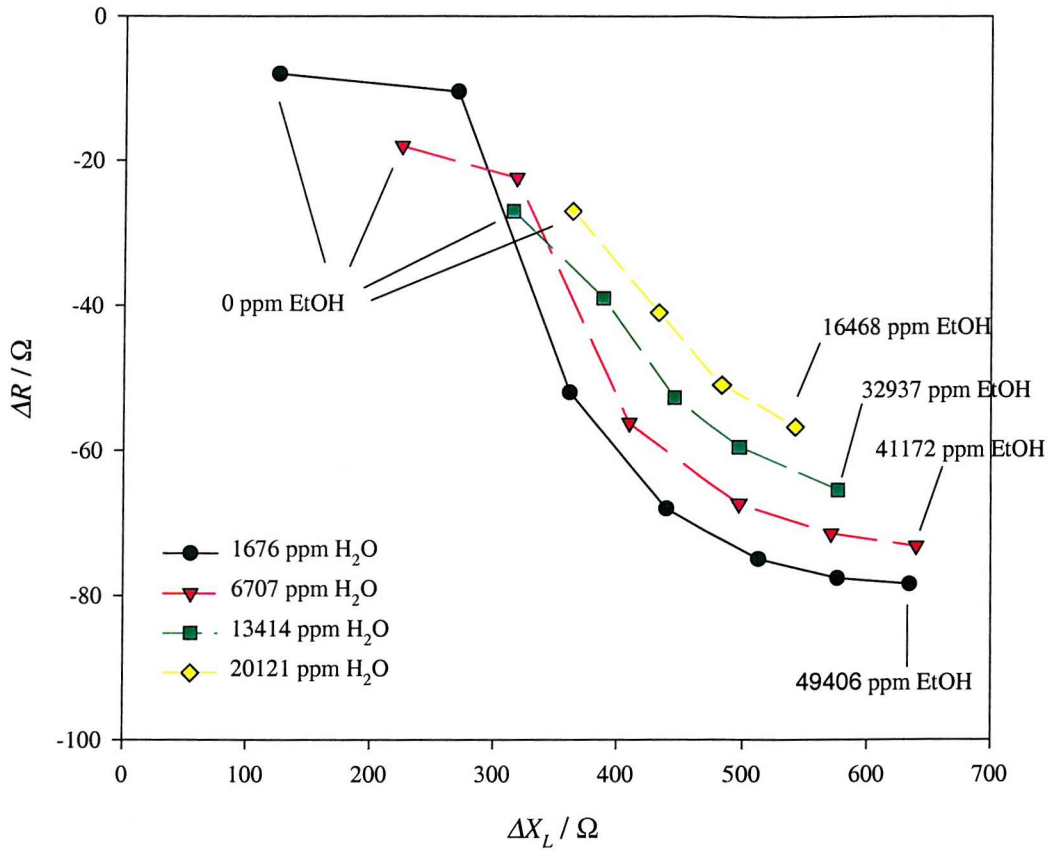

Figure 7. 8: parametric polar plot for poly(pyrrole) decane sulfonate (QCM 8) for a range of ethanol concentrations and humidity levels.

A last implication from the obvious viscoelastic changes revealed in Figure 7. 8 is that again the rigid film criteria defined by Buttry [6] is inappropriate. Indeed it predicts that for the mass of the coating (here 100 μg for the coating plus 5 μg for the water and ethanol vapours), which is inferior to 2% of the crystal mass, the film should behave like a rigid layer.

7.2.1.2.3 - Poly(aniline) pentane sulfonate

The poly(aniline) pentane sulfonate film did not behave rigidly upon exposure to water or ethanol. The viscoelastic effects were significant as revealed by the ratio $\Delta X_L/\Delta R$ of 3 and 3.4 for an exposure from 0 to 26829 ppm water and for an exposure to 41172 ppm ethanol at 6707 ppm H_2O respectively.

As for poly(pyrrole) decane sulfonate the polar plot shows a sigmoid shape upon exposure to water as shown in Figure 7. 9. Even if the change is less sharp than in the poly(pyrrole) case, the transition in behaviour at 10060 ppm H_2O was clear and reproducible.

The same curve (sigmoid) was not observed upon exposure to ethanol, probably because the amount of ethanol adsorbed is much smaller and therefore does not induce transition compared to water as seen by ΔX_L.

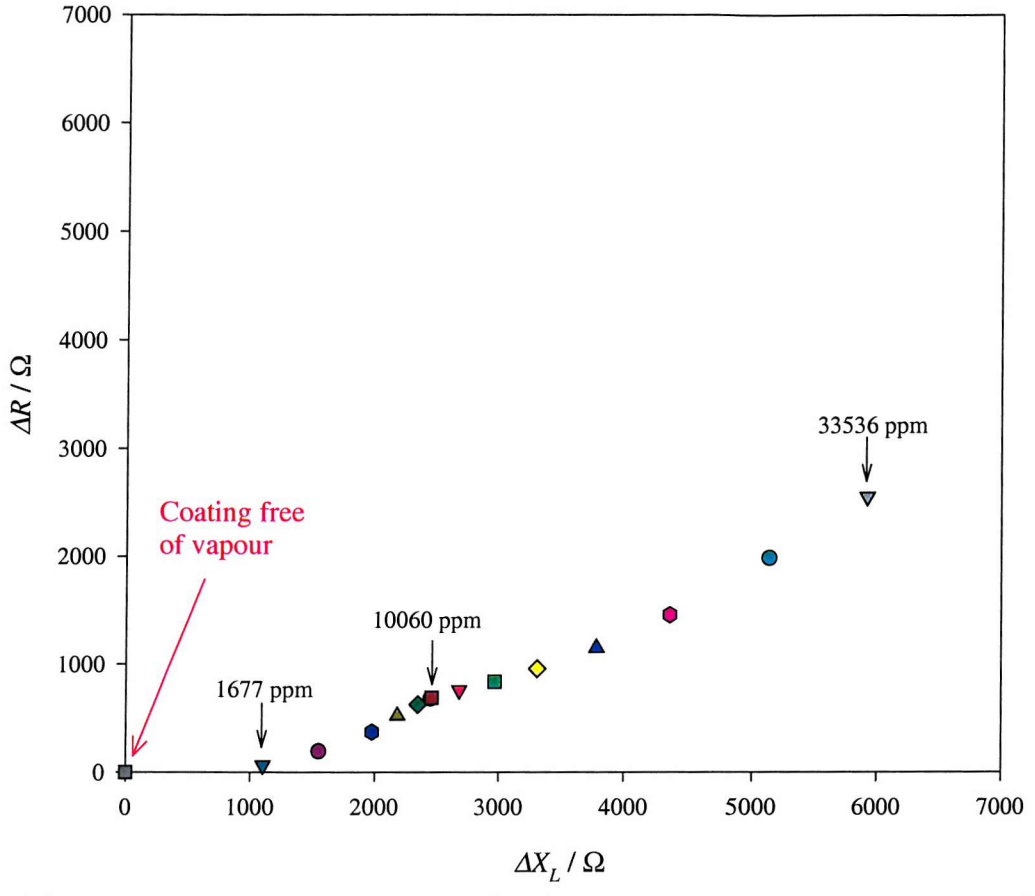

Figure 7. 9: parametric polar plot of poly(aniline) pentane sulfonate (QCM1) exposed to a range of humidities.

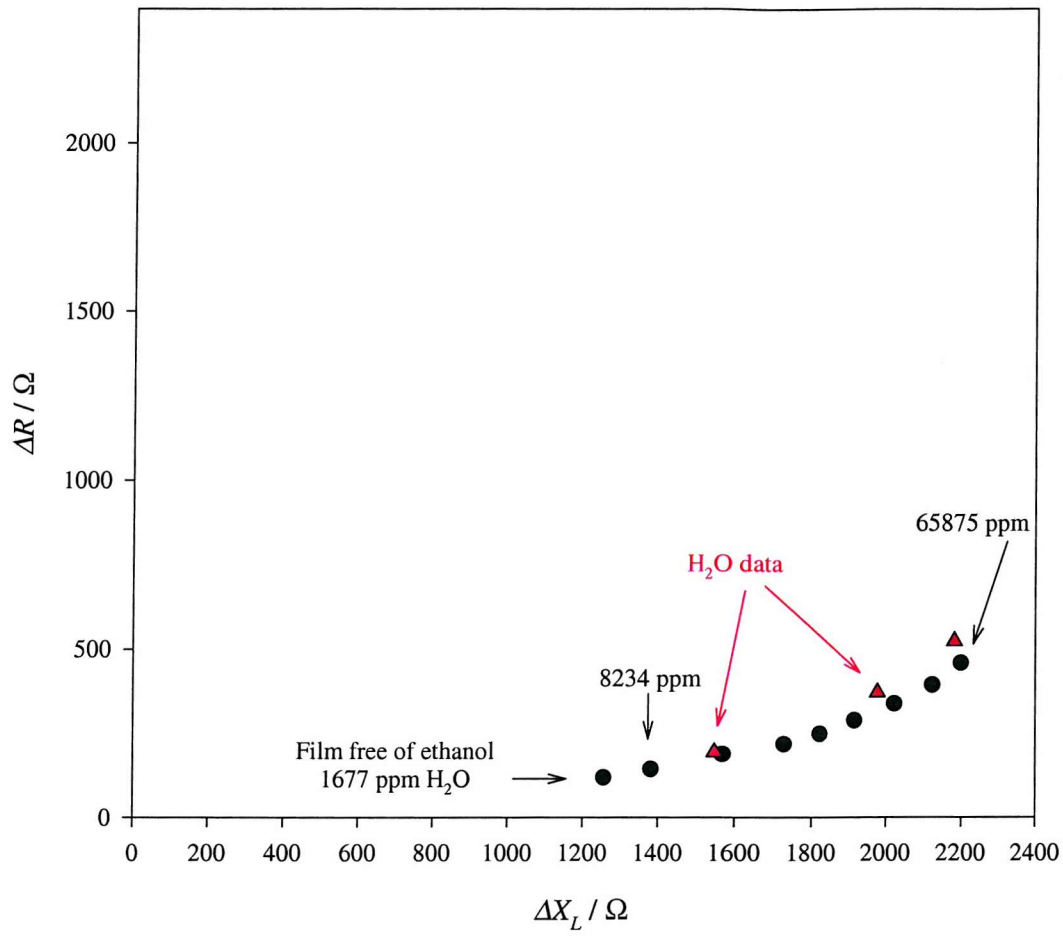

Figure 7. 10: parametric polar plot of poly(aniline) pentane sulfonate (QCM 1) exposed to a range of ethanol concentrations at 1677 ppm H_2O, as well as some data from Figure 7. 9.

For the three coatings investigated using QCM sensors, the ratio between ΔX_L and ΔR was always smaller than 10 upon exposure to water or ethanol, indicating significant viscoelastic effects. The equivalent electroacoustic resistance was used here to reveal viscoelastic effects not shown in the shift in resonant frequency alone. In addition the parametric polar plots were rich in information, revealing some clear transition between different structures.

The conclusion that the conducting polymers investigated do not behave rigidly is in agreement with the results reported by Etchenique [8] who recorded ΔR and ΔX_L upon the removal of residual water in a poly(aniline) film under vacuum. Only once a significant amount of the water had been removed was the equivalent electroacoustic resistance constant. So, in other words, even at low vapour concentrations, conducting polymers behave like viscoelastic layers and more especially in the high concentration ranges investigated in this work.

7.2.2 – Discussion on the validity of the Langmuir isotherm model

To analyse the experimental results obtained during this work regarding the sensing mechanism, the Langmuir isotherm model developed by Gardner and Bartlett [9-11] will be discussed first. It is a fairly complete model, and has been largely discussed in the literature [7,12-15].

7.2.2.1 - Description of the Langmuir isotherm model

Gardner and Bartlett have approached the problem of the sensing mechanism of conducting polymers using a mathematical method. The model they developed couples Fickian diffusion of the vapour in the polymer layer with the adsorption of the vapour at active sites following a Langmuir isotherm.

The Langmuir isotherm

The Langmuir isotherm is the simplest adsorption (physisorption) isotherm. Here it consists in the adsorption of gas molecules, A, into the matrix at given active sites, <S>, leading to occupied sites, <A>, according to:

$$A + <S> \underset{k_d}{\overset{k_a}{\rightleftharpoons}} <A>$$

where k_a and k_d are the adsorption and desorption rate constants respectively.

The coverage, θ , in a Langmuir isotherm is given by:

$$\theta = \frac{KC}{1+KC} \qquad (1)$$

where $K = k_a/k_d$ is the partition coefficient and C the concentration of the gas.

The conditions of the Langmuir isotherm are as following:

- the maximum coverage is one monolayer (one molecule at maximum per active site).
- the ability of a molecule to adsorb at a given site is independent of the occupancy of the adjacent sites.
- all sites are equivalent.

In the model, to relate the site occupancy with the response of the sensors ($\Delta\sigma/\sigma_{ini}$), Bartlett and Gardner assumed a linear relationship between the site occupancy and the conductivity. The conductivity of the polymer is then related to the conductance using a mathematical model for the band-gap structure. In addition, in their model they assume competition for the sites between the vapour, say EtOH, and water molecules to account for the observed effect of H_2O on the ethanol responses.

Fickian diffusion coupled with Langmuir adsorption isotherm

In the model, the polymer is assumed to behave ideally, meaning it is uniform in thickness and homogenous in the bulk. The diffusion is then assumed to be planar, perpendicular to the polymer surface. Then Fick's second law can be expressed for the conducting polymer as:

$$\frac{\partial C}{\partial t} = D\frac{\partial^2 C}{\partial x^2} - k_a N(1-\theta)C + k_d N\theta \qquad (2)$$

where the term $D\frac{\partial^2 C}{\partial x^2}$ represents the change in concentration due to diffusion of the vapour into the film, and the second and third terms on the right hand side express the change in concentration of free vapour due to the interactions of the vapour molecules at the active sites, from adsorption and desorption respectively. In the expression, N represents the concentration of active sites.

According to the Langmuir isotherm, the variation of coverage with time can be expressed as:

$$N\frac{\partial \theta}{\partial t} = k_a N(1-\theta)C - k_d N\theta \qquad (3)$$

So by combining (2) and (3) we obtain:

$$D\frac{\partial^2 C}{\partial x^2} - \frac{\partial C}{\partial t} = N\frac{\partial \theta}{\partial t} \qquad (4)$$

By introducing appropriate dimensionless parameters, Bartlett and Gardner obtained an equation equivalent to (4) (not detailed here but which can be found in references [1-3]). There are no analytical solutions for this last equation, but they identified limiting cases, mainly determined by whether the diffusion or the interaction at the sites was rate limiting.

Several papers cover the discussion of these cases in detail [1-3], and it is not the purpose to repeat this here.

To correlate their model with experimental data, Bartlett *et al.* analysed the response at equilibration of chemoresistors coated with poly(pyrrole) and poly(aniline) films exposed to a range of ethanol concentrations and for a range of humidities [13]. Their results were found to fit well the Langmuir isotherm model.

Following their work, several authors reported the good fitting of their results to the Langmuir isotherm model. Stussi *et al.* [4] employed chemoresistors coated with poly(pyrrole) and investigated the response to toluene. Similarly to Bartlett's work, they employed a model with a Fickian's diffusion into the polymer layer coupled with a Langmuir adsorption isotherm, but limited their study to investigating the effect of the film thickness on the response at equilibrium.

Hwang *et al.* [5] modelled the conducting polymer as a network of resistances, each resistance representing an active site in the polymer, the value of the resistor having two possible values depending whether the site is vacant or occupied. According to their calculations, the reciprocal of the change in resistance is expected to be linear with the reciprocal of the vapour concentration. They verified the model with poly(pyrrole) and composites of poly(pyrrole)-poly(ethylene oxide) upon exposure to ethanol. Their model, limited to equilibrium conditions, does not give any information on the transient response. In addition, the model is expected to be invalid for thick films where the sites at the interface polymer/vapour are less sensitive than the sites at the electrode/polymer interface due to the geometry of the field lines.

Topart and Josowicz [6] also applied a similar Langmuir adsorption model to the response to methanol of poly(pyrrole) doped with tetrafluoroborate or tosylate. The positive aspect of their work is that they were capable of fitting their results to the Langmuir isotherm model using different types of sensors as chemoresistors: Kelvin probe, UV-visible spectroscopy and QCM sensors.

7.2.2.2 - Discussion on the Langmuir isotherm model

7.2.2.2.1 - General comments on the model

Some data have been shown to fit the Langmuir model but the validity is limited. Indeed most of the work is limited in the number of coatings investigated and in the number of

vapours tested. In addition, they mainly treat the response at equilibration and ignore the response transient, which can be rich in information. A last comment is that the sensor type was limited to chemoresistors. This may appear to contradict the comment on the work of Topart *et al.* who employed several sensor types, but the same authors demonstrated that the Langmuir model was limited in concentration. In an earlier report, they showed by the use of QCM sensors that upon exposure to 12% MeOH, a poly(pyrrole) film showed viscoelastic changes not shown by chemoresistors [7].

Coming back to Gardner and Bartlett's model, the first criticism of Ingleby's work [13] is that it is limited in the number of sensor types investigated. In addition, the coatings employed were identical to the ones used in this work, which were found to drift significantly upon exposure to vapour. It is unfortunate that this author reported little on the transient response and in particular how the relative change in resistance was determined. For this reason it may be that the repeated error in the relative change in resistance used to verify the model is significant.

7.2.2.2.2 - Fitting of the chemoresistor/QCM responses to the Langmuir isotherm model

As just discussed the Langmuir isotherm model may fail in explaining the overall responses of conducting polymer gas sensors. Chemoresistor sensors coupled with QCM sensors showed that the experimental data were deviating from the Langmuir model in at least three respects. The first part of this work on the investigation of the sensing mechanism was to determine whether or not the Langmuir isotherm model failed in explaining the experimental data.

1 - Viscoelastic effects

As discussed in section 7.2.1, the QCM sensors revealed that the polymers investigated showed significant viscoelastic effects upon exposure to water and to ethanol, as confirmed by the literature [7,15]. This implies that the Langmuir isotherm model can be suitable to interpret the responses of the chemoresistors, but is incomplete to interpret the behaviour of a conducting polymer coating upon exposure to vapours as it does not take into consideration viscoelastic changes.

2 - Monolayer of adsorbed vapour per site

In the definition of the Langmuir adsorption isotherm model it is assumed that there is at maximum one vapour molecule per site. In order to test this using the results of the QCM experiments and the Sauerbrey equation some assumptions have to be made. The first assumption made here is that the number of active sites is, at most, equal to the number of monomer units in the polymer, since this is the smallest repeat unit in the material. This is a reasonable approximation taking into account the relatively limited space to accommodate the vapour, and also considering that in the model it is assumed that no interaction occurs between molecules on adjacent active sites.

The second approximation is in the number of monomer units as already discussed in Chapter 6. The maximum of the interval was employed here (see Tables 6.2 and 6.4).

These two approximations would allow us to test on the validity of the Langmuir isotherm model if it could be deduced that the number of vapour molecule per site is 1 or higher, as they both lead to an under-estimation of the number of molecules per site. Unfortunately, the Sauerbrey equation itself is an approximation here due to viscoelastic effects and the influence of the later on the mass is not predictable as discussed in Chapter 6. Here it is assumed that at most viscoelastic effects double the calculated mass from the actual mass. Therefore the number of vapour molecules per site should be larger than 2 to be conclusive.

Taking into account the assumptions just discussed, the number of vapour per active site can be determined from the shift in resonant frequency and the number of monomer units.

At saturated **humidity**, it was calculated that 5 water molecules were adsorbed per aniline for poly(aniline) pentane sulfonate. This first example shows that the limits of the Langmuir adsorption isotherm were reached as more than a monolayer was incorporated into the film.

Upon exposure to **ethanol**, no clear conclusion can be drawn. At 1676 ppm H_2O and 65875 ppm ethanol, the number of water and ethanol molecules per aniline unit has been calculated to be 1 and 0.5 respectively. Taking into account the competition between these two vapours for the active sites, a site occupancy of 1.5 was calculated. This number is too low to allow any firm conclusion. An interesting point is that, in contrast to the situation for water, at no point was more than 1 ethanol molecule found per site for the range of concentrations investigated here.

Referring back to Gardner and Bartlett's model, in his work Ingleby [13] also investigated poly(aniline) pentane sulfonate, but over a narrower concentration range (less than 40000 ppm EtOH at 11500 ppm H_2O). Over this range, his conclusions on the validity of the Langmuir adsorption model may be correct but it is expected that the Langmuir isotherm reaches its limits as the number of water molecules is larger than 1.5 per aniline (without taking into account the ethanol- about 0.05 per site).

For **poly(pyrrole),** no conclusion on the validity of the Langmuir adsorption model can be drawn as the ratio of vapour molecules adsorbed is always less than 1. For poly(pyrrole) pentane sulfonate, at saturated humidity, the ratio water:pyrrole is at maximum 1:3, and 1:3.3 for the decane equivalent. Upon exposure to ethanol, only 1 ethanol molecule is adsorbed for 17 pyrrole units at 49406 ppm EtOH and 6707 ppm H_2O for poly(pyrrole) pentane sulfonate. For the decane sulfonate doped film, the ratio EtOH:pyrrole is 1:7.5 under the same conditions. These later conditions may not be exactly leading to the maximum number of vapour molecules per pyrrole unit but are representative of the values obtainable. The low vapour to pyrrole ratio obtained here disagrees with the value of 1:6.7 reported by Topart for only 1% methanol [7,15].
From the QCM measurement, the Langmuir isotherm model can be ruled out only for poly(aniline) pentane sulfonate based on the argument that the coverage is greater than 1. In the other cases, the calculated coverage was close to 1 and therefore no firm conclusion can be drawn due to the difficulty in interpretation of the Quartz Crystal Microbalance data. However, it has to be remembered that in the model it was also assumed that there was no interaction between the molecules on adjacent sites. At the concentrations investigated here, the site occupancy being high, a critical point is reached where this aspect may also be limiting.

Charlesworth *et al.* [16] also investigated the number of molecules per site and concluded that up to 4 water molecules or 4 methanol molecules could be incorporated. They showed that the BET isotherm rather than the Langmuir isotherm was therefore suitable. The BET (Brunauer- Emmett- Teller) isotherm can be described as a Langmuir isotherm with a site occupancy larger than 1, which is agreement with the conclusions drawn here.

3 - Agreement between the chemoresistor and the QCM responses over the range of concentrations

Figure 7. 11 compares the typical response of the chemoresistor with the shift in resonant frequency and demonstrates that the Langmuir isotherm is not exact over the range of concentrations investigated. The chemoresistor sensor saturates at a moderate concentration; this correlates with the results from Ingleby [13]. The response of the QCM sensor varies over the whole range of concentrations. This implies that the chemoresistor coating continues to adsorb vapour at high concentrations but that these molecules have a negligible influence on the resistance, thus they are "invisible" to the chemoresistor sensors, and thus could not be taken into account in the model. The pattern observed in Figure 7. 11 was observed for poly(aniline) for humidity and ethanol, and for both poly(pyrrole) films upon exposure to water. For these later films, the chemoresistor response towards ethanol was difficult to define due to the drift, the small amplitude and the lack of reversibility of the response, allowing no conclusions to be drawn.

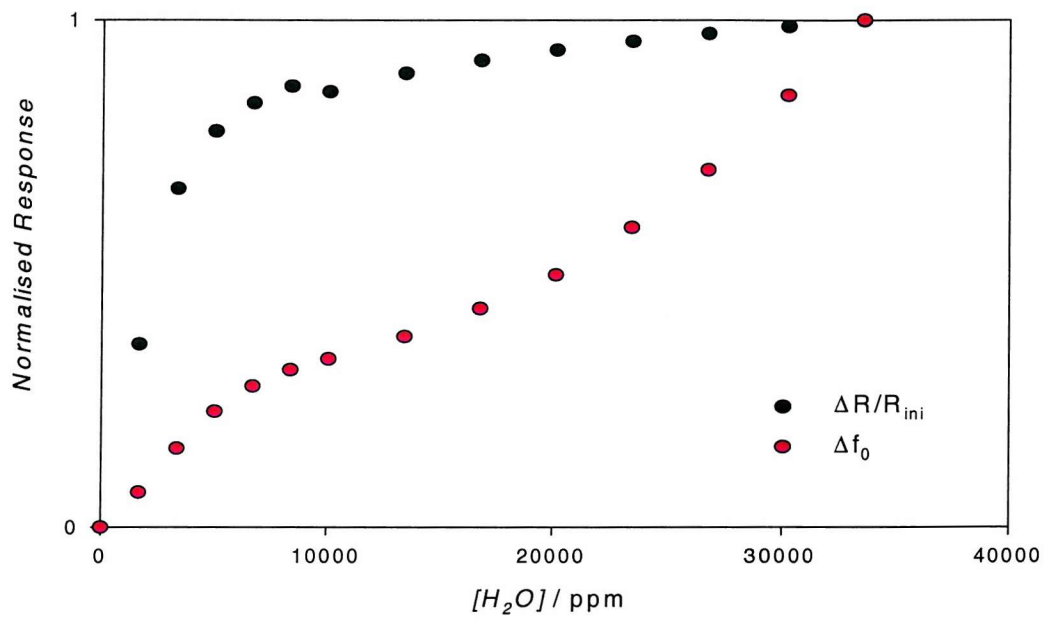

Figure 7. 11: normalised shift in resonant frequency of a QCM coated with poly(aniline) pentane sulfonate (QCM1) and the change in relative resistance of a comparable chemoresistor (IB0042), showing that at a concentration of about 10000 ppm the chemoresistor saturates, whereas the coating further adsorbs vapour molecules as shown by the resonant frequency.

A fourth criteria was investigated in order to rule out the Langmuir isotherm model. In the model defined by Gardner and Bartlett, each vapour molecule is assumed to induce an identical change in resistance, independently of the initial vapour content in the film.

Some calculations were performed in order to determine the effect of one mole of vapour molecules adsorbed on the electrical resistance for the range of concentrations investigated. However due to the large number of approximations required for these calculations, no conclusion could be drawn.

Coupling QCM sensors to chemoresistors rapidly revealed some limitations of the Langmuir adsorption isotherm model. Indeed it fails to take into account viscoelastic effects occurring in the coating upon exposure to vapour. In addition, for the large concentration range tested here, some limitations on the site occupancy and the assumption of non-interaction criteria between vapour molecules in adjacent sites were expected and proven in one case. Unfortunately, the viscoelastic effects limit the conclusions which can be drawn from the QCM data. A clear conclusion on the invalidity of the model defined by Gardner and Bartlett could however be drawn by comparing the response of the two sensor types over a range of concentrations, as both show very different behaviours.

7.2.3 - Alternative model- a double-diffusion model

7.2.3.1 - Description of the double-diffusion model

The data collected on the response of conducting polymers to ethanol, together with the sensitivity to humidity, were found to disagree with the Langmuir isotherm model. An alternative model is proposed here, based on the typical transient response observed for chemoresistor and QCM sensors coated with conducting polymer exposed either to ethanol or to water. The pattern observed was as follows (see Figure 7. 12 for the corresponding sensor response):

- a fast adsorption of the vapour in the coating shown by the rapid shift in resonant frequency of the QCM sensor, inducing little change in the conductivity of the coating but a large change in its viscoelasticity.
- a slow process which largely influences the chemoresistor response without any significant change in the amount of vapour absorbed and in viscoelasticity.

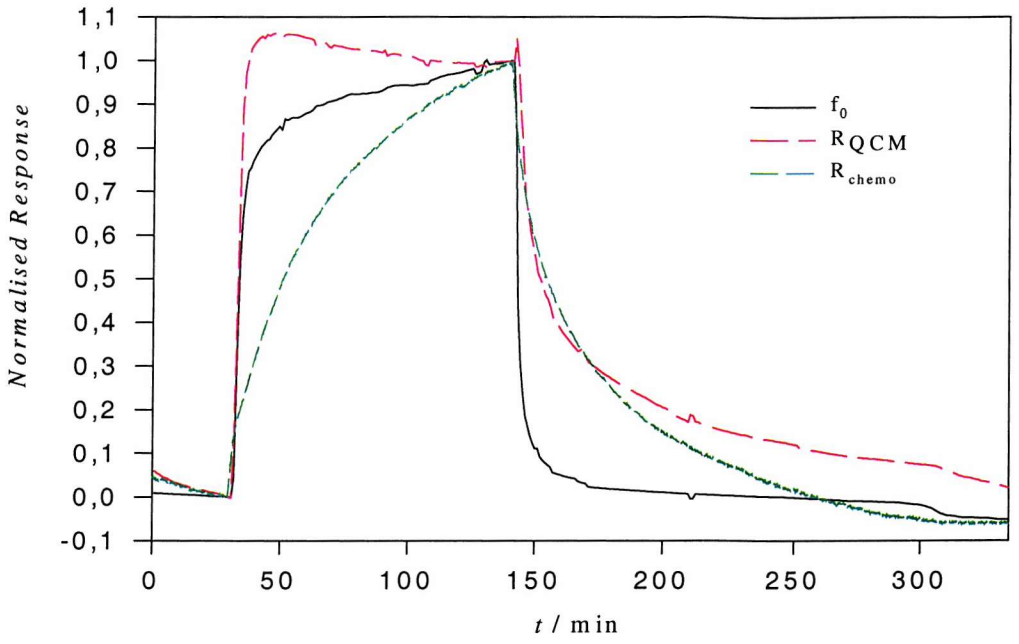

Figure 7. 12: typical transients obtained for the response of the conducting polymers to ethanol, both for the chemoresistor and the QCM sensors. Here is shown the response of poly(pyrrole) decane sulfonate to 32938 ppm ethanol at 6707 ppm H_2O (chemoresistor 65QR and QCM8).

Before discussing further the sensing mechanism, the morphology of conducting polymers has to be recalled. These materials are known to be porous. Even thought both poly(aniline) and poly(pyrrole) have different morphologies, a similar structure can be found: compact zones (of fibres for poly(aniline) or of nodules for poly(pyrrole)), separated by porous zones.

On the basis of the typical response transients observed for R_{chemo}, R_{QCM} and f_0, a double-diffusion model can be proposed. In the double-diffusion model, see Figure 7. 13 for a schematic representation, the vapour is believed to partition in the coating and be trapped in a rapid manner within the pores between the compact zones (step (1)). In a manner similar to that when a QCM is used in liquid media, the molecules of vapour trapped in the coating oscillate with the coating inducing a large and fast response of the piezoelectric device. From a concentration C in the vapour phase, a concentration C_1 is trapped in the layer. Due to the intrinsic poor conduction through the porous zone the influence of the vapour on the conductivity is low.

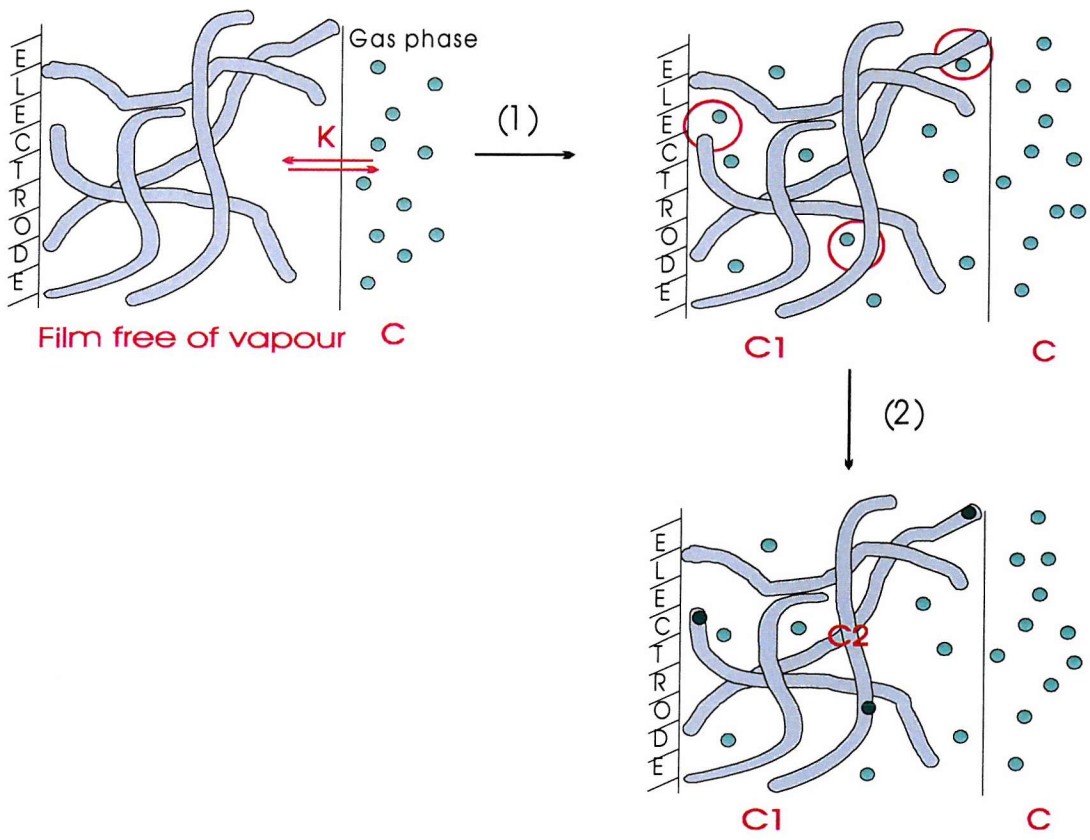

Figure 7. 13: diagram representing the double-diffusion model, where the vapour diffuses in a first stage into porous zones of the conducting polymer before diffusing in a second stage into the compact zones (here symbolised as fibres).

In step (2), a fraction of the vapour molecules trapped in the layer (circled) diffuses slowly into the polymer itself (fibres or nodules), symbolised as darker vapour molecules, to give a concentration C_2. This diffusion is accompanied by a major change in the conductivity of the coating as shown by the transient for the chemoresistor. How the vapour interacts with the polymer inducing the change in conductivity has not been investigated in detail here. As justified in the next paragraph, a BET isotherm is proposed. The overall process is accompanied by viscoelastic effects.

It was earlier shown that the Langmuir isotherm model was not suitable on its own to interpret the behaviour of conducting polymer films upon exposure to vapour, and thus in three respects. In the model defined here, it is clear that viscoelastic effects occur upon exposure, even if they are not noticeable in the response of chemoresistors. The second point was that it was observed that more than one molecule could be adsorbed per "site". This can be here compensated by the use of the BET rather than the Langmuir adsorption isotherm. The BET (Brunauer- Emmett- Teller) adsorption isotherm model was already found to fit the response of conducting polymer sensors by Topart [7]. In addition, the

curve of the BET isotherm [17] has the same shape as the one observed for the QCM sensors as illustrated in Figure 7. 11.
However, the BET isotherm rather than the Langmuir isotherm may not be required in the double-diffusion model as the amount of vapour adsorbed determined by QCM is the sum of the vapour in the pores and in the dense parts, only the later playing a role in the isotherm. Indeed when the response of f_0 is considered, it can be approximated that 95 % of the mass loading is due to adsorption in the pores and 5 % in the dense part. Then the argument that the site occupancy is larger than 1 is no longer valid and the Langmuir adsorption isotherm is sufficient. Another implication from this comment is that it demonstrates that the model developed by Gardner and Bartlett is in fact suitable to simply interpret the response of chemoresistors on their own, if of course, as suggested, the influence of the vapour in the pores of the polymer on the conductivity is negligible.

A similar model to the double-diffusion model was proposed by Blanc [18] to interpret the response of a poly(pyrrole) film to ammonia. He decomposes the response transient into two components. At short times, the response was analysed by the Elovich law, followed by an exponential drift at long time.

7.2.3.2 - Discussion on the model

There is further agreement between the model just defined and the data acquired during this work. One important aspect of the response of chemoresistors coated with conducting polymers, too often ignored, is the "**drift**". There are two types of drift observed: over a long time period and on the time scale of an experiment. Only the later was of interest here. The first one can be considered as a slow oxidation by atmospheric oxygen and/or a loss of adhesion of the polymer on the electrode. In all cases, this corresponds to an increase in resistance. This ageing process is a common concern in the field of sensors.
On the contrary, the sign of the drift on the time scale of an exposure was found to vary with the experimental conditions, so that it could not be explained by the same process. It was rather indicative of a slow process in the response. A significant example was the variation in the sign of the drift of the baseline of a poly(aniline) coated chemoresistor at 20% relative humidity (6707 ppm) as a function of the previous humidity it was conditioned to. If dry air was previously applied, the drift, like the response, was negative (decrease in resistance), corresponding to a slow uptake of water molecules. On the other

hand, the drift was positive if the relative humidity was decreased from 50% to 20%, corresponding to a slow loss in water content.

Before drawing the conclusion that the drift was due to a slow interaction of the vapour with the polymer, any experimental contributions to the phenomena were considered. The signal of the chemoresistor was monitored by applying a direct current trough the polymer film. Even if the potential across the film was carefully maintained below 100 mV, the polarisation of the film due to charge movement in the electrical field had to be considered. A switch was added to enable the current direction to be reversed during the gas tests. This did not lead to any change in the drift. A delay introduced by the gas delivery system was ruled out by the fast response of the QCM sensors.

Several points were further considered regarding the validity of the double-diffusion model.

In the double-diffusion model described here, the response time of two molecules with an identical chemical functional group is expected to increase with increasing size of the molecule. If it is assumed that water and ethanol have a similar chemical nature, the response time should be much larger for ethanol than for water. This is in good agreement with the trend observed (about 10 min for water and 60 min for ethanol). Published results confirm this point as the response time was found to increase with the size of the vapour molecule for a range of alkyl alcohols [19,20]. This conclusion assumes that the increasing hydrophobicity of the alkyl chain here plays a minor role.

In the double-diffusion model, for simplicity, it was assumed that the diffusion of the vapour in the pores of the polymer was fast enough to have a minor contribution to the response time. Of course, this contributes to the response time, as shown for poly(aniline) pentane sulfonate in Chapter 4, where the response time was found to increase with increasing the thickness of the film.

There are several other possible approaches to the problem of the sensing mechanism of conducting polymers. Following the work of Grate and Abraham [21], the interactions can be seen as physical interactions induced by polarity, polarisability, acidity and basicity. The solvents are well documented, but unfortunately to date the necessary coefficients for conducting polymers remain to be determined. Some thermodynamic approaches, similar to the ones commonly employed for polymers [22-25], can also be considered.

The results collected during the work and presented here confirm that the diffusion model described here is suitable to describe the interactions taking place between a vapour and a conducting polymer coating. However, further experiments are required to validate this conclusion. First, the response of a range of chemicals should be investigated and their response should be related to their diffusion coefficient. A more detailed mathematical approach to the response should be performed, mainly to correlate the response for a range of polymers to their physical properties (porosity and dimensions of the dense part). Finally, a wider range of polymers should be studied.

7.2.4 - Conclusions on the sensing mechanism

In the light of the response of the chemoresistor sensors alone to ethanol and water, no conclusion on the sensing mechanism could be drawn. Calculating the mass of vapour adsorbed upon exposure from the shift in resonant frequency was also unsuccessful due to significant viscoelastic effects occurring in the polymers. However, after appropriate approximations, the amount of vapour adsorbed could be estimated, and could be related to the number of monomer units in the coating. The first implication was that the simple Langmuir isotherm model developed by Gardner and Bartlett could be ruled out. In addition, by comparing the transient of the response of the two sensor types, a new model could be proposed. The fast response of the QCM sensor could be explained by a fast diffusion of the vapour in the pores of the conducting polymer and the slow response of the chemoresistor sensors by the slow diffusion of the vapour in the dense parts of the material, the modulation in conductivity following a Langmuir adsorption isotherm. Additional experimental results confirmed these conclusions. Further experiments are still required to validate the model.

As far as the implications for the engineering of the sensitive layer are concerned, in the case of a process limited by the diffusion of the vapour in the dense parts, the dimension of the dense parts should be reduced to improve the response time of the chemoresistors. The response time of conducting polymer sensors can also be decreased if the transduction is chosen as the resonant frequency of a QCM, as revealed by the faster response of this later. No real solution on improving the sensitivity can be offered as the interactions inducing the change in conductivity are not solved yet.

(1) Blair, N., The development and characterisation of conducting polymer based sensors for use in an electronic nose, PhD thesis, SOUTHAMPTON, 1994.

(2) Elliott, J. M., Conducting Polymer Odour Sensors, PhD thesis, SOUTHAMPTON, 1997.

(3) Ingleby, P.; Gardner, J. W., *Sensors and Actuators*, 1999, **B 57**, 17-27.

(4) Gopel, W., *Sensors and Actuators*, 1995, **B 24-25**, 17-32.

(5) Vigmond, S. J.; Kallury, K. M. R.; Ghaemmaghami, V.; Thompson, M., *Talanta*, 1992, **39**, 449-456.

(6) Buttry, D. A.; Ward, M. D., *Chem. Rev.*, 1992, **92**, 1355-1379.

(7) Topart, P.; Josowicz, M., *J. Phys. Chem.*, 1992, **96**, 7824-7830.

(8) Etchenique, R.; Brudny, V. L., *Langmuir*, 2000, **16**, 5064-5071.

(9) Bartlett, P. N.; Gardner, J. W., *Phil. Trans. R. Soc. Lond. A*, 1996, **354**, 35-37.

(10) Gardner, J. W.; Bartlett, P. N.; Pratt, K. F. E., *IEE Proc.-Circuits Devices Syst.*, 1995, **142**, 321-333.

(11) Gardner, J. W.; Bartlett, P. N., *Synthetic Metals*, 1993, **55-57**, 3664-3670.

(12) Hwang, B. J.; Yang, J. Y.; Lin, C. W., *J. Electrochem. Soc.*, 1999, **146**, 1231-1236.

(13) Ingleby, P., Modelling and characterisation of conducting polymer chemorsistors, PhD thesis, WARWICK, 1999.

(14) Stussi, E.; Stella, R.; Rossi, D. D., *Sensors and Actuators B*, 1997, **43**, 180-185.

(15) Topart, P.; Josowicz, M., *J. Phys. Chem.*, 1992, **96**, 8662-8666.

(16) Charlesworth, J. M.; Partridge, A. C.; Garrard, N., *J. Chem. Phys.*, 1993, **97**, 5418-5423.

(17) Brunauer, S.; Deming, L. S.; Deming, W. E.; Teller, E., *J.Am. Chem. Soc.*, 1940, **62**, 1723-1732.

(18) Blanc, J. P.; Derouiche, N.; Hadri, A. E.; Germain, J. P.; Maleysson, C.; Robert, H., *Sensors and Actuators*, 1990, **B1**, 130-133.

(19) Josowicz, M.; Janata, J., *Anal. Chem.*, 1986, **58**, 514-517.

(20) Bartlett, P. N.; Ling-Chung, S. K., *Sensors and Actuators*, 1989, **20**, 287-292.

(21) Grate, J. W.; Abraham, M. H., *Sensors and Actuators B*, 1991, **3**, 85-111.

(22) Chehimi, M. M.; Abel, M. L.; Pigois-Landureau, E.; Delamar, M., *Synthetic Metals*, 1993, **60**, 183-194.

(23) Ganesh, K.; Nagarajan, R.; Duda, J. L., *Ind. Eng. Chem. Res.*, 1992, **31**, 746-755.

(24) Pellegrino, J.; Radebaugh, R.; Mattes, B. R., *Macromolecules*, 1996, **29**, 4985-4992.

(25) Tan, Z.; Vancso, G. J., *Macromolecules*, 1997, **30**, 4665-4673.

Chapter 8 - Conclusions

Numerous improvements have resulted from this work on conducting polymer gas sensors. The first field of improvement concerns the sensor substrates, which were shown to be a crucial point in the quality of the sensors. A new array of devices has been developed and new materials have been tested. During the development of the new substrates, the aspect concerning the mass production was kept in mind.

Much attention was paid to improving the sensing material. New sensing materials have been tested. Polymers were engineered by incorporation of metal phthalocyanines in order to increase the sensitivity towards NO_2. On the material side, it has been shown that the reproducibility of the response of the sensors could be improved, along with the response time and stability, by monitoring *in-situ* the resistance of the polymer during the electropolymerisation.

The sensing mechanism of conducting polymer gas sensors towards VOCs has been investigated, along with the influence of humidity. Both the data acquired and the calculations performed were analysed very critically. A large number of approximations were required, the most limiting one being the incapability of measuring the mass of vapour adsorbed by the coating on the QCM sensors due to significant viscoelastic effects occurring upon exposure to vapour.

The following conclusions on the sensing mechanism were drawn. The Langmuir adsorption isotherm model was ruled out as, on its own, it failed explaining viscoelastic effects associated with vapour adsorption and a coverage close to the monolayer. A double-diffusion model was considered. It consists in a rapid diffusion of the vapour in the pores of the polymer, as revealed by the fast response of the piezoelectric sensors, followed by a slow diffusion of a fraction of the vapour in the dense parts of the material inducing the change in conductivity. Coupled with the double diffusion model and viscoelastic effects, the Langmuir adsorption isotherm model could no longer be ruled out and appeared to be the most appropriate and simple model to interpret the change in conductivity induced by vapour adsorption. The main target of being able to engineer the coating for a given application remains. Parts of this complex problem are still unsolved and further work should be done in this direction.

Annex A – Chemoresistor production

The polymerisation charge of the conducting polymer chemoresistor is given here as an indication of the polymer deposition for each individual sensor.

The substrates employed were SRL123 devices, cleaned by cyclic voltammetry prior to electrodeposition as described in Chapter 3. For each polymer a table containing the reference code (or name) of six to eight sensors, their polymerisation charge as well as the resistances of the dry films is given. The order of the sensors in the table represents the order of production, from the same growth solution. The reference code for the sensors is given here so that the response to vapours from these sensors (reported in Chapter 6) can be correlated with the exact polymerisation results. The resistance of the films was measured 7 days after drying under atmospheric conditions, corresponding to the time required for the resistance to reach a steady behaviour.

POLY(PYRROLE) PENTANE SULFONATE

Sensor	65BR	65CL	65CM	65CR	65DL	65DM	65DR	65EL
Q / mC	15.5	17.0	14.75	14.75	14.5	14.5	14.0	13.5
R / Ω	307	1470	237	760	523	474	338	519

POLY(PYRROLE) DECANE SULFONATE

Sensor	65PL	65PM	65PR	65QM	65QR	65RL
Q / mC	16.0	16.5	15.25	14.5	14.0	14.5
R / Ω	57	31	319	112	122	84

POLY(PYRROLE) *P*-TOLUENE SULFONATE

Sensor	64YM	64YR	64ZL	65AM	65AR	65BL	65BM
Q / mC	17.75	16.25	17.0	15.75	15.5	15.0	15.0
R / Ω	58	124	37	87	65	64	43

POLY(PYRROLE) COPPER PHTHALOCYANINE TETRASULFONATE

Sensor	64VR	64WL	64WM	64WR	64XL	64XM	64XR	64YL
Q / mC	15.75	12.75	13	13	12.25	11	10.5	9.5
R / Ω	695	790	1140	1040	1120	1120	1370	1580

POLY(PYRROLE) NICKEL PHTHALOCYANINE TETRASULFONATE

Sensor	65MR	65NL	65NM	65NR	65OL	65OM	65OR
Q / mC	19.75	16.5	16.0	17.0	15.25	15.25	12.75
t / s	100	120	140	140	140	140	180
R / Ω	590	800	760	820	800	1090	1700

NB: the electropolymerisation presented a lack of reproducibility, so that the deposition time was varied as indicated in the table.

POLY(ANILINE) PENTANE SULFONATE

Sensor	65KM	65KR	65LL	65LM	65LR	65ML	65MM
Q / mC	6.25	5.62	5.06	4.12	5.50	4.87	3.62
R / Ω	17.3	18.4	16.4	20.0	15.2	19.0	24.5

POLY(ANILINE) DECANE SULFONATE

Sensor	65RM	65RR	65SL	65SM	65SR	65TL
Q / mC	28.0	22.0	21.5	21.5	20.5	17.0
R / Ω	3.2	3.5	3.4	3.5	4.0	4.0

POLY(ANILINE) *P*-TOLUENE SULFONATE

Sensor	65ER	65FL	65FR	65GM	65GL	65HL
Q / mC	23.0	16.0	18.0	18.0	18.5	20.0
R / Ω	5.6	7.6	7.8	6.6	7.4	5.8

POLY(ANILINE) COPPER PHTHALOCYANINE TETRASULFONATE

Sensor	65HM	65HR	65IL	65IM	65IR	65JM	65JR
Q / mC	0.87	0.86	0.90	0.99	1.12	1.40	1.99
R / Ω	6200	3500	3400	4300	2100	810	2000

POLY(ANILINE) NICKEL PHTHALOCYANINE TETRASULFONATE

Sensor	65TM	65TR	65UM	65UR	65VL	65VM
Q / mC	6.37	6.37	5.62	7.12	7.25	7.31
R / Ω	62	45	64	37	42	33